

2008

Code comparison of methane hydrate reservoir simulators using CMG STARS

Manohar Gaddipati
West Virginia University

Follow this and additional works at: <https://researchrepository.wvu.edu/etd>

Recommended Citation

Gaddipati, Manohar, "Code comparison of methane hydrate reservoir simulators using CMG STARS" (2008). *Graduate Theses, Dissertations, and Problem Reports*. 1973.
<https://researchrepository.wvu.edu/etd/1973>

This Thesis is protected by copyright and/or related rights. It has been brought to you by the The Research Repository @ WVU with permission from the rights-holder(s). You are free to use this Thesis in any way that is permitted by the copyright and related rights legislation that applies to your use. For other uses you must obtain permission from the rights-holder(s) directly, unless additional rights are indicated by a Creative Commons license in the record and/ or on the work itself. This Thesis has been accepted for inclusion in WVU Graduate Theses, Dissertations, and Problem Reports collection by an authorized administrator of The Research Repository @ WVU. For more information, please contact researchrepository@mail.wvu.edu.

**Code Comparison of Methane Hydrate Reservoir Simulators
using CMG STARS**

Manohar Gaddipati

**Thesis submitted to the
College of Engineering and Mineral Resources
at West Virginia University
in partial fulfillment of the requirements
for the degree of**

**Master of Science
in
Chemical Engineering**

Dr. Brian J. Anderson

Dr. H. Ilkin Bilgesu

Dr. Wu Zhang

Department of Chemical Engineering

Morgantown, West Virginia

2008

Key words: Gas hydrates, CMG STARS, Code comparison, Methane hydrate reservoir simulators, Gas production from hydrates, Sensitivity analysis, Heterogeneity, Depressurization

Code Comparison of Methane Hydrate Reservoir Simulators using CMG STARS

ABSTRACT

Natural gas is an important energy source contributing to 23% of the total energy consumption in United States. Domestic conventional natural gas production does not keep pace with increase in natural gas demand. Development of new alternatives like natural gas from methane hydrate can play a major role in ensuring adequate future energy supplies in the United States.

Methane hydrates are crystalline solids, very similar to ice, in which non-polar molecules are trapped inside the cages of water molecules. Methane hydrates could be potentially a vast source of energy. It is estimated that the total amount of natural gas trapped inside the hydrate is approximately two times the total unconventional oil-gas reserves in the world. The production of natural gas from hydrates economically poses a big challenge to today's scientific world. Over the years, different reservoir simulators were developed and different approaches have been used to model the gas hydrate dissociation behavior. The National Energy Technology Laboratory (NETL) and the U.S Geological Survey (USGS) gas hydrate code comparison project is the first of its kind and it aims at a worldwide understanding of the hypotheses involved in the gas hydrate modeling and problem solving. This code comparison study is conducted to compare various hydrate reservoir simulators like CMG STARS, TOUGH-Fx/Hydrate, MH21, STOMP, HydrateResSim and a code from University of Houston.

The objective of this Project is to generate results for different problems set by the code comparison participants using CMG STARS and to validate its results with other reservoir simulators. Results obtained are in good agreement with other simulators in the study. However minor differences were observed for a problem with ice in the system. Long term simulations were conducted for Mt Elbert, Prudhoe Bay L-PAD like deposits. The Production rates obtained using CMG STARS were in good agreement with other packages.

In addition to the code comparison problems, simulations to analyze the sensitivity to various parameters were performed. Studies were carried out with heterogeneity introduced in the reservoir properties using the Mt. Elbert stratigraphic test well data and results showed that higher production was observed with the incorporation of heterogeneity. Sensitivity analysis of seven reservoir parameters was done using Plackett-Burman design to gain a better understanding on production performance. The reservoir parameters were ranked based on effects of the reservoir parameters on production rates.

Acknowledgements

I thank my research advisor Dr. Brian J. Anderson for his encouragement, guidance and his help throughout the course of my research. Besides being my research advisor, he has been of great support in a foreign country to me. I will remain indebted to him for the inspiration he has given me.

Many thanks to Dr. Huseyin I. Bilgesu and Dr. Wu Zhang for being a part of my advisory committee and for all the help and suggestions they have offered.

I sincerely thank George Moridis, Joseph W. Wilder, Scott Wilson, Mark D. White, Mehran Pooladi-Darvish, Kelly Rose, Ray Boswell, Masanori Kurihara for sharing their research results and indirectly supporting my research project. Together it was a perfect team.

It is family that makes a person and I am very lucky to have a wonderful family. I am very grateful to my father, Narasimha Rao, my mother, Nagamani for their love and my brother Samba who has been my role model since childhood. I also express my genuine gratitude to Lavanya Nyayapathi who has always been there for me.

Thank you one and all.

Manohar Gaddipati

October 31, 2008.

Table of Contents

1. Introduction	1
1.1 Growing Energy demand and importance of Hydrate	2
1.2 Reservoir simulations of gas hydrate reservoirs	6
1.3 Recent developments in the production of natural gas from gas hydrates	8
1.4 International effort for the code comparison project	9
1.6 Objectives of this study	10
1.7 General project description.....	10
1.8 Overview of the report.....	11
2. Literature Review	13
2.1 History	13
2.2 Hydrates in Natural gas Industry	13
2.3 Occurrences	14
2.4 Hydrate structures.....	16
2.5 Stability	20
2.6 Hydrate Properties	21
2.7 Introduction to CMG STARS.....	23
2.8 Role of hydrates in climatic change	23
2.9 Conventional methods for producing gas from hydrates.....	25
3: 1-D Cartesian systems: Problems and Solutions	27
3.1 Problem 1	28
3.1.1 Solution to problem 1 using CMG STARS	33
3.2 Problem 2	45
3.2.1 Solution to Problem 2.....	47
3.3 Problem 3	61
3.3.1 Solution to Problem 3.....	67
4. 1-D and 2-D radial systems: Problems and Solutions	104
4.1 Problem 4	105
4.1.1 Solution to Problem 4.....	109
4.1.2 Results of similarity solution study of hydrate dissociation in radial domain.....	114
4.2 Problem 5	123
4.2.1 Solution to Problem 5.....	131
5. Long term simulations on Prudhoe Bay and Mt. Elbert like sites	144
5.1 Problem 7a.....	145
5.1.1 Solution to Problem 7a	153
5.2 Problem 7b: PBU L-Pad.....	161

5.2.1 Solution to Problem 7b.....	168
5.3 Problem 7c.....	173
5.3.1 Solution to Problem 7c.....	176
6. Sensitivity Analysis of Reservoir Parameters	179
6.1 One at a Time Effect:	180
6.2 Plackett Burman Design.....	188
7. Importance and Incorporation of Heterogeneity in Reservoirs	197
8. Conclusions Recommendations and Future work	202
8.1 Conclusions	202
8.2 Recommendations and Future work.....	203
References	205

List of Figures

Figure 1-1 U.S Energy Consumption by Fuel, projected up to 2030	3
Figure 1-2 Average imported crude oil prices.	4
Figure 1-3 U.S Natural gas consumption and Production.	5
Figure 1-4 U.S Natural gas production by source, projections up to 2030.....	6
Figure 2-1 Locations of known and inferred gas hydrate occurrences ²¹	14
Figure 2-2 Different structures of gas hydrates.	17
Figure 2-3 Structure I and II type hydrate.	19
Figure 2-4 Methane Hydrate Stability Zones ²⁸ (a) Permafrost Regions (b) Oceanic Regions.....	21
Figure 2-5 Equilibrium Pressure-Temperature relationship of methane hydrates ³	22
Figure 2-6 Global methane concentration Vs. Time in the atmosphere from 1980 to 2004 ³¹	24
Figure 3-1 Schematic diagram of the grid for problem 1.	29
Figure 3-2 Capillary Pressures vs. Water Saturation as calculated using the Van Genuchten equation.....	31
Figure 3-3 Relative permeability of water k_{ra} and gas, k_{rg} phases as a function of water saturation	32
Figure 3- 4 Aqueous Saturation Curves for different time steps for Problem 1	40
Figure 3- 5 Temperature profiles for different time steps for Problem 1	41
Figure 3- 6 Aqueous relative permeability for different time steps for problem 1.....	42
Figure 3- 7 Aqueous methane mass fraction for different time steps for Problem 1.....	43
Figure 3- 8 Gas Pressure at different time steps for Problem 1.....	44
Figure 3- 9 Schematic view of problem 2.....	45
Figure 3- 10 Aqueous Saturation profiles for different time steps for Problem 2.	54
Figure 3- 11 Gas Saturation profiles for different time steps for Problem 2.....	55
Figure 3- 12 Hydrate saturation profiles for different time steps for Problem 2.....	56
Figure 3- 13 Profiles of temperature at different time steps for Problem 2.....	57
Figure 3- 14 Aqueous relative permeability curves at different time steps for Problem 2.....	58
Figure 3- 15 Aqueous methane mass fraction profiles for different time steps for Problem 2.....	59
Figure 3- 16 Gas Pressure profiles for different time steps for Problem 2.....	60
Figure 3- 17 Schematic representation of grid for Problem 3	62
Figure 3- 18 Aqueous and Gas Relative permeability curves as a function of Water Saturation.....	65
Figure 3-19 Capillary Pressure vs. Water Saturation	65

Figure 3- 20 Profiles of Aqueous saturation at different times for problem 3 Case 1.....	77
Figure 3- 21 Profiles of gas saturation at different time steps for Problem 3 Case 1	78
Figure 3- 22 Profiles of hydrate saturation at different times for Problem 3 Case 1	79
Figure 3- 23 Profiles of temperature at different times for Problem 3 Case 1.....	80
Figure 3- 24 Profiles of Aqueous relative permeability at different times for Problem 3 Case 1 ..	81
Figure 3- 25 Profiles of Aqueous methane mass fraction at different times for Problem 3 Case 1	82
Figure 3- 26 Profiles of Pressure at different times for Problem 3 Case 1	83
Figure 3- 27 Profiles of capillary pressure at different times for Problem 3 Case 1	84
Figure 3- 28 Production rates for problem 3, Case 2.....	85
Figure 3- 29 Aqueous Saturation for different time steps for Problem 3-case-2.....	86
Figure 3- 30 Gas Saturation for different time steps for Problem 3-case-2.....	87
Figure 3- 31 Hydrate Saturation for different time steps for Problem 3-case-2.....	88
Figure 3- 32 Temperature for different time steps for Problem 3-case-2.....	89
Figure 3- 33 Aqueous relative permeability at different time steps for Problem 3-case-2.....	90
Figure 3- 34 Aqueous relative permeability at different time steps for Problem 3-case-2.....	91
Figure 3- 35 Gas Pressure for different time steps for Problem 3-case-2.....	92
Figure 3- 36 Gas-water capillary pressures for different time steps for Problem 3-case-2.	93
Figure 3- 37 Hydrate saturation curves at different time steps for Problem 3- Case -3	96
Figure 3- 38 Aqueous saturation curves at different time steps for Problem 3, Case 3.....	97
Figure 3- 39 Aqueous phase relative permeability curves at different time steps for Problem 3, Case 3.....	98
Figure 3- 40 Aqueous phase relative permeability curves at different time steps for Problem 3, Case 3.....	99
Figure 3- 41 Ice saturation curves at different time steps for Problem 3, Case 3.....	100
Figure 3- 42 Gas saturation curves at different time steps for Problem 3, Case 3.....	101
Figure 3- 43 Profiles of aqueous phase CH ₄ mass fraction at different time steps for Problem 3, Case 3.....	102
Figure 3- 44 Gas Pressure curves at different time steps for Problem 3, Case 3.....	103
Figure 4-1 Schematic view of the grid for problem 4.....	105
Figure 4- 2 Aqueous and gas relative permeability curves as a function of water saturation for Problem 4.....	107
Figure 4-3 Capillary Pressure vs. Water Saturation for Problem 4.	108

Figure 4- 4 Profiles of Temperature of Problem 4 case 1 for (a) CMG STARS (b) TOUGH-Fx/HYDRATE.....	114
Figure 4- 5 Profiles of Hydrate saturation of Problem 4 case 1 for (a) CMG STARS (b) TOUGH-Fx/HYDRATE.....	115
Figure 4- 6 Profiles of Gas saturation of Problem 4 case 1 for (a) CMG STARS (b) TOUGH-Fx/HYDRATE.....	116
Figure 4- 7 Profiles of Aqueous saturation of Problem 4 case 1 for (a) CMG STARS (b) TOUGH-Fx/HYDRATE.....	116
Figure 4- 8 Profiles of Aqueous saturation of Problem 4 case 1 for (a) CMG STARS (b) TOUGH-Fx/HYDRATE.....	117
Figure 4- 9 Profiles of Gas pressure of Problem 4 case 1 for (a) CMG STARS (b) TOUGH-Fx/HYDRATE.....	117
Figure 4-10 Profiles of Gas pressure of Problem 4 case 2 for (a) CMG STARS (b) TOUGH-Fx/HYDRATE.....	118
Figure 4- 11 Profiles of Temperature of Problem 4 case 2 for (a) CMG STARS (b) TOUGH-Fx/HYDRATE.....	119
Figure 4- 12 Profiles of aqueous saturation of Problem 4 case 2 for (a) CMG STARS (b) TOUGH-Fx/HYDRATE.....	120
Figure 4- 13 Profiles of gas saturation of Problem 4 case 2 for (a) CMG STARS (b) TOUGH-Fx/HYDRATE.....	120
Figure 4- 14 Profiles of hydrate saturation of Problem 4 case 2 for (a) CMG STARS (b) TOUGH-Fx/HYDRATE.....	121
Figure 4- 15 Profiles of aqueous relative permeability of Problem 4 case 2 for (a) CMG STARS (b) TOUGH-Fx/HYDRATE.....	121
Figure 4- 16 Profiles of aqueous CH ₄ mass fraction of Problem 4 case 2 for (a) CMG STARS (b) TOUGH-Fx/HYDRATE.....	122
Figure 4- 17 Profiles of gas-water capillary pressure of Problem 4 case 2 for (a) CMG STARS (b) TOUGH-Fx/HYDRATE.....	122
Figure 4-18 Geometry of the cylindrical grid for Problem 5.....	123
Figure 4-18 a Case A: Aqueous & Gas Relative permeability curves.....	128
Figure 4-18 b Case B: Aqueous & Gas Relative permeability curves.....	128
Figure 4-19 a Case A: Capillary pressure plotted against water saturation for Problem 5.....	129
Figure 4-19 b Case B: Capillary pressure plotted against water Saturation for problem 5	130

Figure 4-20 Gas Rates for problem 5 Cases A-1, A-2, A-3, A-4.	136
Figure 4-21 Gas Rates for problem 5 Cases A-1, A-2, A-3, A-4.	137
Figure 4-22 Cumulative gas production for problem 5 Cases A-1, A-2, A-3, A-4.	138
Figure 4-23 Cumulative water production for Problem 5 Cases A-1, A-2, A-3, A-4.	139
Figure 4-24 Gas rates for problem 5 Cases B-1, B-2, B-3, B-4.....	140
Figure 4-25 Water rates for problem 5 Cases B-1, B-2, B-3, B-4.	141
Figure 4-26 Cumulative gas production for problem 5 Cases B-1, B-2, B-3, B-4.	142
Figure 4-27 Cumulative water production for problem 5 Cases B-1, B-2, B-3, B-4.....	143
Figure 5-1 Schematic view of the grid for problem 7a.....	145
Figure 5-2 Aqueous and Gas relative Permeability curves for Problem 7a.....	151
Figure 5-3 Capillary Pressure as a function of water saturation.....	152
Figure 5-4 Gas rate and cumulative gas rate for 50 years using CMG STARS	159
Figure 5-5 Gas rate and cumulative gas rate for 50 years using MH21	159
Figure 5-6 Water rate and cumulative water rate for 50 years using CMG STARS	160
Figure 5-7 Water rate and cumulative water rate for 50 years using MH21	160
Figure 5- 8 Schematic view of the grid for Problem 7b.	161
Figure 5- 9 Aqueous and Gas relative Permeability curves for problem 7b.....	166
Figure 5-10 Gas rate and cumulative gas rate for 50 years using CMG STARS	170
Figure 5-11 Gas rate and cumulative gas rate for 50 years using MH21	171
Figure 5-12 Water rate and cumulative water rate for 50 years using CMG STARS	171
Figure 5-13 Water rate and cumulative water rate for 50 years using MH21	172
Figure 5-14 Gas rate and cumulative gas production for 50 years using CMG STARS	177
Figure 5-15 Gas production rate and cumulative gas production for 50 years using MH21	177
Figure 5-16 Water rate and Cumulative water production for 50 years using MH21	178
Figure 5-17 Water rate and Cumulative water production for 50 years using CMG STARS	178
Figure 6-1 Effect of Porosity on gas production.....	181
Figure 6-2 Effect of permeability on gas production.....	182
Figure 6-3 Effect of hydrate saturation on gas production	183
Figure 6-4 Effect of temperature on gas production.....	184
Figure 6-5 Effect of pressure on gas production.....	185
Figure 6-6 Effect of bottom- hole pressure on gas production	186
Figure 6-7 Effect of free water saturation on gas production	187
Figure 6-8 Parameter specifications for Design 1	189

Figure 6- 9 Cumulative gas production for designs 1-8	193
Figure 6-10 Effects of the parameters on gas production.....	195
Figure 7-1 Hydrate saturation and Permeability distribution data from Mt Elbert Stratigraphic test well	197
Figure 7-2 Porosity and Irreducible water saturation data from Mt Elbert Stratigraphic test well	198
Figure 7-3 Gas production for Case 1, 2 and 3. Case 1 refers to the reservoir which includes anisotropy in permeability, porosity, hydrate saturation and irreducible water saturation. Only heterogeneity in hydrate saturation is considered in Case 2. Anisotropy in hydrate saturation, porosity and irreducible water saturation (50 layers) is considered in Case 3	201

List of Tables

Table 2-1 Different estimates of Methane Hydrates from 1973 to 2005 ²²	15
Table 2-2 Worldwide Estimates of Gas Hydrates ²³	16
Table 2-3 Geometry of Cages	18
Table 2-4 Physical Properties of Methane Hydrates ²⁹	22
Table 3-1 Parameters and Specifications for Problem 1	30
Table 3-2 Input Parameters for Problem 2	46
Table 4-1 Input Parameters and Specifications	106
Table 4-2 Case Description of Problem 5	125
Table 4-3 Pressures and Temperatures for Models 1 & 3	125
Table 4-4 Pressures and Temperatures for Models 2 & 4	126
Table 4-5 Hydrate and Water Saturation for different case studies	126
Table 4-6 Hydraulic and Thermal Properties for Problem 5	127
Table 4-7 Effect of discretization on production rates for problem 5	134
Table 4-8 Effect of hydrate saturation on production rates for Problem 5	135
Table 5-1 Radius of the individual cells	146
Table 5-2 Cell discretization in the z-direction for Problem 7a	147
Table 5-3 Pressure and Temperature values for the reservoir modeled in Problem 7a	148
Table 5-4 Medium Properties for the Problem 5	150
Table 5-5 Discretization of the grid in z direction	162
Table 5-6 Pressure and Temperature values for Problem 7b	163
Table 5-7 Medium Properties for Problem 7b	166
Table 5-8 Pressure and Temperature values for Problem 7c	173
Table 6-1 Factors and their values used for OAAT effect calculations	180
Table 6- 2 Parameter specifications for different scenarios	190
Table 6-3 Plackett-Burman sensitivity analysis matrix	191
Table 6-4 Effects of variable input parameters on cumulative gas production	195
Table 6-5 Rankings for different parameters involved in each design	196

1. Introduction

Gas Hydrates are non stoichiometric combination of gas and water molecules that form under conditions of high pressures and low temperatures. Hydrates are crystalline solids, very similar to ice, in which non-polar molecules are trapped inside the cages of water molecules. Non-polar molecules are typically low molecular weight gases which include natural gases like methane, ethane and propane. Hydrates are formed wherever suitable conditions of temperature and pressure exist. Methane hydrates are generally found in the Arctic and ocean floor at a depths greater than 500m. Naturally-occurring hydrates are mainly methane hydrates due to the availability of low molecular weight natural gas beneath the surface. Methane hydrates receiving increased attention due to increases in gas prices and because of their high energy density. One volume of hydrate on dissociation releases as much of 164 volumes¹ of natural gas.

Methane hydrates represent a vast source of energy. It is estimated that the total amount of natural gas trapped inside the hydrates is approximately two times the total conventional oil-gas reserves in the world². The production of natural gas from hydrates in an economic manner poses a big challenge to today's scientific world. Different numerical reservoir simulators are developed to model the gas hydrate dissociation behavior. Over the years, different approaches have been used to solve the gas hydrate modeling problems but no unanimity reached. Every approach has its pros and cons. The National Energy Technology Laboratory (NETL) and the U.S Geological Survey (USGS) gas hydrate code comparison project² is the first of its kind and it aims at a worldwide understanding of the hypotheses involved in gas hydrate modeling and problem solving.

Different reservoir simulators used in the code comparison study are

- TOUGH+HYDRATE³, developed at the Lawrence Berkeley National Laboratory (LBNL)
- MH-21⁴ Hydrate Reservoir Simulator (MH-21 HYDRES), developed by the National Institute of Advanced Industrial Science and Technology, Japan Oil Engineering Co., Ltd.
- HydrateResSim⁵ developed at the Lawrence Berkeley National Laboratory (LBNL).
- CMG-STARs⁶ developed by COMPUTER MODELLING GROUP LTD.
- STOMP⁷ developed by Pacific Northwest National Laboratory (PNNL).
- Code from University of Houston

This project is a part of the “Code Comparison Study of Different Hydrate Reservoir Simulators”. It is intended to generate results for CMG STARs and to conduct sensitivity analysis for various reservoir parameters.

1.1 Growing Energy demand and importance of Hydrate

Energy is inevitable to human life and energy requirements around the world are ever increasing. Energy supply and demand plays an important role in the economic development of a country. Energy consumption is expected to increase more than 50% when projected to 2030⁸. Energy demand is expected to grow at an annual rate of 3% from 2004 to 2020⁹. Energy demand for developing countries like India and China is projected to grow at a higher rate (3.75% annually) due to rapid economic growth⁹. The majority of the World’s Energy is generated from non-renewable resources like coal, petroleum and natural gas. Figure 1-1 shows energy consumption by fuel of United States starting from 1980 to 2030⁸.

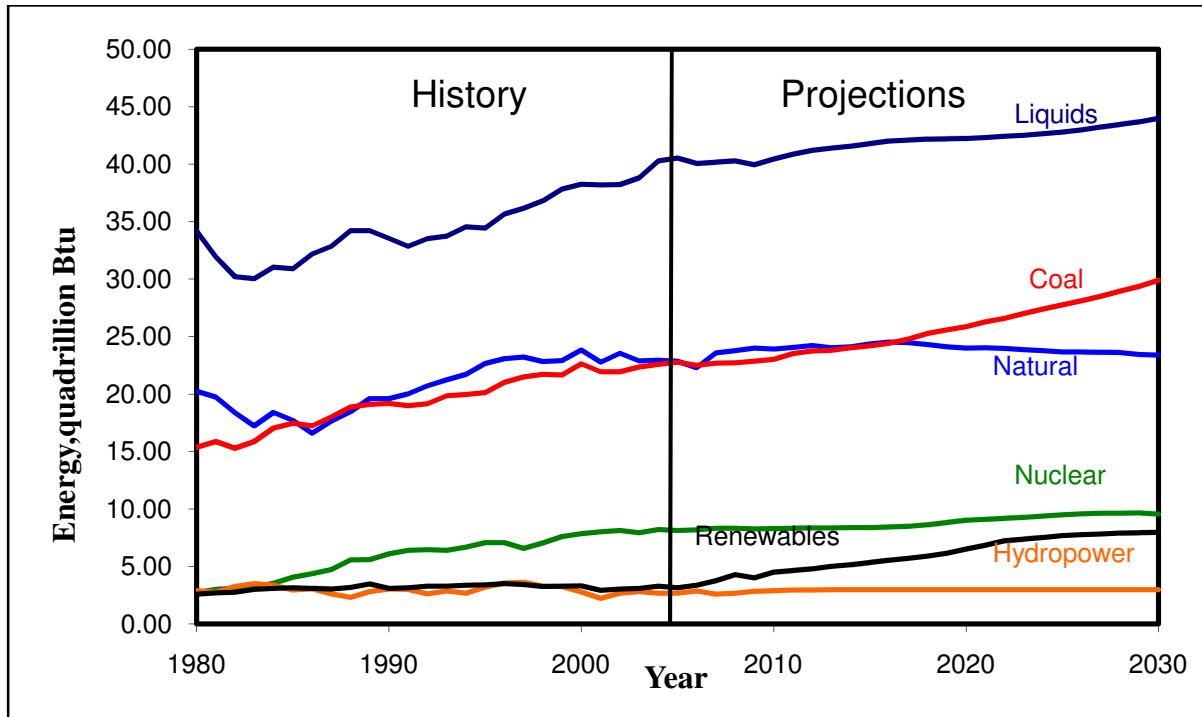


Figure 1-1 U.S Energy Consumption by Fuel, projected up to 2030

There is a significant increase in the projected values for energy consumption. In 2006 renewable energy contributed up to 18% of the total energy consumption, out of which 13% came from biomass, 3% came from hydropower and rest from modern technologies like wind, geothermal and solar⁹. In spite of high gas prices and support from government policies the forecasts do not show much increase in the renewable energy. A small increase of 7.4 to 7.6% for renewable resources is all that is expected by 2030⁹. The three important fossil fuel sources which fuels United States in the future will be crude oil, coal and natural gas. The Energy Information Administration (EIA) reported that, in 2007, the U.S consumed 20 million bbl/day of petroleum products, out of which 12 million bbl/day was imported from other countries¹⁰. As U.S imports 60% of the crude oil, a fluctuation in the crude oil price could have a great impact on U.S economy. Figure 1-2 shows crude oil price

fluctuations in the recent years. In 1994, the U.S imported crude oil at an average price of \$15.54/barrel and now in 2008 the average price is \$116.59/bbl⁸.

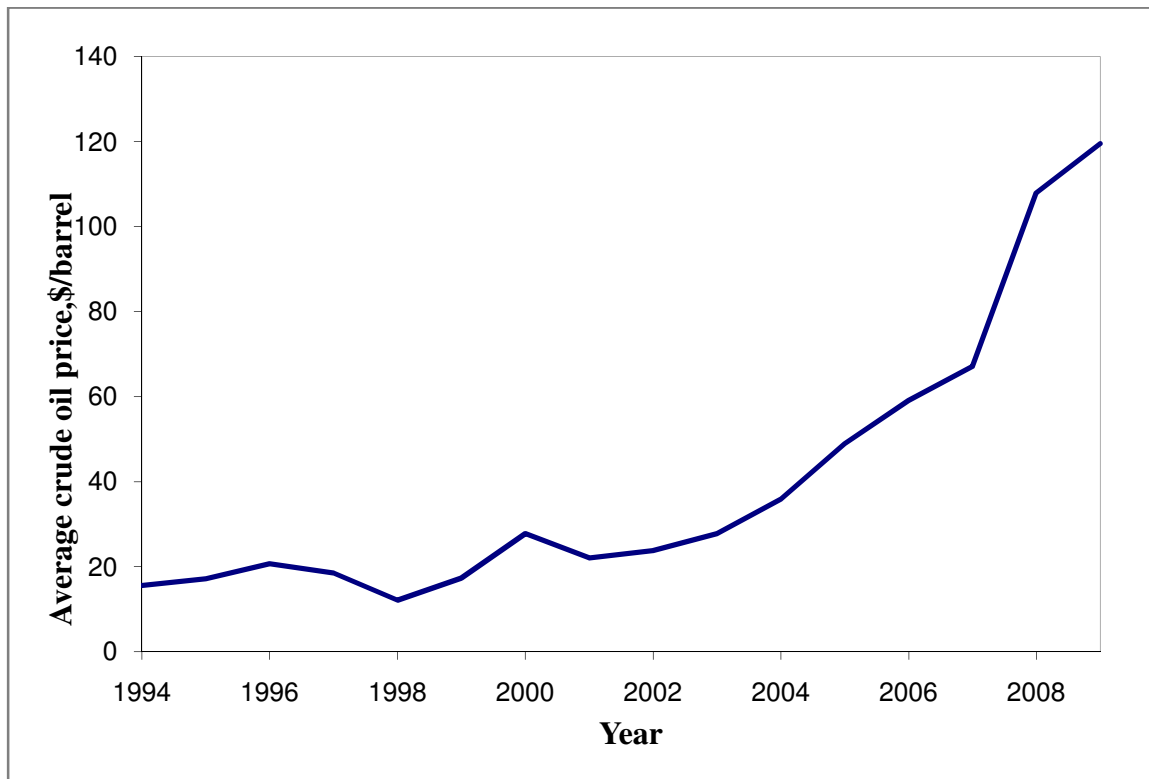


Figure 1-2 Average imported crude oil prices.

Natural gas is an important energy source contributing 23% of the total energy consumption in United States¹¹. Electricity generation from natural gas is expected to increase from 752 billion kilowatt-hours to 930 billion kWh in 2030¹¹. Natural gas is an important fuel for a wide range of industries and natural gas contributes to 19% of the total electricity generation⁸. Compressed natural gas is used as a cleaner alternative to automobile fuels in various countries. U.S and World's natural gas consumption has increased significantly in recent years. The global natural gas consumption in 1990 was 73.4 trillion cubic feet (tcf) and it is projected to be 182 tcf in 2030⁸.

The net imports of natural gas in the U.S. are projected to increase by 21% by the year 2030 and are shown in Figure 1-3⁸. Domestic conventional and unconventional natural gas production does not keep pace with increase in natural gas demand. Development of new alternatives like natural gas from methane hydrate can play major role in ensuring adequate future energy supplies for the U.S.

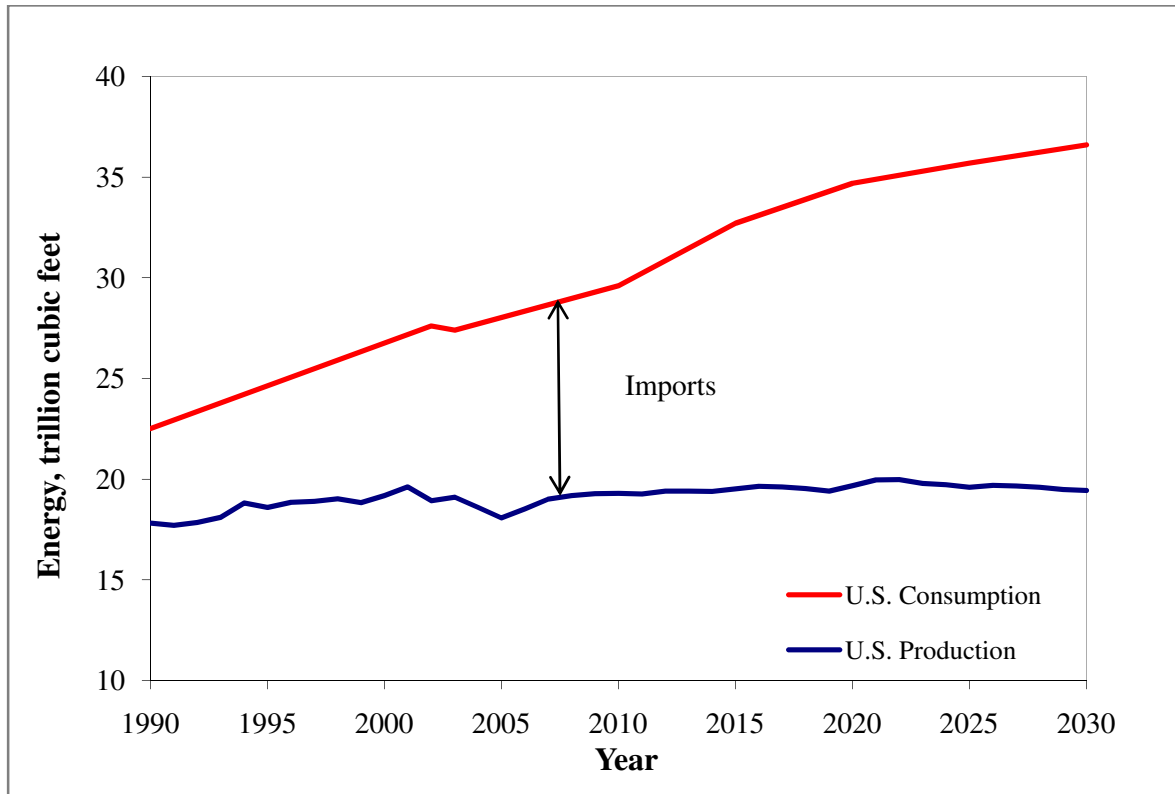


Figure 1-3 U.S Natural gas consumption and Production.

Methane, though it is itself a green house gas produces less carbon dioxide when combusted than other higher hydrocarbons. There is a vast reserve of Hydrate accumulations in the United States itself. A fraction of the methane that is recovered from hydrates can address the energy demand to a great level. The U.S. counts on natural gas a major part of its energy portfolio. Natural gas production by source is shown in Figure 1-4⁸. Onshore and offshore conventional resources show a decline from 1990 to 2030. Production of gas from onshore

unconventional resources like hydrates shows a tremendous increase when projected to 2030. A large portion of the U.S onshore conventional resources have already been used for producing natural gas. The newly discovered reserves such as in Alaska are very remote and costly to exploit.

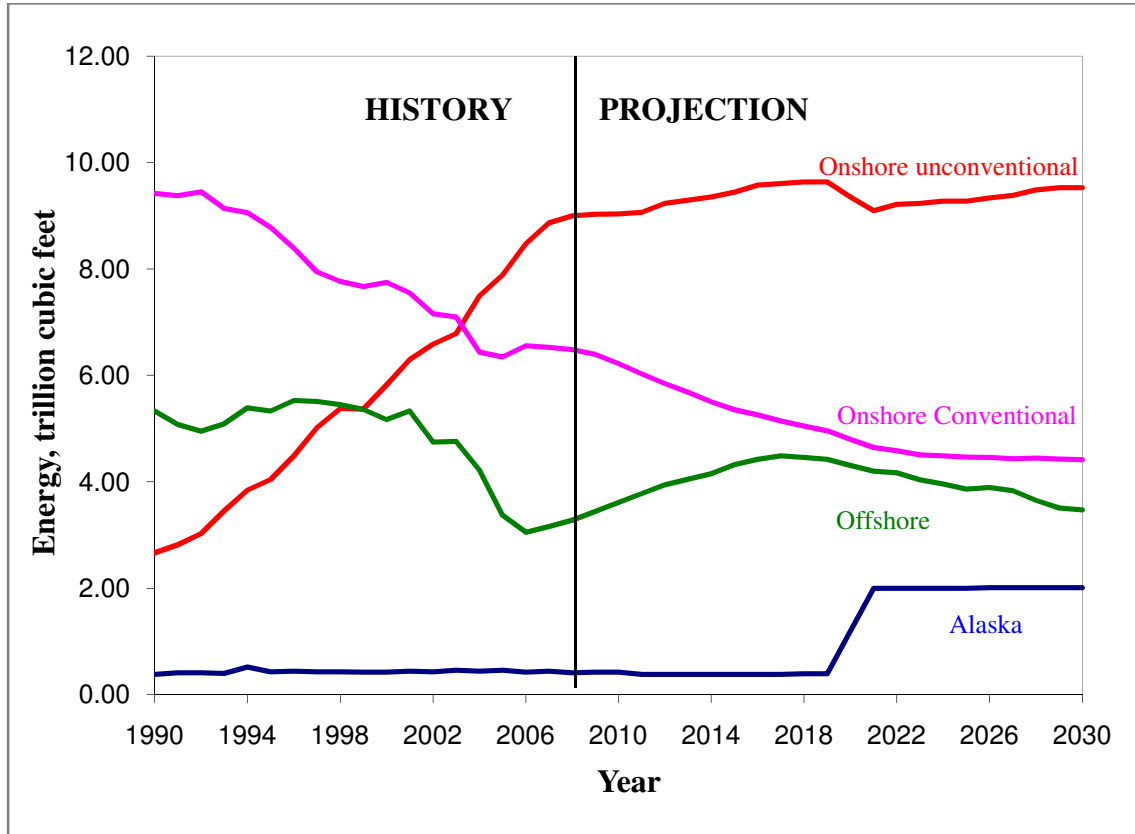


Figure 1-4 U.S Natural gas production by source, projections up to 2030.

1.2 Reservoir simulations of gas hydrate reservoirs

Reservoir simulation is a computational method of modeling the flow of fluid in porous media over time. A reservoir simulator is built on different mathematical models which represent the petrophysical properties of a reservoir. Usually a reservoir simulator is

validated by performing history matching of the data obtained from different production wells. When the reservoir simulator is validated it is used as a tool to predict future production rates which are very important in making investment decisions. Gas Hydrates are a novel field that could potentially produce large amounts of fuel for the mankind but in reality, field scale experiments are prohibitively high. Also, the equipment required for gas production from a hydrate well costs millions of dollars. In this kind of scenario, the best thing that could be done is to get assurance from different reservoir simulators providing motivation for simulating gas hydrates. The crucial decisions about production potentials of hydrate wells have been taken based on reservoir simulations so far.

Gas Hydrate reservoirs require special production techniques due to the low temperature of the reservoir. Secondary hydrate formation and ice formation could make the dissociated gas difficult to produce due to the decreasing permeability of the reservoir due to solid formation. Hence, there are a number of problems like highly coupled heat flow, mass flow, phase transitions, physical and chemical properties that need to be addressed for a successful reservoir model. Based on reservoir simulations, hydrate reservoirs that contain free gas are easier to produce than those with no free gas because free gas can be easily removed from the reservoir. This causes depressurization of the reservoir and promotes hydrate dissociation. Reservoir simulators are an effective tool to decide what technique is best suited to a particular reservoir setting.

1.3 Recent developments in the production of natural gas from gas hydrates

The first hydrate test was carried out at the Mallik field in Canada in 1972¹². Minor methane recovery was observed. A collaborative drilling program was carried out at Mallik field in 1998¹² and hydrate bearing core samples were collected for research and laboratory purposes. A high concentration of hydrate was observed as a result of this drilling program. Later, in 2002¹², at the same field a test well was drilled and 6 days of petro-physical data was collected. That test flared gas over a short period indicating that it was actually possible to recover energy through hydrate dissociation.

In 2004, hydrate bearing sediments were recovered by drilling shallow wells at the Nankai Trough in Japan¹². Before this, in 1999-2000, a deep well was drilled for gas hydrates and conventional oil & gas exploration as well.

In 2006, in India, coring, drilling and down hole logging of gas hydrates was performed and samples were recovered at ten different sites in order to study the distribution, the nature of gas hydrates, the flow processes and the geological factors that control hydrate formation in marine segments¹³.

In 2007, two days of experimental-scale tests were performed at the Mt. Elbert site on the North Slope¹⁴. Modular Dynamics Testing was performed and the flow and pressure build-up data collected indicated that gas was produced. The pressure build up data was used to calculate the permeability of the reservoir. At the Mallik site, a collaboration of Japan and Canada conducted a 60 hour flow test which reinforced the notion that production of gas

from hydrate wells was feasible. In 2008, sustained gas flow was first reported from a hydrate well at the Mallik field and it was concluded that methane gas equivalent to that of coal bed methane well was produced¹⁵.

The economic viability of gas production from hydrates is not yet established but the tests are conducted to get an insight into technical feasibility of gas hydrates.

1.4 International effort for the code comparison project

In order to gain confidence in the predicted productivity of gas hydrate deposits, it is important to have a reliable model that can reliably forecast potential production scenario. To gain such confidence, it is essential that various models be studied and compared paving the way for a code comparison project on the international scale. The initiative of an international comparison of different reservoir simulators to model hydrates has been led by the National Energy Technology Laboratory (NETL) and the U.S. Geological Survey (USGS). The outcome of the project was expected to be the sharing of knowledge, cross validation of results of various simulators, and the acquired self-reliance for future production prediction techniques using those simulators.

The objective set for the participants of the project was to estimate the performance of different model reservoirs of varying properties subject to same reservoir parameters using different reservoir modeling programs.

1.6 Objectives of this study

The international code comparison project is an effort to harmonize various reservoir programs and the study started with formulation of different problems of different complexity levels. The objective of this part of the study is to generate and validate results for the hydrate problems set by the code comparison project using CMG STARS.

Various cases studied include homogenous and heterogeneous reservoirs. The sensitivity analysis of production rates as affected by different parameters is discussed.

1.7 General project description

A detailed literature review about various techniques of hydrate dissociation indicated that depressurization is the best method for production of gas from gas hydrates. This project explores different methods that are feasible to be used in production from gas hydrates using reservoir simulation techniques using CMG STARS.

The problems addressed in the project are called Problems 1-5 and Problem 7(a, b & c). Problem 7 is based on the Mt. Elbert site and data from the Prudhoe Bay L-Pad unit and they are all solved using CMG STARS. Problem 1 is a simple one dimensional problem with no hydrate. It is designed to validate the changes of thermodynamic properties in a reservoir. Problem 2 & 3 have hydrate phase but different geometries of the 1-D grid. Problem 4 contains a cylindrical grid and both thermal and depressurization methods are modeled in this problem. Problem 5 is about a class II hydrate deposit in which hydrate is bound by two shale zones saturated with water.

Data from the Mt. Elbert Stratigraphic Test Well inspired the Problem 7 formulation. Three cases of this problem, a, b & c are studied assuming uniformity of certain parameters such as hydrate saturation, permeability etc. in the reservoir. Later, the effect of homogeneous and heterogeneous reservoirs on production rates is studied. The heterogeneity of the reservoir is recorded from the NMR well log data obtained from Mt. Elbert site. The heterogeneity of porosity, permeability and hydrate saturation is considered in the study.

Gas hydrates reservoir performance is controlled by a complex set of geologic and reservoir parameters. In order to utilize gas hydrate resources it is very important to understand the effect of each reservoir parameter on production rates. For this reason, a parametric study is conducted for seven most important of the several reservoir parameters using design of experiments. Out of the different techniques studied, the Plackett-Burman design is most suitable to the situation. A Plackett-Burman design of size 8 is implemented since the number of factors is 7. The seven parameters studied are permeability, porosity, hydrate saturation, bottom-hole pressure, free water saturation, temperature and pressure.

1.8 Overview of the report

This thesis documents the project findings and CMG STARS' solutions to problems set by the code comparison project team. A brief overview of the report is given below.

Chapter 1 describes the growing energy demand and importance of hydrates. It outlines the objectives and description of the project and introduces modeling of gas hydrate reservoirs and the importance of the study.

Chapter 2 deals with literature review done for the project. It tells briefly about basic properties of gas hydrates, the structure of gas hydrates and the conventional methods of production of gas from gas hydrates.

Chapter 3 details the Problem descriptions for 1-D Cartesian systems which were called Problems 1–3 of the code comparison project and discusses their solutions obtained through CMG STARS.

Chapter 4 contains problem descriptions for 1-D and 2-D radial systems (Problem 4&5) and their results using CMG STARS.

Chapter 5 explains problem descriptions for problem 7(a, b & c) which were defined based on Mt. Elbert and Prudhoe Bay L-Pad deposits and the results for the same solved by using CMG STARS.

Chapter 6 presents a sensitivity analysis of different reservoir parameters using a Plackett-Burman design.

Chapter 7 describes the importance of introducing heterogeneity to the reservoir.

Chapter 8 summarizes the study, includes conclusions and shows recommendations for future work.

2. Literature Review

2.1 History

Gas Hydrates are non stoichiometric combination of Gas and Water molecules that form under conditions of high pressures and low temperatures¹⁶. The water molecules act as the host and the gas molecules are guest molecules embedded in the cages of ice due to Hydrogen bonding and van der Waal's forces. Specialists believe that in 1810, Sir Humphrey Davy first obtained hydrates by cooling a saturated solution of chlorine in water well below 9°C. Also, there is evidence that hydrates were retrieved more than 30 years before Davy. Joseph Priestly in 1778¹⁷ had obtained SO₂ hydrate by cooling an aqueous solution and by combining the gaseous SO₂ in ice as well. Priestly also mentioned the effect of hydrate inhibition¹⁷.

2.2 Hydrates in Natural gas Industry

Natural Gas Hydrates are ice like solids that do not flow but rapidly grow and agglomerate to sizes that can block pipelines¹⁸. Gas Hydrates are a known menace in gas and oil pipelines since many decades. Hydrates are known to plug the pipelines that could cause unexpected fountains because of pipeline rupture. The formation of gas hydrates in natural gas pipe lines mainly depends on the pressure, temperature, and gas-water composition mixture. Hydrates can form in the pipelines whenever the pertinent temperature and pressure conditions are met. Hydrates can form in valves, lines, elbows etc. Hydrate plugs are formed at the hydrocarbon/water interface which eventually hinders flow and cause shutdown of the pipelines. A shut down cold well is very prone to hydrate formation. Gas Hydrates were known to clog cold area pipelines since 1900.

2.3 Occurrences

Knowledge of occurrence of hydrates is incomplete. Majority of the gas hydrates are marine hydrates. Hydrate estimates in the world are based upon the assumptions made by each estimator. Different gas hydrate estimates by different people are shown in Table 2.1. The first estimate was made by Trofimuk¹⁹ in 1973 who assumed that hydrates occurred wherever suitable conditions of temperature and pressure exist. The most recent model was developed by Klaua and Sandler²⁰ in 2005 which estimates $120 \times 10^{15} \text{m}^3$ of methane at standard conditions of temperature and pressure. This is considered as a huge amount as it equals to the energy consumption of United States for 1000 years. This recent estimate includes 68 of 71 occurrences of hydrate. Widespread distribution of worldwide gas hydrate deposits are shown in Figure 2-1.

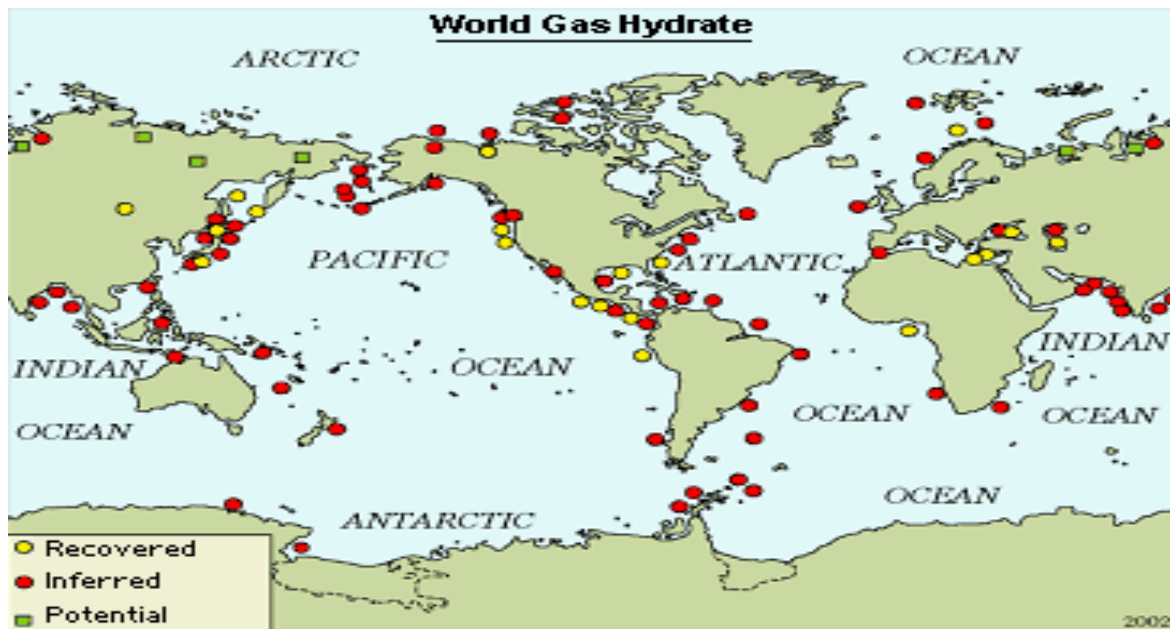


Figure 2-1 Locations of known and inferred gas hydrate occurrences²¹.

Table 2-1 Different estimates of Methane Hydrates from 1973 to 2005²²

Estimates of <i>In Situ</i> Methane Hydrates		
Year	CH ₄ amount 10 ¹⁵ m ³ STP	citations
1973	3053	Trofimuk et al.
1977	1135	Trofimuk et al.
1982	1573	Cheriskiy et al.
1981	120	Trofimuk et al.
1981	301	McIver
1974/1981	15	Makogon
1982	15	Trofimuk et al.
1988	40	Kvenvolden and Claypool
1988	20	Kvenvolden
1990	20	MacDonald
1994	26.4	Gornitz and Fung
1995	45.4	Harvey and Huang
1995	1	Ginsburg and Soloviev
1996	6.8	Holbrook et al.
1997	15	Makogon
2002	0.2	Soloviev
2004	2.5	Milkov
2005	120	Klauda and Sandler

Hydrate potential in the world exceeds conventional gas resources and their values are given in Table 2-2. Estimating techniques are far more conservative today than yesterday. More accurate and precise ways of estimating the amount of hydrates present have come up since 1973, and the amount of gas hydrates estimated has been dropping ever since.

Table 2-2 Worldwide Estimates of Gas Hydrates²³

Hydrate Potential	Value, Tcf
World-Oceanic hydrate potential	30,000 to 49,100,000 x 10 ¹²
World-continental hydrate potential	5,000 to 12,000,000 x 10 ¹²
United States Hydrate potential	1,331 x 10 ¹²
Alaska Hydrate potential	590 x 10 ¹²
India Hydrate Potential	4,307 x 10 ¹²
Japan Hydrate Potential	1,765 x 10 ¹²
World's conventional gas resources	13,000 x 10 ¹²

2.4 Hydrate structures

Hydrates are formed due to the unusual behavior of water molecule and its orientation. Water molecule consists of one oxygen atom covalently bonded to two hydrogen atoms. The angle between the atoms is 104.5°. There are two unbonded electrons which induces partially negative charge on oxygen atom due to its high electro negativity relative to hydrogen atom. The partially induced charges result in one molecule link up with other water molecule in the form of bond which is called hydrogen bond. When the water molecules line up they arrange themselves in different patterns. Hydrates are formed due to this ability of water to form hydrogen bonds. When hydrates are formed the guest molecules and the host molecules are held together by van der Waals force. There is no bonding between the guest and the host molecules.

In ice water molecules are arranged in a hexagonal pattern. When hydrocarbon and water freezes at low temperatures it forms three different crystal structures (Structure I, II, H)

depending upon the size of the hydrocarbon. These three different crystal structures are formed by the combination of different basic cavities. The basic cavities of hydrate structures are labeled as n^m where n is the number of edges and m is the no of faces.

Pentagonal dodecahedron (5^{12}) has 12 pentagonal faces with equal edge lengths and angles. Tetrakaidecahedron ($5^{12}6^2$) has 12 pentagonal faces and two hexagonal faces. Different other cavities like the irregular dodecahedron ($4^35^66^3$) are given in Table 2-3.

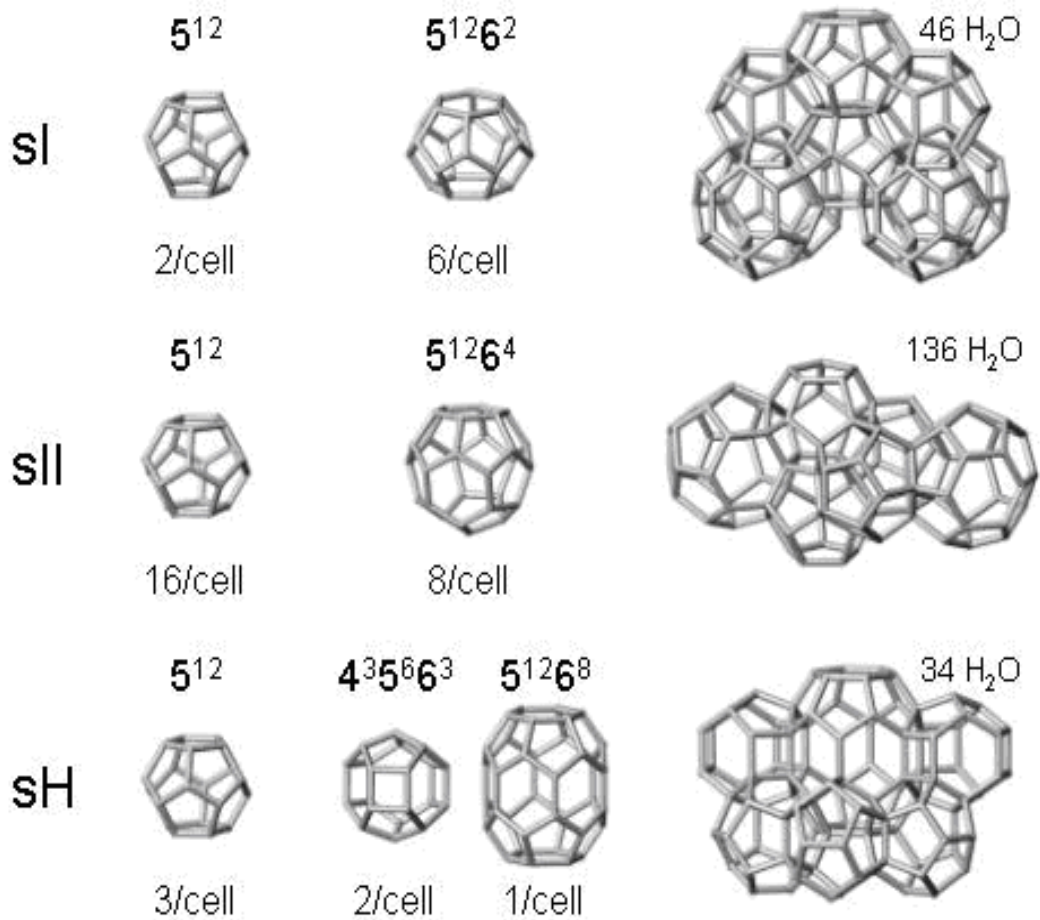


Figure 2-2 Different structures of gas hydrates.

Structure I

This structure was first observed for Ethylene oxide hydrate in 1965 by MC Mullam and Jeffrey²⁴. It is a Base centered cubic structure with a lattice constant of 12 Å, formed by smaller guest molecules like CH₄, C₂H₆, CO₂ and H₂S. There are 46 water molecules arranged to accommodate 8 guest molecules of size 4-6 Å in diameter. There are two small cages of pentagonal dodecahedron and six tetrakaidecahedron. Structural composition is 8G.46H₂O where G is the guest molecule.

Structure II

This Structure was observed by Mc Mullan and Jeffrey for a H₂S hydrate in 1965. It is a face centered cubic structure which can accommodate 24 guest molecules. It has 16 small and 8 large cages with 136 water molecules per unit cell. Hydrate with guest molecules like propane, Iso-butane usually form this structure. Lattice constant is 17.3 Å. Structural composition is 24G. 136 H₂O.

Table 2-3 Geometry of Cages

Structure	I		II		H		
	Small	Large	Small	Large	Small	Medium	Large
Cavity Description	5 ¹²	5 ¹² 6 ²	5 ¹²	5 ¹² 6 ⁴	5 ¹²	4 ³ 5 ⁶ 6 ³	5 ¹² 6 ⁸
Number of cavities/unit cell	2	6	16	8	3	2	1
Average cavity radius(Å)	3.95	4.33	3.91	4.73	3.94	4.04	5.79
Variation in radius(%)	3.4	14.4	5.5	1.73	4.0	8.5	15.1
No. of water molecules/cavity	20	24	20	28	20	20	36

Structure H

It was first identified by Ripmester²⁵ in 1987. These crystals have large volume capacity and can accommodate big molecules like n-butane which has a diameter of 7.1 Å. Structure H is composed of three different types of cavities. It contains 34 water molecules associated with three 5^{12} cavity guest molecules, two $4^35^66^3$ cavity guest molecules and one $5^{12}6^2$ cavity guest molecules. Smaller guest molecules, such as CH₄, N₂ and CO₂ occupy 5^{12} cavities, and large guest molecules such as 2-methylbutane, methylcyclopentane, methylcyclohexane, ethylcyclohexane and cyclooctane occupy $4^35^66^3$ cavities. It bears repeating, Type H hydrates only form if another, small molecule is present.

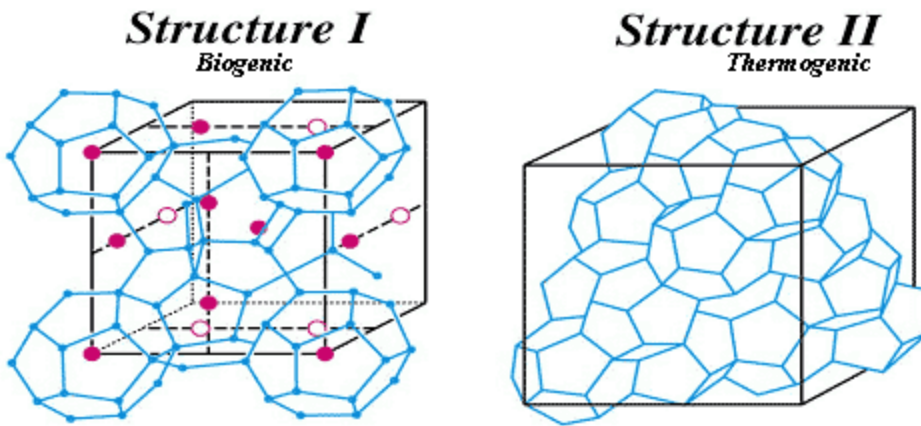


Figure 2-3 Structure I and II type hydrate.

At high pressure it is observed that there is a transition from one structure to the other²⁶. For example argon hydrate forms structure II and is stable at normal pressure (<30MPa). When the pressure is increased to 0.5GPa it forms structure H. Lot of concern in the literature is expressed about the lattice distortions due to change in pressure.

2.5 Stability

Hydrates are formed at conditions of low temperature and high pressure. The required conditions for the hydrate to be stable are

- Low temperature
- High pressure
- Availability of water molecules
- Availability of gas molecules

Gas hydrates are stable in ocean floor sediments at a water depth of 600m and in permafrost regions of depth 150m²⁷.

The figure shows the hydrate stability zone both in permafrost and in oceanic sediments. The dashed line represents geo-thermal gradient. The slopes of the dashed lines are different due to different thermal conductivity which effect thermal gradient. The phase-boundary line is obtained from pressure-temperature Equilibrium curve. The region between the phase-boundary line and the dashed line represents hydrate stability zone. These figures are based upon hydrates which are formed by methane. If we consider other heavy natural gases like propane butane we can observe an increase in the depth of the hydrate stability zone due to the shift of the phase-boundary line. The hydrates which are closer to the phase boundary line dissociates easily.

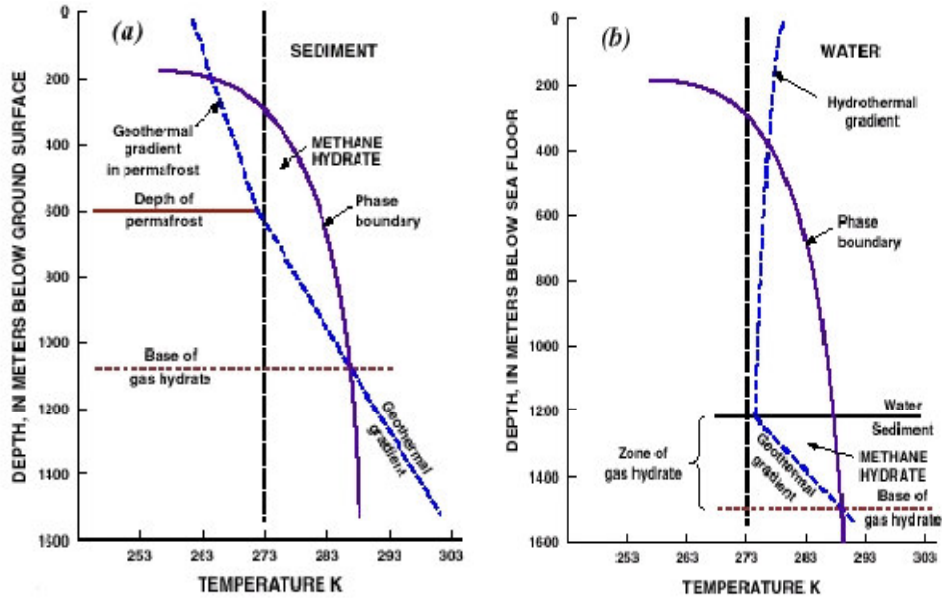


Figure 2-4 Methane Hydrate Stability Zones²⁸ (a) Permafrost Regions (b) Oceanic Regions.

2.6 Hydrate Properties

Methane molecules are tightly packed in a lattice of water molecules due to crystallization forces. Methane hydrates has the highest energy density of any naturally occurring form of methane. Density of methane hydrate is a function of methane saturation and is approximately 0.9 g/cm^3 . Heat of hydrate formation and dissociation are equal in magnitude but of opposite sign. Methane hydrate formation enthalpy at $273 \text{ }^\circ\text{K}$ is 54 kJ/mol ²⁹. Hydrates have a heat capacity of 257 kJ/mol at constant pressure. Hydrate properties are similar to ice; Table 2-3 shows physical properties of ice and hydrate. Pressure-Temperature Equilibrium curve is given in Figure 2-5.

Table 2-4 Physical Properties of Methane Hydrates²⁹

Property	Ice	Hydrate
Dielectric constant at 273°K	94	58
Water molecule reorientation time at 273°K (μsec)	21	10
Isothermal Young's modulus at 268°K (109Pa)	9.5	8.4
Poisson' ratio	0.33	0.33
Bulk modulus (272°K)	8.8	5.6
Shear modulus (272°K)	3.9	2.4
Bulk density (gm/cm ³)	0.916	0.912
Adiabatic bulk compressibility at 273°K 10 ⁻¹¹ Pa	12	14
Thermal Conductivity at 263°K (W/m-K)	2.25	0.49±0.02
Heat of Fusion (KJ/mol)	6	54(measured), 57(calculated)

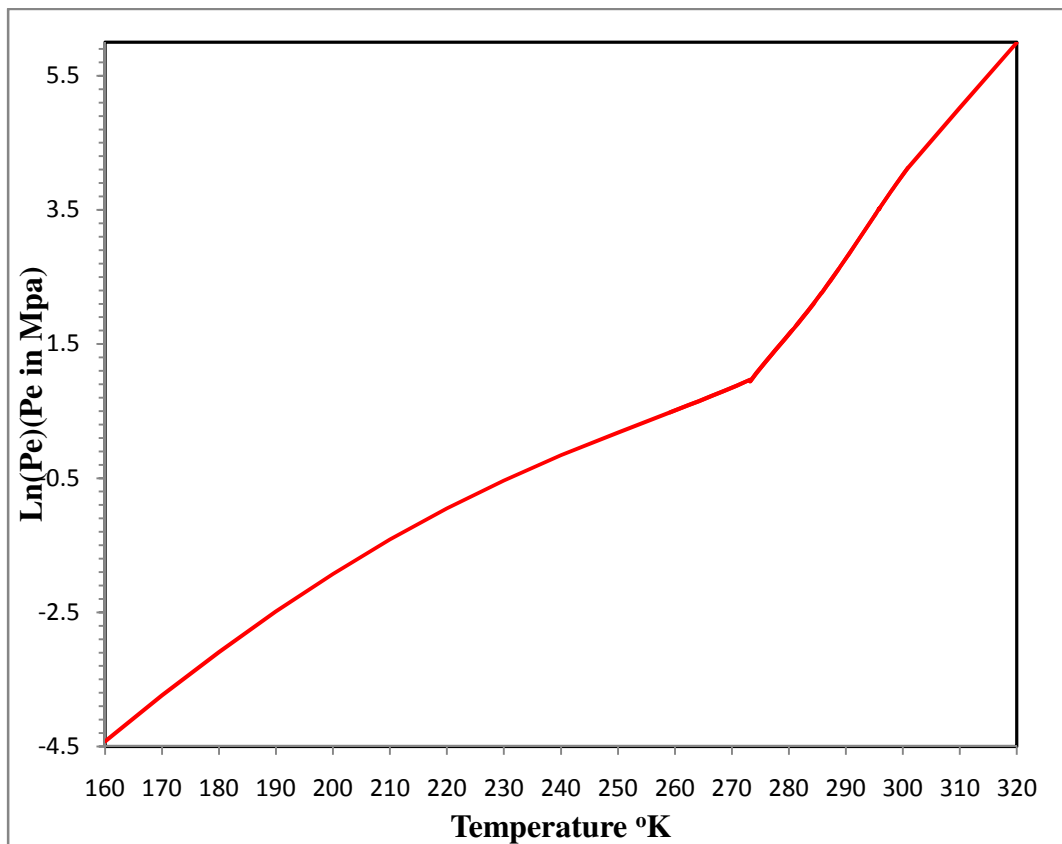


Figure 2-5 Equilibrium Pressure-Temperature relationship of methane hydrates³.

2.7 Introduction to CMG STARS

STARS (Steam Thermal and Advanced Processes Reservoir simulator) ⁶ are a new generation reservoir simulator developed by Computer Modeling group Ltd for modeling the flow of three phases, multi-component fluids.

STARS can be used to model compositional, steam, geo mechanical, dispersed component (polymers, gels, fines, emulsions, and foams) and in-situ combustion process. STARS uses a discretized wellbore model which improves modeling by discretizing the well bore and solving the resulting coupled well bore and reservoir flow problem simultaneously

The adaptive implicit mode in STARS decides from time-step to time-step which blocks must be solved in implicit or explicit modes. Local Grid Refinement can be applied to Cartesian, cylindrical and mixed coordinates to match as closely as possible to the geological model. Chemical reactions between components can also be specified with fixed rate dependence.

2.8 Role of hydrates in climatic change

Gas hydrates are formed at conditions of high pressure and low temperature. They are not stable at room temperatures. Today, gas hydrates are considered as a future energy source because lot of gas is trapped inside the hydrates. The hydrate reservoir is so large that a small fraction of methane release can have a good impact on Earth's climate. Hydrates dissociate to give gas and water when they are out of the stability zone. Rise in sea temperature can trigger hydrate dissociation releasing methane into the atmosphere. Methane is a powerful greenhouse gas, about 20 times stronger than CO₂³⁰. Global concentrations have been

increasing during the past due to various reasons. The figure shows methane concentration in the atmosphere from 1980 to 2004³¹.

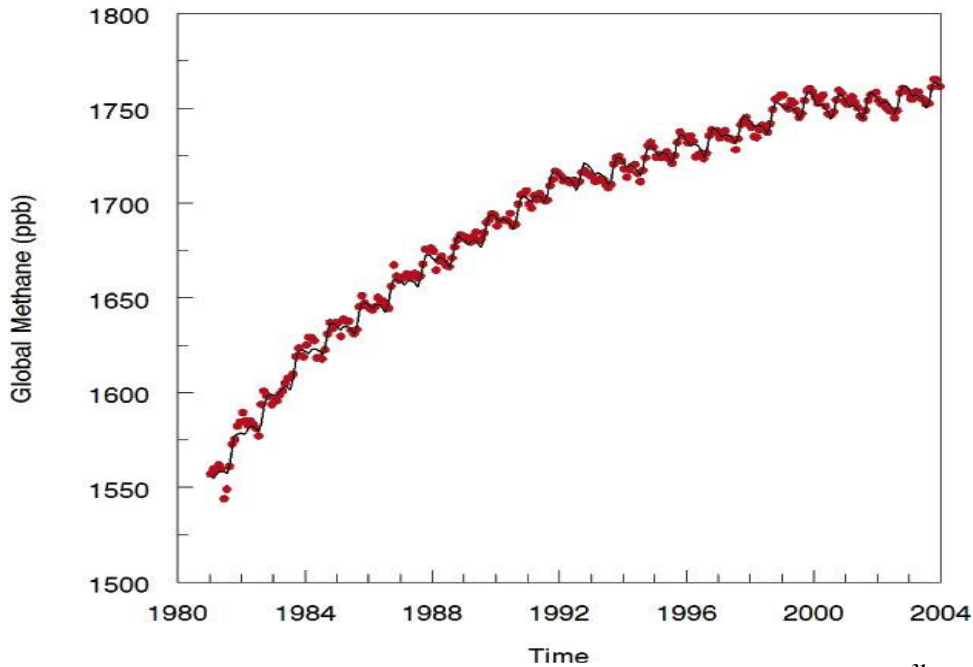
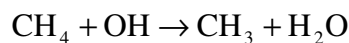


Figure 2-6 Global methane concentration Vs. Time in the atmosphere from 1980 to 2004³¹.

CO₂ and CH₄ are the dominant greenhouse gases in the atmosphere. Methane once released into the atmosphere oxidizes to CO₂. The necessary intermediate 'OH' for this oxidation process is provided by the sunlight. CH₃ is a reactive radical compound which immediately reacts with water vapor and gases to form CO₂³².



Sea Pockmarks are formed when methane gas is explosively vented into the atmosphere by decomposition of hydrates. Warming or sea level fall may trigger hydrate dissociation provoking Landslides, causing tsunamis which have an effect on an entire ocean basin. Some

calculation also shows that landslides can release up to 5 G tons of methane into the atmosphere³³.

Deep ocean temperature change has been detected at intermediate depths due to anthropogenic greenhouse gas warming³³. It is important to take this gas out of the gas hydrates and use it as a fossil fuel before it causes an impact on earth's climate.

2.9 Conventional methods for producing gas from hydrates

Methods of dissociation of hydrates are based on shifting the thermodynamic equilibrium of the three phase system (water-hydrate-gas). Gas can be produced from hydrates either by changing the pressure and temperature of the hydrate bearing media or by injection of inhibitors. Three main methods for producing gas from hydrates are Depressurization – Pressure is reduced below the equilibrium value at a fixed temperature, Thermal stimulation – Temperature is increased to trigger hydrate dissociation and adding inhibitors which shifts the pressure temperature equilibrium.

Depressurization

Depressurization is often considered the best method for commercial production of hydrates. In this case a production well is drilled into the hydrate reservoir and a pressure difference is created between the wellbore and adjacent blocks. Pressure reduction frees the methane molecules from hydrate. A reduction in the reservoir pressure is obtained by removing the associated free gas or formation water. Hydrate dissociates giving gas and water molecules, which migrate towards the wellbore. Different models were developed to describe the

process of hydrate decomposition in the porous media. This method is economically feasible as there is no extra heat to be introduced into the system.

Thermal Injection

In this method heat is introduced into the hydrate bearing layer through an injector well. Injection wells require high pressure pumps to inject water or steam into the reservoir. The fluids injected are generally hot fluids which rises the temperature of the hydrate layer causing hydrate dissociation. Methane gases mix with hot water and return to the surface. Hydrate bearing layers are generally found in permafrost and in ocean's at a depth of 150m and 600m respectively. Considering heat loses, lot of energy is being wasted to provide heat to the hydrate layer. It is not economically feasible to produce gas from this method.

Adding Chemical Inhibitors

Commonly used inhibitors are salts, alcohols and glycols. Injection of inhibitors shifts the pressure-temperature equilibrium leading to rapid dissociation of gas hydrates. In this method of production of gas from gas hydrates inhibitors are injected from the surface to the hydrate bearing sediment. When the inhibitor is added through a well, it does not necessarily come into contact with the entire hydrate bearing sediment but this process of dissociation is well accepted for an initial hydrate dissociation which is later followed by depressurization.

3: 1-D Cartesian systems: Problems and Solutions

The problems that will be discussed in this chapter are the result of an effort by the U.S. D.O.E. and U.S.G.S. to reach a consensus between various gas hydrate reservoir simulation codes. They have been collectively formulated by a team of researchers working on gas hydrate reservoir modeling. Certain parameters are fixed in this Code Comparison Project for each problem and these parameters are constant among every reservoir simulator so that all the simulators captured the basic properties of the hydrate model in the same way. The problems start with simple cases and become more advanced and complex as the project proceeds.

The project starts with a relatively simple case and it is named Problem 1, in which there is only one dimension and there is no hydrate phase. The objective of the problem is to study the mass and heat flow in a porous media in the defined one dimensional domain.

The next case, called Problem 2, is a similar grid to that of problem 1; the only difference is the presence of gas hydrate in one half of the domain. There will be a hydrate phase in all the problems of this study hence forth. High temperature in the other half of the domain leads to dissociation of the hydrate and hence the gas-flow in the entire domain. The simulation is continued until equilibrium is attained in the domain.

Problem 3 has three different cases. It is a one dimensional problem with different grid dimensions than Problems 1 & 2. The three different cases modeled in this problem are adapted basically from the different techniques proposed to produce gas from hydrate wells. In the third case of Problem 3, the possibility of ice formation is included to make it a more complex situation in the reservoir.

3.1 Problem 1

A closed horizontal, one-dimensional domain, 20 m in length is considered as the base case for the NETL USGS gas hydrate code comparison project. This simplified horizontal domain is used to remove gravitational body forces from the problem. The gas hydrate phase is not considered in this case to avoid complexities, the only water-CH₄ system is selected in the entire domain. The whole 20 m horizontal domain is discretized uniformly into 20 grid cells each of length 1 m. The grid is defined in such a way that there is no mass and heat flow outside the blocks, like a closed, isolated system. High pressure, temperature gradients and complete aqueous saturation conditions are specified in the first 10 grid cells and aqueous unsaturated conditions in the next 10 grid cells. As the simulation proceeded, equilibrium conditions are obtained in the entire domain due to mass and heat flow in the domain. The results of simulations of methane hydrate formations in geological media mainly depend upon how the tool or the simulator calculates the thermodynamic and transport properties. As there is no gas hydrate there is no dissociation or formation of hydrate.

Different processes simulated in the case are

- Heat transfer in the multi-fluid porous media with phase-advection
- Aqueous-gas multi fluid flow with phase transition from aqueous saturated to unsaturated
- Methane solubility changes with pressure and temperature
- Change in the thermodynamic and transport properties with pressure and temperature.

A schematic of the grid is shown in Figure 3-1. Considering x as the horizontal distance, the pressure and temperature at three different locations ($x=0$, 10m, 20m) are specified in the

problem. The same properties for other grid cells are calculated based on their gradients in the horizontal direction.

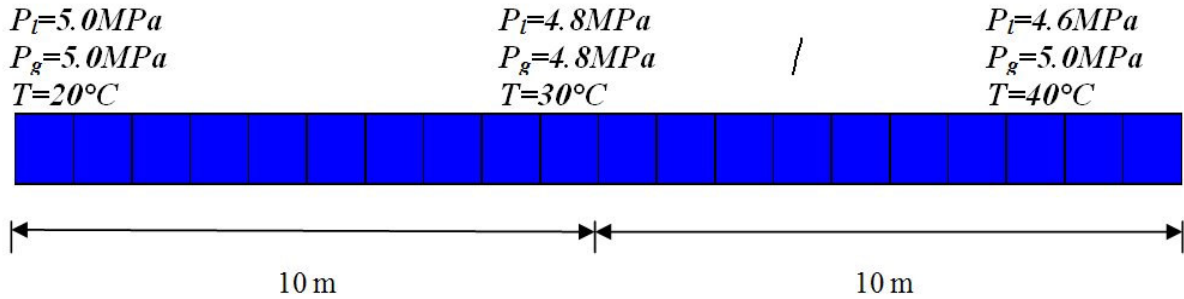


Figure 3-1 Schematic diagram of the grid for problem 1.

The absolute permeability, or the ability to conduct fluids, is set at 100 mD for all the grid cells. The porosity, the ratio of void volume to the bulk volume, Φ is set at 0.3 for the entire grid. Parameters such as porosity, bulk density, grain density, bulk specific heat, grain specific heat, hydraulic conductivity, dry thermal conductivity, water-saturated thermal conductivity and pore compressibility for the entire domain are specified in Table 3.1. The values of different parameters used in the capillary pressure model and the relative permeability model are also given in Table 3-1.

The aqueous saturation in the first ten grid cells is equal to one. The aqueous saturation for the next ten grid cells is calculated using the capillary pressure head specified for the problem. Gas saturation is calculated from the following equations.

$$S_w + S_g + S_H = 1$$

However for problem 1 $S_H = 0$ (No hydrate phase)

Therefore $S_w + S_g = 1$

Table 3-1 Parameters and Specifications for Problem 1

Parameter	Value
Porosity	0.3
Bulk Density	1855 kg/m ³
Grain Density	2650 kg/m ³
Bulk Specific Heat	525 J/kg K
Grain Specific Heat	750 J/kg K
Hydraulic Conductivity	0.1 Darcy
Dry Thermal Conductivity	2.0 W/m K
Water-Saturated Thermal conductivity	2.18 W/m K
pore compressibility	5.0 x 10 ⁻¹⁰ Pa ⁻¹
Capillary Pressure Model	Van Genuchten Equation ³⁴
α parameter	0.132m ⁻¹
n parameter	2.823
β_{gl} parameter	1
s_{lr} parameter	0
Aqueous Relative Permeability Model	Mualem Equations ³⁵
m parameter	0.6458
Gas Relative Permeability Model	Mualem Equations ³⁵
m parameter	0.6458

Capillary Pressure Model

Capillary pressure is the pressure difference existing across the interface of two immiscible fluids in a porous system. The Van Genuchten capillary pressure model³⁴ expresses the relationship between capillary pressure and aqueous saturation. It is expressed as the following:

$$\bar{s}_l = \frac{s_l - s_{lr}}{1 - s_{lr}} = \left[1 + (\alpha \beta_{gl} h_{gl})^n \right]^{-m}$$

where \bar{s}_l is the effective aqueous saturation, s_l is the aqueous saturation, β_{gl} is the interfacial tension scaling factor, and h_{gl} is the gas-aqueous capillary pressure head. Figure 3-2 illustrates the relation between Capillary Pressure and Water Saturation.

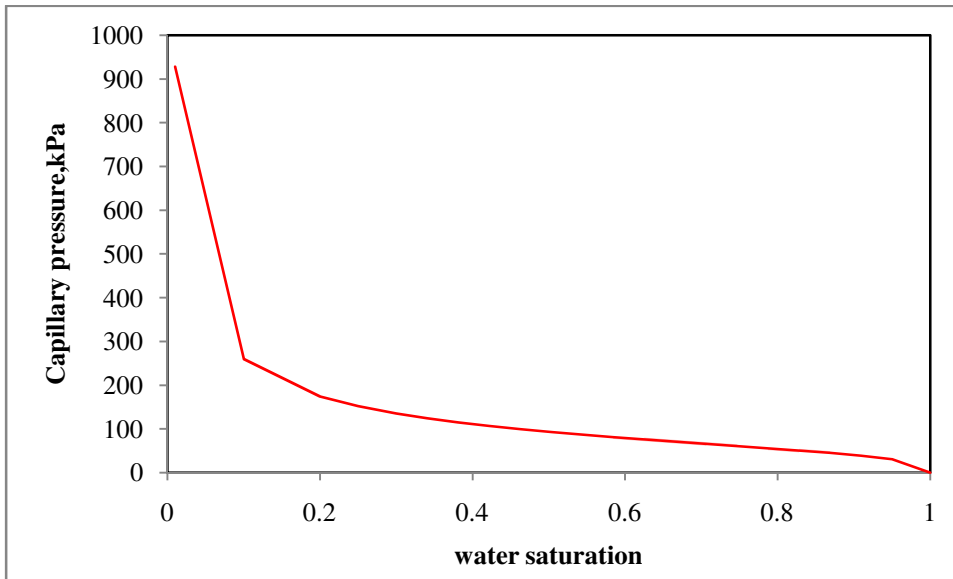


Figure 3-2 Capillary Pressures vs. Water Saturation as calculated using the Van Genuchten equation

Relative Permeability Functions

The relative permeability phenomenon is encountered when more than one fluid phase flows through a porous media. Relative permeability is the ratio of the effective permeability of a fluid at any saturation to the permeability at 100 percent saturation. Effective permeability is the ability of the porous material to allow a fluid at saturation less than 100 percent. Relative permeability functions for both aqueous and gas phases are calculated using a combined

equation of Van Genuchten capillary pressure function and Mualem porosity distribution function³⁵. The combined equation is expressed as the following:

$$K_{rl} = (\bar{s}_l)^{1/2} \left[1 - \{1 - (\bar{s}_l)^{1/m}\}^m \right]^2$$

$$K_{rg} = (1 - \bar{s}_l)^{1/2} \left[1 - \{1 - (\bar{s}_l)^{1/m}\}^m \right]^2$$

Where, \bar{s}_l is the effective aqueous saturation, k_{rl} is the aqueous phase relative permeability and k_{rg} is the gas phase relative permeability. Figure 3-3 shows a plot between relative permeability and water saturation.

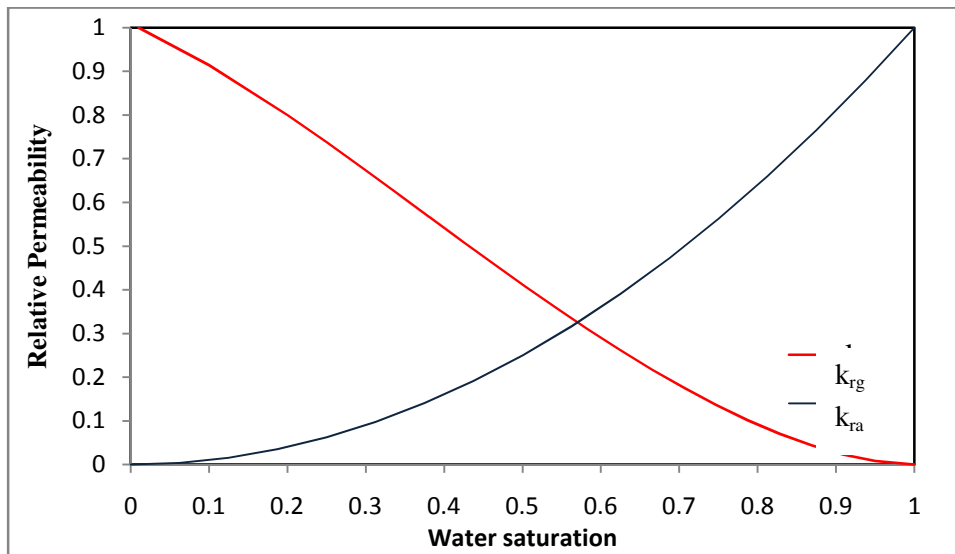


Figure 3-3 Relative permeability of water k_{ra} and gas, k_{rg} phases as a function of water saturation

Data and sampling frequency

Profiles of water saturation, temperature, aqueous relative permeability, and aqueous methane mass fraction and aqueous pressure are obtained for different time steps. Data is recorded for selected times (0, 1 day, 10 days, 100 days, 1000 days, and 10,000 days). Equilibrium is expected in the entire reservoir after 10,000 days.

3.1.1 Solution to problem 1 using CMG STARS

STARS is basically designed for black-oil models and can be used to model the hydrate dissociation behavior by making some adjustments to the input parameters. There is a step by step procedure to simulate problems and to obtain final equilibrium conditions for the entire grid.

- Constructing the grid using CMG BUILDER.
- Assigning medium and rock properties like permeability, porosity, thermal conductivity, pore-compressibility and volumetric heat capacity.
- Defining components, properties and all the reactions and phase transitions between the components.
- Specifying rock fluid properties, capillary pressure model, and initial conditions like temperature, pressure, water saturation and mole fraction of components in all phases.
- Boundary Conditions specified in the problem by defining wells in the reservoir.
- Running the simulation for different time steps specified in the problem.

Problem 1 is a one dimensional horizontal domain of 20m in length and is discretized into 20 cells each of length 1m. In CMG builder, grid is constructed using “GRID VARI I J K” where I J&K represents the dimensions in X Y and Z directions. The further discretization of the grid is done by using keywords DI DJ and DK. The thickness of the grid top is taken as 500m.

```
**$ Definition of fundamental Cartesian grid
GRID VARI 20 1 1
KDIR DOWN
DI IVAR 20*1
DJ JVAR 1
DK ALL 20*1
DTOP
20*500
```

Permeability and porosity for the entire reservoir are constant as specified in the problem description.

```
**$ Property: Porosity Max: 0.3 Min: 0.3
POR CON 0.3
**$ Property: Permeability I (md) Max: 100 Min: 100
PERMI CON 100
```

```

**$ Property: Permeability J (md)   Max: 100   Min: 100
PERMJ CON                           100
**$ Property: Permeability K (md)   Max: 100   Min: 100
PERMK CON                           100

```

Rock Compressibility, thermal Properties like heat capacity, thermal conductivity are specified by defining a rock type. Different rock types can be defined within a reservoir.

```

ROCKTYPE 1
PRPOR 101.3      **Porosity reference pressure
CPOR 5e-7        **Pore compressibility
ROCKCP 1.988e+6 0 **Volumetric heat capacity
THCONR 2.47E+5   **Rock thermal conductivity
THCONS 2.47E+5   **Thermal conductivity of solid
THCONW 5.183E+4 **Thermal conductivity of water
THCONG 2.59e5    **Thermal conductivity of gas
THCONMIX SIMPLE **Thermal conductivity model
PERMCK 4.5       **Variable permeability Model

```

The next step is to specify different components and their properties. In this case only water-CH₄ system is considered, which is a 2-component and 2-phase system. Different components and their physical properties can be directly imported from the builder's inbuilt library. A value of '0' input for any property returns a standard value already set up in the library of the builder. CMM refers to component molecular weight in Kg/gmol. Densities, gas-liquid K values, critical temperature and pressure, aqueous and gas phase viscosities are specified as following

```

**$ Model and number of components
MODEL 2 2 2 2
COMPNAME 'Water' 'CH4'
CMM      ** component molecular weight
0 0.016043
PCRIT    **critical pressure
0 4600
TCRIT    **critical temperature
0 -82.55
KVTABLIM 4000 5000 20 35  ** KVTABLIM plow phigh Tlow Thigh
KVKEYCOMP 'Water' W 0 1
**$ Gas-liquid K Value tables
KVTABLE 'CH4'
**$
          987.6      790  ** K(Tlow,plow) K(Tlow,phigh)
          1175      940  ** K(Thigh,plow) K(Thigh,phigh)
PRSR 101      ** Reference values
TEMR 30
PSURE 101
TSURE 16.85

MOLDEN      ** mole densities in gmol/m3
55509.1 62332.3
CP          ** liquid compressibility at constant temperature
1e-005 1e-005

```

CT1 ** First coefficient of thermal expansion
2.47148e-007 2.47148e-007

Viscosity table for water and methane at different temperatures from 5°C to 540°C

VISCTABLE**\$	temp	Water	CH ₄
	5	1.90124	1.90124
	15	1.42069	1.42069
	25	1.1155	1.1155
	30	1	1
	40	0.817524	0.817524
	65	0.542214	0.542214
	90	0.397513	0.397513
	115	0.306284	0.306284
	140	0.244739	0.244739
	165	0.210104	0.210104
	190	0.183079	0.183079
	215	0.1621	0.1621
	240	0.145113	0.145113
	265	0.131269	0.131269
	290	0.117908	0.117908
	315	0.108632	0.108632
	340	0.09987	0.09987
	365	0.092478	0.092478
	390	0.086039	0.086039
	415	0.08034	0.08034
	440	0.075263	0.075263
	465	0.070712	0.070712
	490	0.06661	0.06661
	515	0.062892	0.062892
	540	0.059507	0.059507

Aqueous and Gas relative permeability values are calculated using the equations mentioned in the problem description. Capillary pressure is calculated from the Van-Genuchten capillary pressure model. These values are entered in the form of tables in the ROCK FLUID section of the data file. Capillary pressure of water-gas is included as PCOG in the gas-oil table. In the absence of hydrate phase or the oil phase there is confusion whether to use capillary pressure as PCOW or PCOG. Using capillary pressure as PCOG gave results which are in agreement with other codes. Vertical Equilibrium calculations are not performed in this problem.

ROCKFLUID

RPT 1

SWT

**\$

SLT

SMOOTHEND CUBIC

**\$

Sw	krw	krow	Pcow	Sl	krq	krog	Pcog
0.00	0.00E+00	0.00000007	0	0.01	1	0	928.16
0.05	8.75E-06	0	0	0.1	0.914	0	259.87
0.10	1.07E-04	0	0	0.2	0.8	0	174.086
0.15	4.62E-04	0	0	0.25	0.738	0	151.975
0.20	1.32E-03	0	0	0.3	0.673	0	135.379
0.25	2.97E-03	0	0	0.341	0.62	0	124.462
0.30	5.82E-03	0	0	0.381	0.566	0	115.139
0.35	1.03E-02	0	0	0.422	0.513	0	106.99
0.40	1.70E-02	0	0	0.463	0.46	0	99.727
0.45	2.65E-02	0	0	0.503	0.408	0	93.143
0.50	3.96E-02	0	0	0.544	0.357	0	87.081
0.55	5.74E-02	0	0	0.584	0.308	0	81.419
0.60	8.08E-02	0	0	0.625	0.261	0	76.056
0.65	1.11E-01	0	0	0.666	0.217	0	70.902
0.70	1.51E-01	0	0	0.706	0.175	0	65.875
0.75	2.02E-01	0	0	0.747	0.136	0	60.889
0.80	2.69E-01	0	0	0.788	0.101	0	55.846
0.85	3.56E-01	0	0	0.828	0.07	0	50.617
0.90	4.72E-01	0	0	0.869	0.044	0	45.007
0.95	6.40E-01	0	0	0.909	0.023	0	38.659
1.00	1.00E+00	0	0	0.95	0.008	0	30.7
						7.00E-	
				1	0	08	0

INITIAL
VERTICAL
OFF

Initial conditions like pressure, temperature, saturations, aqueous and gas mole fractions are initially specified a constant and are then modified by using 'MOD' keyword.

**\$ Property: Pressure (kPa) Max: 4800 Min: 4800

PRES CON 4800

*MOD

1:1	1:1	1:1	= 4990	11:11	1:1	1:1	= 4810
2:2	1:1	1:1	= 4970	12:12	1:1	1:1	= 4830
3:3	1:1	1:1	= 4950	13:13	1:1	1:1	= 4850
4:4	1:1	1:1	= 4930	14:14	1:1	1:1	= 4870
5:5	1:1	1:1	= 4910	15:15	1:1	1:1	= 4890
6:6	1:1	1:1	= 4890	16:16	1:1	1:1	= 4910
7:7	1:1	1:1	= 4870	17:17	1:1	1:1	= 4930
8:8	1:1	1:1	= 4850	18:18	1:1	1:1	= 4950
9:9	1:1	1:1	= 4830	19:19	1:1	1:1	= 4970
10:10	1:1	1:1	= 4810	20:20	1:1	1:1	= 4990

**\$ Property: Temperature (C) Max: 20 Min: 20
TEMP CON 20

*MOD

1:1	1:1	1:1	= 20.5	11:11	1:1	1:1	= 30.5
2:2	1:1	1:1	= 21.5	12:12	1:1	1:1	= 31.5
3:3	1:1	1:1	= 22.5	13:13	1:1	1:1	= 32.5
4:4	1:1	1:1	= 23.5	14:14	1:1	1:1	= 33.5
5:5	1:1	1:1	= 24.5	15:15	1:1	1:1	= 34.5
6:6	1:1	1:1	= 25.5	16:16	1:1	1:1	= 35.5
7:7	1:1	1:1	= 26.5	17:17	1:1	1:1	= 36.5
8:8	1:1	1:1	= 27.5	18:18	1:1	1:1	= 37.5
9:9	1:1	1:1	= 28.5	19:19	1:1	1:1	= 38.5
10:10	1:1	1:1	= 29.5	20:20	1:1	1:1	= 39.5

**\$ Property: Water Saturation Max: 0.8 Min: 0.8
SW CON 0.8

*MOD

1:10	1:1	1:1	= 1				
11:11	1:1	1:1	= 0.984	16:16	1:1	1:1	= 0.134
12:12	1:1	1:1	= 0.754	17:17	1:1	1:1	= 0.1
13:13	1:1	1:1	= 0.461	18:18	1:1	1:1	= 0.077
14:14	1:1	1:1	= 0.285	19:19	1:1	1:1	= 0.062
15:15	1:1	1:1	= 0.189	20:20	1:1	1:1	= 0.051

**\$ Property: Gas Saturation Max: 0.05 Min: 0.05
SG CON 0.05

*MOD

1:10	1:1	1:1	= 0	16:16	1:1	1:1	= 0.866
11:11	1:1	1:1	= 0.016	17:17	1:1	1:1	= 0.9
12:12	1:1	1:1	= 0.246	18:18	1:1	1:1	= 0.923
13:13	1:1	1:1	= 0.539	19:19	1:1	1:1	= 0.938
14:14	1:1	1:1	= 0.715	20:20	1:1	1:1	= 0.949
15:15	1:1	1:1	= 0.811				

Aqueous and gas mole fraction are calculated based on the pressure and temperature prevailing at that particular cell.

**\$ Property: Water Mole Fraction(CH4) Max: 0.0001 Min: 0.0001
MFRAC_WAT 'CH4' CON 0.0001

*MOD

1:1	1:1	1:1	= 0.000976	11:11	1:1	1:1	= 0.000792
2:2	1:1	1:1	= 0.000954	12:12	1:1	1:1	= 0.000783
3:3	1:1	1:1	= 0.000932	13:13	1:1	1:1	= 0.000774
4:4	1:1	1:1	= 0.000912	14:14	1:1	1:1	= 0.000766
5:5	1:1	1:1	= 0.000892	15:15	1:1	1:1	= 0.000758
6:6	1:1	1:1	= 0.000874	16:16	1:1	1:1	= 0.00075
7:7	1:1	1:1	= 0.000855	17:17	1:1	1:1	= 0.000743
8:8	1:1	1:1	= 0.000838	18:18	1:1	1:1	= 0.000736
9:9	1:1	1:1	= 0.000821	19:19	1:1	1:1	= 0.000729
10:10	1:1	1:1	= 0.000805	20:20	1:1	1:1	= 0.000723

**\$ Property: Gas Mole Fraction(CH4) Max: 1 Min: 1

MFRAC_GAS 'CH4' CON 1

**\$ Property: Gas Mole Fraction(Water) Max: 0 Min: 0

MFRAC_GAS 'Water' CON 0

A dummy shut-in well is defined and simulation is run for 10,000 days. The start date is set as Jan 1st 2007. Data is recorded for selected times (i.e. 1, 10, 100, 1000, 10000 days). Equilibrium is reached in 10,000 days. Different time intervals are entered into the data file by using keyword “DATE”. Simulation is stopped after 10,000 days (May 19th 2034). The default geometry of the well is used and is operated at a Bottom hole pressure of 5000 kPa.

```

NUMERICAL
RUN
DATE 2007 1 1
DTWELL 0.001
**$
WELL 'Well-1'
PRODUCER 'Well-1'
OPERATE MIN BHP 5000. SHUTIN
**$      rad geofac wfrac skin
GEOMETRY K 0.086 0.249 1. 0.
PERF GEO 'Well-1'
**$ UBA   ff Status Connection
      1 1 1 1. OPEN   FLOW-TO 'SURFACE'
DATE 2007 1 2
DATE 2007 1 11
DATE 2007 4 11
DATE 2009 9 27
DATE 2034 5 19
STOP

```

Results and Discussion

Aqueous saturation: As per the problem description saturated conditions are maintained in the first half of the domain and unsaturated conditions in the other. As the simulation proceeds due to mass transfer water flows from one part to the other. The aqueous saturation curves match well with other hydrate codes in this problem. By the thousandth day, mechanical equilibrium is seen in the reservoir. Profiles of aqueous saturation are plotted at different time steps shown in Figure 3-4.

Relative permeability: Relative permeability is a function of aqueous saturation. At a high aqueous saturation, even a small change in the saturation brings a huge variation in the relative permeability curves. This can be seen in Figure 3-6.

Temperature: Initially the temperature at $x = 0$ is 20°C and at $x = 20$ m it is 40°C. Due to heat transfer, thermal equilibrium is reached by ten thousandth day. This scenario is in excellent agreement with all codes. It is given in Figure 3-5.

Aqueous CH₄ Mass Fraction: In the grid, the pressure and temperature are different at different locations. The solubility of methane in water is dependent on temperature and pressure. Initially, there is varying amount of dissolved methane at different coordinates in the grid. As the simulation proceeds, the pressure and temperature come to equilibrium and hence the dissolved methane is the same everywhere in the grid. This is given in Figure 3-7

Aqueous Pressure: The aqueous phase pressure at $x = 0$ is 5 MPa and at $x = 20$ m it is 4.6 MPa. Equilibrium is reached at 100 days. This is plotted in Figure 3-8.

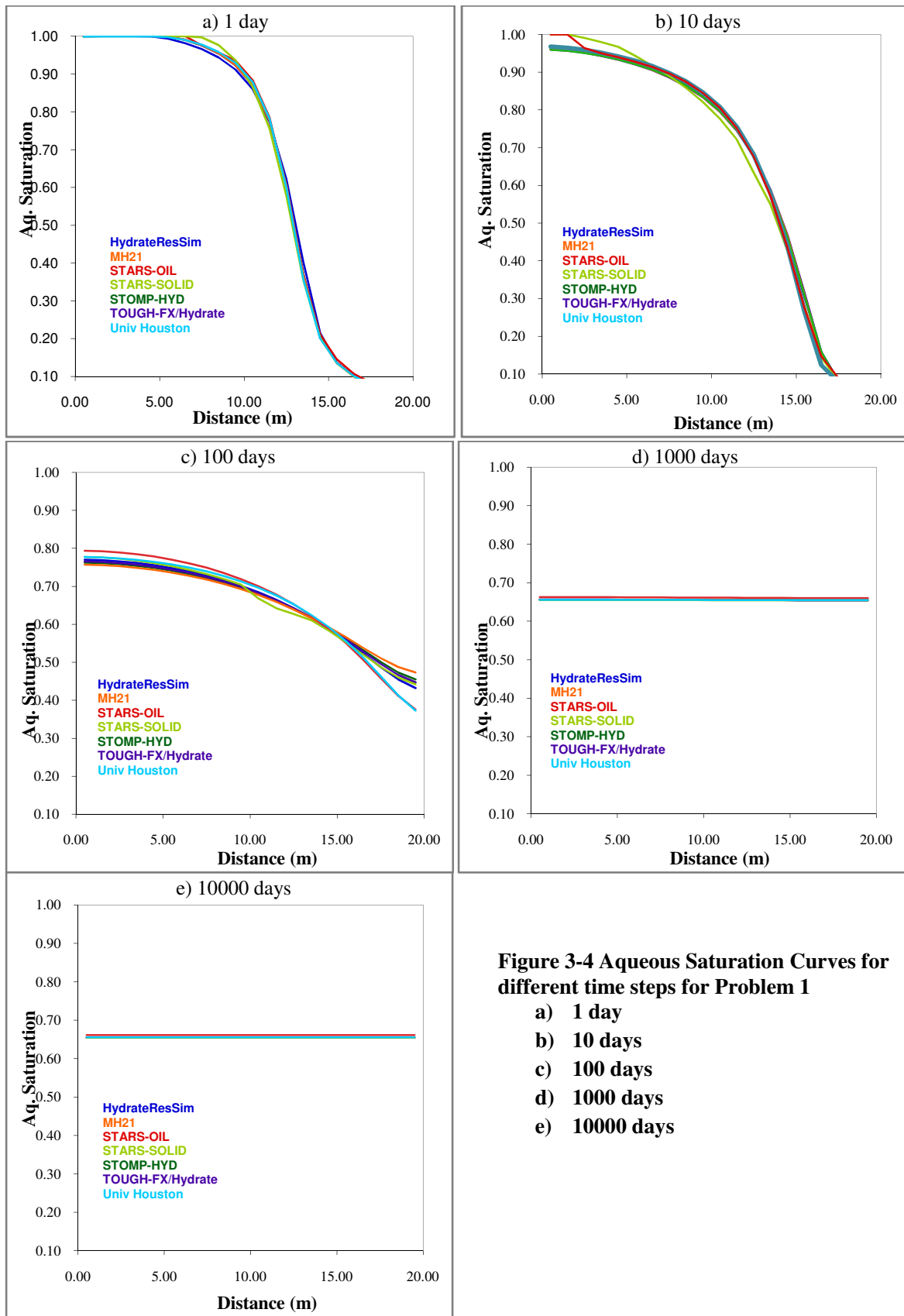


Figure 3-4 Aqueous Saturation Curves for different time steps for Problem 1

- a) 1 day
- b) 10 days
- c) 100 days
- d) 1000 days
- e) 10000 days

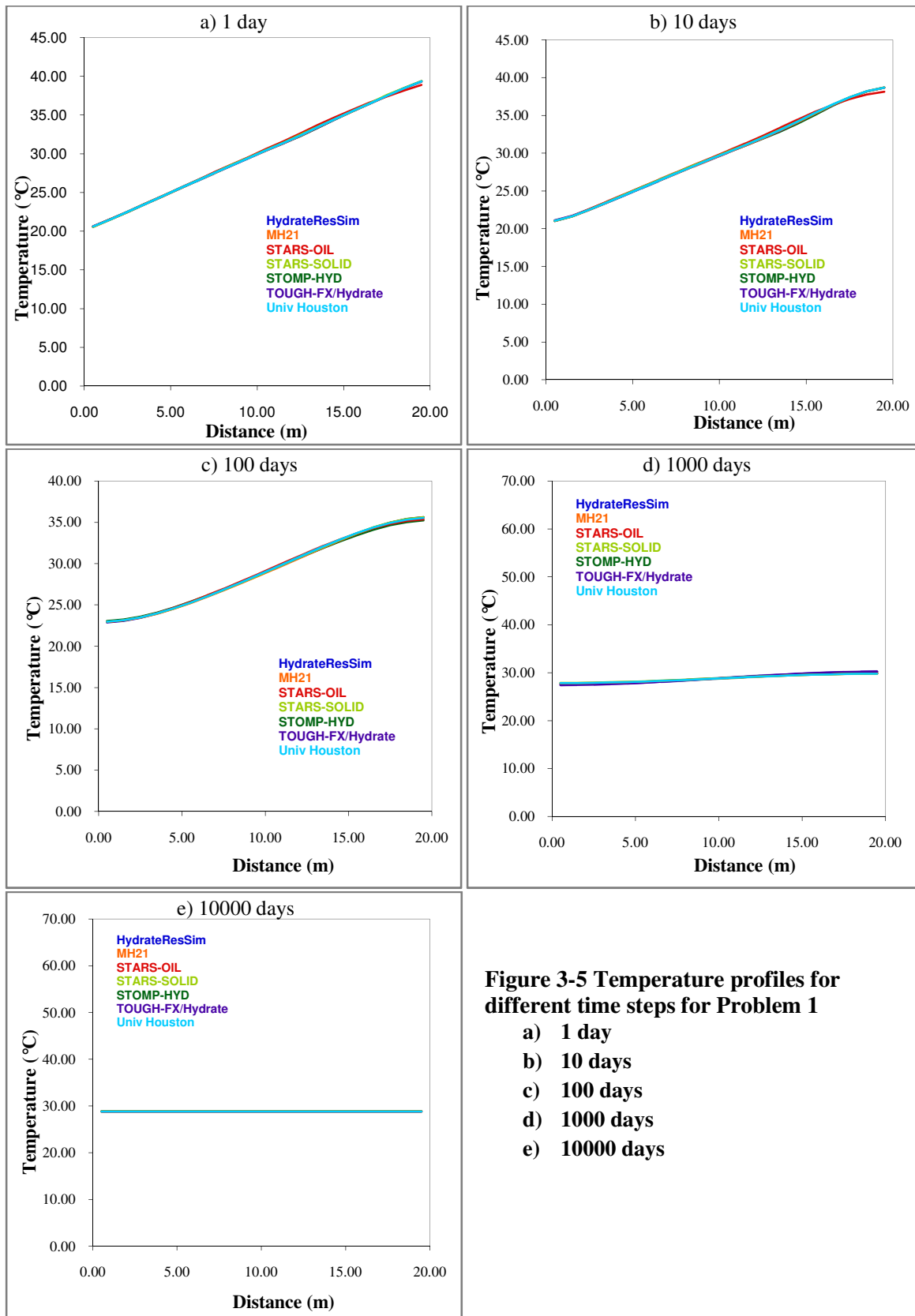


Figure 3-5 Temperature profiles for different time steps for Problem 1

- a) 1 day
- b) 10 days
- c) 100 days
- d) 1000 days
- e) 10000 days

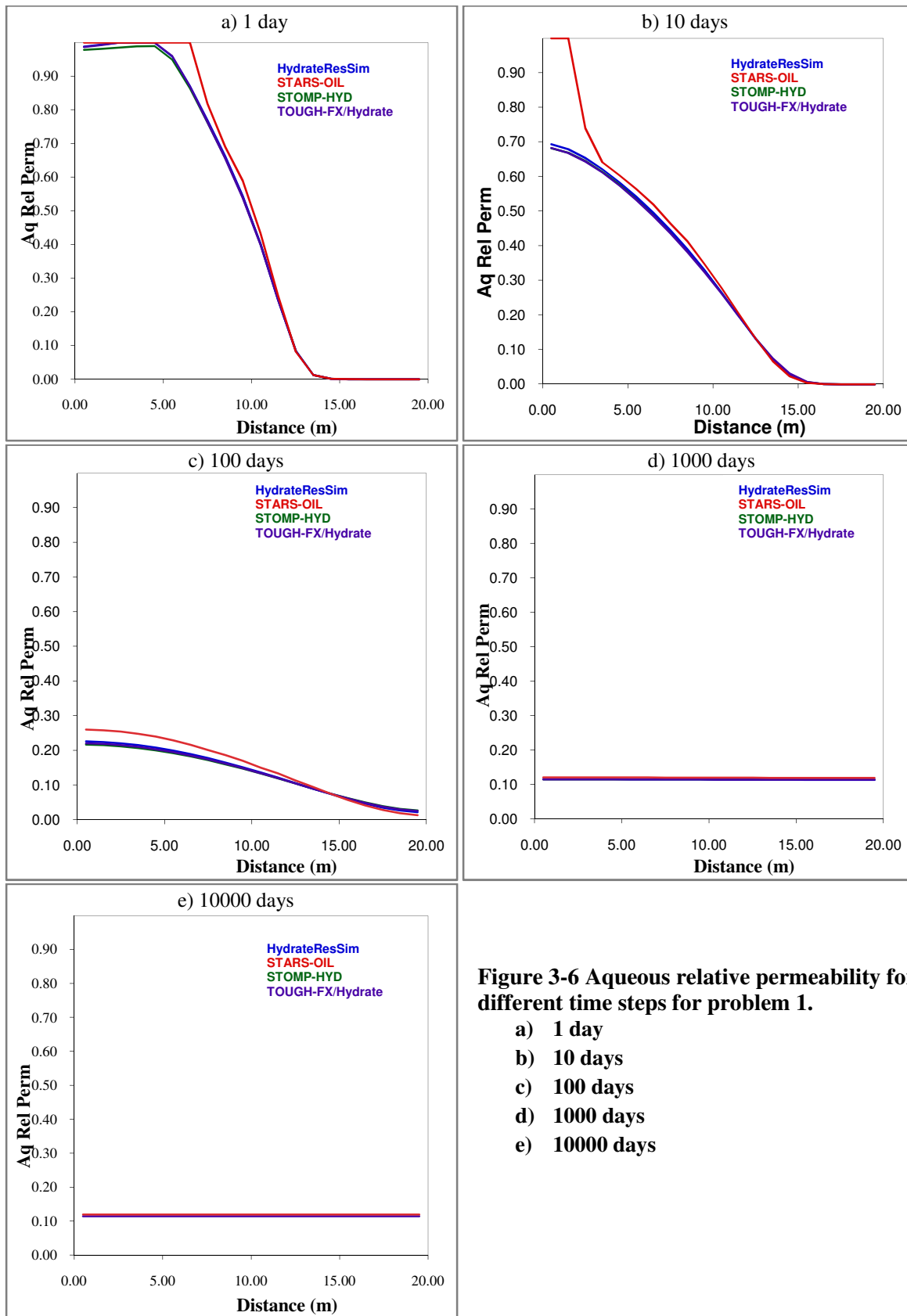


Figure 3-6 Aqueous relative permeability for different time steps for problem 1.

- a) 1 day
- b) 10 days
- c) 100 days
- d) 1000 days
- e) 10000 days

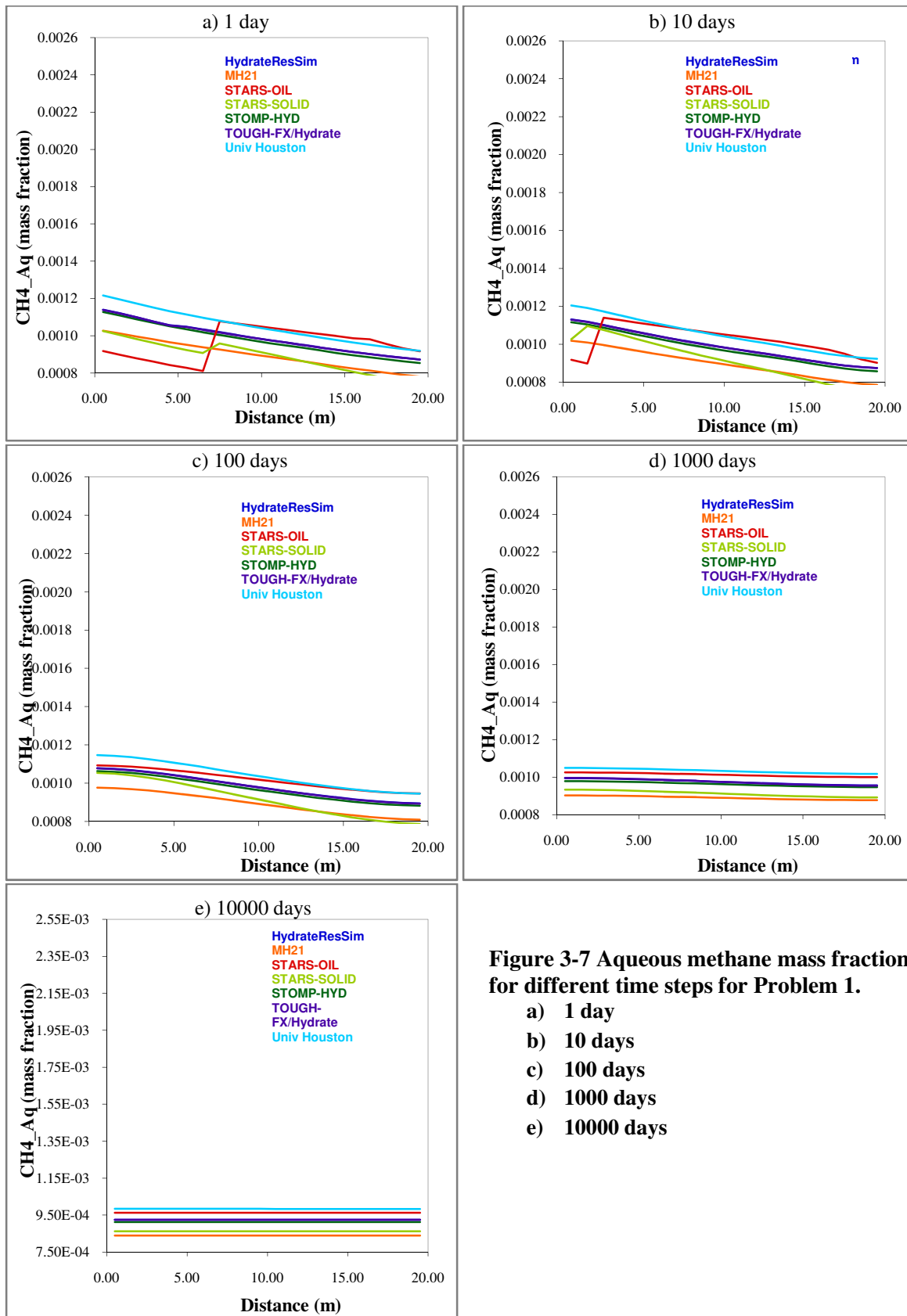


Figure 3-7 Aqueous methane mass fraction for different time steps for Problem 1.

- a) 1 day
- b) 10 days
- c) 100 days
- d) 1000 days
- e) 10000 days

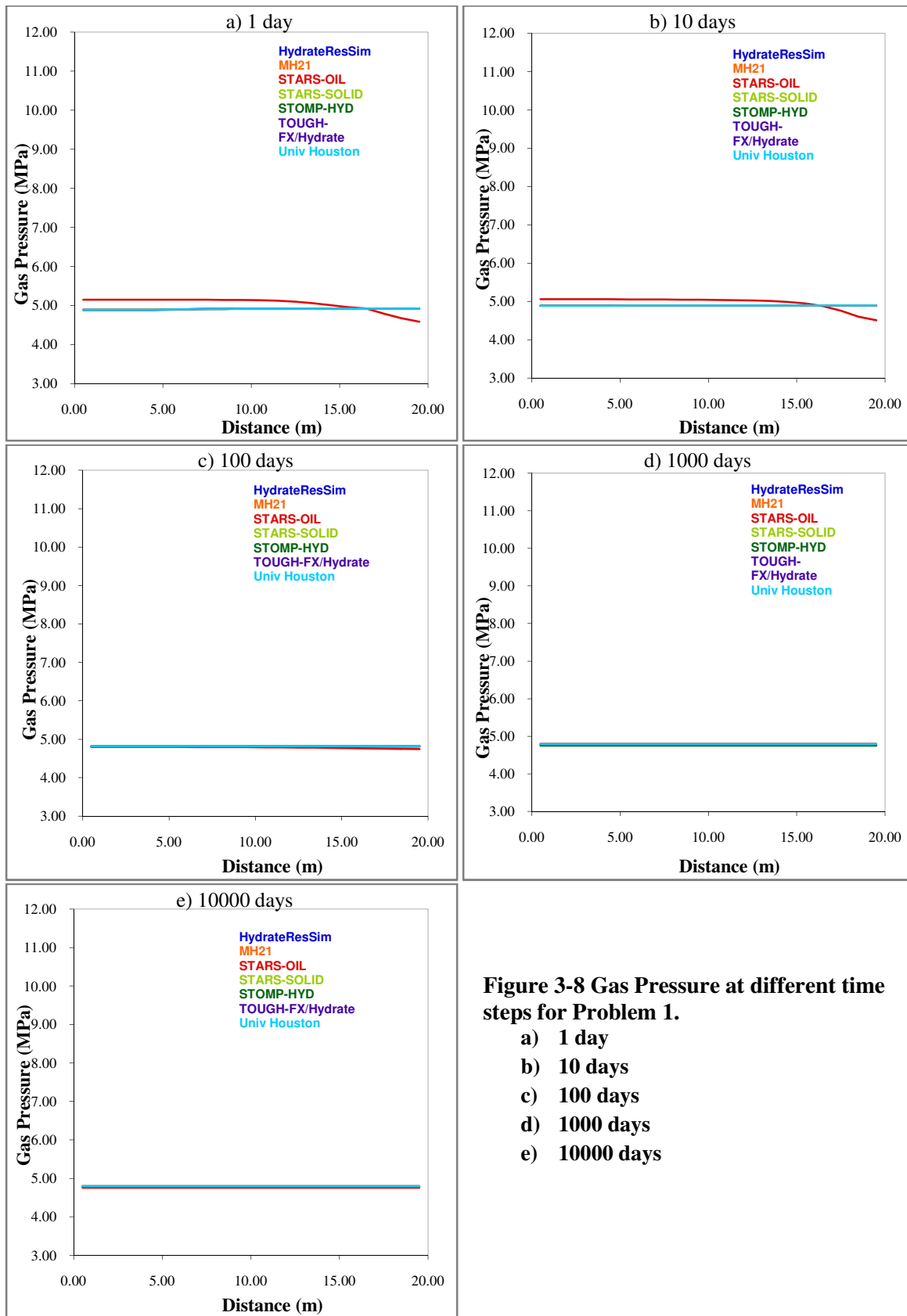


Figure 3-8 Gas Pressure at different time steps for Problem 1.

- a) 1 day
- b) 10 days
- c) 100 days
- d) 1000 days
- e) 10000 days

3.2 Problem 2

This problem of the code comparison study uses the same grid as suggested in problem 1. The difference between these two problems is that there is a hydrate phase in the first half of the domain. Hydrate dissociates due to the thermal conditions prevailing in the second half of the domain. The hydrate dissociation and formation process is simulated using a kinetic model. The simulation proceeds to equilibrium conditions leading to complete hydrate dissociation.

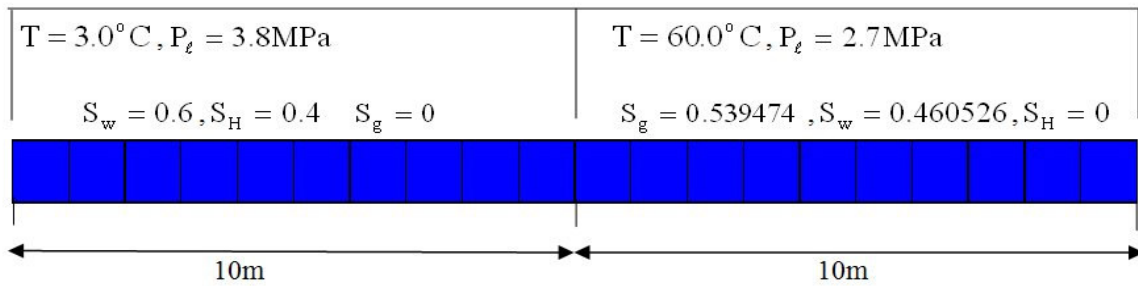


Figure 3- 9 Schematic view of problem 2

Processes simulated in this problem

- Multi-fluid flow for a water-CH₄-hydrate system in a porous media subject to relative permeability, capillarity and phase transitions.
- Hydrate dissociation due to thermal stimulation
- Heat transfer across the porous media with phase advection
- Change in thermodynamic and transport properties with pressure and temperature
- Solubility changes of methane in water with pressure and temperature

Hydrate Equilibrium pressure, hydration number, densities of liquid gas and hydrate, methane composition in liquid and solid phases are specified in Table 3-2.

Table 3-2 Input Parameters for Problem 2

$P_h^{eq} = 3.420 \text{ MPa}$	$P_g = 2.8 \text{ MPa}$
$N_h^w = 6.176$	$\rho_l = 983.889 \text{ kg/m}^3$
$y_{lc}^{CH_4} = 0.9650$	$\mu_l = 4.6642 \times 10^{-4}$
$y_{sc}^{CH_4} = 0.8392$	$\rho_g = 16.7376 \text{ kg/m}^3$
$\rho_h = 911.04 \text{ kg/m}^3$	$\mu_g = 1.2198 \times 10^{-5} \text{ Pa s}$
10 m	10 m

Different input parameters like porosity, specific heat, thermal conductivity and pore compressibility are same as in Problem 1 and are specified in Table 3-1. Capillary pressure model and Relative permeability model used in this problem are same as in Problem 1.

Data and sampling frequency

Profiles of water saturation, hydrate saturation, gas saturation, temperature, pressure, aqueous methane mass fraction, cumulative methane release, and rate of methane release are studied for different time steps (0, 1 day, 10 days, 100 days, 1000 days, 10,000 days).

3.2.1 Solution to Problem 2

Problem 2 has the same grid dimensions as that of Problem 1. It is a 20m-length horizontal domain divided into 20 cells each of length 1m. Porosity and permeability for the entire grid are 0.3 and 100mD respectively. Medium properties and thermal properties are same as that of Problem 1.

```
**$ Definition of fundamental Cartesian grid
GRID VARI 20 1 1 *Rw          0.02
KDIR DOWN
DI IVAR
  20*1
DJ JVAR
  1
DK ALL
  20*1
DTOP
  20*500
**$ Property: NULL Blocks Max: 1 Min: 1
**$ 0 = null block, 1 = active block
NULL CON          1
**$ Property: Porosity Max: 0.3 Min: 0.3
POR CON           0.3
**$ Property: Permeability I (md) Max: 100 Min: 100
PERMI CON         100
**$ Property: Permeability J (md) Max: 100 Min: 100
PERMJ CON         100
**$ Property: Permeability K (md) Max: 100 Min: 100
PERMK CON         100
**$ Property: Pinchout Array Max: 1 Min: 1
**$ 0 = pinched block, 1 = active block
PINCHOUTARRAY CON          1
END-GRID
ROCKTYPE 1
PRPOR 101.3
CPOR 5e-7
ROCKCP 1.988e+6 0
THCONR 1.728E+5
THCONS 1.728E+5
THCONW 2.24633E+5
THCONO 3.395237E+04
THCONG 5.183567E+04
THCONMIX TEMPER
**$ Property: Thermal/rock Set Num Max: 1 Min: 1
THTYPE CON          1
```

The difference between Problem 2 and Problem 1 is that there is an extra component hydrate in the first half of the domain. The system defined in this problem is water-CH₄-hydrate. It is

a 3- component, 3-phase system. Hydrate can be defined as either the oil phase with very high viscosity or as a solid phase. Each method has its own advantages and disadvantages.

Hydrate modeled as an oil

Hydrate saturation when expressed as an oil phase represents liquid saturation. Relative permeability and Capillary pressure curves are a function of water saturation. In CMG STARS, gas relative permeability and capillary pressure have to be entered as a function of liquid saturation ($S_l = S_w + S_{H=oil}$). This small variation in the relative permeability and capillary pressure curves makes it difficult to match the results of STARS to other codes. The dependence of permeability on porosity cannot be modeled in this method. The hydrate (oil), water and gas are specified in the pores of the medium according to following equations.

$$S_l + S_g = 1$$

$$S_l = S_w + S_{H=oil}$$

Hydrate modeled as a solid

In CMG STARS, water and gas saturations are measured on a scale that does not include hydrate. The assumption is that hydrate is a solid and it is not related to/contained in the pore spaces. The equation used to calculate water and gas saturation is $S_w + S_g = 1$. Relative permeabilities depend on water saturation and hence these results are difficult to match with other codes.

Hydrate properties like molecular weight, critical temperature, critical pressure are specified in the data file. Due to wide range of pressure and temperature values in the entire grid, gas-liquid K values for water and methane are calculated using the following correlation.

$$K = \left(\frac{KV1}{P} + KV2 * P + KV3 \right) * EXP\left(\frac{KV4}{T - KV5}\right)$$

The values of *KV1*, *KV2*, *KV3*, *KV4* and *KV5* for water and methane are pre-defined in CMG Builder.

Gas and liquid heat capacities are a function of temperature and are calculated by the correlation

$$CPG = CPG1 + CPG2 \times T + CPG3 \times T^2 + CPG4 \times T^3$$

$$CPL = CPL1 + CPL2 \times T + CPL3 \times T^2 + CPL4 \times T^3$$

CPG1, *CPG2*, *CPG3*, *CPG4* are the gas heat capacity coefficients

CPL1, *CPL2*, *CPL3*, *CPL4* are the liquid heat capacity coefficients

The gas component viscosity is given by

$$visg(i) = avg(i) \times T^{bvg(i)}$$

The liquid component viscosity is given by

$$viso(i) = avisc(i) \times \exp\left(\frac{bvisc(i)}{T}\right)$$

Gas phase and liquid phase viscosities are calculated based upon the gas and liquid component viscosity in STARS. Thermal Expansion Coefficient is expressed as *CT1*+*T*×*CT2* where *CT1* and *CT2* are first and second thermal expansion coefficients.

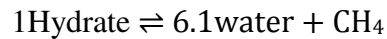
```

**$ Model and number of components          KVTABLIM 4000 5000 25 35
MODEL 3 3 3 2                               PRSR 101
COMPNAME 'Water' 'CH4' 'Hydrate'           TEMR 30
CMM                                           PSURF 101
0 0.016043 0.125962                         TSURF 16.85
PCRIT                                        CPG1
0 4600 10000                                0.0 19.251 0.0E+0
TCRIT                                        CPG2
0 -82.55 1000                               0.0 5.213E-2 0.0E+0
KV1                                          CPG3
1.186e7 9.5e7 0.0                          0.0 1.197E-5 0.0E+0
KV4                                          CPG4
-3816.44 -879.8 0.0                        0.0 -1.132E-8 0.0E+0
KV5                                          CPL1
-207.02 -245.0 0.0                        0.0E+0 0.0E+0 191.2

```

CPL2	-1.9095e-3 0 0.0E+0
0.0E+0 0.0E+0 0.0E+0	CT2
CPL3	7.296e-6 0 0.0E+0
0.0E+0 0.0E+0 0.0E+0	AVG
CPL4	0.0E+0 3.8E-3 0.0E+0
0.0E+0 0.0E+0 0.0E+0	BVG
MOLDEN	0.0E+0 0.0E+0 0.0E+0
55501.5 18723 7696.23	AVISC
CP	.00752 0.137849 9999.0
5.0E-7 0.0 5.0E-7	BVISC
CT1	1384.86 114.14 0.0

Hydrate formation and dissociation reactions are specified by Equilibrium kinetics. Hydrate dissociation is an endothermic first order reaction with an enthalpy of -51857.9364J/gmol and activation energy of 150218.3525 J/gmol.



Equilibrium K value for forward and backward reaction is given by the correlation.

$$K(P, T) = \left(\frac{rxk1}{P} + rxk2 \times P + rxk3 \right) \times \exp \left(\frac{rxk4}{T - rxk5} \right)$$

rxk1, *rxk2*, *rxk3*, *rxk4* and *rxk5* are the correlation coefficients.

```

**$ Reaction specification
**Hydrate Dissociation Reaction

** 1Hydrate = 6.1water + CH4
STOREAC  ** Stoichiometric coefficient of the reacting components
0 0 1
STOPROD  ** Stoichiometric coefficient of the producing components
6.1 1 0
RORDER  ** Order of the reaction, dependent on reactant concentration
0 0 1

FREQFAC 2.176565E+31 ** Reaction Frequency factor
RENTH -51857.9364 ** Reaction Enthalpy
EACT 150218.3525 ** Activation Energy

**Equilibrium K value for forward reaction
RXEQFOR 'Hydrate' 4.16949E+16 0 0 -8315.389 -263.15

**$ Reaction specification
**Hydrate Formation Reaction
** 6.1water + CH4 → 1Hydrate
STOREAC
6.1 1 0
STOPROD

```

```

0 0 1
RORDER
0 0 1
FREQFAC 1.0e28
RENTH 51857.9364
EACT 150218.3525
RXEQFOR 'Hydrate' 4.16949E+16 0 0 -8315.389 -263.15

```

Rock Fluid Properties are same as in problem 1

```

SWT
**$      Sw          krw          krow          Pcow
         0          0.00E+00      0.00000007      0
         0.05        8.75E-06      0.000000      0
         0.1         1.07E-04      0.000000      0
         0.15        4.62E-04      0.000000      0
         0.2         1.32E-03      0.000000      0
         0.25        2.97E-03      0.000000      0
         0.3         5.82E-03      0.000000      0
         0.35        1.03E-02      0.000000      0
         0.4         1.70E-02      0.000000      0
         0.45        2.65E-02      0.000000      0
         0.5         3.96E-02      0.000000      0
         0.55        5.74E-02      0.000000      0
         0.6         8.08E-02      0.000000      0
         0.65        1.11E-01      0.000000      0
         0.7         1.51E-01      0.000000      0
         0.75        2.02E-01      0.000000      0
         0.8         2.69E-01      0.000000      0
         0.85        3.56E-01      0.000000      0
         0.9         4.72E-01      0.000000      0
         0.95        6.40E-01      0.000000      0
         1          1.00E+00      0.000000      0

```

```

SLT
SMOOTHEND LINEAR
**$      S1          krg          krog          Pcoc
         0.01        1.000          0          928.16
         0.100        0.914          0          259.870
         0.200        0.800          0          174.086
         0.250        0.738          0          151.975
         0.300        0.673          0          135.379
         0.341        0.620          0          124.462
         0.381        0.566          0          115.139
         0.422        0.513          0          106.990
         0.463        0.460          0          99.727
         0.503        0.408          0          93.143
         0.544        0.357          0          87.081
         0.584        0.308          0          81.419
         0.625        0.261          0          76.056
         0.666        0.217          0          70.902
         0.706        0.175          0          65.875
         0.747        0.136          0          60.889

```

0.788	0.101	0	55.846
0.828	0.070	0	50.617
0.869	0.044	0	45.007
0.909	0.023	0	38.659
0.950	0.008	0	30.700
1.000	0.000	7.0000E-08	0.000

Initial conditions like pressure, temperature, saturations, aqueous and gas mole fractions are initially specified a constant and are then modified by using ‘MOD’ keyword.

```
**$ Property: Pressure (kPa)   Max: 4800   Min: 4800
PRES CON          4800
*MOD
 1:10    1:1    1:1    = 3800
11:20    1:1    1:1    = 2700
```

```
**$ Property: Temperature (C)   Max: 20   Min: 20
TEMP CON          20
*MOD
 1:10    1:1    1:1    = 13
11:20    1:1    1:1    = 70
```

```
**$ Property: Water Saturation   Max: 0.8   Min: 0.8
SW CON           0.8
*MOD
 1:10    1:1    1:1    = 0.6
11:20    1:1    1:1    = 0.460526
```

```
**$ Property: Gas Saturation   Max: 0.05   Min: 0.05
SG CON           0
*MOD
11:20    1:1    1:1    = 0.539474
```

```
**$ Property: Oil Saturation   Max: 0.05   Min: 0.05
SO CON           0
*MOD
 1:10    1:1    1:1    = 0.4
```

```
**$ Property: Water Mole Fraction(CH4)   Max: 0.002   Min: 0.002
MFRAC_WAT 'CH4' CON          0.002
```

```
**$ Property: Water Mole Fraction(Water)   Max: 0.998   Min: 0.998
MFRAC_WAT 'Water' CON          0.998
```

```
**$ Property: Oil Mole Fraction(Hydrate)   Max: 1   Min: 1
MFRAC_OIL 'Hydrate' CON          1
```

```
**$ Property: Gas Mole Fraction(Water)   Max: 0.0003   Min: 0.0003
MFRAC_GAS 'Water' CON          0.0003
```

```
**$ Property: Gas Mole Fraction(CH4)   Max: 0.9997   Min: 0.9997
MFRAC_GAS 'CH4' CON          0.9997
```

Well Conditions and the time interval chosen to run the simulation is same as in Problem 1

```
NUMERICAL
RUN
```



```

DATE 2007 1 1
DTWELL 0.001
**$

WELL 'Well-1'
PRODUCER 'Well-1'
OPERATE MIN BHP 5000. SHUTIN

**$          rad geofac wfrac skin
GEOMETRY K 0.086 0.249 1. 0.
PERF GEO 'Well-1'

**$ UBA      ff Status Connection
      1 1 1 1. AUTO      FLOW-TO 'SURFACE'
SHUTIN 'Well-1'

DATE 2007 1 2
DATE 2007 1 11
DATE 2007 4 11
DATE 2009 9 27
DATE 2034 5 19
STOP

```

Results

Thermal stimulation as well as depressurization cause hydrates dissociation initially. As, the simulation time proceeds, dissociation is principally due to thermal stimulation as a result of the propagation of a thermal wave from the second half of the domain. Initially hydrate dissociation occurs without hydrate formation. After 10 days, hydrate formation is observed along with dissociation due to the migration of released methane gas from the other half of the reservoir as shown in Figure 3-12. Equilibrium is reached in the reservoir. All the reservoir properties at different time steps are in perfect agreement with other simulators participating in the study which is shown in Figures 3-10 to Figure 3-16.

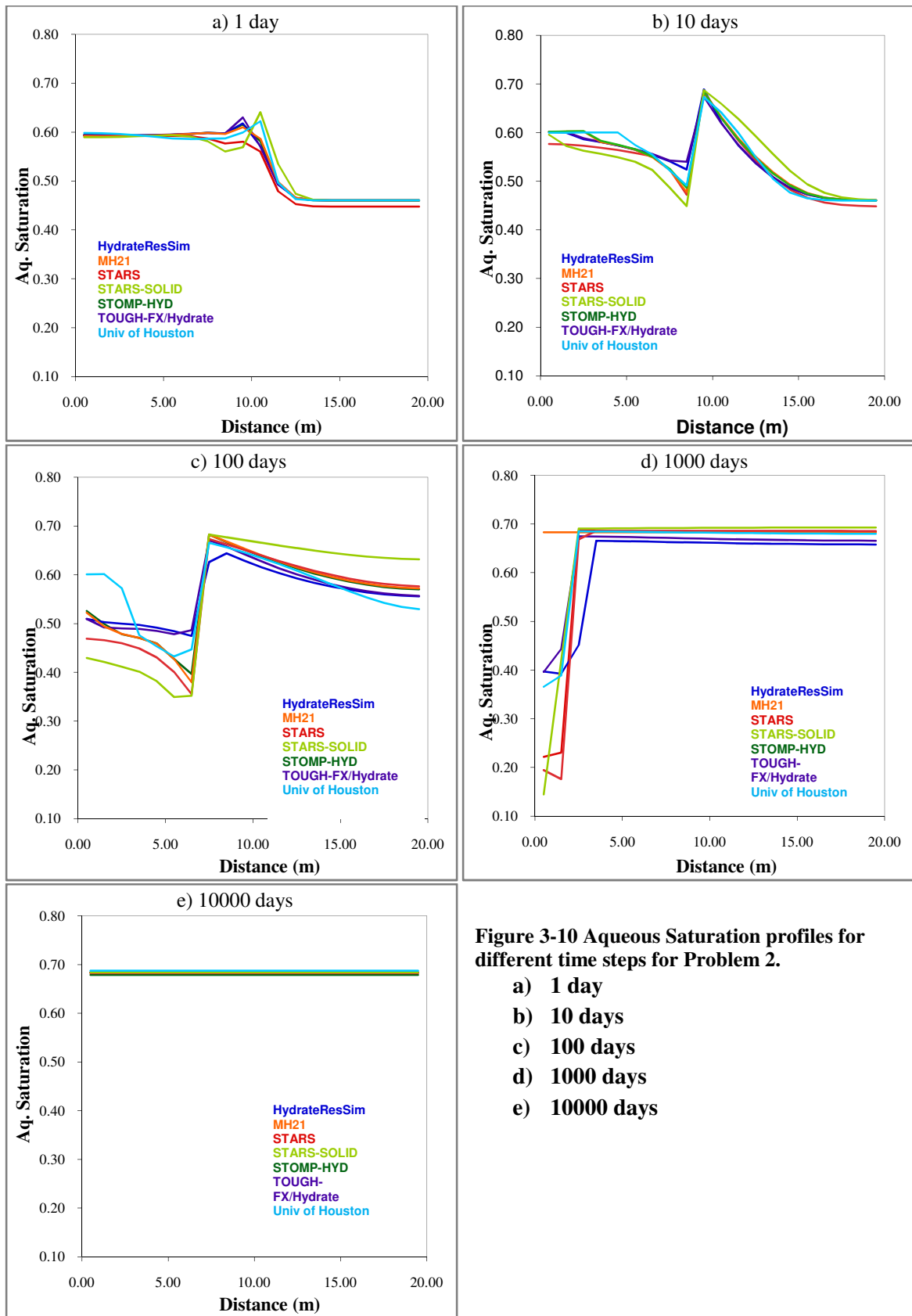


Figure 3-10 Aqueous Saturation profiles for different time steps for Problem 2.

- a) 1 day
- b) 10 days
- c) 100 days
- d) 1000 days
- e) 10000 days

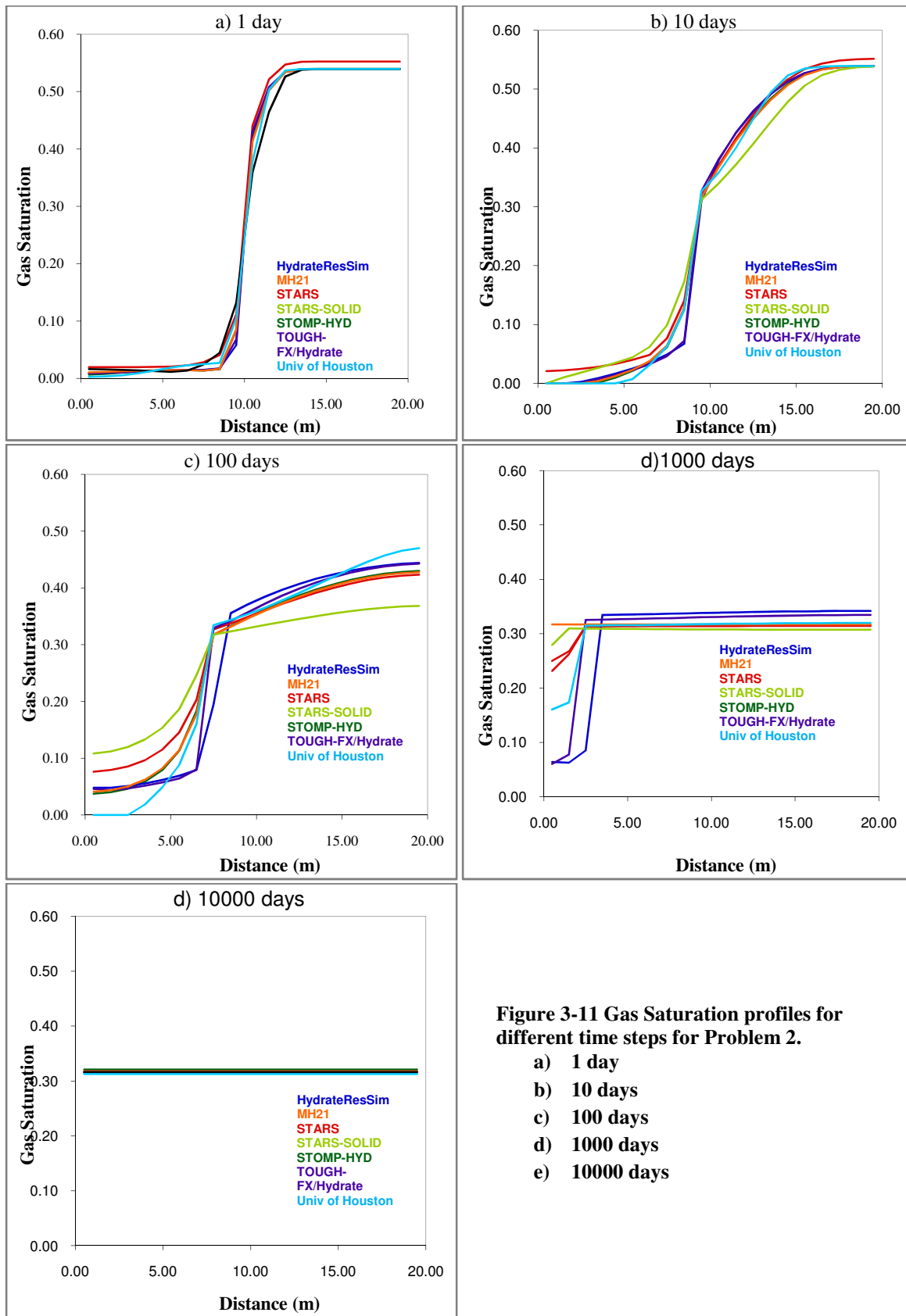


Figure 3-11 Gas Saturation profiles for different time steps for Problem 2.

- a) 1 day
- b) 10 days
- c) 100 days
- d) 1000 days
- e) 10000 days

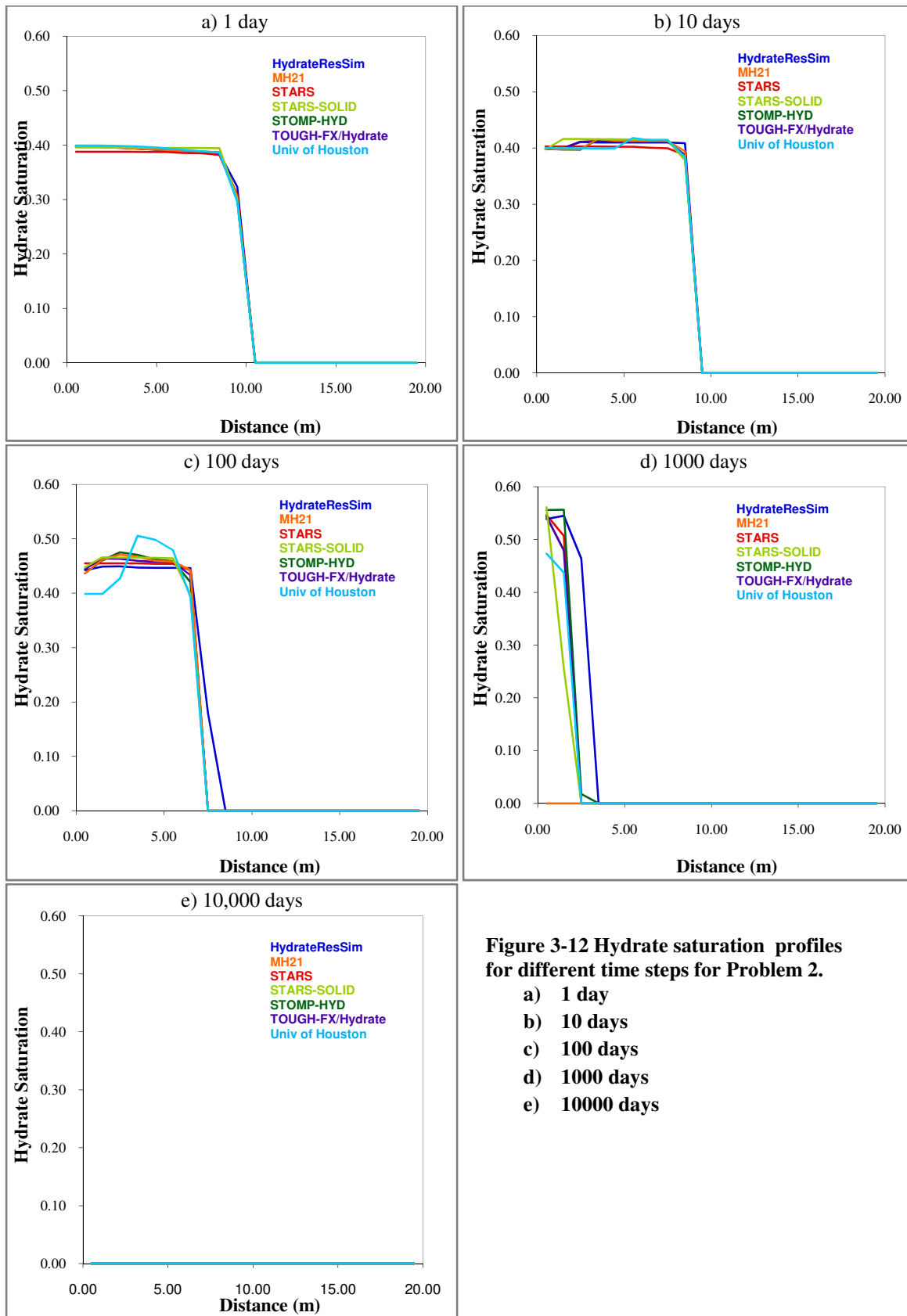


Figure 3-12 Hydrate saturation profiles for different time steps for Problem 2.

- a) 1 day
- b) 10 days
- c) 100 days
- d) 1000 days
- e) 10000 days

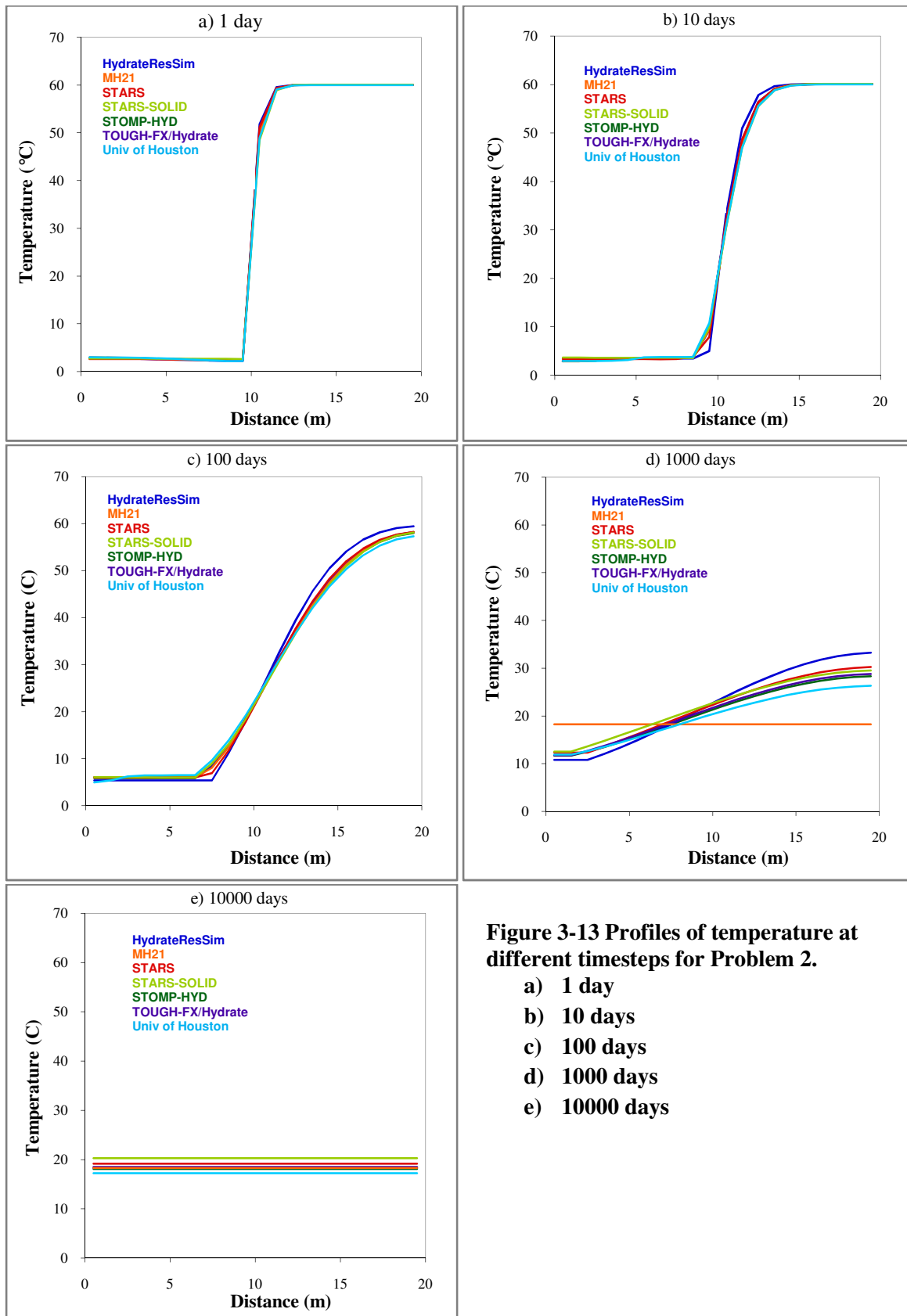


Figure 3-13 Profiles of temperature at different timesteps for Problem 2.

- a) 1 day
- b) 10 days
- c) 100 days
- d) 1000 days
- e) 10000 days

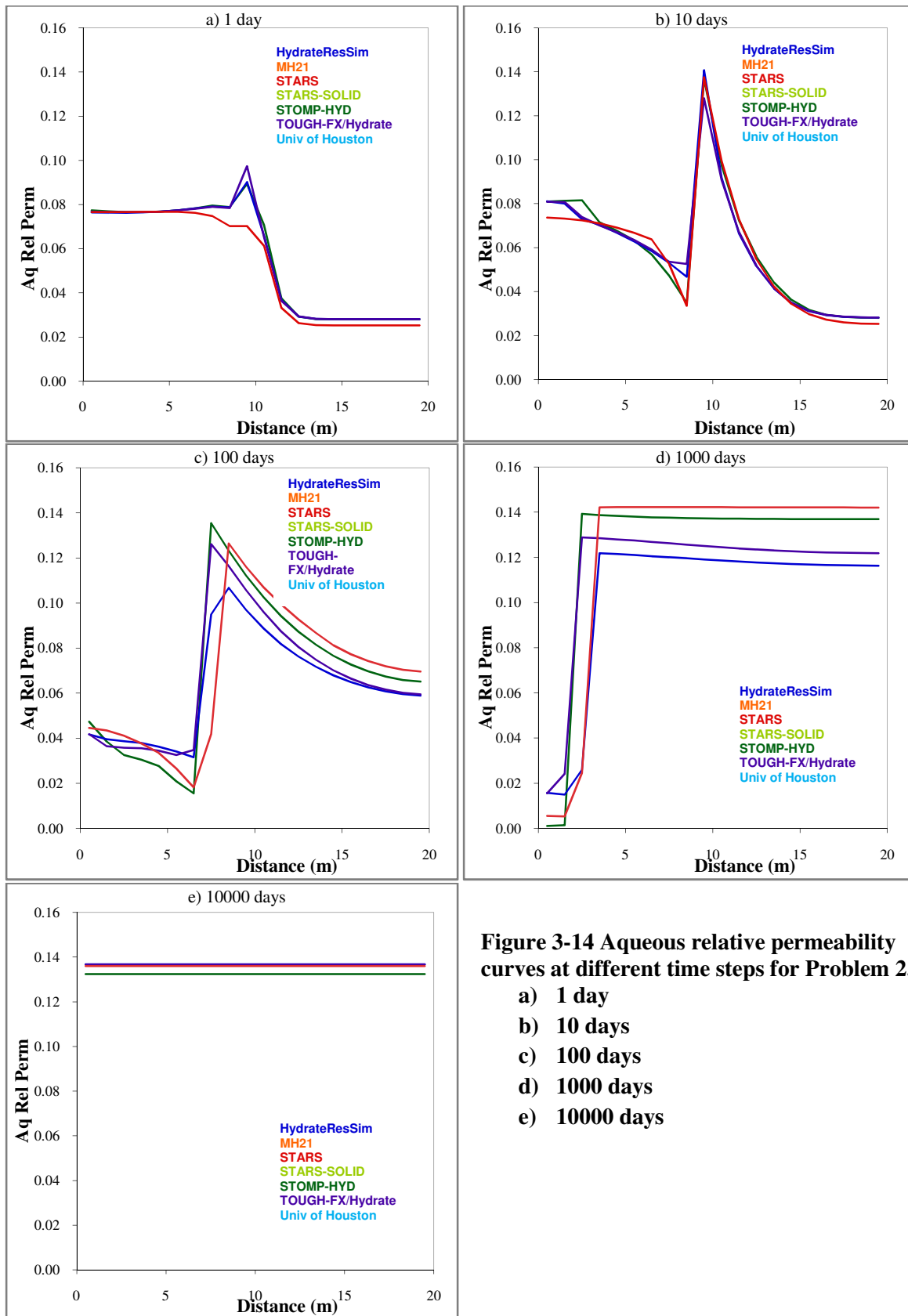


Figure 3-14 Aqueous relative permeability curves at different time steps for Problem 2.

- a) 1 day
- b) 10 days
- c) 100 days
- d) 1000 days
- e) 10000 days

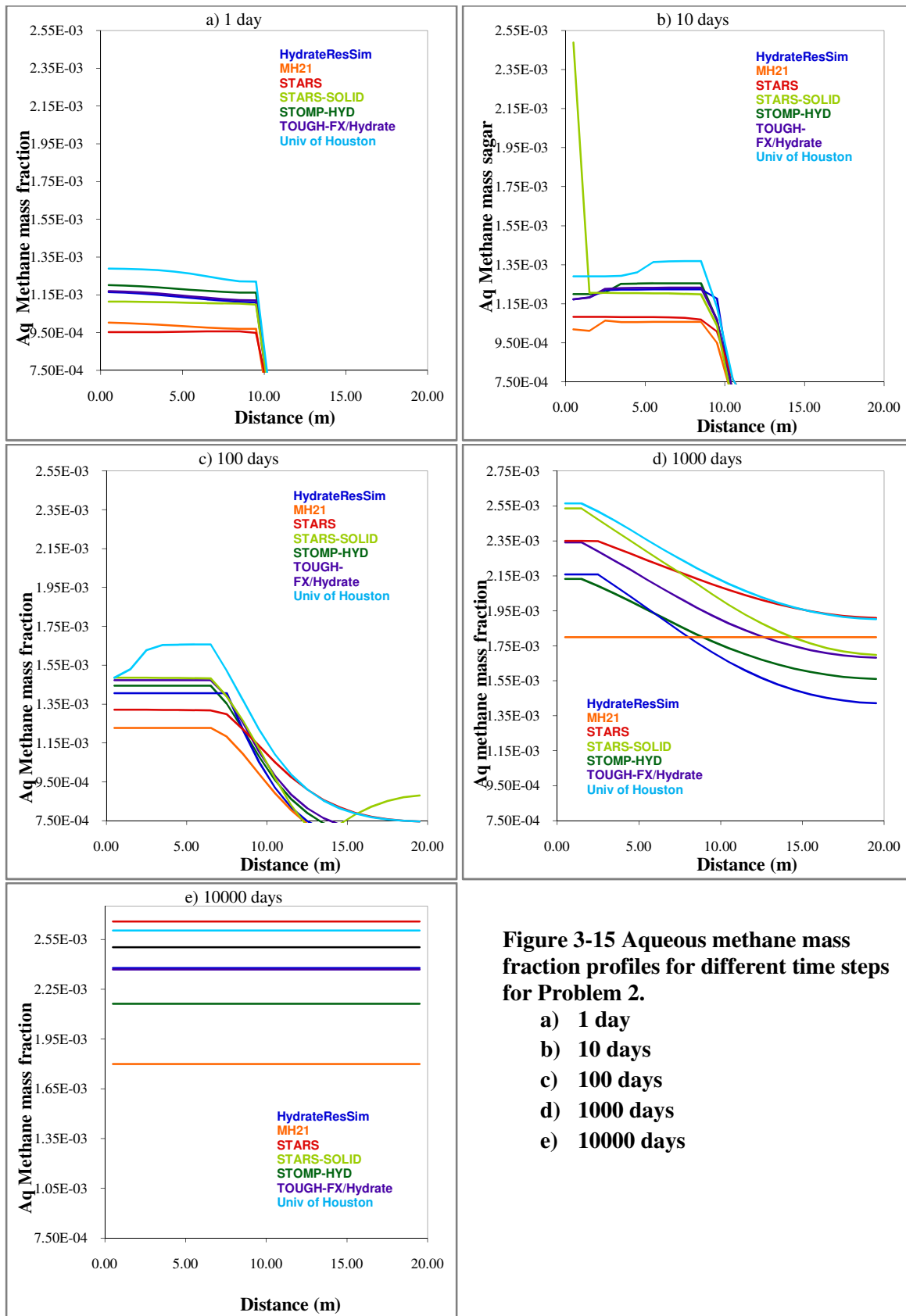


Figure 3-15 Aqueous methane mass fraction profiles for different time steps for Problem 2.

- a) 1 day
- b) 10 days
- c) 100 days
- d) 1000 days
- e) 10000 days

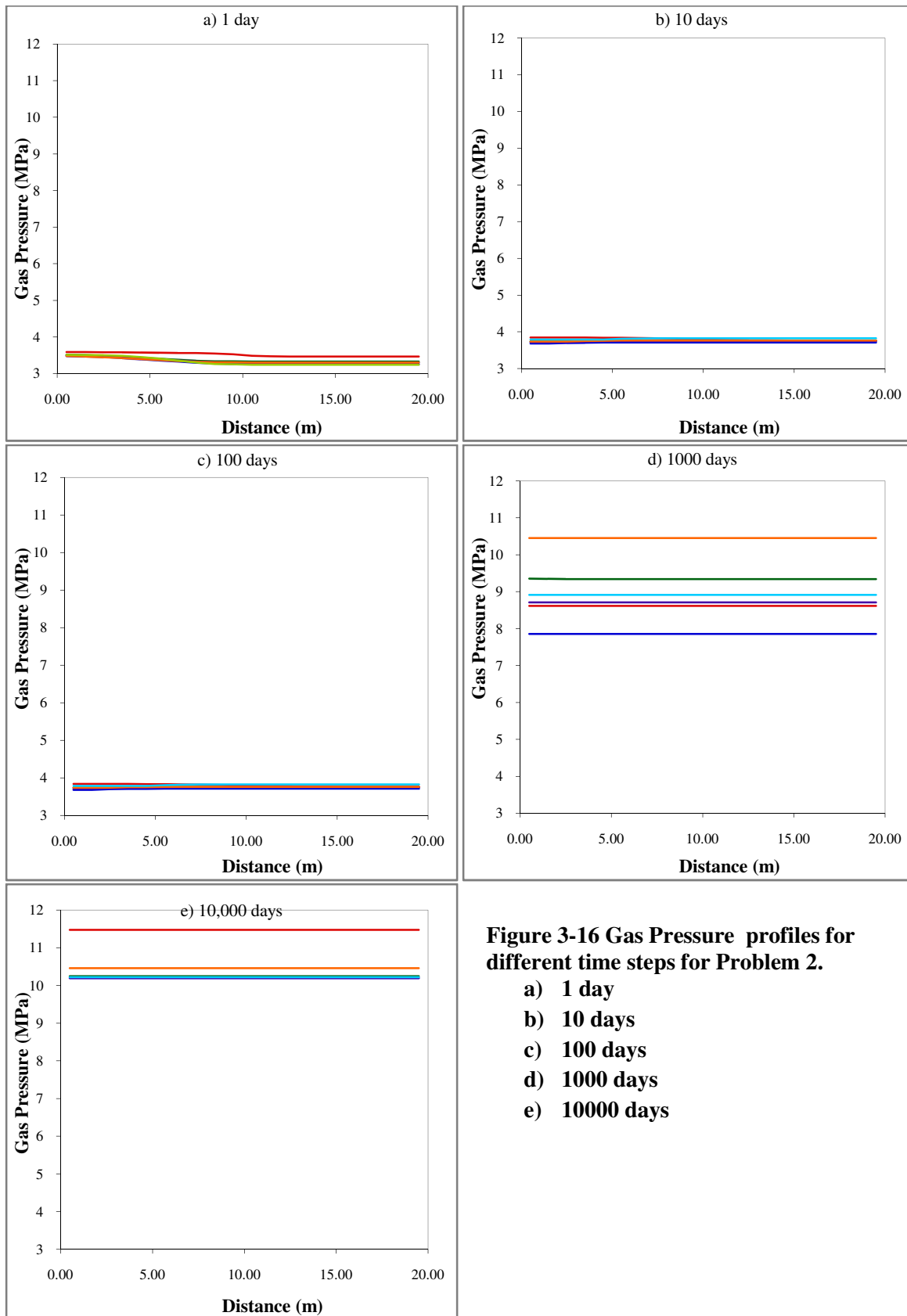


Figure 3-16 Gas Pressure profiles for different time steps for Problem 2.

- a) 1 day**
- b) 10 days**
- c) 100 days**
- d) 1000 days**
- e) 10000 days**

3.3 Problem 3

This problem is defined to explore the basic differences between the simulators when a hydrate reservoir is subjected to different production techniques (depressurization and thermal stimulation). In problem 2 there is a heat transfer from one part of the domain to other part leading to hydrate dissociation. In this problem heat is supplied to the system to trigger hydrate dissociation. Hydrate dissociation is an endothermic reaction. During dissociation, formation of ice and secondary hydrate are more likely to occur. Three cases are defined in this problem to closely observe hydrate dissociation and ice formation.

Case 1: Hydrate dissociation due to thermal stimulation

Case 2: Depressurization to a pressure above the Quadruple point (no ice formation)

Case3: Depressurization to a pressure below the Quadruple point leading to ice formation.

Domain Description

A closed horizontal one dimensional domain is chosen for this problem.

1-D Cartesian system, $L \times W \times H = 1.5\text{m} \times 1.0\text{m} \times 1.0\text{m}$.

The entire length is uniformly discretized into 30 cells each of length 0.05m.

So $\Delta x = 0.05\text{m}$, $\Delta y = \Delta z = 1\text{m}$

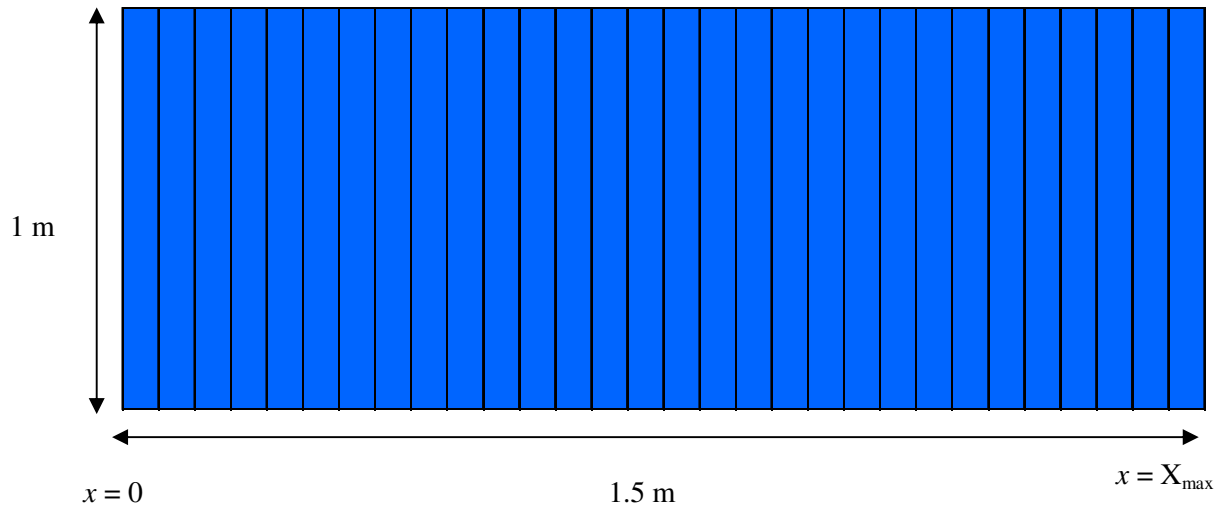


Figure 3- 17 Schematic representation of grid for Problem 3

Case 1: Thermal stimulation

Pressure and temperature of the entire reservoir are 8MPa and 2⁰C. A constant heat supply is maintained in the first block for the hydrate to dissociate. Initial and Boundary conditions for the entire reservoir are

Initial Conditions

Pressure: $P_i = 8 \text{ MPa}$

Temperature: $T_i = 2^{\circ}\text{C}$

Saturations: $S_H = 0.5, S_W = 0.5, S_G = 0.0$

Boundary Conditions

At $x = X_{max}$: No mass or heat flow

At $x = 0$: $S_W = 1.0$

$P_0 = 8 \text{ MPa}$

$T_0 = 45^{\circ}\text{C}$

Case 2: Depressurization to a pressure above the Quadruple point

There is no ice formation in this case. The entire reservoir is at an initial pressure of 8 MPa and is depressurized to 2.8 MPa. A constant water saturation of 100% is maintained in the first block.

Initial Conditions

Pressure: $P_i = 8 \text{ MPa}$

Temperature: $T_i = 6^\circ\text{C}$

Saturations: $S_H = 0.5, S_W = 0.5, S_G = 0.0$

Boundary Conditions

At $x = X_{max}$: No mass or heat flow

At $x = 0$: $S_W = 1.0$

$P_0 = 2.8 \text{ MPa}$

$T_0 = 6^\circ\text{C}$

Case 3: Depressurization below the Quadruple point leading to ice formation

In this case pressure is depressurized up to 0.5 MPa to allow ice to form. The remaining boundary conditions are same as in case 1

Initial Conditions:

Pressure: $P_i = 8 \text{ MPa}$

Temperature: $T_i = 6^\circ\text{C}$

Saturations: $S_H = 0.5, S_W = 0.5, S_G = 0.0$

Boundary Conditions:

At $x = X_{max}$: No mass or heat flow

At $x = 0$: $S_W = 1.0$

$P_0 = 0.5 \text{ MPa}$

$T_0 = 6^\circ\text{C}$

The following properties and models used are same for all the cases.

Medium properties:

Hydraulic and thermal properties play an important role in the production of gas from gas hydrates. These properties are constant in the entire reservoir.

Thermal properties

Grain specific heat $C = 1000 \text{ J/kg/K}$

Dry Thermal Conductivity $k_{\Theta D} = 2 \text{ W/m/K}$

Wet Thermal Conductivity $k_{\Theta w} = 2 \text{ W/m/K}$

Hydraulic properties

Intrinsic Permeability: $k = 3.0 \times 10^{-13} \text{ m}^2$ (0.3 Darcys)

Porosity: $\phi = 0.3$

Pore compressibility: $\beta = 5.0 \times 10^{-9} \text{ Pa}^{-1}$

Grain Density: $\rho_R = 2600 \text{ kg/m}^3$

Relative permeability model

The relative permeability model used in this problem is developed by Stone³⁶ and Aziz³⁷.

$$k_{rG} = (S_G^*)^n, \quad S_G^* = (S_G - S_{irG}) / (1 - S_{irA})$$

$$k_{rA} = (S_A^*)^n, \quad S_A^* = (S_A - S_{irA}) / (1 - S_{irA})$$

Where S_{irG}, S_{irA} represents irreducible gas and aqueous saturation.

In this problem $S_{irG} = 0.02$, $S_{irA} = 0.12$ and $n = 3.0$.

A plot of relative permeability vs. water saturation is shown in Figure 3-18.

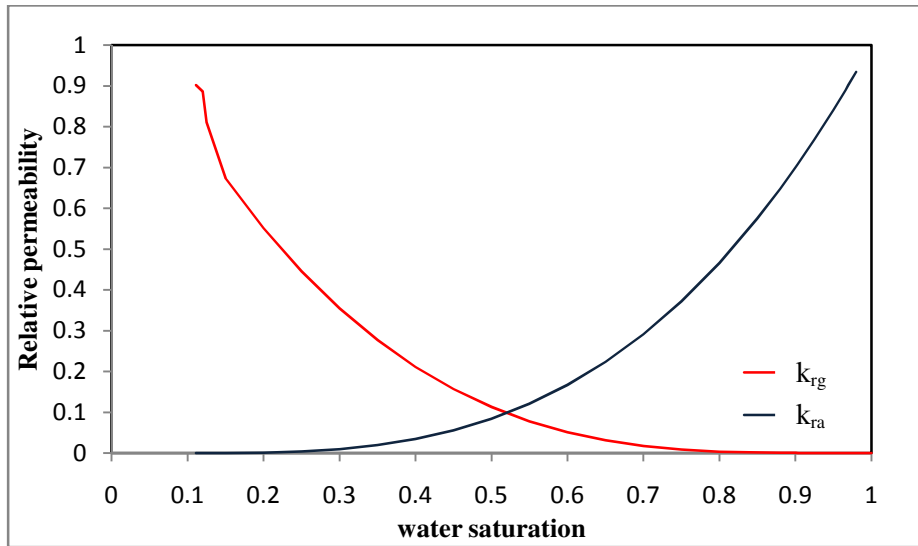


Figure 3- 18 Aqueous and Gas Relative permeability curves as a function of Water Saturation

Capillary pressure Model

Capillary pressure model used is same as in the above problems. A plot of capillary pressures vs. water saturation is shown in Figure 3-19. Different parameters used in this model are specified in Table 3-3.

$$P_{cap} = -P_0[(S^*)^{-1/\lambda} - 1]^\lambda, \quad S^* = \frac{(S_A - S_{irA})}{(S_{mA} - S_{irA})}$$

Where $-P_{max} \leq P_{cap} \leq 0$

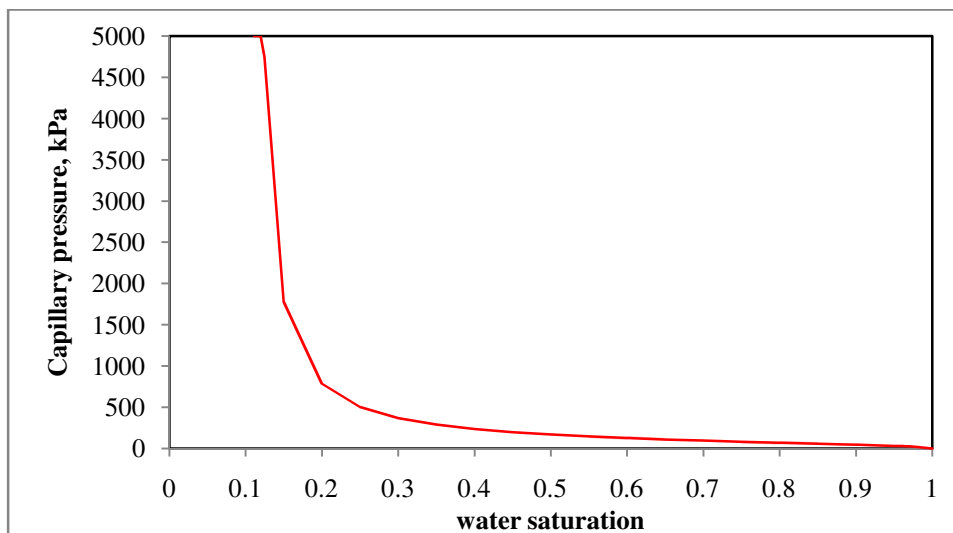


Figure 3-19 Capillary Pressure vs. Water Saturation

Data and sampling frequency

Profiles of water saturation, temperature, pressure, aqueous relative permeability, and aqueous methane mass fraction and capillary pressure, gas rate, cumulative gas rate are compared for different time steps. The time steps considered here are different for each case.

Case 1: Thermal stimulation

Data recorded at 1 hr, 3 hrs, 6 hrs, 12 hrs, 1 day, 2 days, 3 days, and 5 days

Case 2: Depressurization to a pressure above the Q point

Results reported at 2min, 5min, 20min, 1hr, 1.5hrs, 12 hrs, 1 day, 2 days, and 3 days

Case 3: Depressurization to a pressure below Q point

Results reported at 2min, 5min, 10min, 20min, 30 min, 45 min, 1hr, 1 day, 5 days.

3.3.1 Solution to Problem 3

The grid in problem 1 is a 1-D domain of length 1.5 m. The entire length is uniformly discretized into 30 cells each of length 0.05m. The same grid is used for all the cases. The grid is modified to meet the boundary conditions of the problem. The difficulty in this problem lies in maintaining the boundary conditions applied for each case throughout the run. All the cases have a boundary condition that water saturation at $x=0$ is always 100% throughout the simulation. In STARS, it is not practical to maintain a constant boundary in a block. The boundary conditions are achieved and have to be maintained so by making some other changes in the system. Other simulators can treat the block as a single entity and assign fixed properties. STARS have an inbuilt well bore model. Once a well is defined, it is not a block anymore. For each block a water saturation of 100% is difficult to attain and even if it is specified, the saturation later changes due to mass transfer and the boundary condition is abandoned. This was a major difficulty in solving this problem.

For each $s_w=1$ boundary condition is difficult to attain.

To overcome this problem a bigger block was incorporated but even then water saturation did not match with other codes. To match the results with other codes and to fix the boundary condition problem, two extra blocks were defined. Water is injected at high rate of 50,000 m³/day in the first block and then produced at the same rate. The permeability's of the two blocks are set very high so that these two blocks do not affect the properties like pressure temperature and saturations of the rest of the blocks. Temperature of the water that is injected is set according to the boundary condition required for each case.

The modified grid is of length 2.5 m. The first two cells are each of length 0.5 m. The next 30 cells are of 0.05 m in length as per the problem description. A constant porosity of 0.3 is used. Permeability for the first two cells is constant and is 1e6 mD. Other 30 cells have a constant permeability of 300 mD.

Grid description, component properties, Hydrate dissociation formation reactions and rock-fluid properties are same for all the cases (1, 2 & 3) and are specified below in the input data file.

```

*****
$ Definition of fundamental cartesian grid
*****
GRID VARI 32 1 1
KDIR DOWN
DI IVAR
2*0.5 30*0.05
DJ JVAR
1
DK ALL
32*1
DTOP
32*500
**$ Property: NULL Blocks Max: 1 Min: 1
**$ 0 = null block, 1 = active block
NULL CON 1
**$ Property: Porosity Max: 0.3 Min: 0.3
POR CON 0.3
**$ Property: Permeability I (md) Max: 300 Min: 300
PERMI CON 300
*MOD
1:2 1:1 1:1 = 1e+006
**$ Property: Permeability J (md) Max: 300 Min: 300
PERMJ CON 300
*MOD
1:2 1:1 1:1 = 1e+006
**$ Property: Permeability K (md) Max: 300 Min: 300
PERMK CON 300
*MOD
1:2 1:1 1:1 = 1e+006
END-GRID
ROCKTYPE 1
PRPOR 101.3
CPOR 5e-7
ROCKCP 1.988e+6 0
THCONR 1.728E+5
THCONS 1.728E+5
THCONW 2.24633E+5
THCONO 3.395237E+04
THCONG 5.183567E+04
THCONMIX SIMPLE
PERMCK 4.5
**$ Property: Thermal/rock Set Num Max: 1 Min: 1
THTYPE CON 1

**$ Model and number of components
MODEL 3 3 3 1
COMPNAME 'H2O' 'CH4' 'hydrate'
CMM
0 16.043e-3 127.333e-3
PCRIT
0 4.600E+3 1e4
TCRIT
0 -8.255E+1 1e3
KV1
1.186e7 3.65e9 0
KV4
-3816.44 -1942 0
KV5
-227.02 -265.99 0
CPG1
0.0E+0 1.9251E+1 0
CPG2
0.0E+0 5.213E-2 0
CPG3
0.0E+0 1.197E-5 0
CPG4
0.0E+0 -1.132E-8 0
CPL1
0.0E+0 0.0E+0 0

```



```

CPL2
0.0E+0 0.0E+0 0
CPL3
0.0E+0 0.0E+0 0
CPL4
0.0E+0 0.0E+0 0
MOLDEN
0 31800 7458
CP
0 5e-14 5e-14
CT1
0.0E+0 0 0
CT2
0.0E+0 0 0
AVG
0.0E+0 0.012198 0
BVG
0.0E+0 0.0E+0 0
AVISC
0.46642 0.137849 1e9
BVISC
0 114.14 0

```

```

** Reaction 1: 1 HYDRATE + 1 CH4 ---> 7.176 WATER + 1 CH4
**$ Reaction specification
STOREAC
1 0 1
STOPROD
7.176 1 0
RORDER
1 0 1
FREQFAC 1.e28
RENTH -51857.9364
EACT 146711.70
RXEQFOR 'H2O' 9.02843e15 0 0 -7893.6136 -273.15

```

```

** Reaction 2: 6.176 WATER + 1 CH4 --> 1 HYDRATE
**$ Reaction specification
STOREAC
6.176 1 0
STOPROD
0 0 1
RORDER
1 1 0
FREQFAC 1.e27
RENTH 51857.9364
EACT 146711.70
RXEQBAK 'H2O' 9.02843e15 0 0 -7893.6136 -273.15

```

```

ROCKFLUID
RPT 1 WATWET
SWT

```

```

**$
      Sw      krw      krow      Pcow
0.111      0 1.0000E-07 0.0000E+00
0.12      1.4185E-06 9.0000E-08 0.0000E+00
0.125      4.78744E-06 8.0000E-08 0.0000E+00
0.15      9.07841E-05 8.0000E-08 0.0000E+00
0.2      0.001034088 7.0000E-08 0.0000E+00
0.25      0.00389237 6.0000E-08 0.0000E+00
0.3      0.009729506 5.0000E-08 0.0000E+00
0.35      0.019609373 4.0000E-08 0.0000E+00
0.4      0.034595847 3.0000E-08 0.0000E+00
0.45      0.055752806 2.0000E-08 0.0000E+00
0.5      0.084144125 1.0000E-08 0.0000E+00
0.55      0.120833682 1.0000E-08 0.0000E+00
0.6      0.166885352 1.0000E-08 0.0000E+00
0.65      0.223363013 1.0000E-08 0.0000E+00
0.7      0.291330541 1.0000E-08 0.0000E+00
0.75      0.371851812 1.0000E-08 0.0000E+00
0.8      0.465990703 1.0000E-08 0.0000E+00

```

0.85	0.574811091	1.0000E-08	0.0000E+00
0.88	0.647593015	1.0000E-08	0.0000E+00
0.9	0.699376852	1.0000E-08	0.0000E+00
0.903	0.707374731	1.0000E-08	0.0000E+00
0.925	0.767896709	1.0000E-08	0.0000E+00
0.95	0.840751863	1.0000E-08	0.0000E+00
0.958	0.865002847	1.0000E-08	0.0000E+00
0.96	0.871137596	1.0000E-08	0.0000E+00
0.966	0.889715741	1.0000E-08	0.0000E+00
0.97	0.902246765	1.0000E-08	0.0000E+00
0.98	0.934087882	0	0.0000E+00

SLT

SMOOTHEND LINEAR

**\$	S1	krq	krog	Pcog
0.111	0.902246765	0	5000	
0.12	0.886601219	6.0000E-08	5000	
0.125	0.811081055	6.0000E-08	4746.421788	
0.15	0.673153004	6.0000E-08	1779.187755	
0.2	0.551821428	6.0000E-08	788.9195842	
0.25	0.446022449	6.0000E-08	504.7999693	
0.3	0.354692192	6.0000E-08	369.2345198	
0.35	0.27676678	6.0000E-08	289.3000514	
0.4	0.211182336	6.0000E-08	236.1567439	
0.45	0.156874983	6.0000E-08	197.9230752	
0.5	0.112780846	6.0000E-08	168.8010783	
0.55	0.077836047	6.0000E-08	145.6154878	
0.6	0.05097671	6.0000E-08	126.4702926	
0.65	0.031138958	6.0000E-08	110.1491143	
0.7	0.017258915	6.0000E-08	95.81611475	
0.75	0.008272704	6.0000E-08	82.84907637	
0.8	0.003116449	6.0000E-08	70.72867486	
0.85	0.001418502	6.0000E-08	58.93392089	
0.88	0.000726273	6.0000E-08	51.73975692	
0.9	0.000647593	6.0000E-08	46.7629846	
0.903	0.000236003	6.0000E-08	45.99679873	
0.925	3.82996E-05	6.0000E-08	40.14794759	
0.95	1.51042E-05	7.0000E-08	32.71657413	
0.958	1.1348E-05	8.0000E-08	30.03839527	
0.96	3.89237E-06	1.0000E-07	29.33544567	
0.966	1.4185E-06	1.0000E-07	27.12672049	
0.97	1.4185E-09	1.0000E-07	25.55391808	
0.98	1.4185E-09	1.0000E-07	21.11325599	
1	0	1.0000E-07	0	

**\$ Property: Rel Perm Set Num Max: 1 Min: 1

RTYPE CON

1

INITIAL

VERTICAL OFF

INITREGION 1

REFDEPTH 500.5

Pressure, temperature, saturations of the grid blocks are different for each case and are specified according to the problem description. Well constraints are different in all the cases and are specified in the input data file for each case.

Case 1

Pressure of the reservoir is 8MPa and temperature of the reservoir is 2°C. The temperature of the first three blocks is maintained at a constant temperature of 45°C. Water is injected in the first block through an injector well (well 1) at rate of 50, 000 m³/day. A producer well is introduced in the second block and water is produced at the same rate of 50,000 m³/day. The temperature of the injected stream (water) is 45°C. Initially there is no gas in the reservoir. Hydrate saturation is 50% in the entire reservoir. The time steps at which the simulations are carried out are different for each case and are specified according to the problem description.

```

**$ Property: Pressure (kPa)   Max: 8000   Min: 8000
PRES CON           8000
**$ Property: Temperature (C)   Max: 2   Min: 2
TEMP CON           2

*MOD

    1:3      1:1      1:1      = 45
**$ Property: Water Saturation   Max: 0.5   Min: 0.5
SW CON           0.5

*MOD

    1:3      1:1      1:1      = 1
**$ Property: Oil Saturation   Max: 0.5   Min: 0.5
SO CON           0.5

*MOD

    1:3      1:1      1:1      = 0
**$ Property: Gas Saturation   Max: 0   Min: 0
SG CON           0
**$ Property: Oil Mole Fraction(hydrate)   Max: 1   Min: 1
MFRAC_OIL 'hydrate' CON           1
**$ Property: Gas Mole Fraction(CH4)   Max: 0.9999   Min: 0.9999
MFRAC_GAS 'CH4' CON           0.9999
**$ Property: Gas Mole Fraction(H2O)   Max: 0.0001   Min: 0.0001
MFRAC_GAS 'H2O' CON           0.0001
NUMERICAL
CONVERGE TEMP 10
NEWTONCYC 30
NCUTS 15
RUN
DATE 2007 12 17
DTWELL 0.001
**$
WELL 'Well-1'
INJECTOR UNWEIGHT 'Well-1'
INCOMP WATER 1. 0. 0.
TINJW 45.
OPERATE MAX STW 50000. CONT
**$      rad geofac wfrac skin
GEOMETRY K 0.086 0.249 1. 0.
PERF GEO 'Well-1'
**$ UBA   ff Status Connection
    1 1 1 1. OPEN   FLOW-FROM 'SURFACE'
**$

```

```

WELL 'Well-2'
PRODUCER 'Well-2'
OPERATE MIN BHP 8000. STOP
OPERATE MAX STW 50000. CONT
**$      rad geofac wfrac skin
GEOMETRY K 0.086 0.249 1. 0.
PERF GEO 'Well-2'
**$ UBA  ff Status Connection
    2 1 1 1. OPEN  FLOW-TO 'SURFACE'
**$
WELL 'Well-3'
PRODUCER 'Well-3'
OPERATE MIN BHP 8000. CONT
**$      rad geofac wfrac skin
GEOMETRY K 0.086 0.249 1. 0.
PERF GEO 'Well-3'
**$ UBA  ff Status Connection
    3 1 1 1. OPEN  FLOW-TO 'SURFACE'
DATE 2007 12 17.04167
DATE 2007 12 17.12500
DATE 2007 12 17.25000
DATE 2007 12 17.50000
DATE 2007 12 18
DATE 2007 12 19
DATE 2007 12 20
DATE 2007 12 22
STOP

```

Case 2

The reservoir in this case is depressurized to a Bottom-hole pressure of 2.8 MPa leading to hydrate dissociation. Pressure and temperature for the entire reservoir are 8 MPa and 6°C. Three wells are defined in the first three blocks as in the previous case. Water is injected at a rate of 10,000 m³/day in the first block and produced at the same rate in the second block by a producer well. The temperature of the injected stream (water) is 6°C. This flow rate gave better match of results of CMG STARS with other hydrate codes. The part of data file different from the previous case is given below.

```

**$ Property: Pressure (kPa)  Max: 8000  Min: 8000
PRES CON      8000
**$ Property: Temperature (C)  Max: 6  Min: 6
TEMP CON      6
**$ Property: Water Saturation  Max: 0.5  Min: 0.5
SW CON        0.5

*MOD

    1:2      1:1      1:1      = 1
    3:3      1:1      1:1      = 1
**$ Property: Oil Saturation  Max: 0.5  Min: 0.5
SO CON        0.5

*MOD

```

```

1:2      1:1      1:1      = 0
3:3      1:1      1:1      = 0
**$ Property: Gas Saturation Max: 0 Min: 0
SG CON          0
**$ Property: Water Mole Fraction(H2O) Max: 0.999 Min: 0.999
MFRAC_WAT 'H2O' CON          0.999
**$ Property: Water Mole Fraction(CH4) Max: 0.001 Min: 0.001
MFRAC_WAT 'CH4' CON          0.001
**$ Property: Oil Mole Fraction(hydrate) Max: 1 Min: 1
MFRAC_OIL 'hydrate' CON          1
**$ Property: Gas Mole Fraction(CH4) Max: 0.9999 Min: 0.9999
MFRAC_GAS 'CH4' CON          0.9999
**$ Property: Gas Mole Fraction(H2O) Max: 0.0001 Min: 0.0001
MFRAC_GAS 'H2O' CON          0.0001
NUMERICAL
RUN
DATE 2007 12 17
DTWELL 0.001
**$
WELL 'Well-1'

INJECTOR UNWEIGHT 'Well-1'
INCOMP WATER 1. 0. 0.
TINJW 6.
OPERATE MAX STW 10000. CONT
**$          rad geofac wfrac skin
GEOMETRY K 0.086 0.249 1. 0.
PERF GEO 'Well-1'

**$ UBA      ff Status Connection
      1 1 1 1. OPEN      FLOW-FROM 'SURFACE'

**$
WELL 'Well-2'
PRODUCER 'Well-2'
OPERATE MIN BHP 2800. CONT
OPERATE MAX STW 10000. CONT
**$          rad geofac wfrac skin
GEOMETRY K 0.086 0.249 1. 0.
PERF GEO 'Well-2'
**$ UBA      ff Status Connection
      2 1 1 1. OPEN      FLOW-TO 'SURFACE'
**$
WELL 'Well-3'
PRODUCER 'Well-3'
OPERATE MIN BHP 2800. STOP
**$          rad geofac wfrac skin
GEOMETRY K 0.086 0.249 1. 0.

PERF GEO 'Well-3'
**$ UBA      ff Status Connection
      3 1 1 1. OPEN      FLOW-TO 'SURFACE'
DATE 2007 12 17.00139
DATE 2007 12 17.00347
DATE 2007 12 17.01389
DATE 2007 12 17.04167
DATE 2007 12 17.06250
DATE 2007 12 17.50000
DATE 2007 12 18
DATE 2007 12 19
DATE 2007 12 20
STOP

```

Case 3

In this case the reservoir is depressurized to a lower pressure of 500 kPa. Ice formation is included in the system by adding “*ICE” keyword in the component property section in the input data file. Three wells are defined as in the previous case to ensure that the water saturation in the first block is always one and the bottom-hole pressure applied is 500 kPa.

```
WELL 'Well-1'
INJECTOR UNWEIGHT 'Well-1'
INCOMP WATER 1. 0. 0.
TINJW 6.
OPERATE MAX STW 50000. CONT
**$      rad geofac wfrac skin
GEOMETRY K 0.086 0.249 1. 0.
PERF GEO 'Well-1'
**$ UBA  ff Status Connection
      1 1 1 1. OPEN  FLOW-FROM 'SURFACE'
WELL 'Well-2'
PRODUCER 'Well-2'
OPERATE MIN BHP 500. CONT
OPERATE MAX STW 50000. CONT
**$      rad geofac wfrac skin
GEOMETRY K 0.086 0.249 1. 0.
PERF GEO 'Well-2'
**$ UBA  ff Status Connection
      2 1 1 1. OPEN  FLOW-TO 'SURFACE'
WELL 'Well-3'
PRODUCER 'Well-3'
OPERATE MIN BHP 500. STOP
**$      rad geofac wfrac skin
GEOMETRY K 0.086 0.249 1. 0.
PERF GEO 'Well-3'
**$ UBA  ff Status Connection
      3 1 1 1. OPEN  FLOW-TO 'SURFACE'
```

Results

CASE 1

Profiles of aqueous saturation for CMG STARS are in good agreement with other codes. Initially water saturation is 0.5 for the entire reservoir. It is subject to a boundary condition $S_w = 1.0$ at $x=0$. In STARS the boundary condition is obtained by continuous injection and production of water from the first and second blocks. Unlike other codes STARS took a little longer time to maintain this boundary condition. It can be seen from Figure 3-20 that aqueous saturation for the first half of the domain is highly affected by the boundary

condition. There is a drop in the aqueous saturation values due to secondary hydrate formation. Figure 3-20 shows profiles of aqueous saturation for selected time steps (1 hr, 3 hrs, 6 hrs, 12 hrs, 1 day, 2 days, 3 days, 5 days).

Initially there is no gas in the reservoir. Hydrate dissociates due to the heat given to the system in the form of boundary condition at $x = 0$, $T_o = 45^\circ\text{C}$. Gas saturation at $x = 0$, is not zero initially because the water saturation at this point is not 1. Higher saturations are observed near the well bore for different time steps given in Figure 3-21. Results of CMG STARS are in good agreement with other codes.

Hydrate saturation is 0.5 initially for the entire reservoir. Due to thermal stimulation hydrate which is near to the well bore quickly dissociates. Hydrate formation is also observed in this case. All the simulators captured the movement of dissociation front in the same way. As the simulation proceeds hydrate dissociates slowly which indicates the slow movement of the thermal wave in the reservoir as shown in Figure 3-22. At the end of the simulation which is at 5 days hydrate in the first half of the domain dissociates completely.

This is a thermal stimulation case so it is very important to match temperature profiles. CMG STARS are in excellent agreement with other codes as seen from Figure 3-23. Small peaks in the profiles of temperature show the movement of dissociation front.

Aqueous relative permeability is a function of aqueous saturation. As the simulation proceeds and boundary condition of water saturation equal to 100% is attained in the first block there is a complete match of the permeability curves. Figure 3-24 shows the aqueous permeability curves at different time steps. Due to the injector and the producer wells in the system the

pressure of the reservoir is shifted to a higher value. This is shown in Figure 3-26. Due to higher pressure values aqueous mass fraction is also shifted as shown in Figure 3-25. Capillary pressure is expressed as a function of liquid saturation in STARS. However the profiles of capillary pressure look similar to other codes as in Figure 3-27

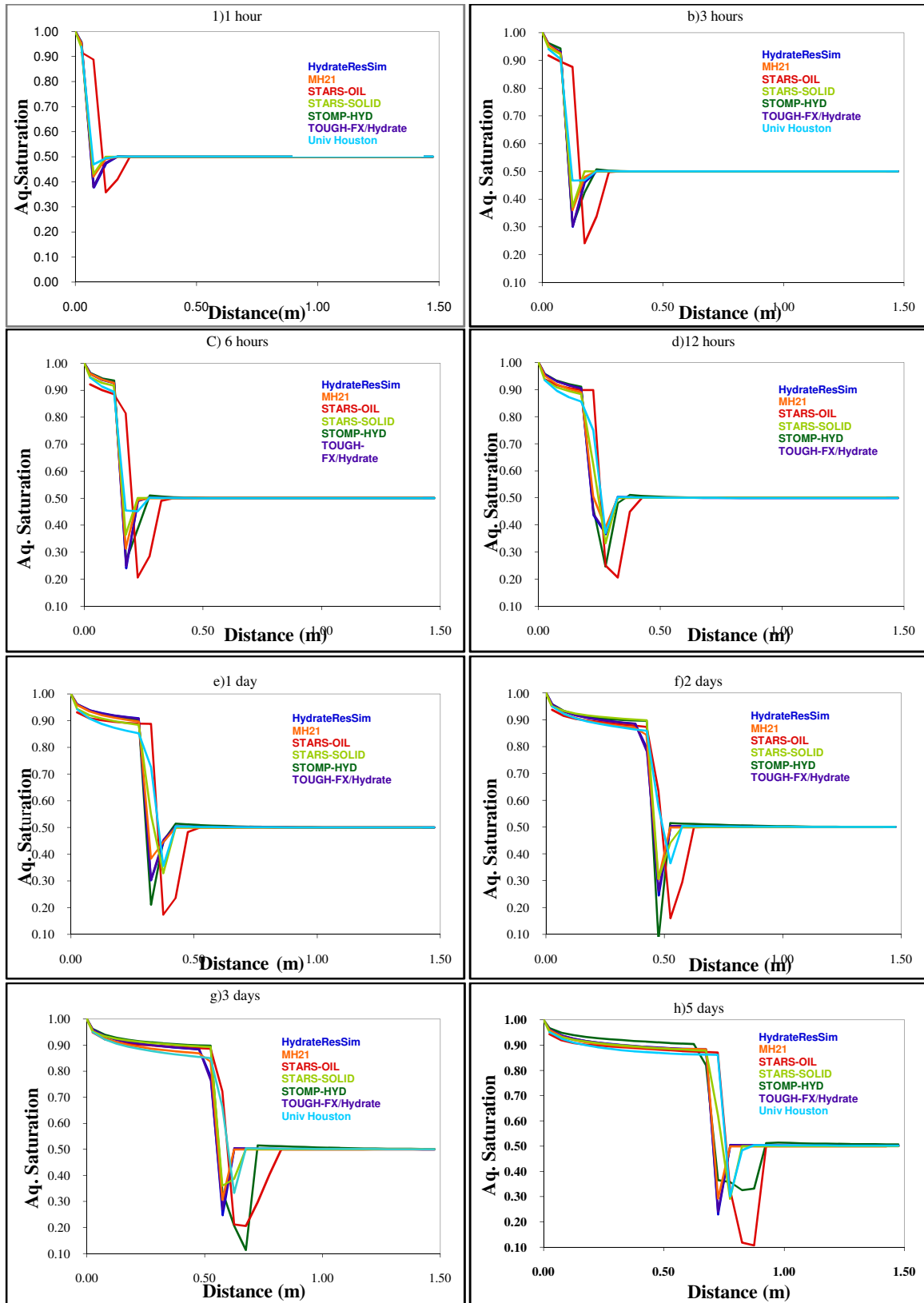


Figure 3- 20 Profiles of Aqueous saturation at different times for problem 3 Case 1

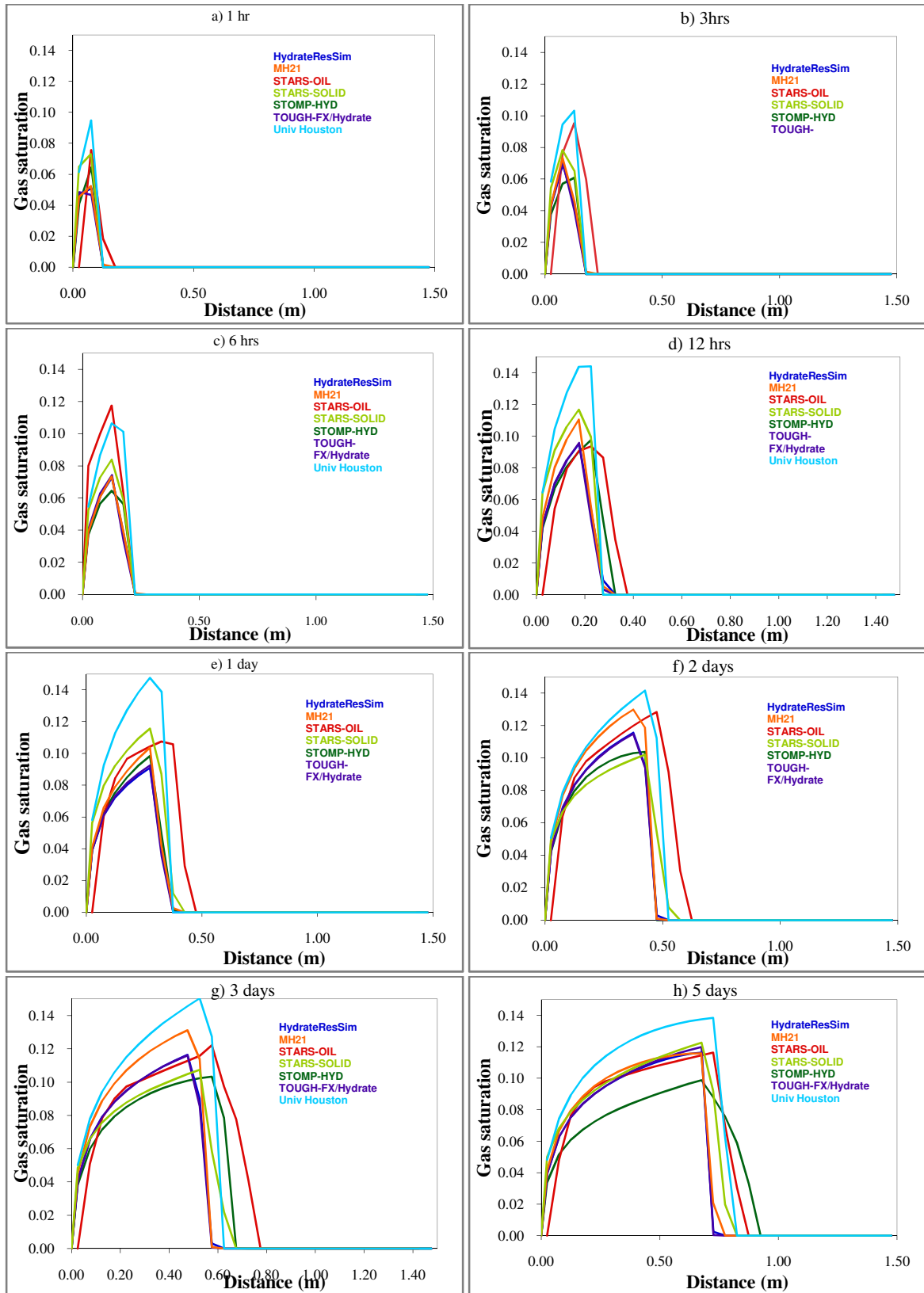


Figure 3- 21 Profiles of gas saturation at different time steps for Problem 3 Case 1

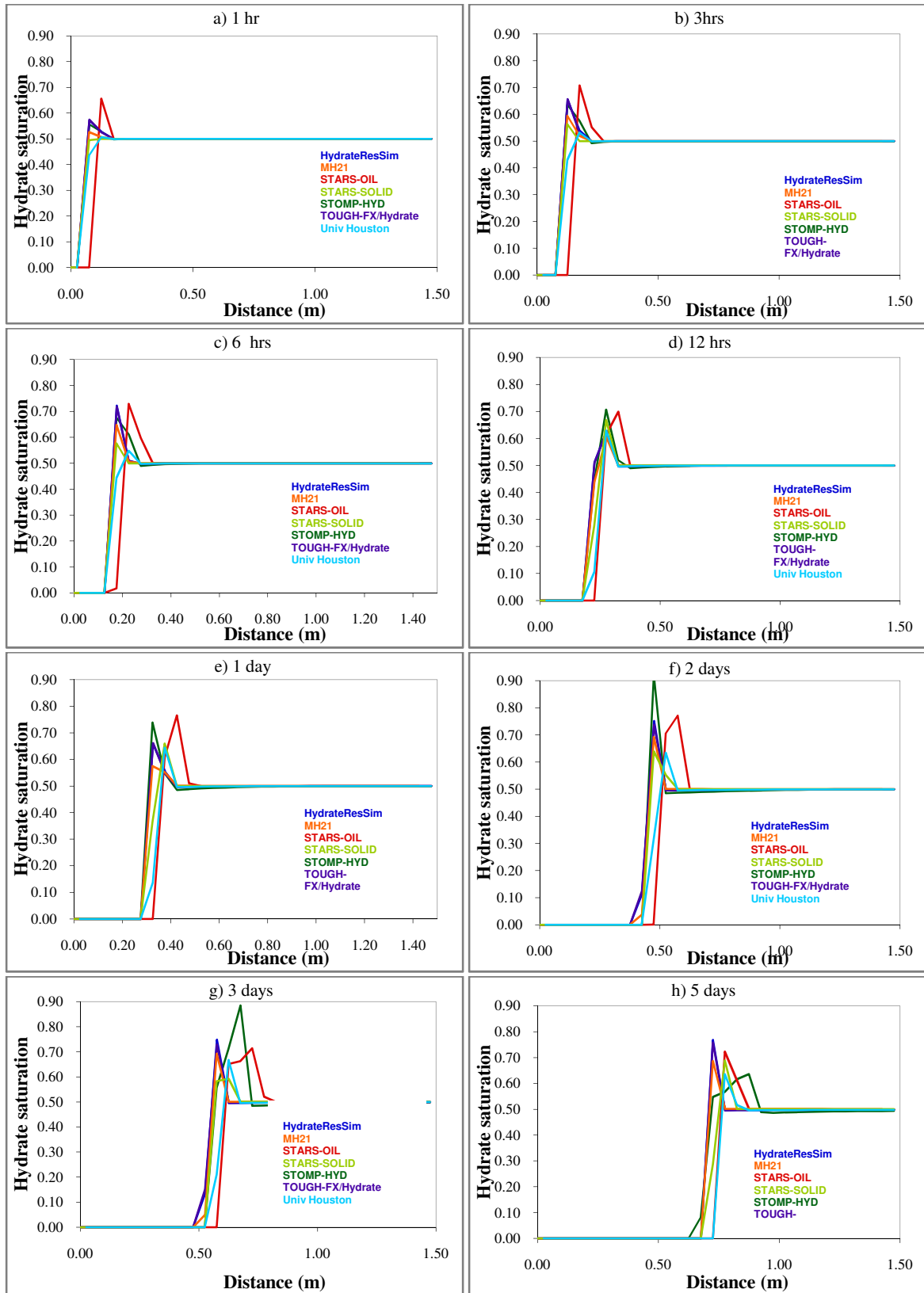


Figure 3- 22 Profiles of hydrate saturation at different times for Problem 3 Case 1

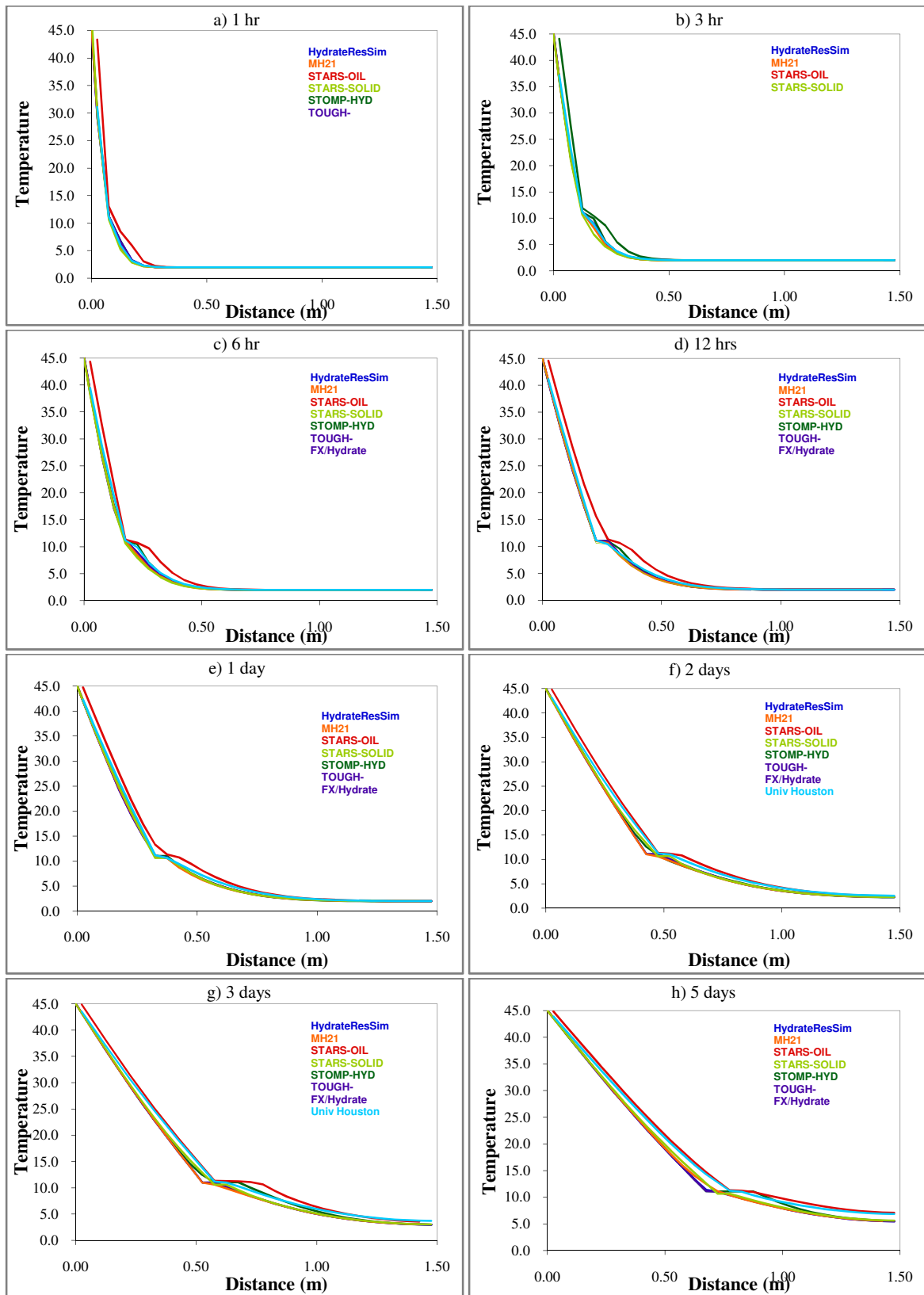


Figure 3- 23 Profiles of temperature at different times for Problem 3 Case 1

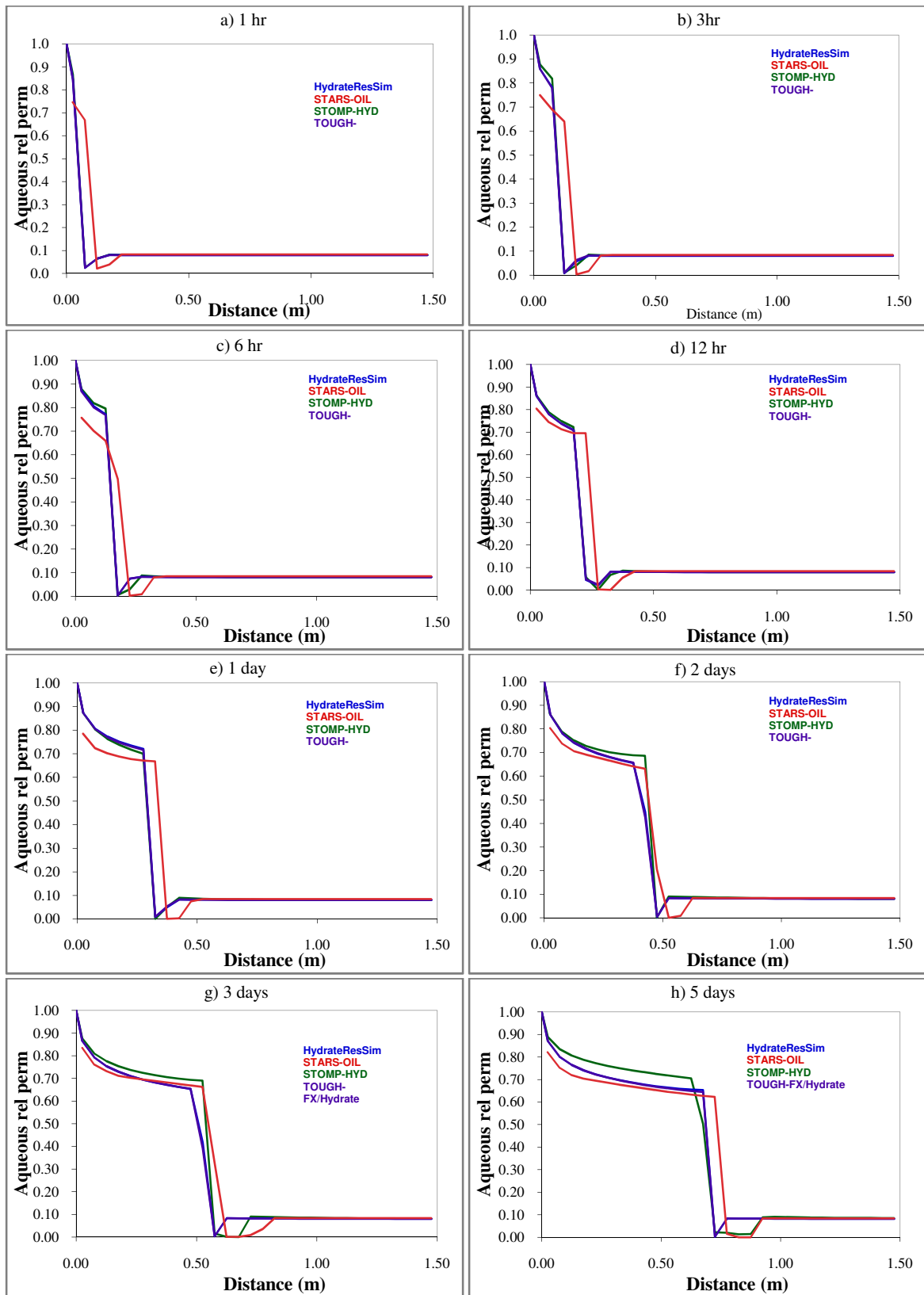


Figure 3- 24 Profiles of Aqueous relative permeability at different times for Problem 3 Case 1

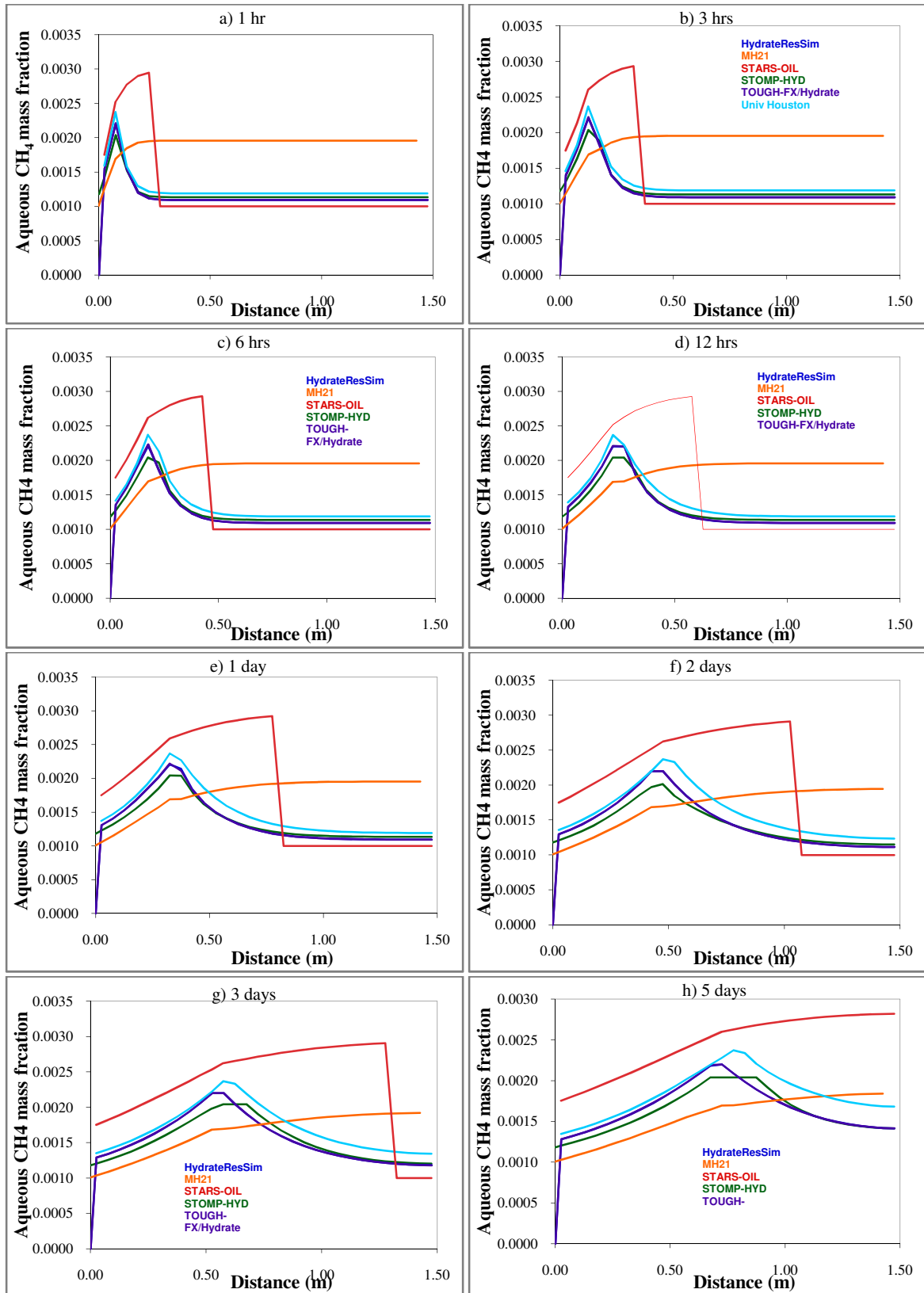


Figure 3- 25 Profiles of Aqueous methane mass fraction at different times for Problem 3 Case 1

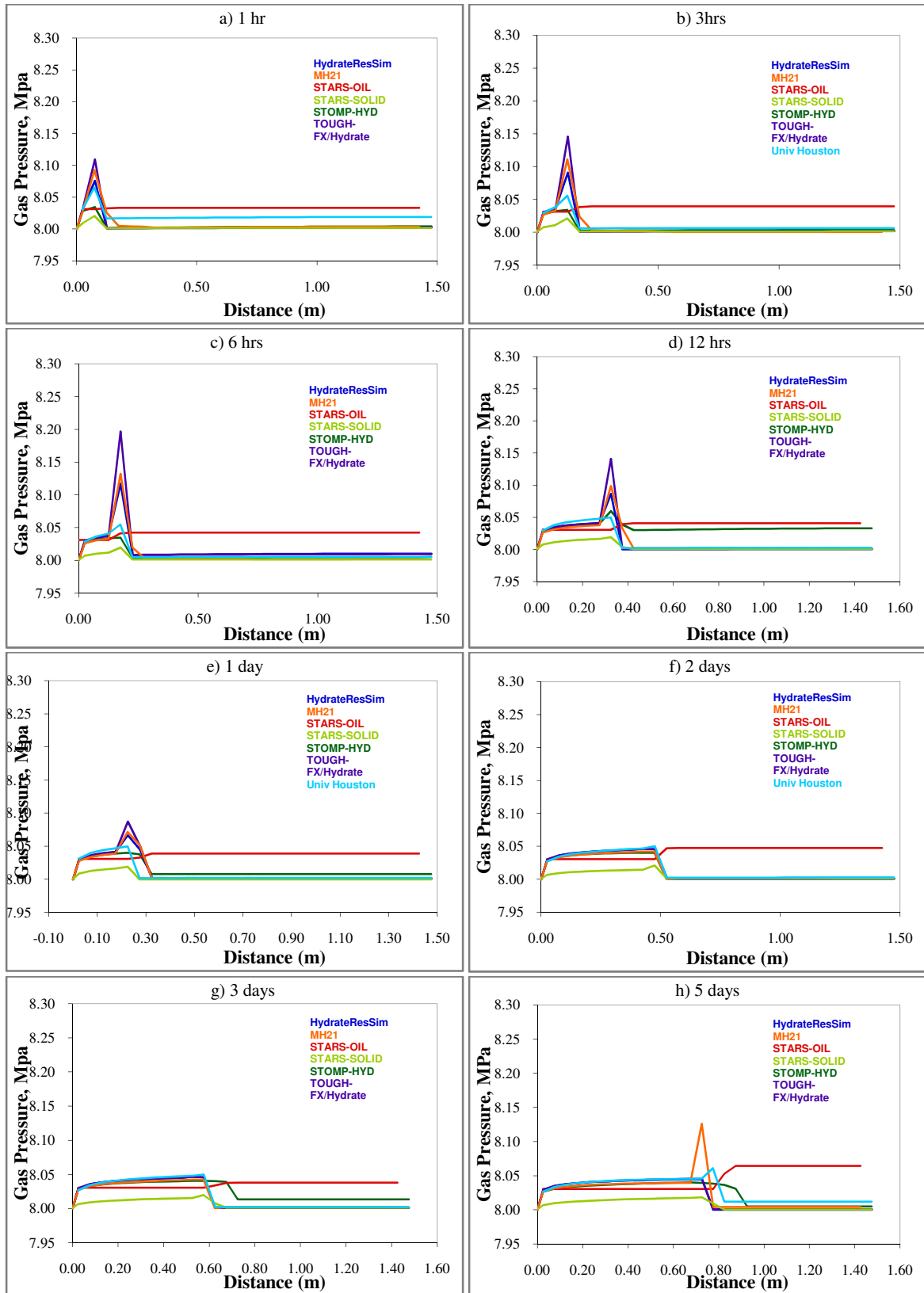


Figure 3- 26 Profiles of Pressure at different times for Problem 3 Case 1

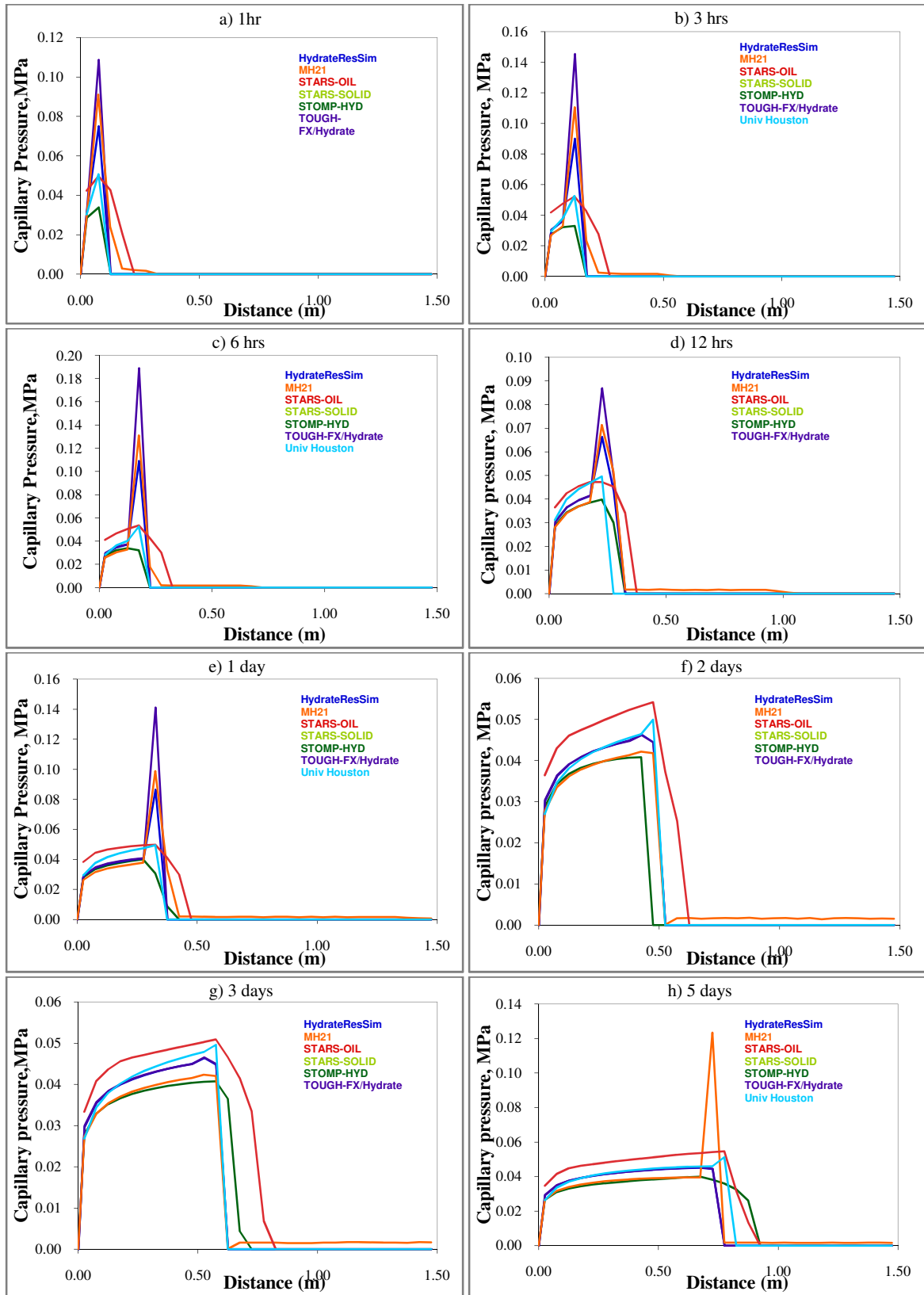


Figure 3- 27 Profiles of capillary pressure at different times for Problem 3 Case 1

CASE 2

As in the previous discussion the boundary condition ($x = 0, S_w = 1.0$) is not maintained initially but after some time as the simulation proceeds this difficulty is also achieved. Figure 3-29 shows profiles of aqueous saturation in good agreement with other codes

Initially there is no gas in the reservoir. Hydrate dissociates due to depressurization of the well. Figure 3-30 shows the profiles of gas saturation. Profiles of hydrate saturation, temperature and aqueous methane mass fraction are in good agreement with other codes as shown in Figure 3-31, Figure 3-32 and Figure 3-34.

Aqueous relative permeability curves are affected initially due to the boundary condition problem as shown in Figure 3-33. As the time proceeds good match of permeability curves with other codes for CMG STARS is obtained. Profiles of gas pressure as in Figure 3-35 shows the propagation of the pressure wave when the reservoir is depressurized. Initially the reservoir pressure is at 8 MPa and is depressurized to 2.8 MPa. Capillary pressure is expressed as a function of liquid saturation (water + hydrate) in STARS. However the profiles of capillary pressure look similar to other codes as shown in Figure 3-36. Figure 3.28 shows cumulative and gas rates for CMG STARS.

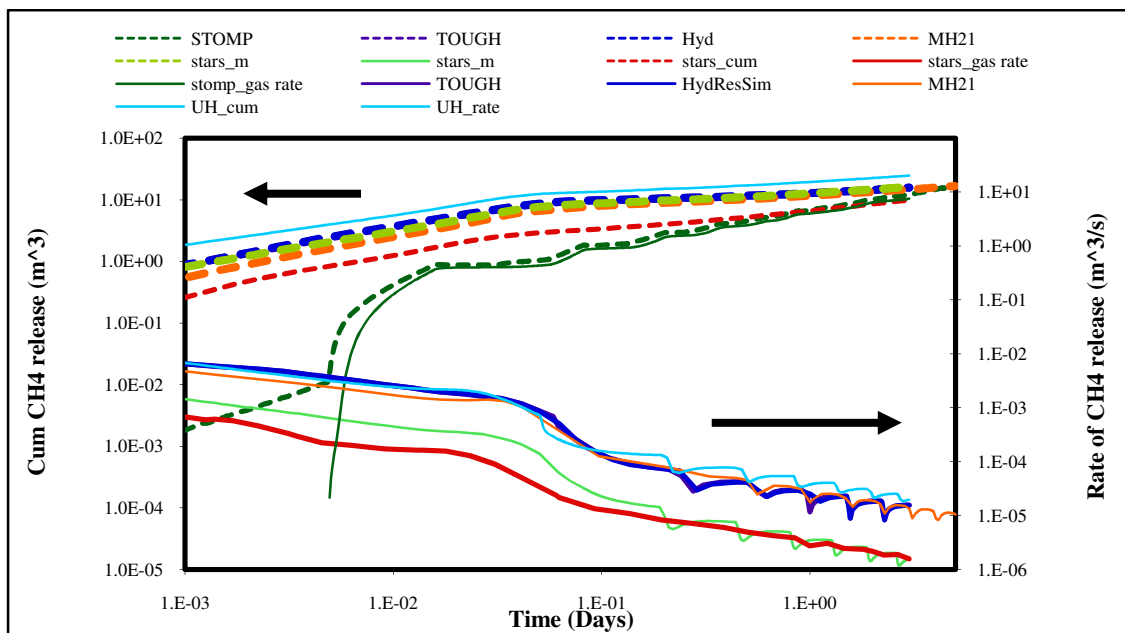
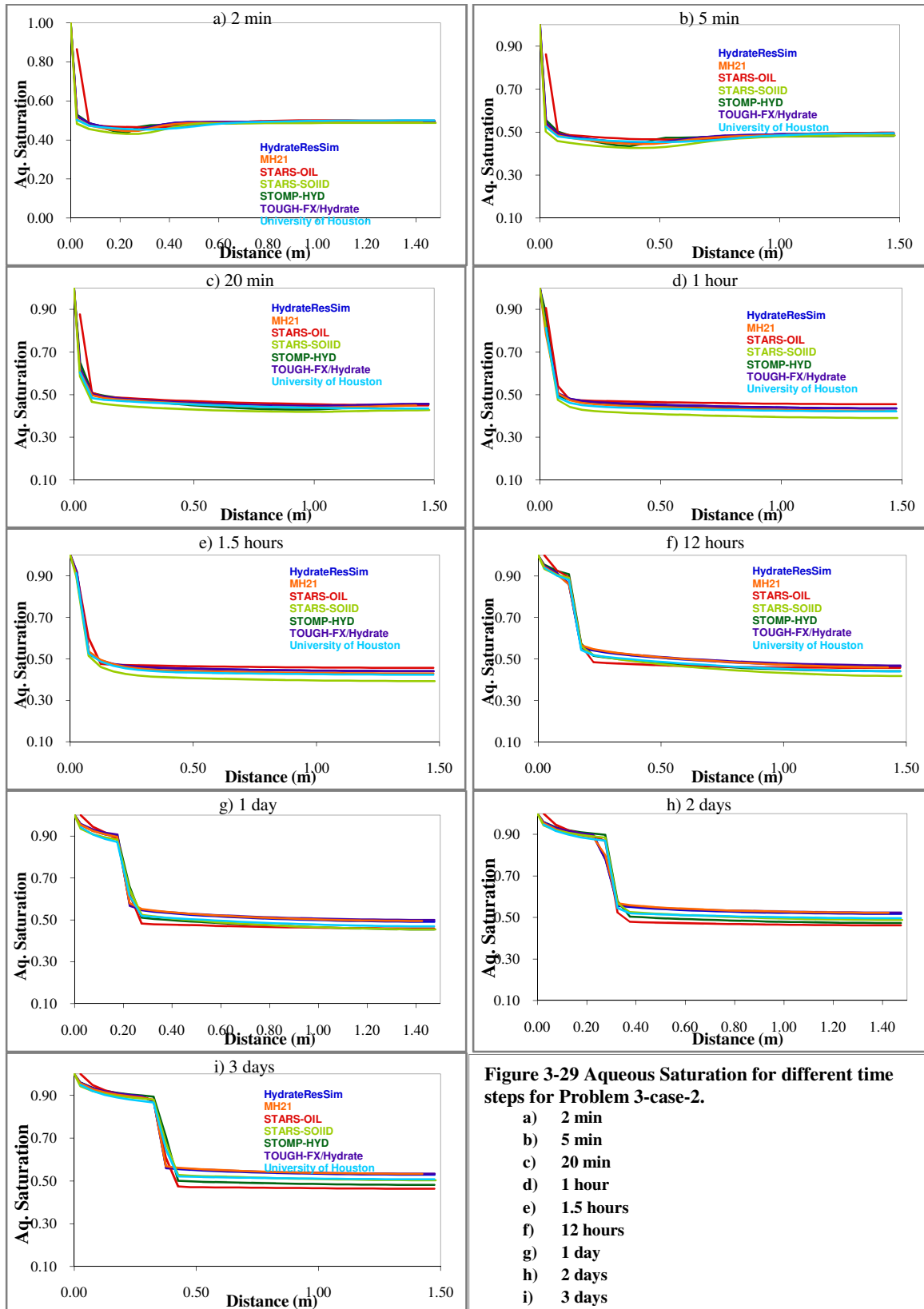


Figure 3- 28 Production rates for problem 3, Case 2

Aqueous Saturation



Gas Saturation

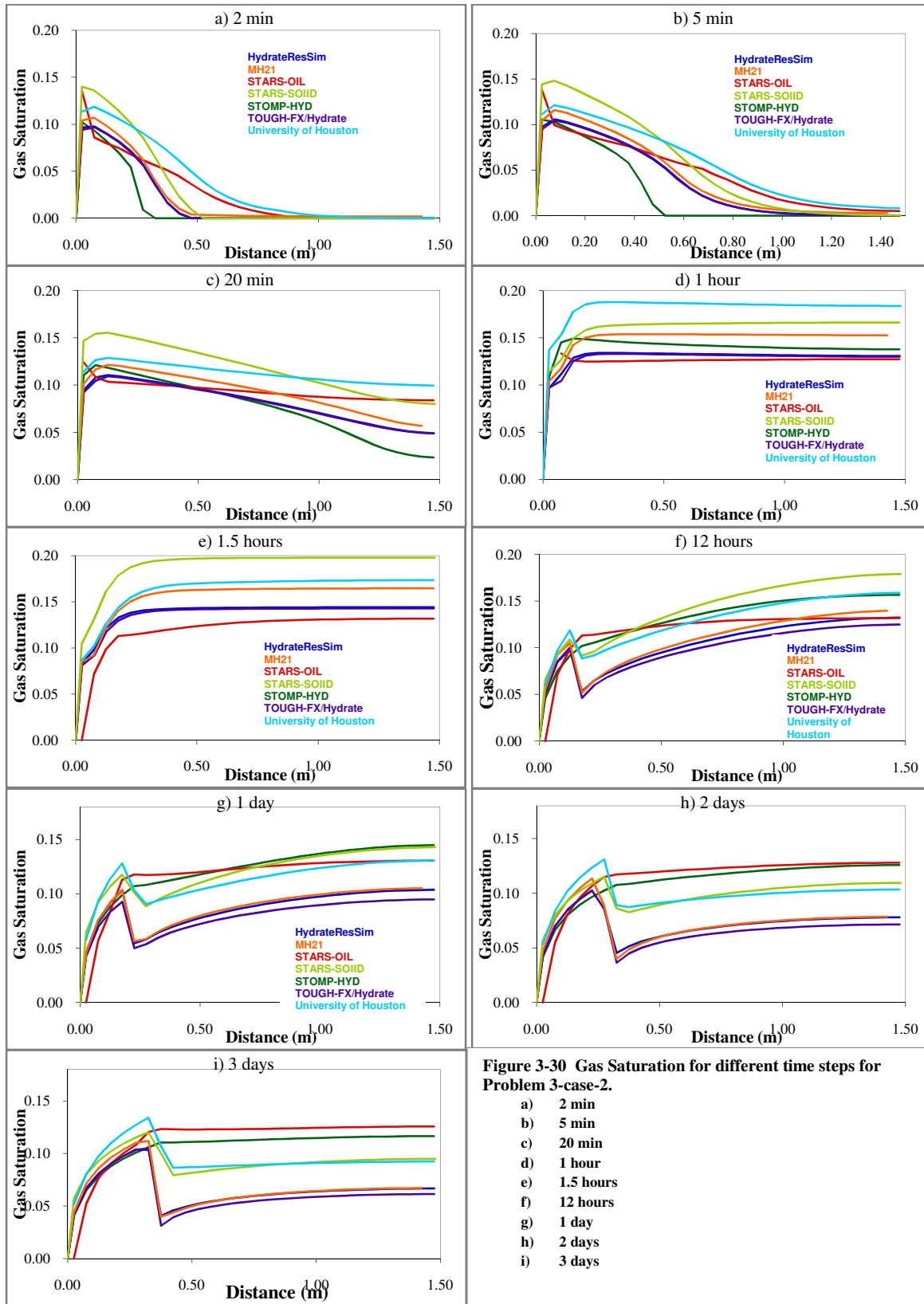


Figure 3-30 Gas Saturation for different time steps for Problem 3-case-2.

- a) 2 min
- b) 5 min
- c) 20 min
- d) 1 hour
- e) 1.5 hours
- f) 12 hours
- g) 1 day
- h) 2 days
- i) 3 days

Hydrate Saturation

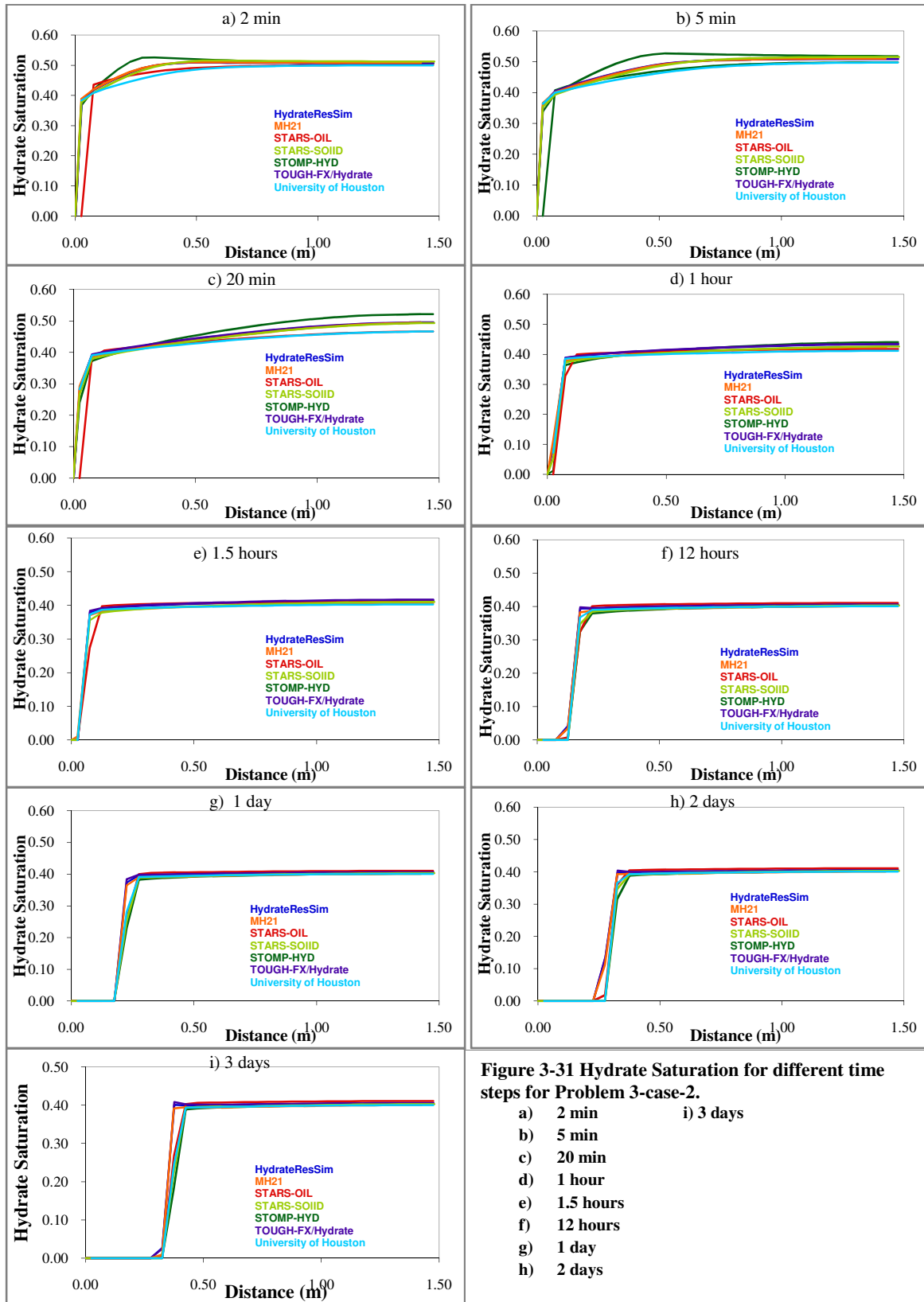


Figure 3-31 Hydrate Saturation for different time steps for Problem 3-case-2.

- a) 2 min
- b) 5 min
- c) 20 min
- d) 1 hour
- e) 1.5 hours
- f) 12 hours
- g) 1 day
- h) 2 days
- i) 3 days

Temperature

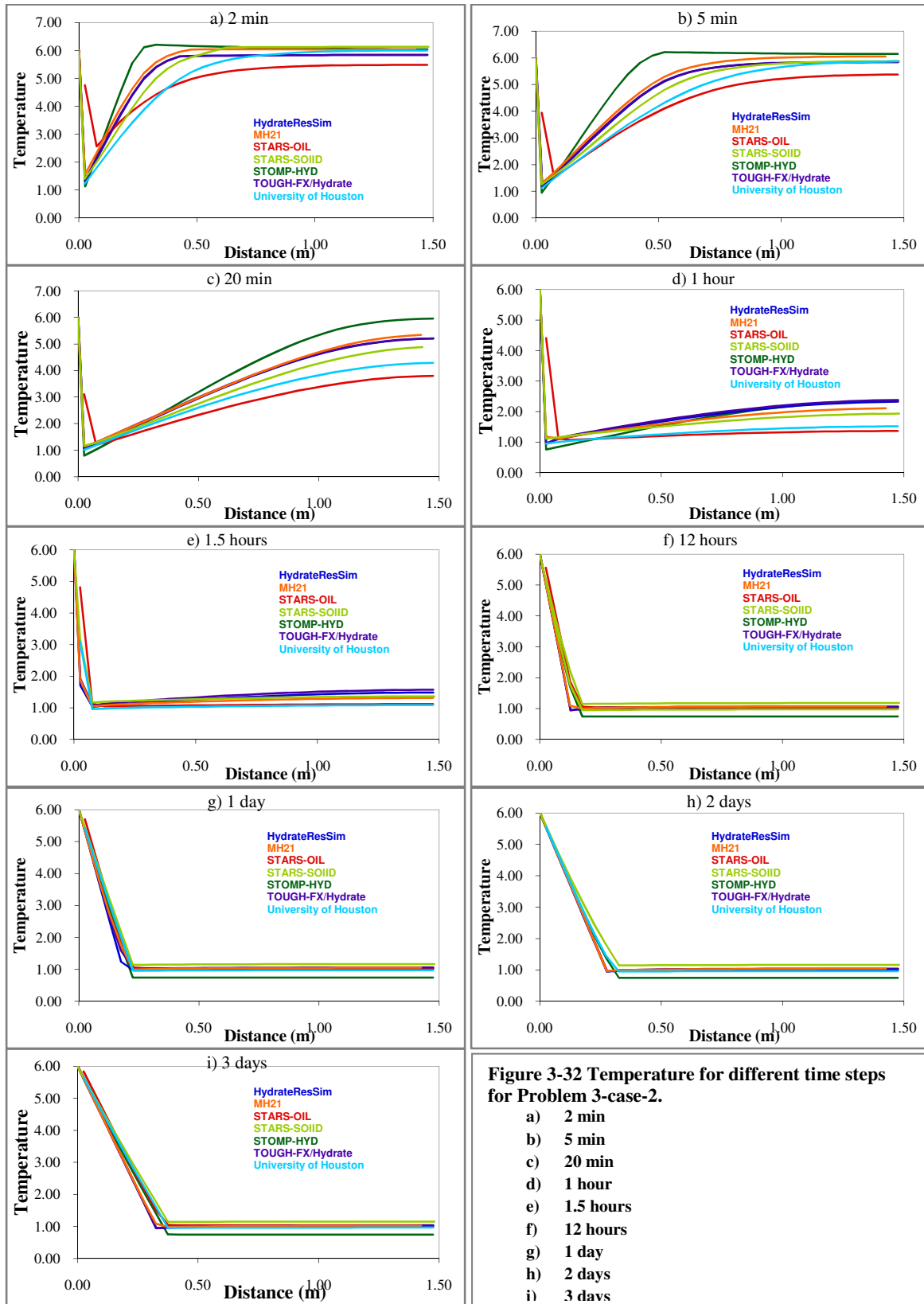
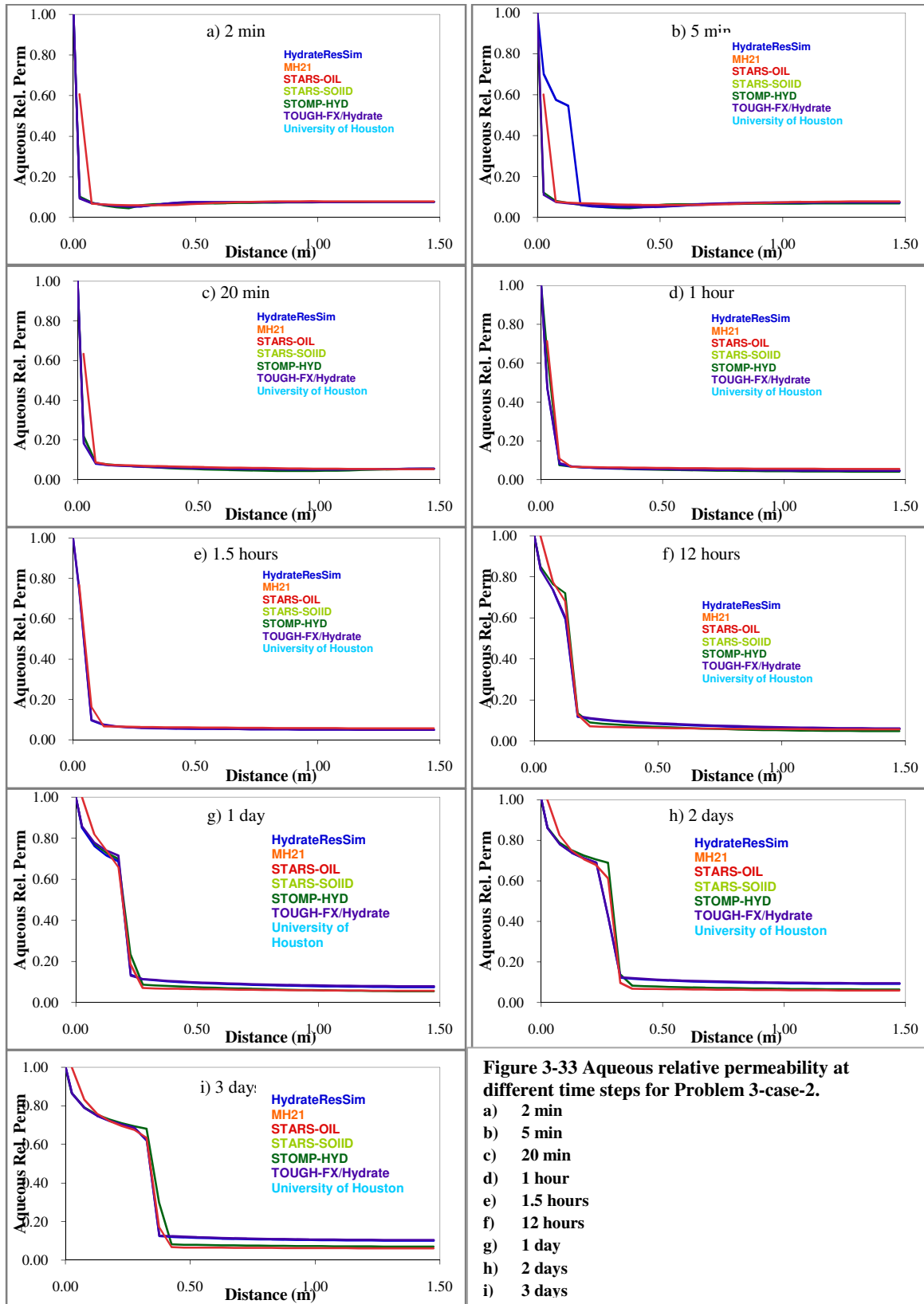


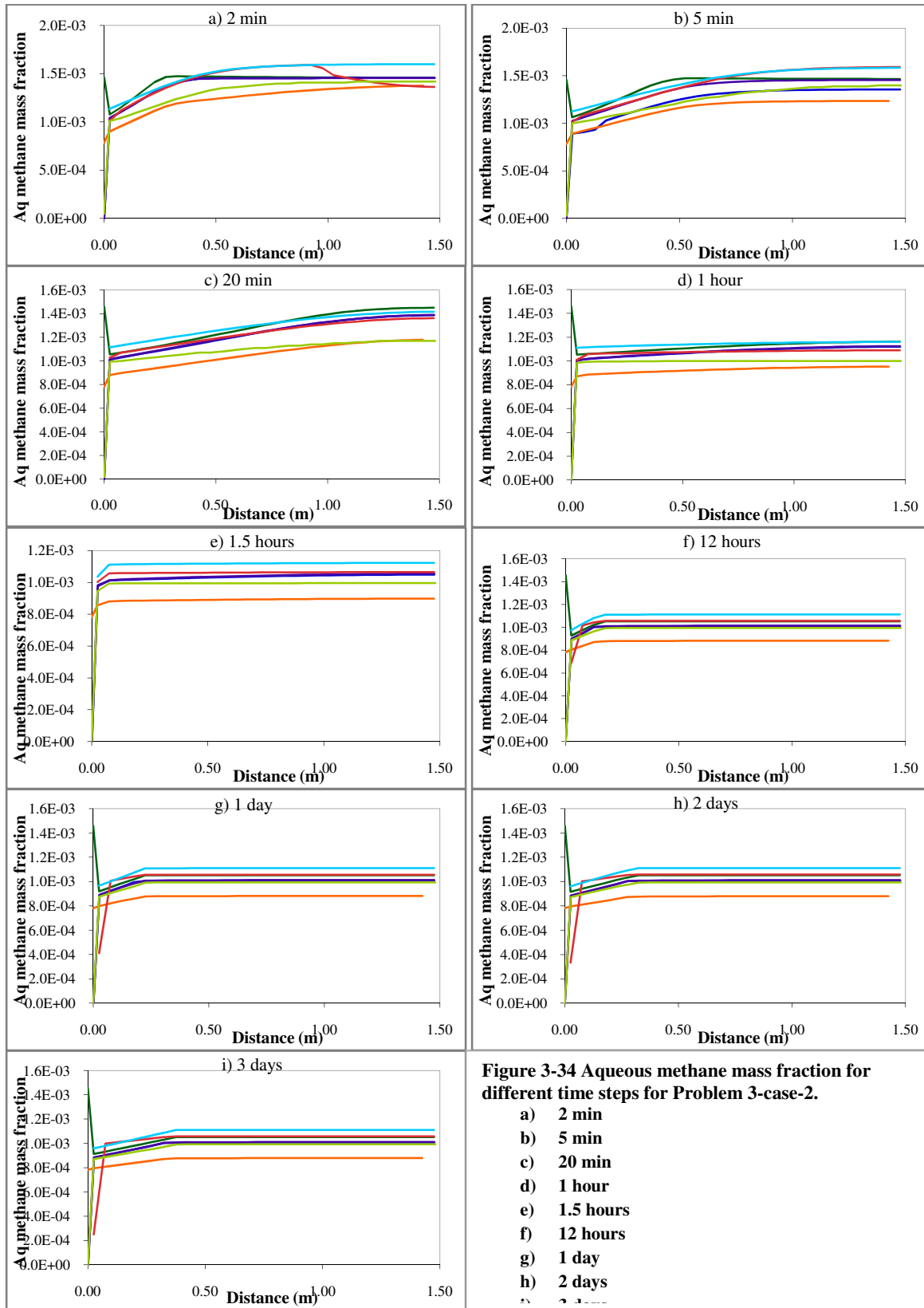
Figure 3-32 Temperature for different time steps for Problem 3-case-2.

- a) 2 min
- b) 5 min
- c) 20 min
- d) 1 hour
- e) 1.5 hours
- f) 12 hours
- g) 1 day
- h) 2 days
- i) 3 days

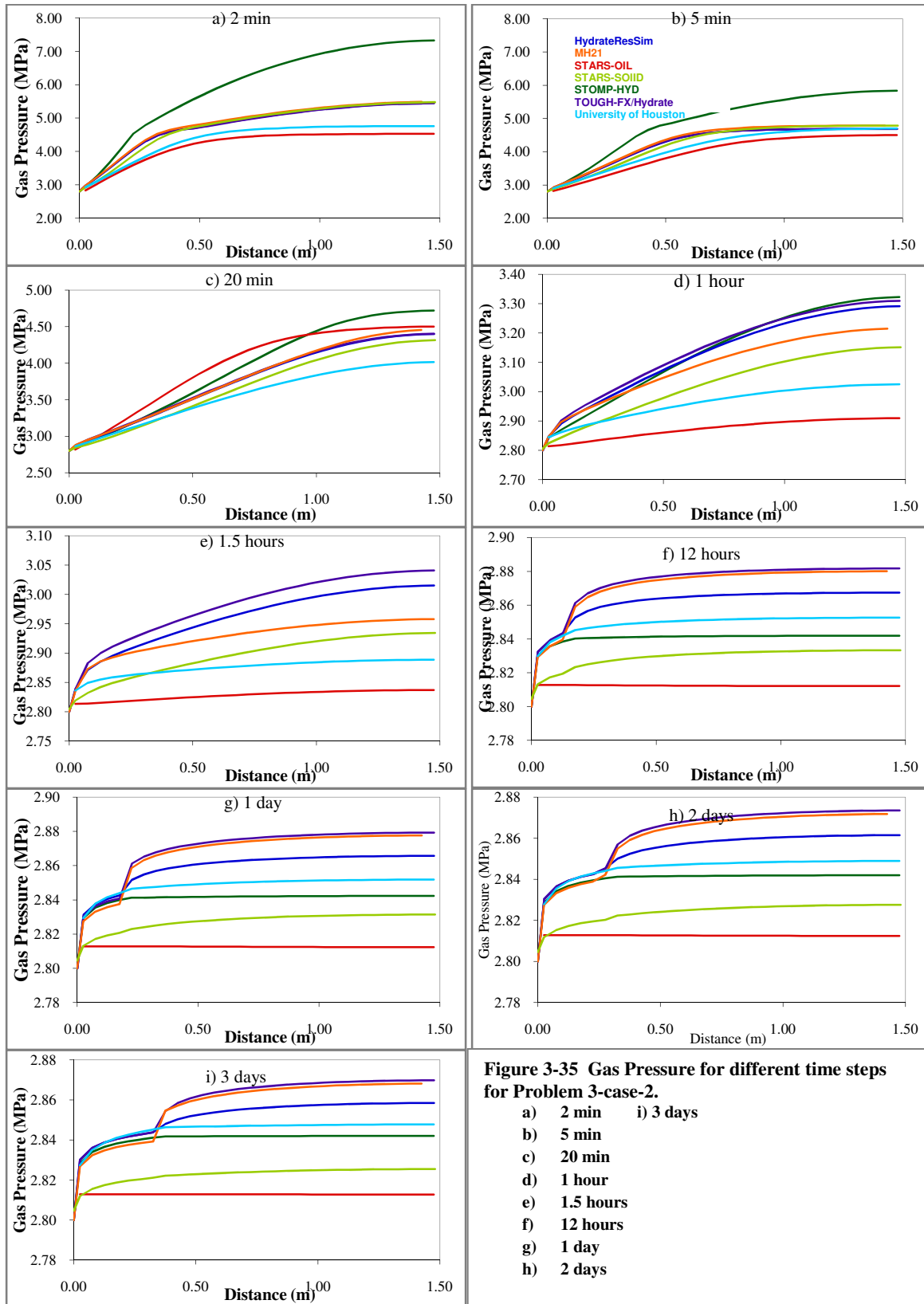
Aqueous phase relative permeability



Aqueous phase methane mass fraction



Gas pressure



Gas water capillary pressure

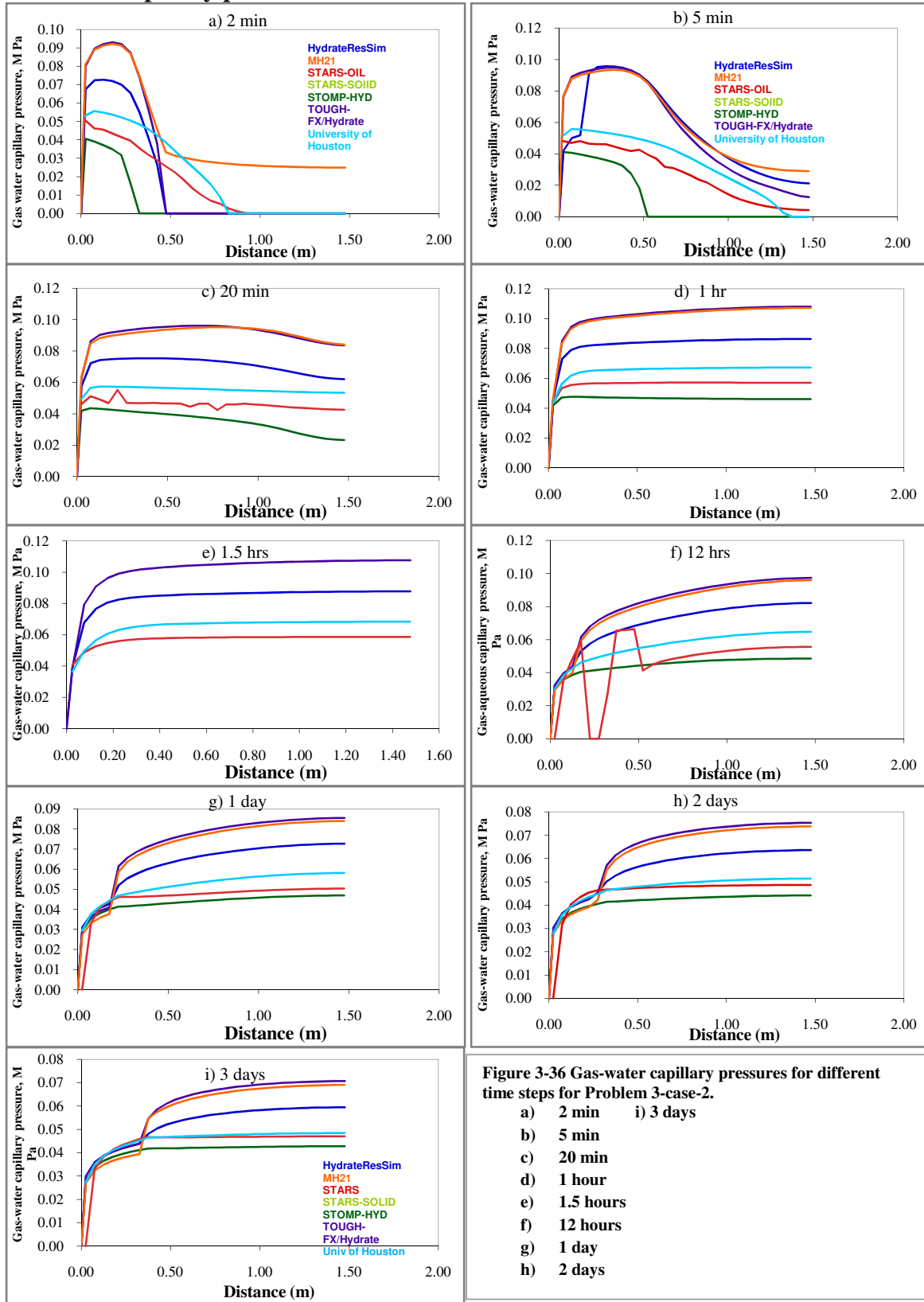


Figure 3-36 Gas-water capillary pressures for different time steps for Problem 3-case-2.

- a) 2 min
- b) 5 min
- c) 20 min
- d) 1 hour
- e) 1.5 hours
- f) 12 hours
- g) 1 day
- h) 2 days
- i) 3 days

Case 3

In this case, the reservoir is depressurized to a pressure below the Quadruple point leading to ice formation. Differences in the results of various simulators are obtained due to ice formation in the system. The observed differences are due to the way each simulator calculates the ice formation phenomena. There are two ways in which ice can be specified in the input data file of CMG STARS. Ice can be specified by adding the keyword *ICE in the component property section of the input data file. When this is used, temperatures down to -100°C can be tolerated in the reservoir. The other way is not using this default, but to specify ice as a component and include its reactions (melting & formation). In this method, the minimum temperature allowed is 0.85° and so the entire reservoir and its reactions are scaled up to a higher temperature during the simulation and reset again in the results. Both methods were used to run the simulations for matching results with the other codes. The results that will be presented in this document will be of those obtained from *ICE method of specifying the ice component.

Initially hydrate and aqueous saturation are 0.5 each. As the simulation proceeds, hydrate dissociates giving gas and water molecules. In this problem hydrate dissociation occurs at different points for different simulators. Figure 3-37 shows the movement of dissociation front for CMG STARS at different time steps. Profiles of aqueous saturation, aqueous phase relative permeability and temperature for CMG STARS are shown in Figure 3-38, 3-39 and 3-40 respectively. They are found to be in good agreement with other codes.

More ice formation is seen in STARS simulations at the beginning of the run itself (shown in Figure 3-41). Due to this extra ice in the first few blocks of the grid, there is no void space

for the dissociated methane to escape in the gas phase and as a result increase in the aqueous phase methane mass fraction is observed as in Figure 3-43. There is no much increase in the gas pressure (shown in Figure 3-44) initially, which shows there is something wrong in the whole calculation process of CMG. This also explains the high irregularity in the gas saturation curves as shown in Figure 3-42.

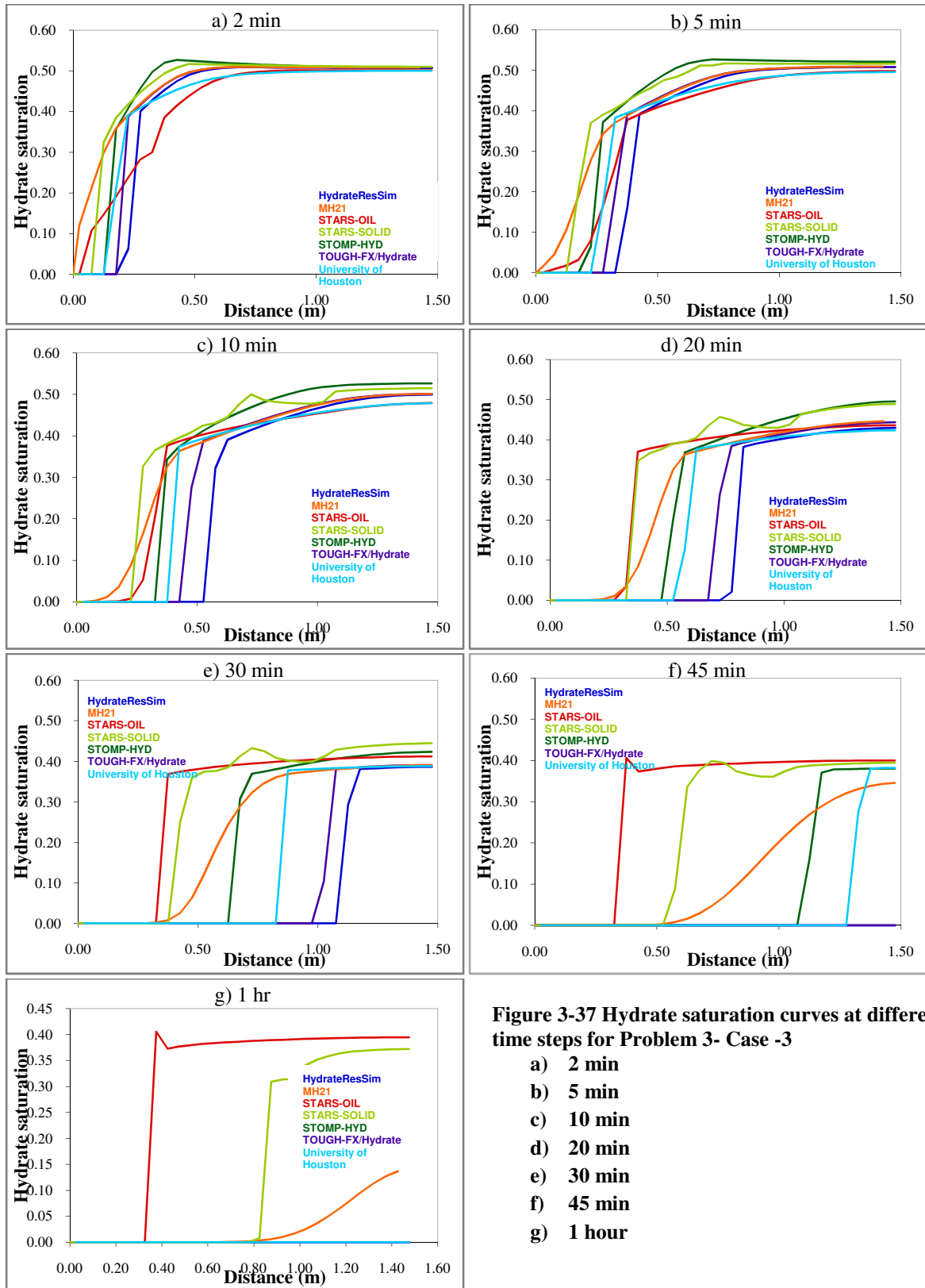


Figure 3-37 Hydrate saturation curves at different time steps for Problem 3- Case -3

- a) 2 min
- b) 5 min
- c) 10 min
- d) 20 min
- e) 30 min
- f) 45 min
- g) 1 hour

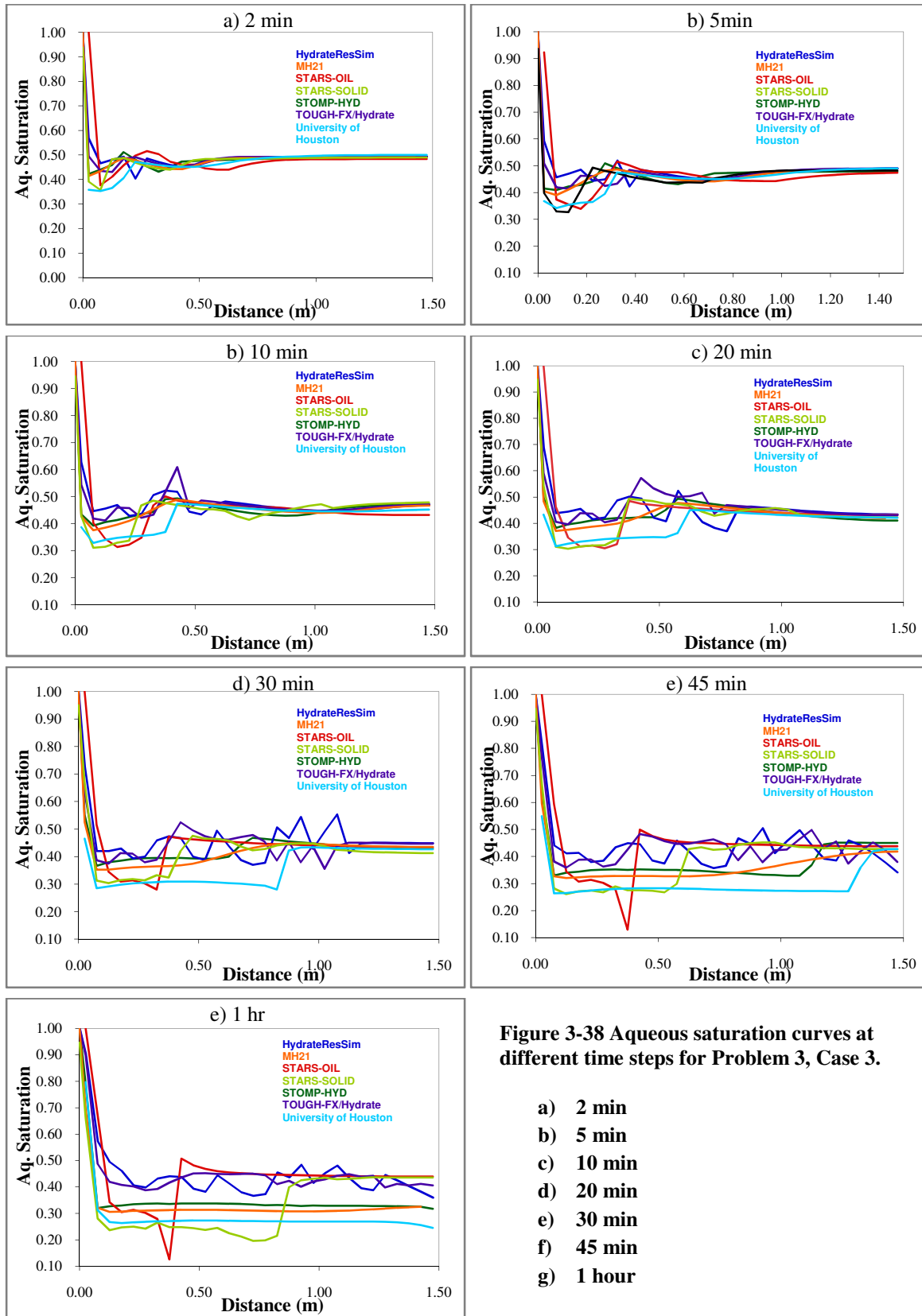


Figure 3-38 Aqueous saturation curves at different time steps for Problem 3, Case 3.

- a) 2 min
- b) 5 min
- c) 10 min
- d) 20 min
- e) 30 min
- f) 45 min
- g) 1 hour

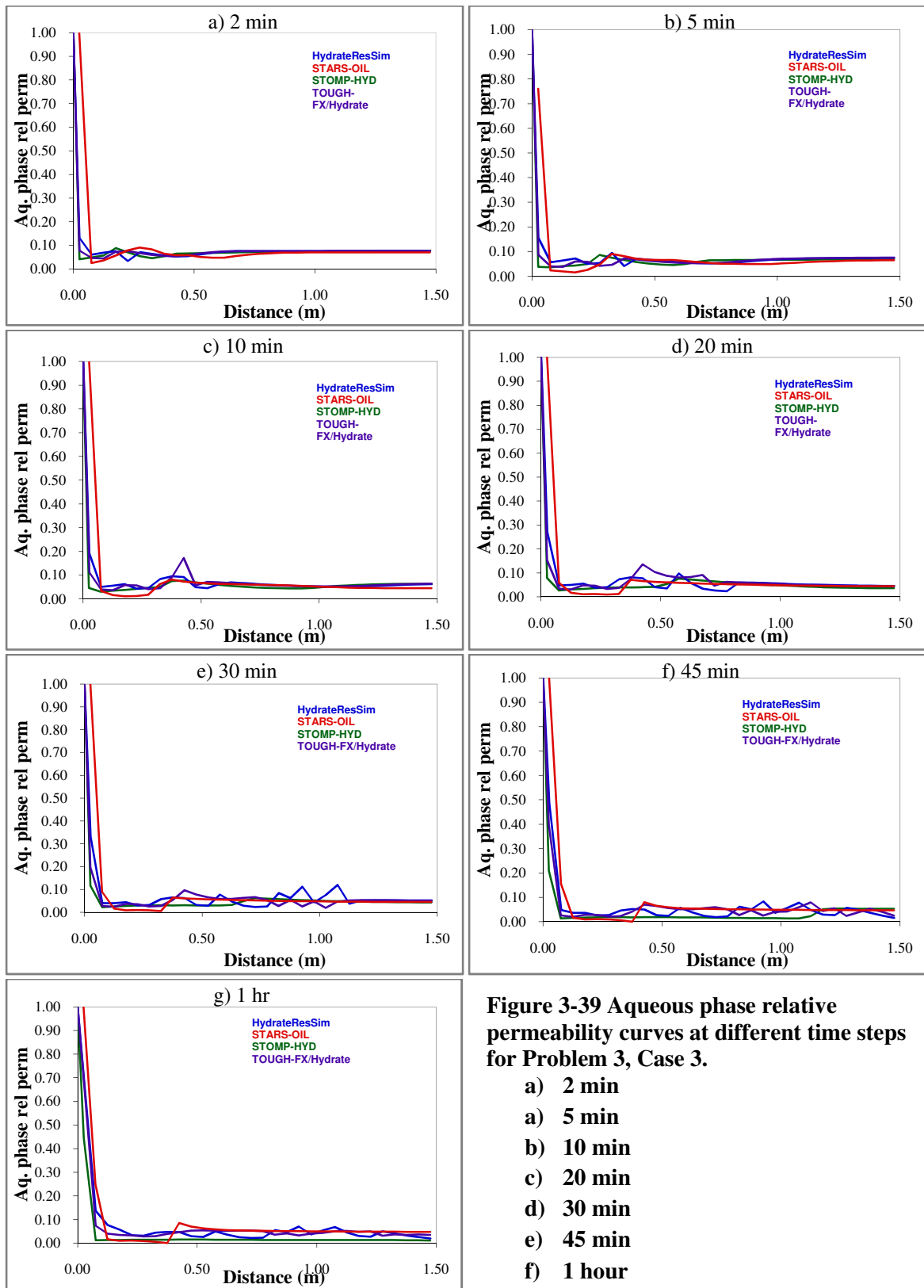
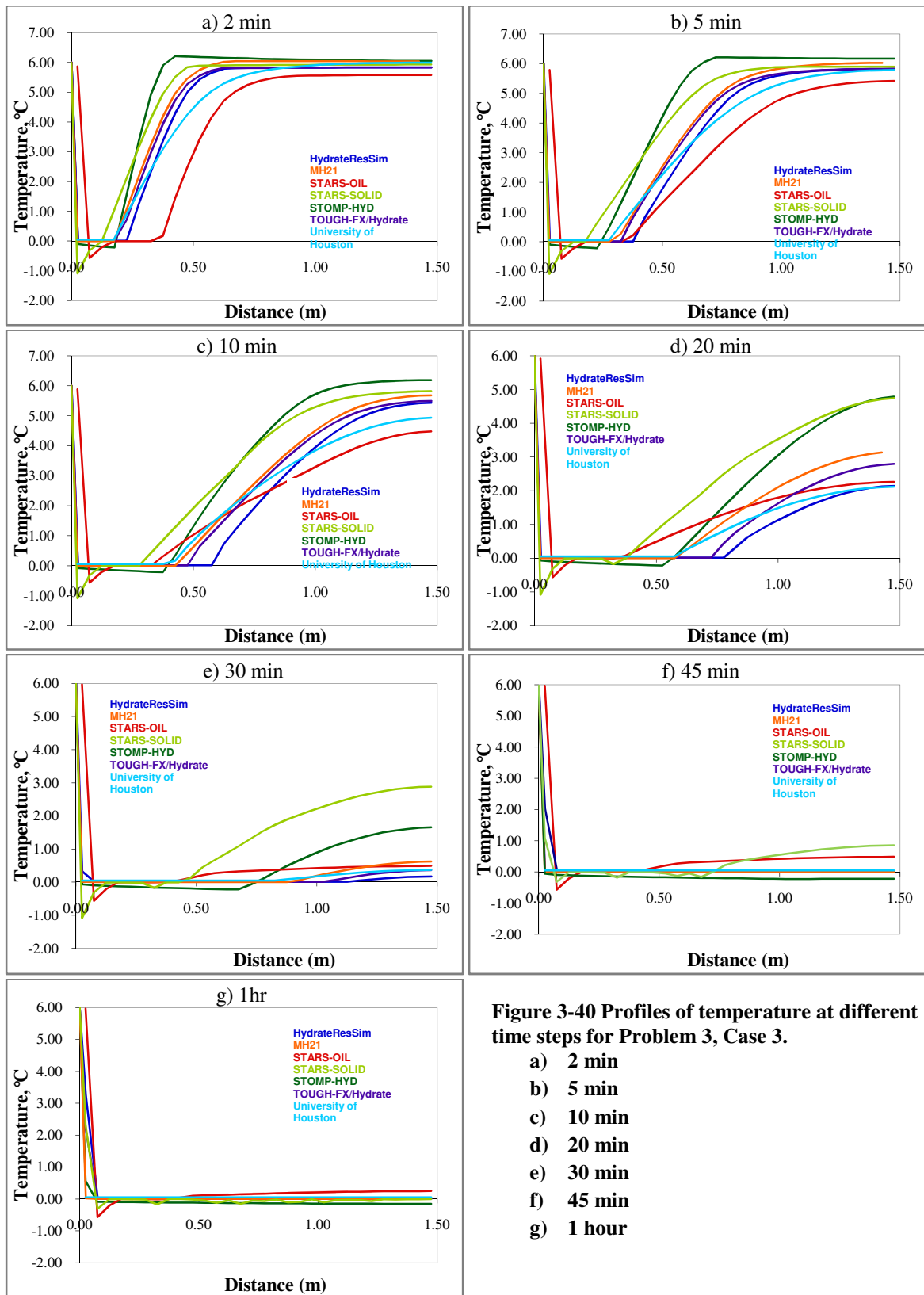


Figure 3-39 Aqueous phase relative permeability curves at different time steps for Problem 3, Case 3.

- a) 2 min
- a) 5 min
- b) 10 min
- c) 20 min
- d) 30 min
- e) 45 min
- f) 1 hour



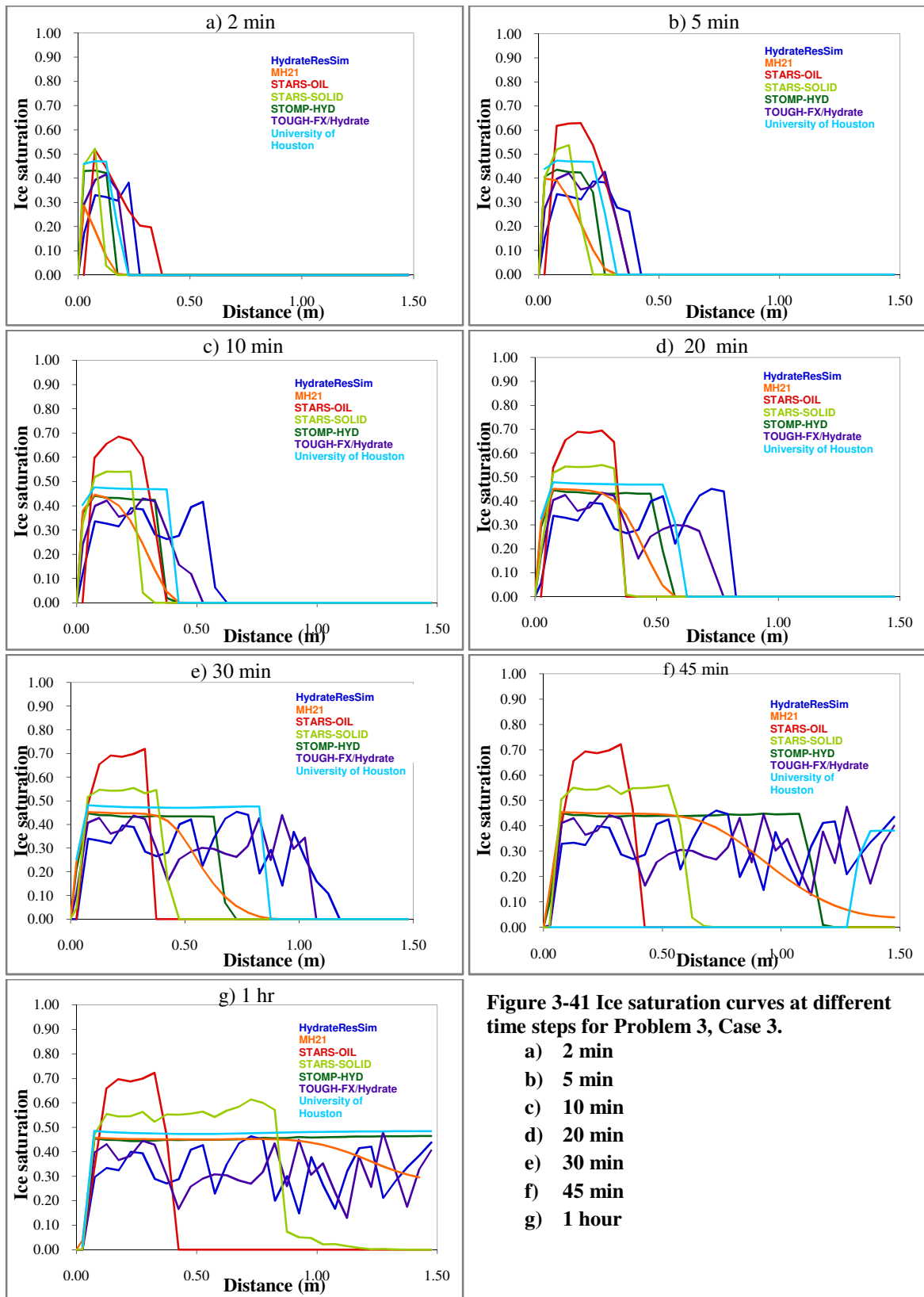


Figure 3-41 Ice saturation curves at different time steps for Problem 3, Case 3.

- a) 2 min
- b) 5 min
- c) 10 min
- d) 20 min
- e) 30 min
- f) 45 min
- g) 1 hour

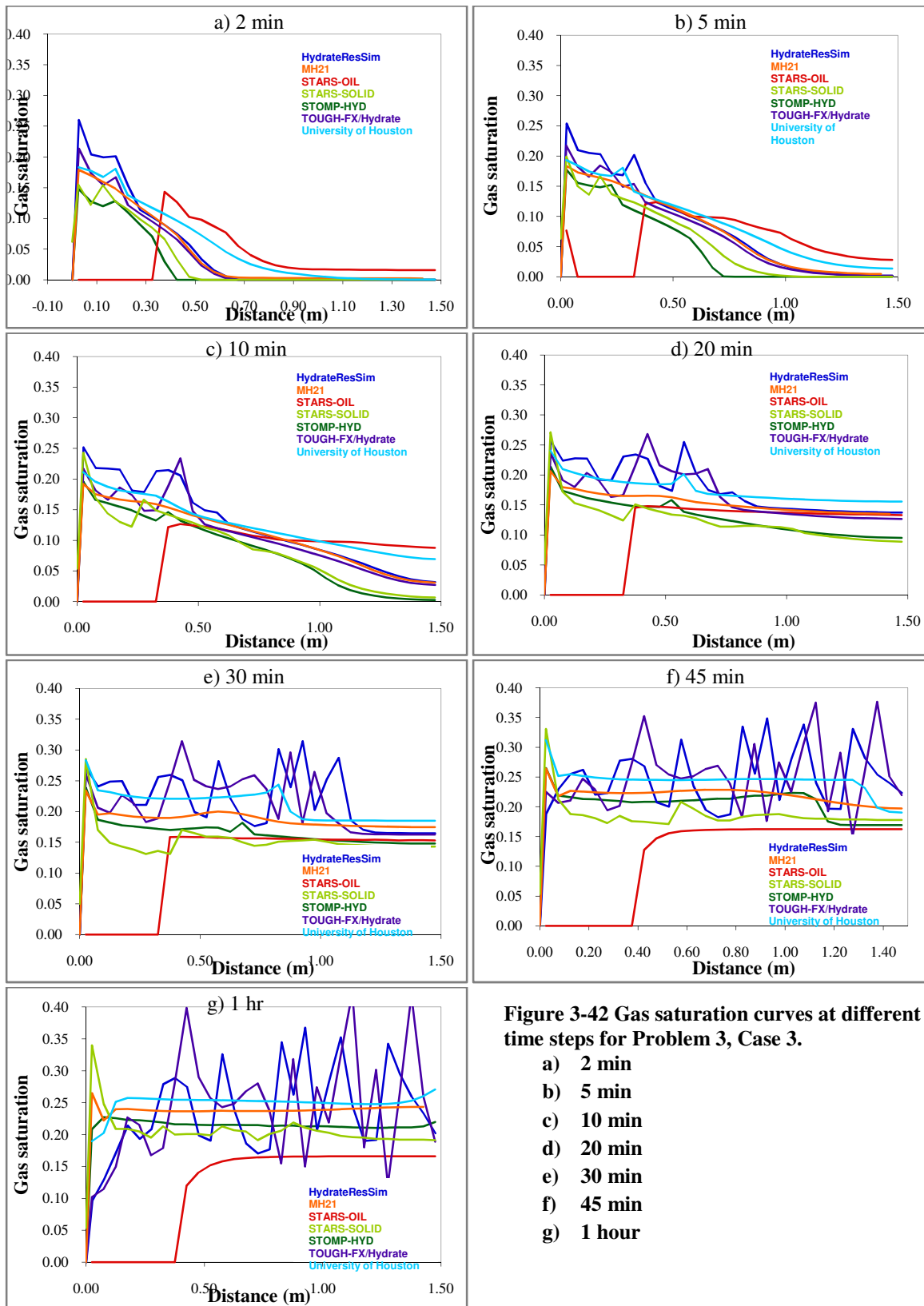


Figure 3-42 Gas saturation curves at different time steps for Problem 3, Case 3.

- a) 2 min
- b) 5 min
- c) 10 min
- d) 20 min
- e) 30 min
- f) 45 min
- g) 1 hour

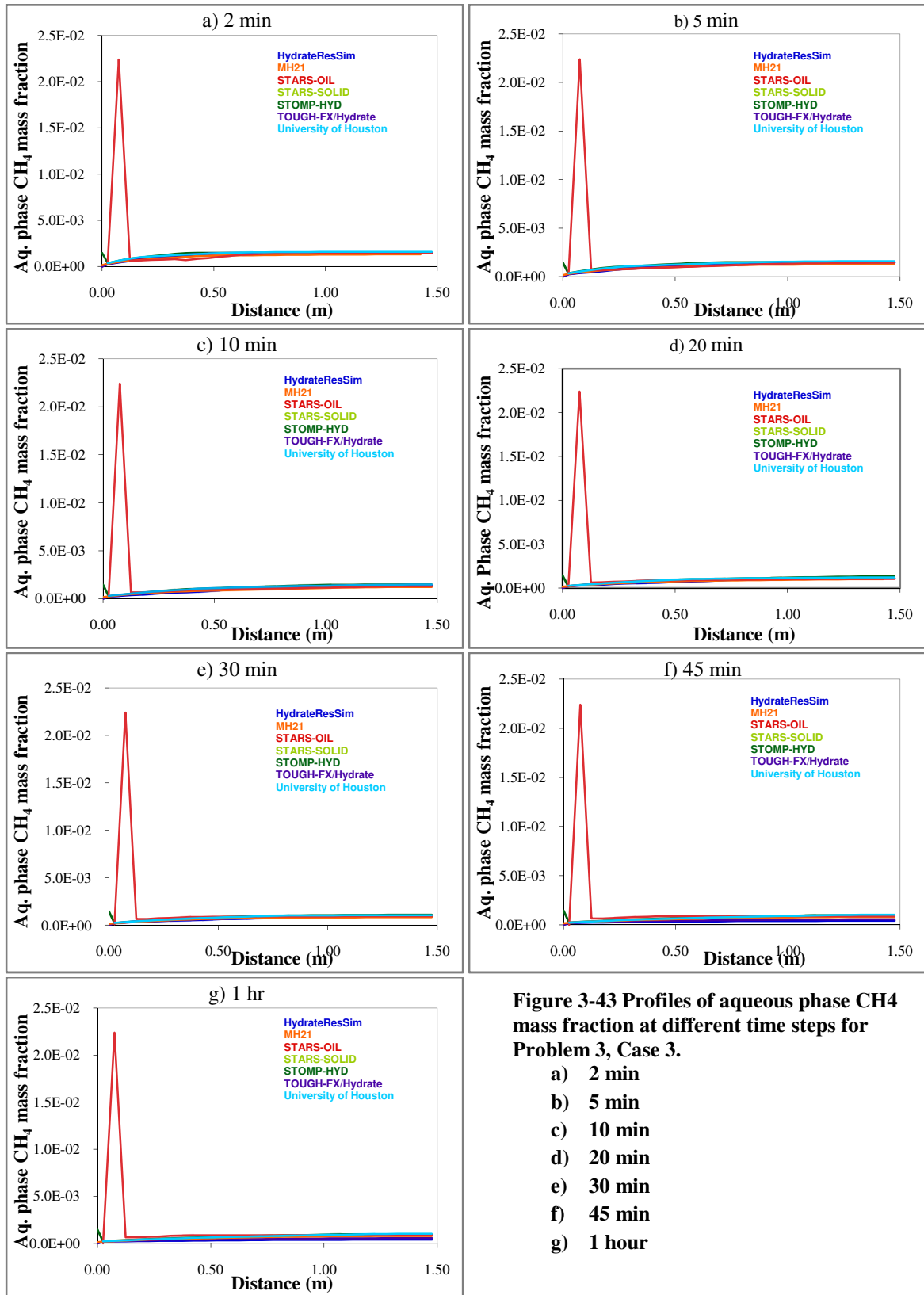


Figure 3-43 Profiles of aqueous phase CH_4 mass fraction at different time steps for Problem 3, Case 3.

- a) 2 min
- b) 5 min
- c) 10 min
- d) 20 min
- e) 30 min
- f) 45 min
- g) 1 hour

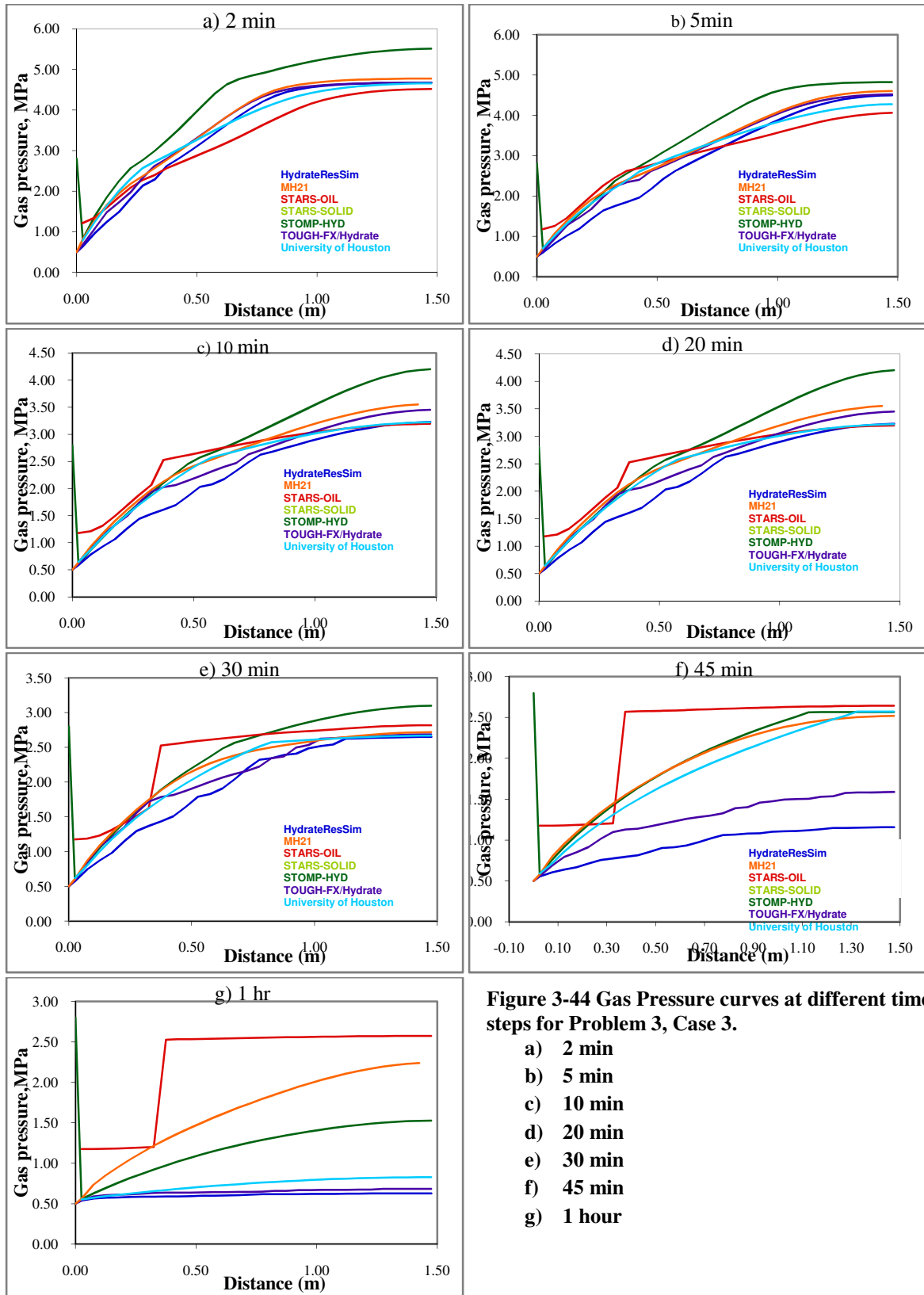


Figure 3-44 Gas Pressure curves at different time steps for Problem 3, Case 3.

- a) 2 min
- b) 5 min
- c) 10 min
- d) 20 min
- e) 30 min
- f) 45 min
- g) 1 hour

4. 1-D and 2-D radial systems: Problems and Solutions

In Problem 4, a radial cylindrical grid is defined. There are two cases in this problem; they arise from different methods of hydrate dissociation too, Thermal Stimulation and Depressurization.

Problem 5 shows a typical example of a Class 2 Hydrate Deposit in which the hydrate layer is bound by two water saturated shale zones. Eight different cases have been modeled in this problem. The effect of hydrate saturation and finite discretization of the grid is also studied in this problem.

4.1 Problem 4

A cylindrical domain is considered in this problem. A fine discretization is used to capture the dissociation front and to understand the transport properties in a radial domain. This problem is defined to introduce similarity solutions to hydrate dissociation processes. Two different cases are defined to study the thermal stimulation and depressurization process in a radial domain.

Grid Description

A one dimensional radial domain of 1000 m x 1.0 m ($r \times z$) is considered. It is further discretized into 1500 cells, 1000 radial cells with a $\Delta r = 0.02m$ followed by 500 radial cells logarithmically distributed from $r = 20$ m to $r = 1000$ m.

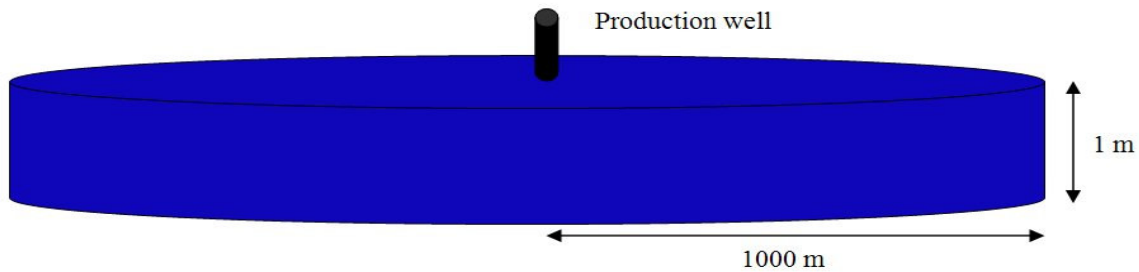


Figure 4-1 Schematic view of the grid for problem 4.

Case 1: Thermal Stimulation

Initial conditions

Pressure: $P_i = 4.6$ MPa

Temperature: $T_i = 3^\circ\text{C}$

Saturations: $S_H = 0.5, S_W = 0.5, S_G = 0.0$

Boundary Conditions:

At $r = R_{max}$: constant thermodynamic conditions

At $r = 0$: $Q_H = 150$ W

Case 2: Depressurization to a pressure below Q point

Initial conditions:

Pressure: $P_i = 9.5$ MPa

Temperature: $T_i = 3^\circ\text{C}$

Saturations: $S_H = 0.4$, $S_W = 0.6$, $S_G = 0.0$

Boundary Conditions:

At $r = R_{max}$: constant thermodynamic conditions

At $r = 0$: $Q = 0.1$ kg/s; Fluid rate

Medium properties:

Hydraulic and thermal properties are specified in Table 4.1

Table 4-1 Input Parameters and Specifications

Parameter	Value
Porosity	0.3
Permeability	1000 mD
Bulk Density	1855 kg/m ³
Grain Density	2600 kg/m ³
Grain Specific Heat	750 J/kg K
Bulk Specific heat	525 J/kg K
Dry Thermal Conductivity	2.0 W/m K
Water-Saturated Thermal Conductivity	2.18 W/m K
Pore Compressibility	5.0×10^{-10} Pa ⁻¹
composite thermal conductivity Model	linear
Capillary Pressure Model	Van-Genuchten Equation ³⁴
λ parameter	0.132m-1
S_{irA} parameter	2.823
$1/P_o$ parameter	1
P_{max} parameter	5.0×10^6 Pa
S_{mxA} parameter	1
Aqueous Relative Permeability Model	Stone ³⁶ + Aziz ³⁷
S_{irA} parameter	0.12
n parameter	3
Gas Relative Permeability Model	Stone ³⁶ + Aziz ³⁷
S_{irG} parameter	0.02

Relative Permeability Model

The relative permeability model used in this problem is same as in problem 3 and is developed by Stone and Aziz.

$$k_{rG} = (S_G^*)^n, \quad S_G^* = (S_G - S_{irG}) / (1 - S_{irA})$$

$$k_{rA} = (S_A^*)^n, \quad S_A^* = (S_A - S_{irA}) / (1 - S_{irA})$$

Where, S_{irG}, S_{irA} represents irreducible gas and aqueous saturation.

In this problem $S_{irG}=0.02$, $S_{irA}=0.12$ and $n = 3.0$.

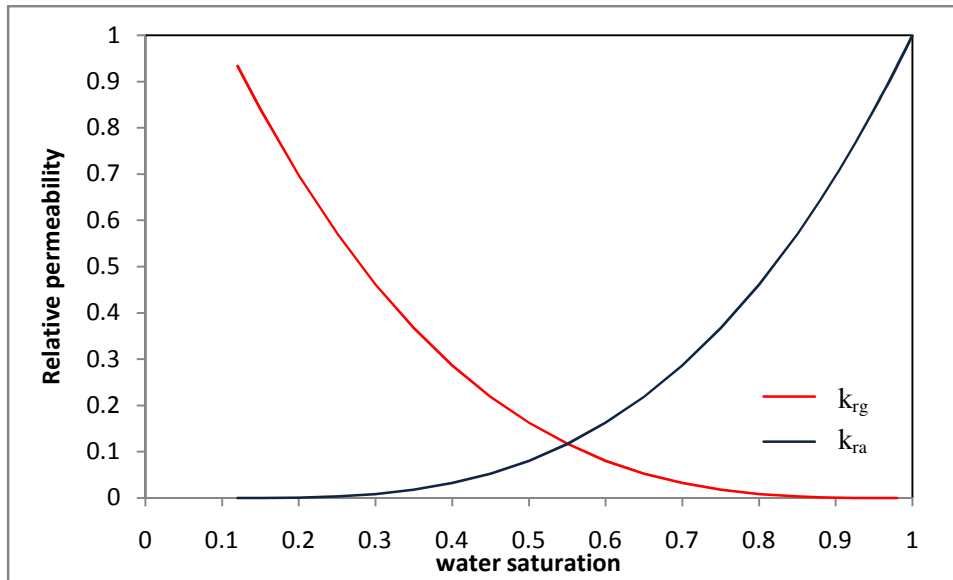


Figure 4- 2 Aqueous and gas relative permeability curves as a function of water saturation for Problem 4

Capillary pressure model:

To avoid complexities, capillary pressure is not considered for the thermal case (case 1). For the depressurization case (Case-2) capillary pressure used is the same as in problem3.

$$P_{cap} = -P_0[(S^*)^{-1/\lambda} - 1]^\lambda, \quad S^* = \frac{(S_A - S_{irA})}{(S_{mxA} - S_{irA})} \text{ where } -P_{max} \leq P_{cap} \leq 0$$

Different parameters in this model are specified in Table 4-1

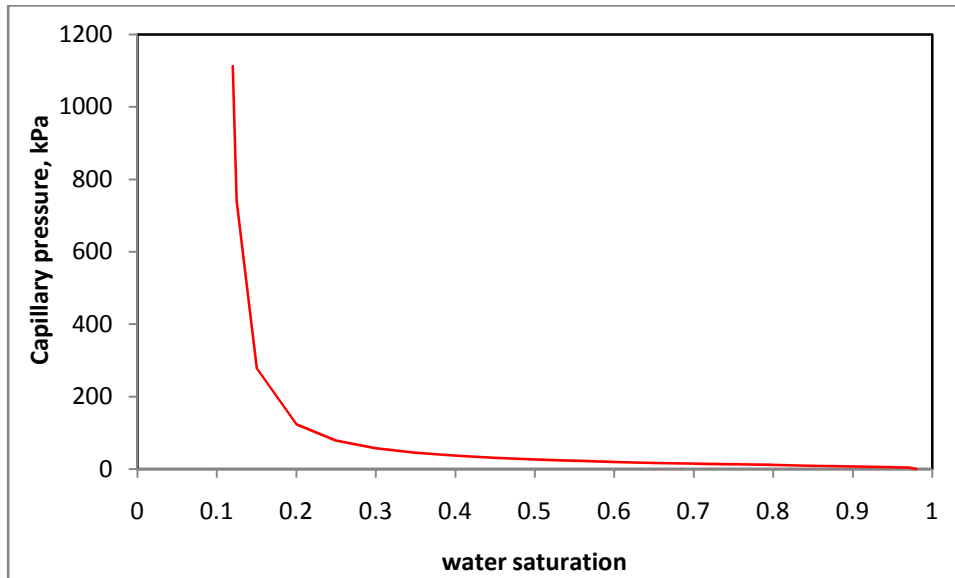


Figure 4-3 Capillary Pressure vs. Water Saturation for Problem 4.

Data and sampling frequency

Profiles of water saturation, temperature, pressure, aqueous relative permeability, and aqueous methane mass fraction and capillary pressure, gas rate, cumulative gas rate are compared for different time steps. The time steps considered here are different for each case.

Case 1: Thermal Stimulation

Data is recorded at 2 days, 5 days, 10 days, 15 days, 20 days, 30 days, 45 days and 60 days.

Case 2: Depressurization to a pressure above Q point

Data is recorded at 2 days, 5 days, 10 days, 15 days, 20 days, 30 days and 45 days.

4.1.1 Solution to Problem 4

The cylindrical grid is very finely discretized into 1500 cells in the radial direction. Two cases are defined based on the method of hydrate dissociation chosen. Grid description, medium and rock-fluid properties are same for both the cases. To avoid complexities, capillary pressure is not considered for the thermal case. As given in the problem description the only difference between case 1 & 2 is their initial and boundary conditions. Porosity and permeability are 0.3 and 300 mD. The input data file used in this problem is specified below.

```
**$ *****  
**$ Definition of fundamental cylindrical grid  
**$ *****  
GRID RADIAL 1501 1 1 *RW          0.02  
KDIR DOWN  
DI IVAR  
  ** 1000 radial cells of  $\Delta r = 0.02$  m  
    0.02    0.0202594  
0.0205222  0.0207883    0.0210579    0.021331    0.0216077    0.0218879  
0.0221718  0.0224594    0.0227507    0.0230458    0.0233446    0.0236474  
0.0239541  0.0242648    0.0245795    0.0248983    0.0252212    0.0255483  
0.0258797  0.0262153    0.0265553    0.0268997    0.0272486    0.027602  
  0.02796  0.0283226        0.02869    0.0290621    0.029439    0.0298208  
0.0302076  0.0305994    0.0309962    0.0313982    0.0318055    0.032218  
0.0326358  0.0330591    0.0334879    0.0339222    0.0343622    0.0348078  
0.0352593  0.0357166    0.0361798    0.036649    0.0371244    0.0376059  
0.0380936  0.0385877    0.0390881    0.0395951    0.0401086    0.0406288  
0.0411558  0.0416895    0.0422302    0.042778    0.0433328    0.0438948  
0.0444641  0.0450408    0.0456249    0.0462167    0.0468161    0.0474233  
0.0480383  0.0486614    0.0492925    0.0499318    0.0505794    0.0512354  
0.0518999  0.052573    0.0532549    0.0539456    0.0546452    0.055354  
0.0560719  0.0567991    0.0575358    0.058282    0.0590379    0.0598036  
0.0605792  0.0613649    0.0621608    0.062967    0.0637837    0.0646109  
0.0654489  0.0662978    0.0671576    0.0680286    0.068911    0.0698047  
  0.07071  0.0716271    0.0725561    0.0734971    0.0744504    0.075416  
0.0763941  0.0773849    0.0783886    0.0794052    0.0804351    0.0814783  
0.0825351  0.0836055    0.0846898    0.0857882    0.0869009    0.088028  
0.0891696  0.0903261    0.0914977    0.0926843    0.0938864    0.0951041  
0.0963376  0.097587    0.0988527    0.100135    0.101434    0.102749  
0.104082  0.105432    0.106799    0.108184    0.109587    0.111009  
0.112448  0.113907    0.115384    0.116881    0.118396    0.119932  
0.121488  0.123063    0.124659    0.126276    0.127914    0.129573  
0.131253  0.132956    0.13468    0.136427    0.138196    0.139989  
0.141804  0.143643    0.145506    0.147393    0.149305    0.151242  
0.153203  0.15519    0.157203    0.159242    0.161307    0.163399  
0.165518  0.167665    0.16984    0.172042    0.174274    0.176534  
0.178824  0.181143    0.183492    0.185872    0.188283    0.190725  
0.193198  0.195704    0.198242    0.200813    0.203418    0.206056  
0.208729  0.211436    0.214178    0.216956    0.21977    0.22262  
0.225507  0.228432    0.231395    0.234396    0.237436    0.240515  
0.243635  0.246795    0.249996    0.253238    0.256522    0.259849  
0.263219  0.266633    0.270092    0.273594    0.277143    0.280737  
0.284378  0.288067    0.291803    0.295587    0.299421    0.303305  
0.307238  0.311223    0.31526    0.319348    0.32349    0.327686  
0.331936  0.336241    0.340602    0.345019    0.349494    0.354027  
0.358618  0.36327    0.367981    0.372754    0.377588    0.382485  
0.387446  0.392471    0.397561    0.402718    0.407941    0.413232  
0.418591  0.42402    0.429519    0.43509    0.440733    0.446449  
  0.45224  0.458105    0.464046    0.470065    0.476162    0.482337
```

0.488593	0.49493	0.501349	0.507851	0.514438	0.52111
0.527869	0.534715	0.54165	0.548675	0.555791	0.563
0.570301	0.577698	0.585191	0.59278	0.600468	0.608256
0.616145	0.624136	0.632231	0.640431	0.648737	0.657151
0.665674	0.674308	0.683053	0.691912	0.700886	0.709976
0.719185	0.728512	0.737961	0.747532	0.757227	0.767048
0.776996	0.787074	0.797282	0.807622	0.818097	0.828707
0.839455	0.850343	0.861372	0.872543	0.88386	0.895323
0.906935	0.918698	0.930613	0.942683	0.954909	0.967294
0.979839	0.992548	1.00542	1.01846	1.03167	1.04505
1.0586	1.07233	1.08624	1.10033	1.1146	1.12906
1.1437	1.15853	1.17356	1.18878	1.2042	1.21982
1.23564	1.25166	1.2679	1.28434	1.301	1.31787
1.33496	1.35228	1.36982	1.38758	1.40558	1.42381
1.44228	1.46098	1.47993	1.49912	1.51857	1.53826
1.55821	1.57842	1.59889	1.61963	1.64064	1.66192
1.68347	1.7053	1.72742	1.74983	1.77252	1.79551
1.8188	1.84239	1.86628	1.89049	1.915	1.93984
1.965	1.99049	2.0163	2.04245	2.06894	2.09578
2.12296	2.15049	2.17838	2.20664	2.23526	2.26425
2.29361	2.32336	2.35349	2.38402	2.41494	2.44626
2.47798	2.51012	2.54268	2.57566	2.60906	2.6429
2.67718	2.7119	2.74707	2.7827	2.81879	2.85535
2.89238	2.9299	2.9679	3.00639	3.04538	3.08488
3.12489	3.16542	3.20647	3.24806	3.29019	3.33286
3.37608	3.41987	3.46422	3.50915	3.55467	3.60077
3.64747	3.69478	3.7427	3.79124	3.84041	3.89022
3.94067	3.99178	4.04356	4.096	4.14912	4.20294
4.25745	4.31266	4.3686	4.42526	4.48265	4.54079
4.59968	4.65934	4.71977	4.78098	4.84299	4.9058
4.96943	5.03388	5.09917	5.1653	5.23229	5.30016
5.3689	5.43853	5.50907	5.58052	5.65289	5.72621
5.80048	5.87571	5.95191	6.02911	6.1073	6.18651
6.26675	6.34803	6.43036	6.51376	6.59824	6.68382
6.7705	6.85831	6.94726	7.03737	7.12864	7.2211
7.31475	7.40962	7.50572	7.60307	7.70168	7.80157
7.90275	8.00525	8.10907	8.21424	8.32078	8.4287
8.53801	8.64875	8.76092	8.87455	8.98965	9.10624
9.22435	9.34398	9.46517	9.58793	9.71228	9.83825
9.96585	10.0951	10.226	10.3587	10.493	10.6291
10.767	10.9066	11.0481	11.1913	11.3365	11.4835
11.6325	11.7833	11.9362	12.091	12.2478	12.4066
12.5675	0.001				

DJ JVAR 360
DK ALL
1501*1
DTOP
1501*500
POR CON 0.3
PERMI CON 300
PERMJ CON 300
PERMK CON 300
END-GRID
ROCKTYPE 1
PRPOR 101.3
CPOR 5e-7

**\$ Property: Thermal/rock Set Num Max: 1
Min: 1
THTYPE CON 1
**\$ Model and number of components

MODEL 3 3 3 2
COMPNAME 'H2O' 'CH4' 'hydrate'
CMM
0 0.016043 0.125962
PCRIT
0 4600 10000
TCRIT
0 -82.55 1000

ROCKCP 1.988e+6 0
THCONR 1.728E+5
THCONS 1.728E+5
THCONW 2.24633E+5
THCONO 3.395237E+04
THCONG 5.183567E+04
THCONMIX SIMPLE
PERMCK 5
**\$ Property: Thermal/rock Set Num Max: 1
Min: 1
THTYPE CON 1

KV1
1.186e7 9.5e7 0.0
KV4
-3816.44 -879.8 0.0
KV5
-207.02 -245.0 0.0
KVTABLIM 4000 5000 25 35
PRSR 101
TEMR 30
PSURF 101
TSURF 16.85
CPG1
0.0 19.251 0.0E+0
CPG2

```

0.0 5.213E-2 0.0E+0
CPG3
0.0 1.197E-5 0.0E+0
CPG4
0.0 -1.132E-8 0.0E+0
CPL1
0.0E+0 0.0E+0 191.2
CPL2
0.0E+0 0.0E+0 0.0E+0
CPL3
0.0E+0 0.0E+0 0.0E+0
CPL4
0.0E+0 0.0E+0 0.0E+0
MOLDEN
55501.5 18723 7696.23
**$ Reaction specification
STOREAC
0 0 1
STOPROD
6.1 1 0
RORDER

**$ Reaction specification
STOREAC
6.1 1 0
STOPROD
0 0 1
FREQFAC 1e28
RENTH 51857.9364
.15
** There is no capillary pressure for case 1
ROCKFLUID
RPT 1 WATWET
SWT
**$
      Sw      krw      krow      Pcow
0.1200000 0.0000000 1.0000E-07 0.0000E+00
0.1250000 0.0000002 9.0000E-08 0.0000E+00
0.1500000 0.0000396 8.0000E-08 0.0000E+00
0.2000000 0.0007513 8.0000E-08 0.0000E+00
0.2500000 0.0032239 7.0000E-08 0.0000E+00
0.3000000 0.0085579 6.0000E-08 0.0000E+00
0.3500000 0.0178540 5.0000E-08 0.0000E+00
0.4000000 0.0322126 4.0000E-08 0.0000E+00
0.4500000 0.0527344 3.0000E-08 0.0000E+00
0.5000000 0.0805198 2.0000E-08 0.0000E+00
0.5500000 0.1166695 1.0000E-08 0.0000E+00
0.6000000 0.1622840 1.0000E-08 0.0000E+00
0.6500000 0.2184639 1.0000E-08 0.0000E+00
0.7000000 0.2863096 1.0000E-08 0.0000E+00
0.7500000 0.3669219 1.0000E-08 0.0000E+00
0.8000000 0.4614012 1.0000E-08 0.0000E+00
0.8500000 0.5708481 1.0000E-08 0.0000E+00
0.8800000 0.6441585 1.0000E-08 0.0000E+00
0.9000000 0.6963632 1.0000E-08 0.0000E+00
0.9030000 0.7044291 1.0000E-08 0.0000E+00
0.9250000 0.7654902 1.0000E-08 0.0000E+00
0.9500000 0.8390469 1.0000E-08 0.0000E+00
0.9580000 0.8635431 1.0000E-08 0.0000E+00
0.9600000 0.8697408 1.0000E-08 0.0000E+00
0.9660000 0.8885115 1.0000E-08 0.0000E+00
0.9700000 0.9011742 1.0000E-08 0.0000E+00
0.9800000 0.9333560 1.0000E-08 0.0000E+00
0.9900000 0.9662950 1.0000E-08 0.0000E+00
1.0000000 1.0000000 0 0.0000E+00

CP
5.0E-7 0.0 5.0E-7
CT1
-1.9095e-3 0 0.0E+0
CT2
7.296e-6 0 0.0E+0
AVG
0.0E+0 3.8E-3 0.0E+0
BVG
0.0E+0 0.0E+0 0.0E+0
AVISC
.00752 0.137849 9999.0
BVISC
1384.86 114.14 0.0
0 0 1
FREQFAC 1e31
RENTH -51857.9364
EACT 150218.3525
RXEQFOR 'hydrate' 4.16949E+16 0 0
-8315.389 -273.15

0 0 1
RORDER
EACT 150218.3525
RXEQFOR 'hydrate' 4.16949E+16
0 0 -8315.389 -273

```

```

SLT
**$      Sl          krg          krog          Pcog
0.1200000 0.9333560          0 1112.47669
0.1250000 0.9171710 6.0000E-08 741.62840
0.1500000 0.8390469 6.0000E-08 277.99809
0.2000000 0.6963632 6.0000E-08 123.268685
0.2500000 0.5708481 6.0000E-08 78.874995
0.3000000 0.4614012 6.0000E-08 57.692894
0.3500000 0.3669219 6.0000E-08 45.203133
0.4000000 0.2863096 6.0000E-08 36.899491
0.4500000 0.2184639 6.0000E-08 30.925481
0.5000000 0.1622840 6.0000E-08 26.375168
0.5500000 0.1166695 6.0000E-08 22.752420
0.6000000 0.0805198 6.0000E-08 19.760983
0.6500000 0.0527344 6.0000E-08 17.210799
0.7000000 0.0322126 6.0000E-08 14.9712679
0.7500000 0.0178540 6.0000E-08 12.9451682
0.8000000 0.0085579 6.0000E-08 11.0513554
0.8500000 0.0032239 6.0000E-08 9.2084251
0.8800000 0.0014674 6.0000E-08 8.0843370
0.9000000 0.0007513 6.0000E-08 7.3067163
0.9030000 0.0006699 6.0000E-08 7.1869998
0.9250000 0.0002441 6.0000E-08 6.2731168
0.9500000 0.0000396 6.0000E-08 5.1119647
0.9580000 0.0000156 6.0000E-08 4.6934993
0.9600000 0.0000117 6.0000E-08 4.5836634
0.9660000 0.0000040 7.0000E-08 4.2385501
0.9700000 0.0000015 8.0000E-08 3.9927997
0.9800000 0.0000000 1.0000E-07 0
INITIAL
VERTICAL OFF

```

Case 1 Thermal Stimulation

Reservoir pressure and temperature are at 4.6 MPa and 3°C. A constant heat supply of 1.296×10^7 J/day at $r = 0$ is specified by keyword 'HEATR CON'. Hydrate saturation is 0.5 in the entire reservoir. A extra constraint of bottom hole pressure of 4607 kPa is added in the well to ensure that all hydrate that is dissociated is due to thermal stimulation.

```

**$ Property: Pressure (kPa) Max: 4600 Min: 4600
PRES CON 4600
**$ Property: Temperature (C) Max: 3 Min: 3
TEMP CON 3
**$ Property: Water Saturation Max: 0.5 Min: 0.5
SW CON 0.5
**$ Property: Oil Saturation Max: 0.5 Min: 0.5
SO CON 0.5
**$ Property: Gas Saturation Max: 0 Min: 0
SG CON 0
**$ Property: Water Mole Fraction(CH4) Max: 7e-005 Min: 7e-005
MFRAC_WAT 'CH4' CON 7E-005
**$ Property: Water Mole Fraction(H2O) Max: 0.99993 Min: 0.99993
MFRAC_WAT 'H2O' CON 0.99993
**$ Property: Oil Mole Fraction(hydrate) Max: 1 Min: 1
MFRAC_OIL 'hydrate' CON 1
**$ Property: Gas Mole Fraction(CH4) Max: 0.9999 Min: 0.9999
MFRAC_GAS 'CH4' CON 0.9999
**$ Property: Gas Mole Fraction(H2O) Max: 0.0001 Min: 0.0001
MFRAC_GAS 'H2O' CON 0.0001
NUMERICAL
RUN

```

```

DATE 2007 9 14
DTWELL 0.001

**$
WELL 'Well-1'
PRODUCER 'Well-1'
OPERATE MIN BHP 4607. CONT
**$      rad geofac wfrac skin
GEOMETRY K 0.029 0.249 1. 0.
PERF GEO 'Well-1'
**$ UBA  ff Status Connection
      1 1 1 1. OPEN FLOW-TO 'SURFACE'
**$ Property: Heat Transfer Rate (J/day)  Max: 0  Min: 0
HEATR CON      0
*MOD
      1:1      1:1      1:1      = 1.296e+007
DATE 2007 9 16      DATE 2007 10 14
DATE 2007 9 19      DATE 2007 10 29
DATE 2007 9 24      DATE 2007 11 13
DATE 2007 9 29      STOP
DATE 2007 10 4

```

Case 2 Depressurization

Initial and boundary conditions are different from the previous case. Reservoir pressure is 9500 kPa and is depressurized by taking out fluid through a well at a constant rate of 0.1 kg/sec. Hydrate saturation is 0.4 in the entire reservoir as specified in the problem description.

```

**$ Property: Pressure (kPa)  Max: 9500  Min: 9500
PRES CON      9500
**$ Property: Temperature (C)  Max: 12  Min: 12
TEMP CON      12
**$ Property: Water Saturation  Max: 0.6  Min: 0.6
SW CON      0.6
**$ Property: Oil Saturation  Max: 0.4  Min: 0.4
SO CON      0.4
**$ Property: Gas Saturation  Max: 0  Min: 0
SG CON      0
MFRAC_WAT 'H2O' CON      0.999
MFRAC_WAT 'CH4' CON      0.002
MFRAC_OIL 'hydrate' CON      1
MFRAC_GAS 'CH4' CON      0.998
MFRAC_GAS 'H2O' CON      0.001
NUMERICAL
RUN
DATE 2007 9 14
DTWELL 0.001
WELL 'Well-1'
PRODUCER 'Well-1'
OPERATE MAX BHP 8.64 CONT
**$      rad geofac wfrac skin
GEOMETRY K 0.029 0.249 1. 0.
PERF GEO 'Well-1'
**$ UBA  ff Status Connection
      1 1 1 1. OPEN FLOW-TO 'SURFACE'
DATE 2007 9 16      DATE 2007 10 14
DATE 2007 9 19      DATE 2007 10 29
DATE 2007 9 24      DATE 2007 11 13
DATE 2007 9 29      STOP
DATE 2007 10 4

```

4.1.2 Results of similarity solution study of hydrate dissociation in radial domain.

Similarity solution can provide a simple and robust tool to evaluate the production potential of hydrate accumulations. If a problem has a similarity solution, there is no need to conduct long term simulations; Short term simulation results can be used to predict long term results. Results at any time are sufficient to describe system behavior and performance at any time. Different properties like pressure, temperature, saturations, aqueous phase relative permeability are plotted against r^2/t and the results showed that the curves are invariant confirming that this problem has a similarity solution. Similarity solutions were found for both the cases of problem 4 in all the reservoir simulators.

Case I: Thermal Stimulation

Temperature: In this case, hydrate dissociates due to constant heat supply of 1.29×10^7 J/day in the well bore. To validate the results of CMG STARS with other codes, it is first important to match the temperature profiles. Figure 4-4 shows temperature profiles for CMG STARS and TOUGH/Fx-Hydrate in good agreement.

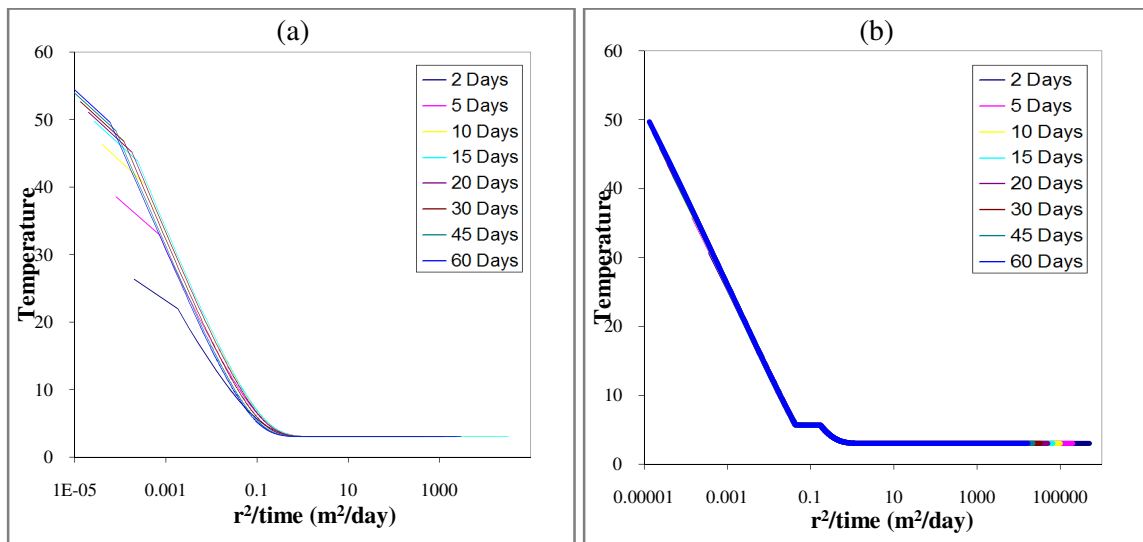


Figure 4- 4 Profiles of Temperature of Problem 4 case 1 for (a) CMG STARS (b) TOUGH-Fx/HYDRATE.

Saturations: The hydrate, gas and water saturation distributions for all other simulators except STARS (when used hydrate as oil phase) indicates a very sharp dissociation front. In CMG STARS unlike in other codes, a property change applied to a block affects the neighboring blocks also. When heat is added to the system from the block at $r = 0$, hydrate in the neighboring blocks also feels that heat and as a result, there is no sharp dissociation front and hence no secondary hydrate formation. Figure 4-5 to Figure 4-7 shows saturation curves for STARS and TOUGH/Fx-Hydrate.

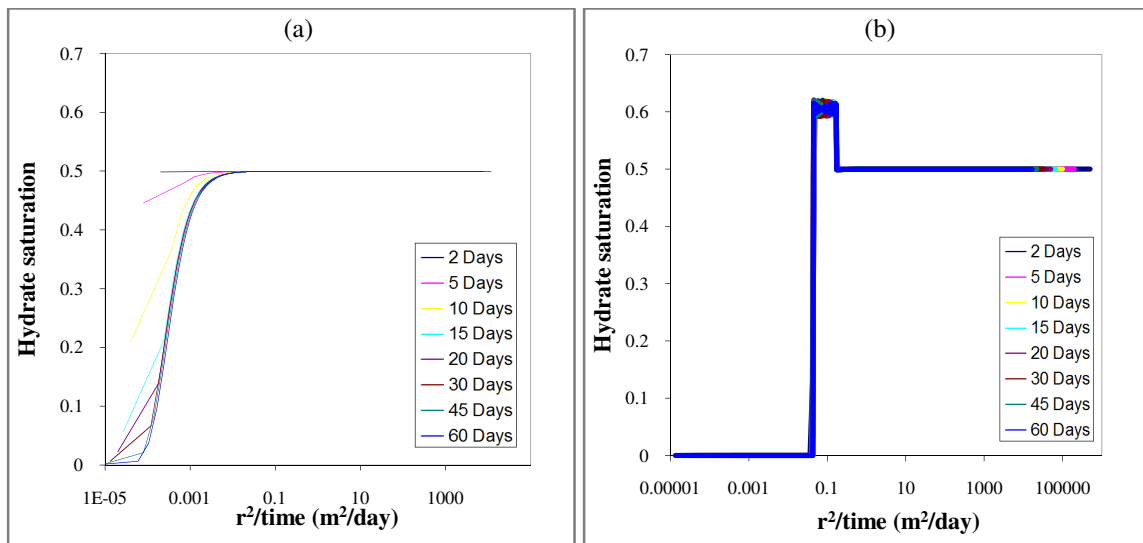


Figure 4- 5 Profiles of Hydrate saturation of Problem 4 case 1 for (a) CMG STARS (b) TOUGH-Fx/HYDRATE.

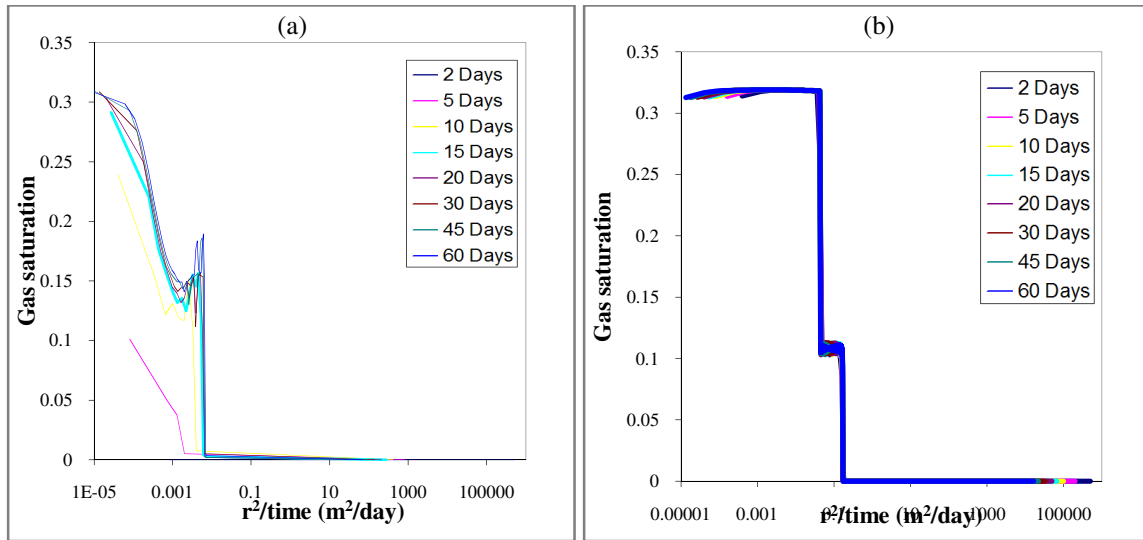


Figure 4- 6 Profiles of Gas saturation of Problem 4 case 1 for (a) CMG STARS (b) TOUGH-Fx/HYDRATE.

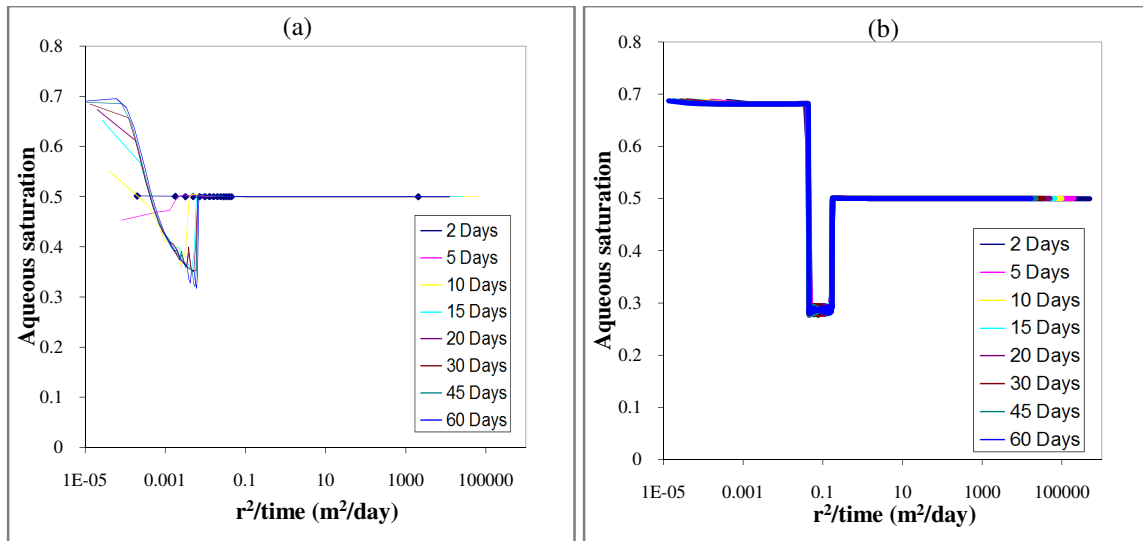


Figure 4- 7 Profiles of Aqueous saturation of Problem 4 case 1 for (a) CMG STARS (b) TOUGH-Fx/HYDRATE.

Aqueous phase relative permeability: Relative permeability is a function of water saturation.

Aqueous phase relative permeability is calculated based on water saturation at every time step. So, same kind of behavior is seen for this property also as shown in Figure 4-8.

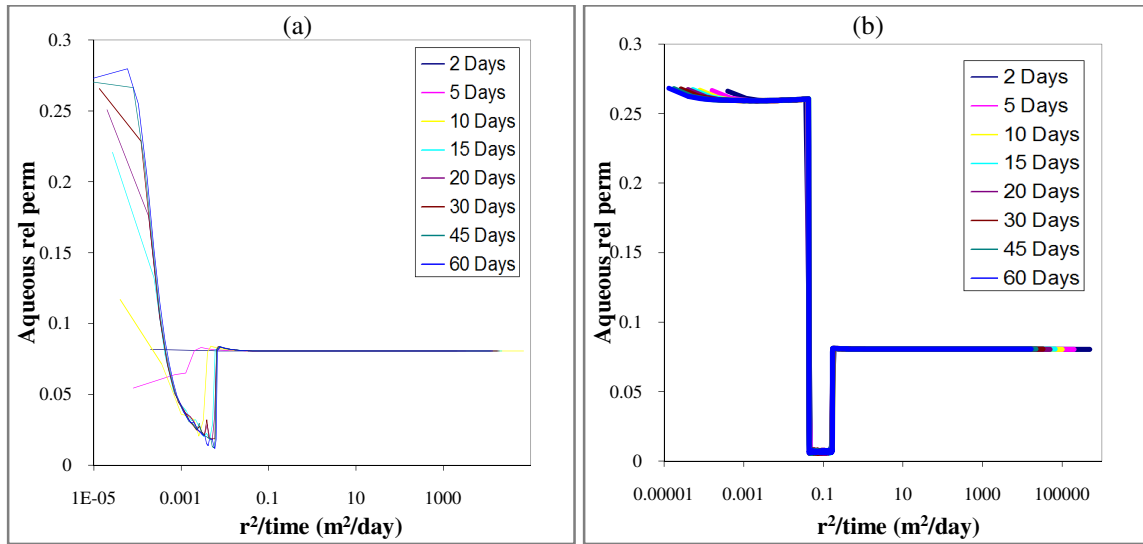


Figure 4- 8 Profiles of Aqueous saturation of Problem 4 case 1 for (a) CMG STARS (b) TOUGH-Fx/HYDRATE.

A Bottom-hole pressure of 4600 kPa is added as an extra boundary condition to ensure that hydrate is dissociated only through thermal stimulation and not by depressurization. Figure 4-9 shows the small differences in the profiles of gas pressure for STARS and TOUGH-Fx/HYDRATE.

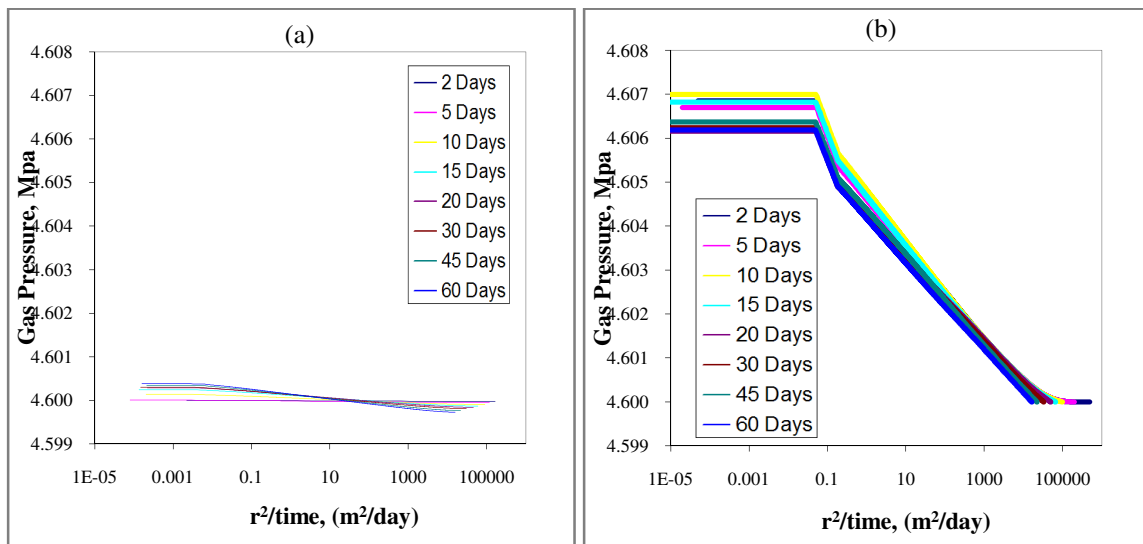


Figure 4- 9 Profiles of Gas pressure of Problem 4 case 1 for (a) CMG STARS (b) TOUGH-Fx/HYDRATE.

Case II: Depressurization to a Pressure below Q point

In this case of depressurization, fluids are removed through a well at a constant rate of 0.1 kg/s causing depressurization. There is no restriction in the fluid distribution in the production stream. Pressure, temperature, saturations, aqueous phase relative permeability and mass fraction of CH₄ in the aqueous phase are plotted vs r^2/t and the results for CMG STARS confirm the presence of similarity solution to this problem. Profiles of all these properties are in excellent agreement with other codes. There is no sharp hydrate dissociation front in this case. Results also confirmed that depressurization yields higher production rates. Hydrate dissociation reaction is an endothermic reaction, so it cools the reservoir resulting in the drop of temperatures which may even sometimes lead to secondary hydrate formation. In this case there is no secondary hydrate formation due to higher temperatures in the reservoir. Profiles of pressure and temperature for STARS and TOUGH-Fx/HYDRATE are shown in Figure 4-10 and Figure 4-11.

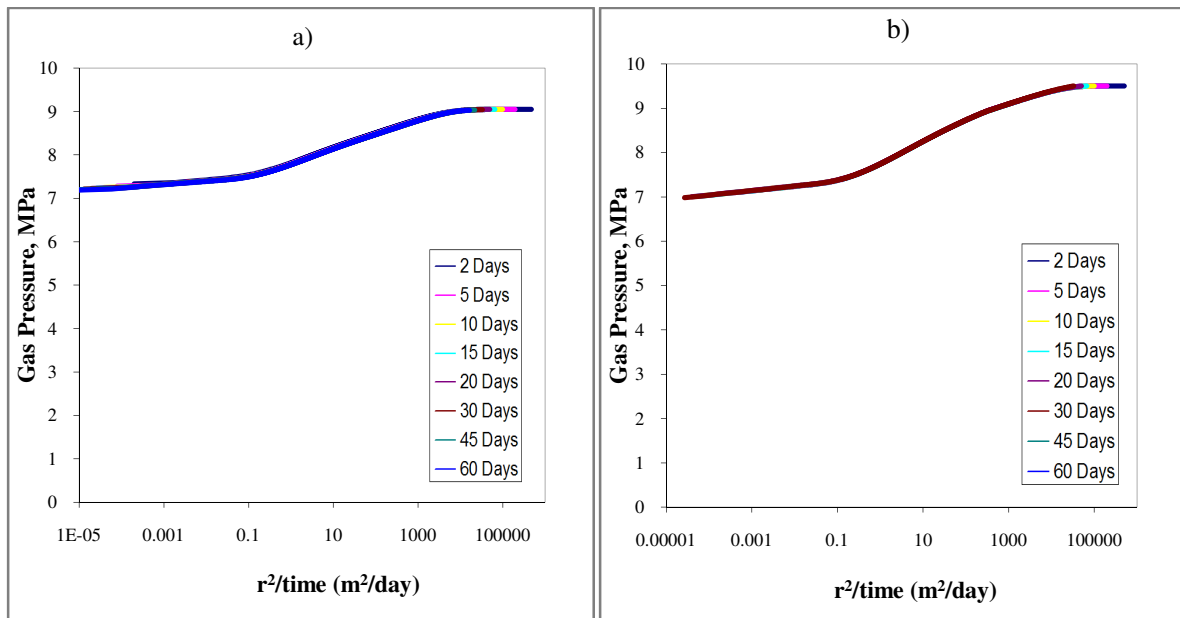


Figure 4-10 Profiles of Gas pressure of Problem 4 case 2 for (a) CMG STARS (b) TOUGH-Fx/HYDRATE.

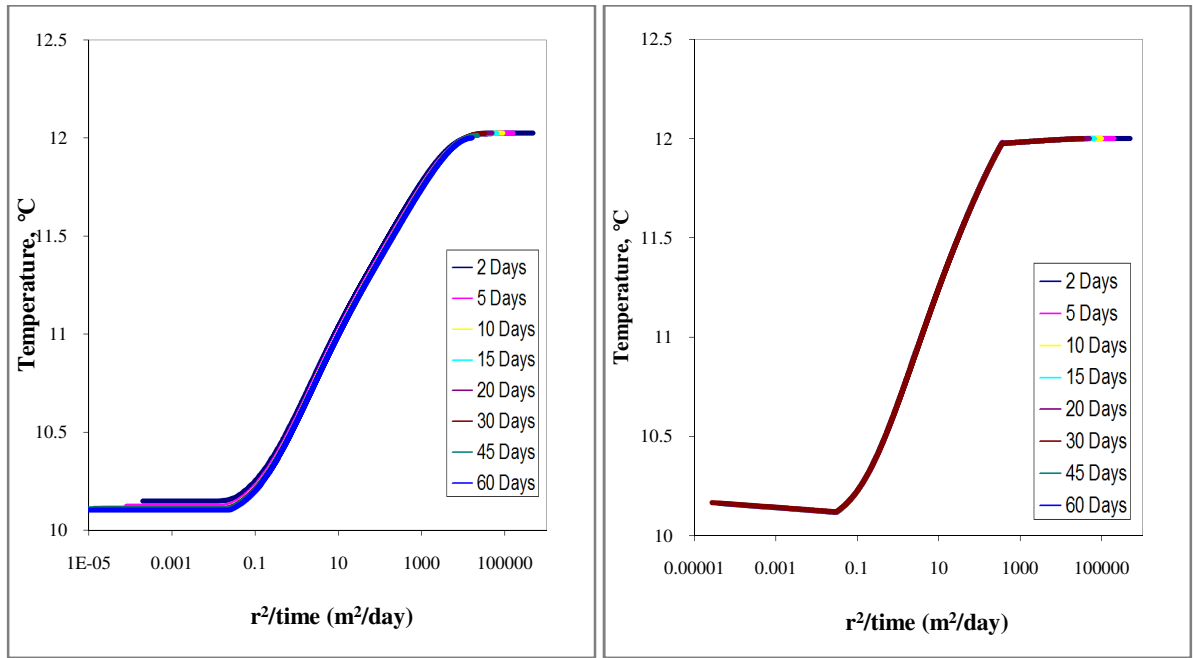


Figure 4- 11 Profiles of Temperature of Problem 4 case 2 for (a) CMG STARS (b) TOUGH-Fx/HYDRATE.

Profiles of hydrate saturation, aqueous saturation and gas saturation are given in Figures 4-11 to Figure 4-13. They are in excellent agreement with other code results. Small fluctuation about the mean is observed in the results for STARS due to numerical difficulties caused by fine discretization of the grid. Aqueous relative permeability for STARS and TOUGH are given in Figure 4-14. Differences in the profile for aqueous CH₄ mass fraction for STARS and TOUGH are observed as shown in Figure 4-15. Luckily gas-water capillary pressure for STARS also showed good agreement with TOUGH as shown in Figure 4-16.

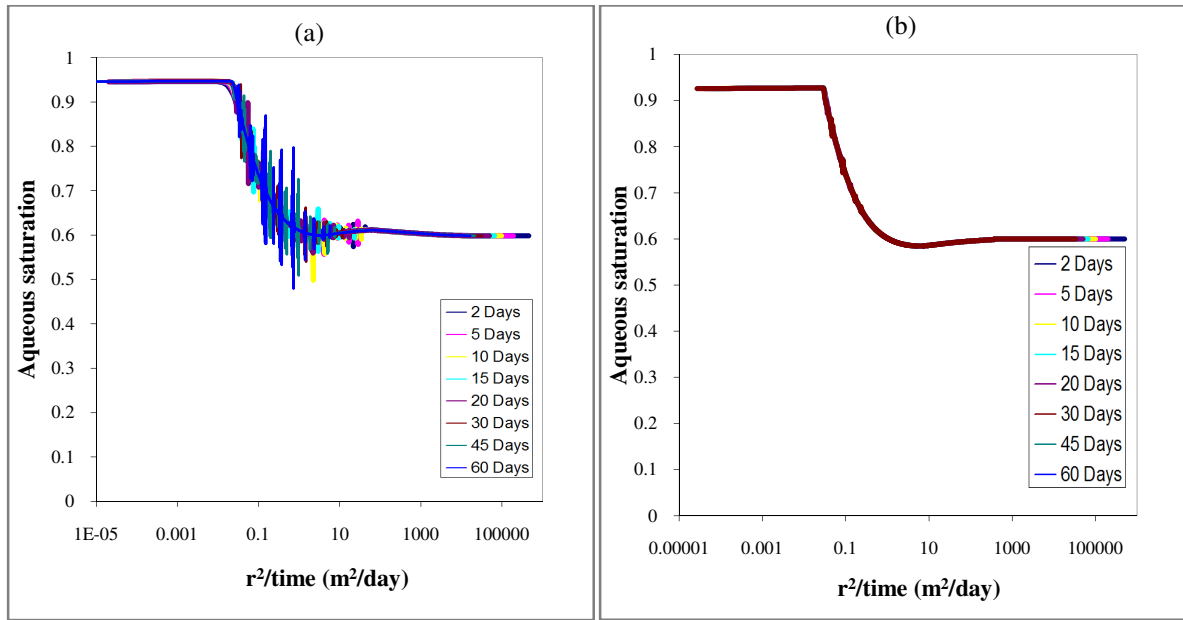


Figure 4- 10 Profiles of aqueous saturation of Problem 4 case 2 for (a) CMG STARS (b) TOUGH-Fx/HYDRATE.

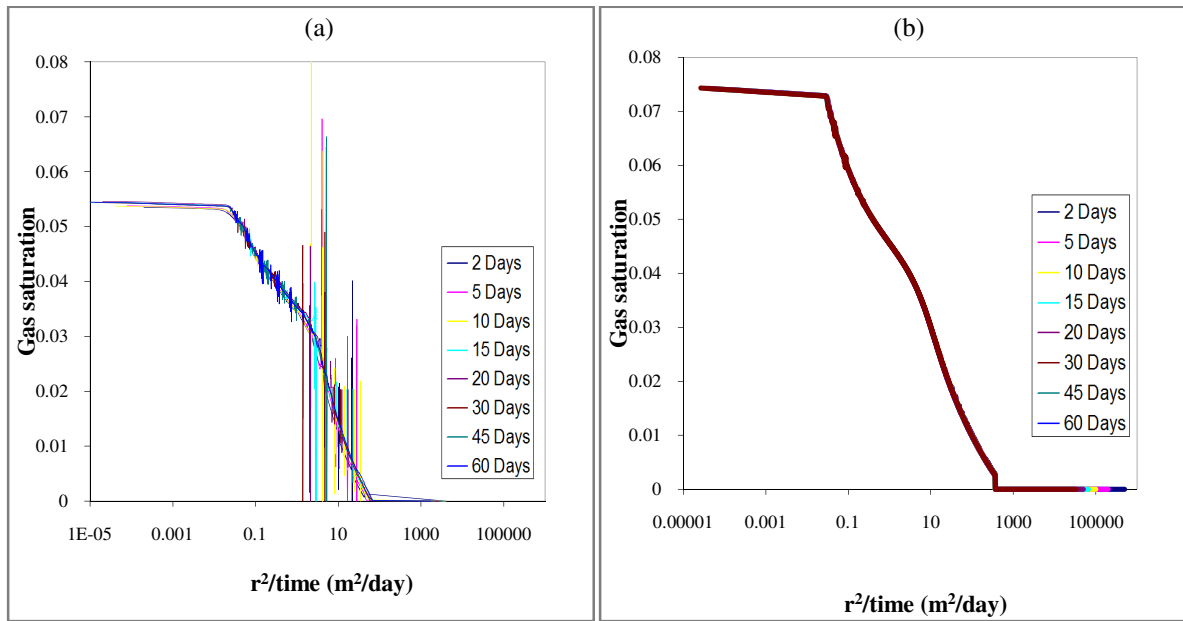


Figure 4- 113 Profiles of gas saturation of Problem 4 case 2 for (a) CMG STARS (b) TOUGH-Fx/HYDRATE.

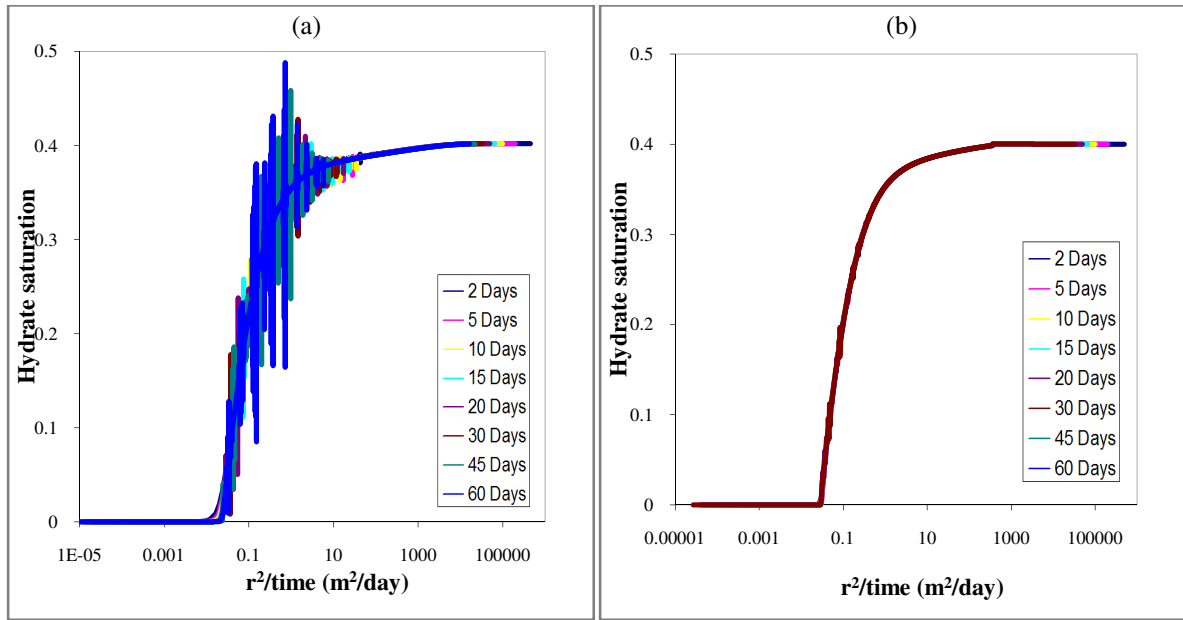


Figure 4- 14 Profiles of hydrate saturation of Problem 4 case 2 for (a) CMG STARS (b) TOUGH-Fx/HYDRATE.

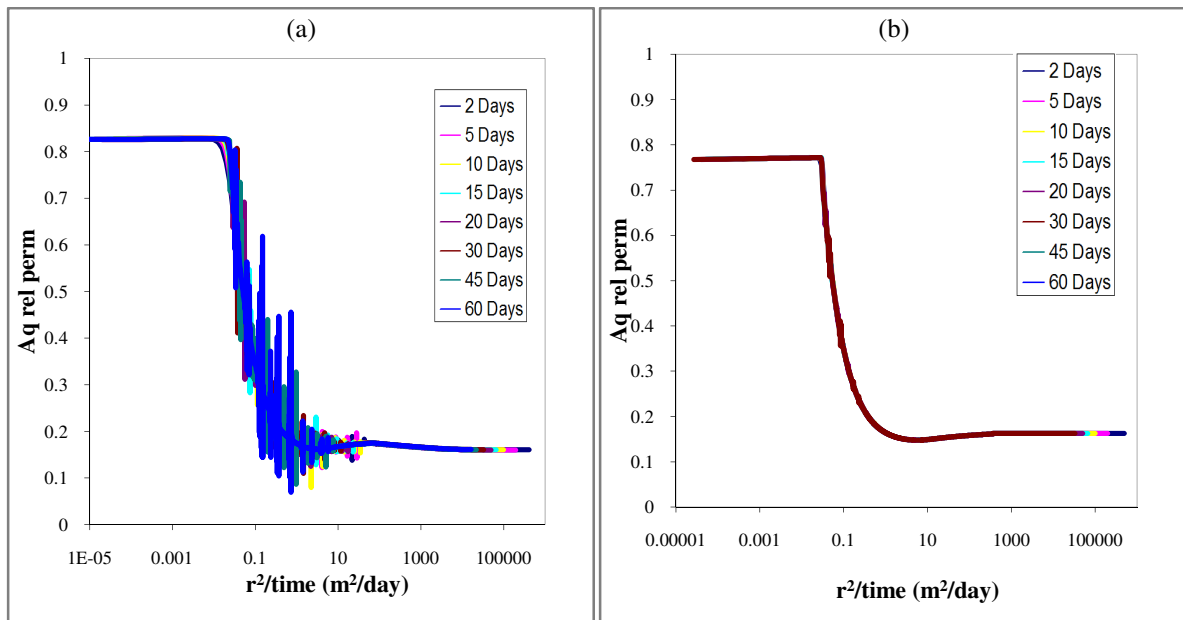


Figure 4- 15 Profiles of aqueous relative permeability of Problem 4 case 2 for (a) CMG STARS (b) TOUGH-Fx/HYDRATE.

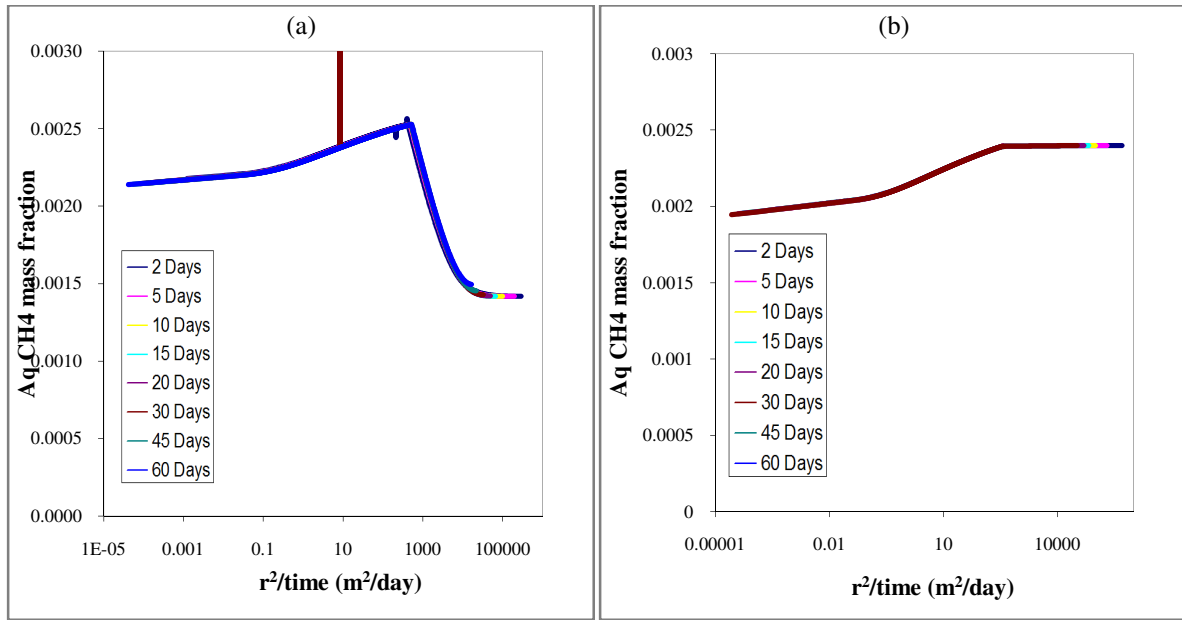


Figure 4- 16 Profiles of aqueous CH4 mass fraction of Problem 4 case 2 for (a) CMG STARS (b) TOUGH-Fx/HYDRATE.

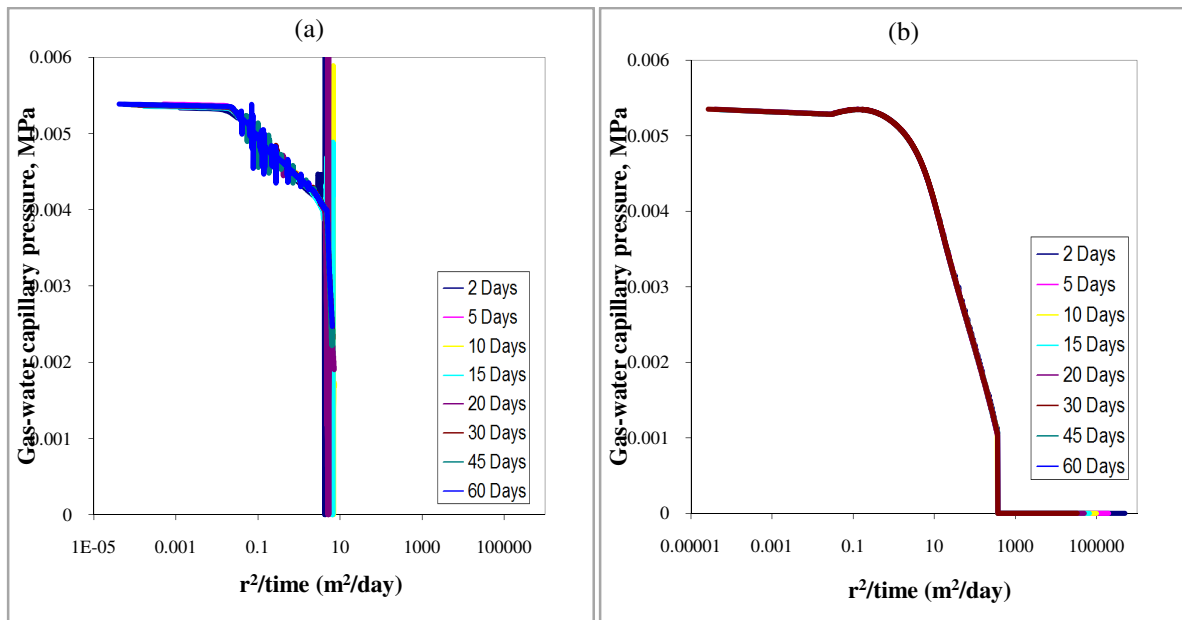


Figure 4- 17 Profiles of gas-water capillary pressure of Problem 4 case 2 for (a) CMG STARS (b) TOUGH-Fx/HYDRATE.

4.2 Problem 5

This problem is a typical example of Class 2 hydrate deposits in which hydrate layer is bounded by saturated water zone. This problem models gas hydrate dissociation behavior in a two dimensional radial domain. The grid consists of a hydrate zone which is bounded at the top and bottom by two shale zones. The thickness of the hydrate layer is 10 m and the corresponding shale zones are 25 m. Two different cases, cases A and B are defined to evaluate the effect of hydrate saturation on the production rates. The problem is set up to verify the effect of discretization on the responses. For the same case four different models are developed to understand the effect of discretization.

Grid Description:

The length and height of the 2-D radial grid system is 1000 m x 60 m. The schematic of the radial grid is shown in Figure 4-18

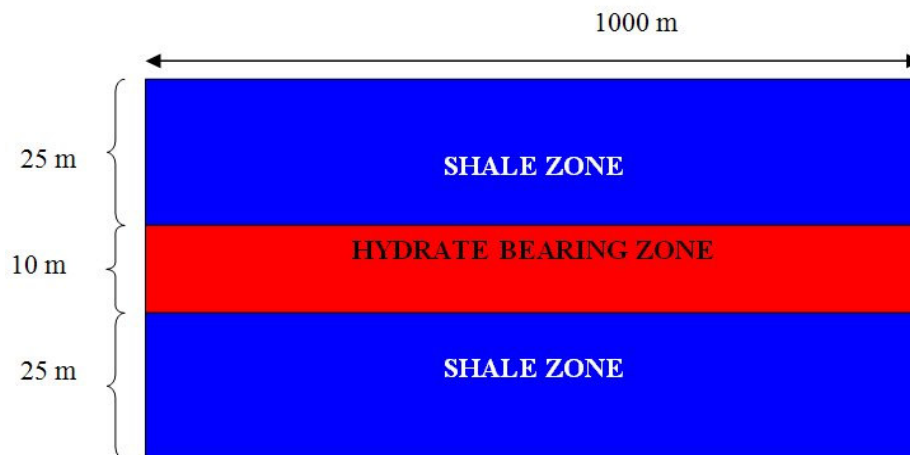


Figure 4-18 Geometry of the cylindrical grid for Problem 5.

The method for hydrate dissociation is chosen as depressurization. The bottom-hole pressure for the depressurization is chosen in such a way that there is no ice formation, i.e. the

pressure is maintained above the quadruple point. There is no mass or heat flow to the surroundings.

Discretization of the grid:

The entire reservoir is discretized in four different ways. However, for all four discretizations the grid is logarithmically distributed in the r - direction. The innermost grid have a Δr of 0.02 m. The logarithmic distribution is calculated by the following formula

$$\Delta r_{n+1} = f * \Delta r_n, \text{ where } f \text{ is a constant which is fixed for every model.}$$

Model 1 (200 x 30)

r direction : 200 cells logarithmically distributed from $r_w = 0.10795$ m to $r_{200} = 1000$ m,

z direction : 30 cells (5 x 5 m, 20 x 0.5 m, 5 x 5 m), $\Delta r_1 = 0.02$ and $f = 1.03856$

Model 2 (200 x 11)

r direction : 200 cells logarithmically distributed from $r_w = 0.10795$ m to $r_{200} = 1000$ m

z direction : 11 cells (5 x 5 m, 1 x 10.0 m, 5 x 5 m), $\Delta r_1 = 0.02$ and $f = 1.03856$

Model 3 (50 x 30)

r direction : 50 cells logarithmically distributed from $r_w = 0.10795$ m to $r_{50} = 1000$ m

z direction : 30 cells (5 x 5 m, 20 x 0.5 m, 5 x 5 m), $\Delta r_1 = 0.02$ and $f = 1.20257$

Model 4 (50 x 11)

r direction : 50 cells logarithmically distributed from $r_w = 0.10795$ m to $r_{50} = 1000$ m

z direction : 11 cells (5 x 5 m, 1 x 10.0 m, 5 x 5 m), $\Delta r_1 = 0.02$ and $f = 1.20257$

Case Description

Considering the four different discretizations used for this problem, the introduction of two cases, A and B means that eight different cases are modeled in this problem. The hydrate

saturation for case A and case B are 0.8 and 0.75. Different cases and their parameters are given in Table 4-2.

Table 4-2 Case Description of Problem 5

Case	Discretization	S_H	S_W	Pressure & Temperature
Case A-1	Model 1	0.8	0.2	Table 4-3
Case A-2	Model 2	0.8	0.2	Table 4-4
Case A-3	Model 3	0.8	0.2	Table 4-3
Case A-4	Model 4	0.8	0.2	Table 4-4
Case B-1	Model 1	0.75	0.25	Table 4-3
Case B-2	Model 2	0.75	0.25	Table 4-4
Case B-3	Model 3	0.75	0.25	Table 4-3
Case B-4	Model 4	0.75	0.25	Table 4-4

Initial Conditions

Pressure and temperature for different layers are specified in Table 4-3 and Table 4-4.

Pressure & Temperature:

Model 1 & Model 3

Table 4-3 Pressures and Temperatures for Models 1 & 3

Layer	Pressure	Temperature	Layer	Pressure	Temperature
	(MPa)	(K)		(MPa)	(K)
1	10.382	285.676	16	10.654	286.507
2	10.431	285.827	17	10.658	286.521
3	10.48	285.979	18	10.663	286.536
4	10.529	286.13	19	10.668	286.55
5	10.578	286.281	20	10.673	286.564
6	10.604	286.364	21	10.678	286.579
7	10.609	286.379	22	10.683	286.593
8	10.614	286.393	23	10.688	286.607
9	10.619	286.407	24	10.693	286.622
10	10.624	286.421	25	10.698	286.636
11	10.629	286.436	26	10.724	286.719
12	10.634	286.45	27	10.773	286.87
13	10.639	286.464	28	10.822	287.022
14	10.644	286.479	29	10.871	287.173
15	10.649	286.493	30	10.92	287.324

Table 4- 4 Pressures and Temperatures for Models 2 & 4

Layer	Pressure (MPa)	Temperature (K)
1	10.382	285.676
2	10.431	285.827
3	10.480	285.979
4	10.529	286.130
5	10.578	286.281
6	10.651	286.500
7	10.724	286.719
8	10.773	286.870
9	10.822	287.022
10	10.871	287.173
11	10.920	287.324

Hydrate Saturation & Water Saturation:

There is no gas in the entire reservoir. The hydrate and water saturations are distributed in the entire reservoir as shown in Table 4-5.

Table 4- 5 Hydrate and Water Saturation for different case studies

Case	Hydrate Saturation (S_H)		Water saturation(S_W)	
	Shale Zone	Hydrate zone	Shale Zone	Hydrate zone
Case A	0	0.8	1	0.2
Case B	0	0.75	1	0.25

Boundary Conditions:

There is no mass and heat flow outside the grid. The upper and lower boundary temperature are maintained a constant value of 285.6 K and 287.4 K.

Medium Properties:

Hydraulic and thermal properties for this problem are specified in Table 4-6.

Table 4-6 Hydraulic and Thermal Properties for Problem 5

Parameter	Value
Porosity	Shale zone (0.1), hydrate zone (0.4)
Permeability	Shale zone (0.0), hydrate zone (1000 md)
Rock Density	2600 kg/m ³
Rock Specific heat	1000 J/kg K
Dry Thermal Conductivity	2.0 W/m K
Pore Compressibility	10 ⁻⁹ Pa ⁻¹
Composite Thermal Conductivity Model	linear
Capillary Pressure Model	Van Genuchten Equation ³⁴
λ parameter	0.45
S_{irA} parameter	Case A(0.14), Case B(0.19)
l/P_o parameter	8 x 10 ⁻⁵ Pa ⁻¹
P_{max} parameter	5.0 x 10 ⁶ Pa
S_{mxA} parameter	1
Aqueous Relative Permeability Model	Stone ³⁶ + Aziz ³⁷
S_{irA} parameter	case A(0.15), case B (0.20)
n parameter	3
Gas Relative Permeability Model	Stone ³⁶ + Aziz ³⁷
S_{irG} parameter	case A(0.02), case B (0.02)

Relative permeability model

Aqueous and gas relative permeability model used in this problem is same as that in problem

3. Irreducible water and gas saturation values for this problem are specified in Table 4-6.

$$k_{rG} = (S_G^*)^n, \quad S_G^* = (S_G - S_{irG}) / (1 - S_{irA})$$

$$k_{rA} = (S_A^*)^n, \quad S_A^* = (S_A - S_{irA}) / (1 - S_{irA})$$

where S_{irG}, S_{irA} represent irreducible gas and aqueous saturation.

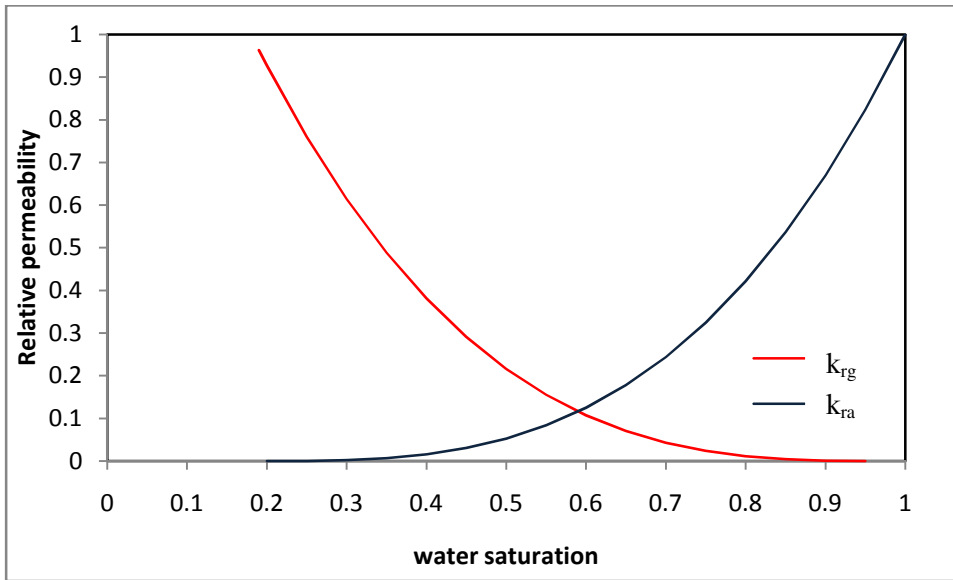


Figure 4-18 a Case A: Aqueous & Gas Relative permeability curves

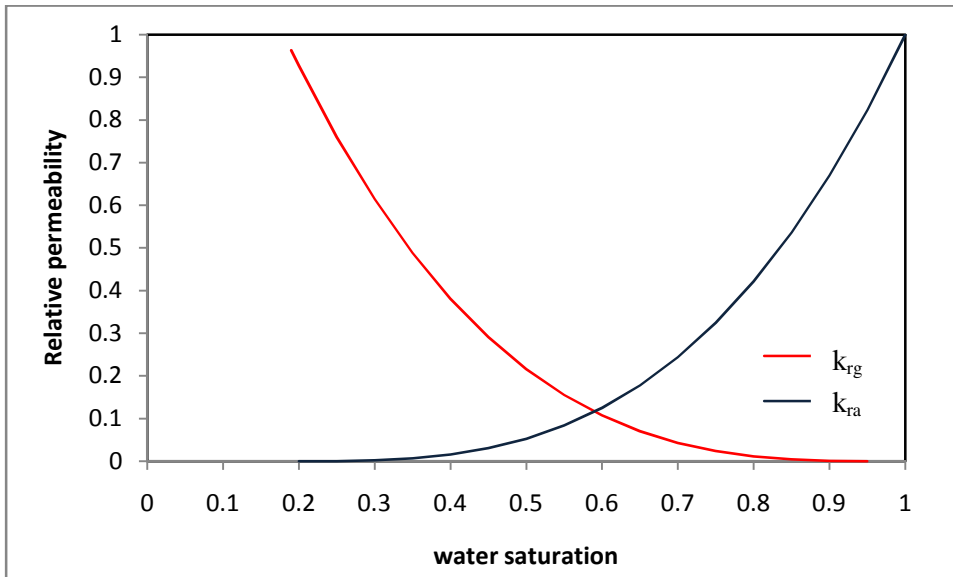


Figure 4-18 b Case B: Aqueous & Gas Relative permeability curves

Capillary pressure model

Capillary pressure model used in this problem is same as in problem 3. Different parameters and their specifications are given in Table 4-6. Plots of Capillary pressure for both cases are shown in Figure 4-19 (a) and (b)

$$P_{cap} = -P_0[(S^*)^{-1/\lambda} - 1]^\lambda, \quad S^* = \frac{(S_w^* - S_{wir})}{1 - S_{wir}}$$

$$S_w^* = \frac{S_w}{1 - S_H - S_I}, \quad \lambda = 0.45$$

Where $-P_{max} \leq P_{cap} \leq 0$

$$P_{max} = 5000 \text{ kPa}$$

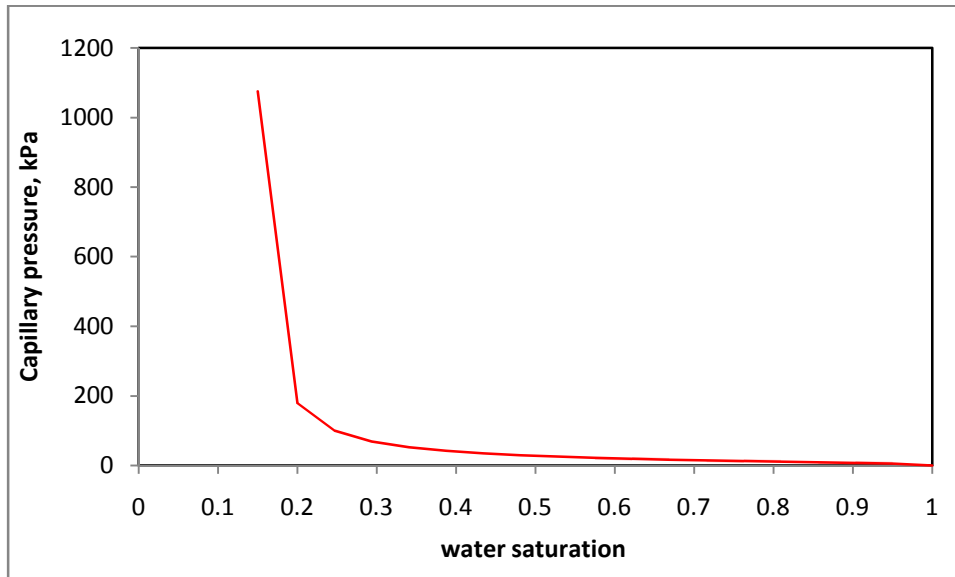


Figure 4-19 a Case A: Capillary pressure plotted against water saturation for Problem 5

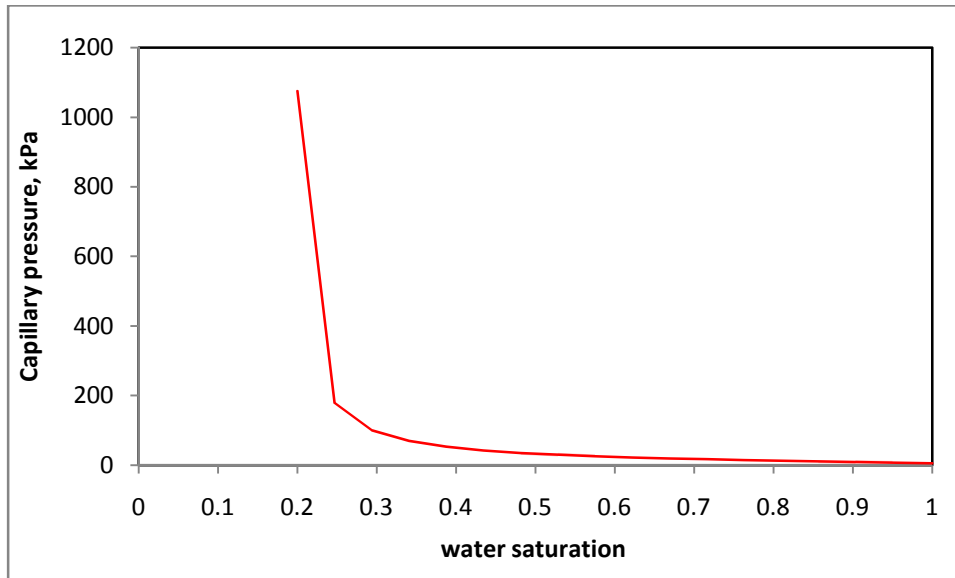


Figure 4-19 b Case B: Capillary pressure plotted against water Saturation for problem 5

Well Details

There is one vertical producer well at the center of the cylindrical grid of wellbore radius 0.10795 m. The bottom hole flowing pressure is constant and is equal to 2.7 MPa which is slightly above the Q point to avoid ice formation in the reservoir.

Data and Sampling Frequency

The simulations are carried out over a time period of 360 days. The production data is sampled every 10 days and the property distribution data is sampled every 90 days. The factors considered for data comparison are gas pressure, water pressure, methane hydrate saturation, water saturation, gas saturation, mass fraction of CH₄ in the aqueous phase, gas production rate, water production rate, cumulative gas production, and cumulative water production

4.2.1 Solution to Problem 5

The length and height of this 2-D radial grid is 1000 m x 60 m. The grid is discretized in four different ways which are mentioned as models (1, 2, 3 & 4) and the discretization for each model are specified in the problem description. The input data file used for case 5-A-1 is specified below. Different data files are adapted based on this data file.

```
**$ *****  
**$ Definition of fundamental cylindrical grid  
**$ *****  
GRID RADIAL 200 1 30 *RW          0.10795 ** MODEL 1  
KDIR DOWN  
**DIFFERENT FOR EACH MODEL  
DI IVAR  
  
    0.020          0.058          0.166          0.479          1.383  
    0.021          0.060          0.173          0.498          1.436  
    0.022          0.062          0.179          0.517          1.491  
    0.022          0.065          0.186          0.537          1.549  
    0.023          0.067          0.193          0.558          1.608  
    0.024          0.070          0.201          0.579          1.670  
    0.025          0.072          0.209          0.602          1.735  
    0.026          0.075          0.217          0.625          1.802  
    0.027          0.078          0.225          0.649          1.871  
    0.028          0.081          0.234          0.674          1.943  
    0.029          0.084          0.243          0.700          2.018  
    0.030          0.087          0.252          0.727          2.096  
    0.031          0.091          0.262          0.755          2.177  
    0.033          0.094          0.272          0.784          2.261  
    0.034          0.098          0.282          0.814          2.348  
    0.035          0.102          0.293          0.846          2.438  
    0.037          0.106          0.305          0.878          2.532  
    0.038          0.110          0.316          0.912          2.630  
    0.040          0.114          0.328          0.947          2.731  
    0.041          0.118          0.341          0.984          2.837  
    0.043          0.123          0.354          1.022          2.946  
    0.044          0.128          0.368          1.061          3.059  
    0.046          0.133          0.382          1.102          3.177  
    0.048          0.138          0.397          1.144          3.300  
    0.050          0.143          0.412          1.189          3.427  
    0.051          0.148          0.428          1.234          3.559  
    0.053          0.154          0.445          1.282          3.696  
    0.056          0.160          0.462          1.331          3.839
```

3.987	6.277	9.882	15.558	24.494
4.140	6.519	10.263	16.157	25.438
4.300	6.770	10.658	16.780	26.418
4.466	7.031	11.069	17.427	27.437
4.638	7.302	11.496	18.099	28.494
4.817	7.583	11.939	18.796	29.592
5.002	7.876	12.399	19.521	30.733
5.195	8.179	12.877	20.273	31.918
5.395	8.494	13.373	21.055	33.148
5.603	8.822	13.889	21.866	34.426
5.819	9.162	14.424	22.709	35.753
6.044	9.515	14.980	23.585	37.131

```

DJ JVAR          360
DK KVAR
5      5      5      5      5
0.5    0.5    0.5    0.5    0.5
0.5    0.5    0.5    0.5    0.5
0.5    0.5    0.5    0.5    0.5
0.5    0.5    0.5    0.5    0.5
5      5      5      5      5
DTOP
  200*10
NULL CON          1
**$ Property: Porosity Max: 0.4 Min: 0.1
POR KVAR
  5*0.1 20*0.4 5*0.1
PERMI KVAR
  5*0.0001 20*1000 5*0.0001
PERMJ KVAR
  5*0.0001 20*1000 5*0.0001
PERMK KVAR
  5*0.0001 20*1000 5*0.0001
END-GRID
ROCKTYPE 1
** SAME AS IN THE PREVIOUS PROBLEM
**$ Model and number of components
Same as previous problem
ROCKFLUID ** CASE A ONLY
RPT 1 WATWET
SWT
**$
      Sw          krw          krow          Pcow
0.15          0  0.00000009          0
0.2  0.000203542  0.00000008          0
0.25  0.001628333  0.00000008          0
0.3  0.005495624  0.00000007          0
0.35  0.013026664  0.00000006          0
0.4  0.025442703  0.00000005          0
0.45  0.043964991  0.00000004          0
0.5  0.069814777  0.00000003          0
0.55  0.104213312  0.00000002          0
0.6  0.148381844  0.00000001          0
0.65  0.203541624  0.00000001          0
0.7  0.270913902  0.00000001          0
0.75  0.351719927  0.00000001          0
0.8  0.447180949  0.00000001          0
0.85  0.558518217  0.00000001          0
0.9  0.686952982  0.00000001          0
0.95  0.833706493  0.00000001          0
      1          1          0          0
SLT
**$      Sl          krg          krog          Pcog

```


0.15	0.931059638	0	1074.975692
0.2	0.772728679	0.00000006	178.9493308
0.25	0.633449216	0.00000006	97.27040457
0.3	0.512	0.00000006	66.46254911
0.35	0.40715978	0.00000006	50.17405093
0.4	0.317707307	0.00000006	40.01647498
0.45	0.242421331	0.00000006	33.0124855
0.5	0.180080602	0.00000006	27.83735789
0.55	0.129463871	0.00000006	23.81053609
0.6	0.089349888	0.00000006	20.54464579
0.65	0.058517403	0.00000006	17.80056682
0.7	0.035745166	0.00000006	15.41944379
0.75	0.019811928	0.00000006	13.2868432
0.8	0.009496438	0.00000006	11.31057562
0.85	0.003577448	0.00000007	9.401695899
0.9	0.000833706	0.00000008	7.444769663
0.95	4.3965E-05	0.00000009	5.199377579
1	0	0.00000009	0

INITIAL
VERTICAL OFF

INITREGION 1

REFPRES 3000

**\$ Property: Pressure (kPa) Max: 10920.4 Min: 10381.6

PRES KVAR

10381.6 10430.7 10479.9 10529 10578.2 10604.3 10609.2 10614.1 10619
10623.9 10628.9 10633.8 10638.7 10643.6 10648.5 10653.5 10658.4 10663.3
10668.2 10673.1 10678.1 10683 10687.9 10692.8 10697.7 10723.8 10773
10822.1 10871.3 10920.4

**\$ Property: Temperature (C) Max: 14.1743 Min: 12.5257

TEMP KVAR

12.5257 12.6771 12.8285 12.9799 13.1313 13.2142 13.2285 13.2428 13.2571
13.2714 13.2857 13.3 13.3143 13.3286 13.3429 13.3572 13.3714 13.3857
13.4 13.4143 13.4286 13.4429 13.4572 13.4715 13.4858 13.5687 13.7201
13.8715 14.0229 14.1743

**\$ Property: Water Saturation Max: 1 Min: 0.2

SW KVAR

5*1 20*0.2 5*1

**\$ Property: Oil Saturation Max: 0.8 Min: 0

SO KVAR

5*0 20*0.8 5*0

**\$ Property: Gas Saturation Max: 0 Min: 0

SG CON 0

**\$ Property: Water Mole Fraction(CH4) Max: 0.0003 Min: 0.0003

MFRAC_WAT 'CH4' CON 0.0003

**\$ Property: Water Mole Fraction(H2O) Max: 0.9997 Min: 0.9997

MFRAC_WAT 'H2O' CON 0.9997

**\$ Property: Oil Mole Fraction(hydrate) Max: 1 Min: 1

MFRAC_OIL 'hydrate' CON 1

**\$ Property: Gas Mole Fraction(H2O) Max: 0.0003 Min: 0.0003

MFRAC_GAS 'H2O' CON 0.0003

**\$ Property: Gas Mole Fraction(CH4) Max: 0.9997 Min: 0.9997

MFRAC_GAS 'CH4' CON 0.9997

NUMERICAL

NORM PRESS 1000

CONVERGE PRESS 100

NEWTONCYC 30

NCUTS 15

RUN

DATE 2008 1 1

DTWELL 0.01

```

**$
WELL 'Well-1'
PRODUCER 'Well-1'
OPERATE MIN BHP 2700. CONT
**$      rad geofac wfrac skin
GEOMETRY K 0.10795 0.249 1. 0.
PERF GEO 'Well-1'
OPEN 'Well-1'

DATE 2008 3 31
DATE 2008 6 29
DATE 2008 9 27
DATE 2008 12 26
STOP

```

Results

Effect of discretization on production rates

Considering the four different discretizations used for this problem, the introduction of two cases A and B means that eight different cases are modeled. The hydrate saturation for Case A and Case B are 0.8 and 0.75 respectively. To study the effect of discretization on production rates profiles of case A-1 to A-4 and Case B-1 to B-4 are compared as given in Table 4-7.

Table 4-7 Effect of discretization on production rates for problem 5

Case	Model	Discretization (<i>r x z</i>)	Avg Gas rates (360 days), m ³ /day	Avg water rates (360 days), m ³ /day
case A-1	Model 1	200 x 30	50,000	60
case A-2	Model 2	200 x 11	10,000	20
case A-3	Model 3	50 x 30	40,000	50
case A-4	Model 4	50 x 11	9,000	20
case B-1	Model 1	200 x 30	100,000	150
case B-2	Model 2	200 x 11	15,000	60
case B-3	Model 3	50 x 30	100,000	120
case B-4	Model 4	50 x 11	25,000	60

Figures 4-21 to Figure 4-28 also show that the difference in the radial discretization of the grid did not affect production rates. Huge difference in the production rates is observed when discretization is changed in the z direction. In cases A-2, A-4, B-2 and B-4, the hydrate zone is treated as a single

block due which lesser production rates are observed. Case (A-1, A-3) and Case (A-2, A-4) have similar production rates. The same is also found within Case B.

Effect of hydrate saturation on production rates

Hydrate saturation is varied for Case-A and Case B. Increase in the production rate is observed when hydrate saturation is varied from 0.8 to 0.75. Table 4-8 shows the difference in the average production rates in both Cases A&B.

Table 4- 8 Effect of hydrate saturation on production rates for Problem 5

Case	S_H	Avg Gas rates (360 days), m³/day	Avg water rates (360 days), m³/day
Case-A	0.8	27,250	40
Case B	0.75	60,000	100

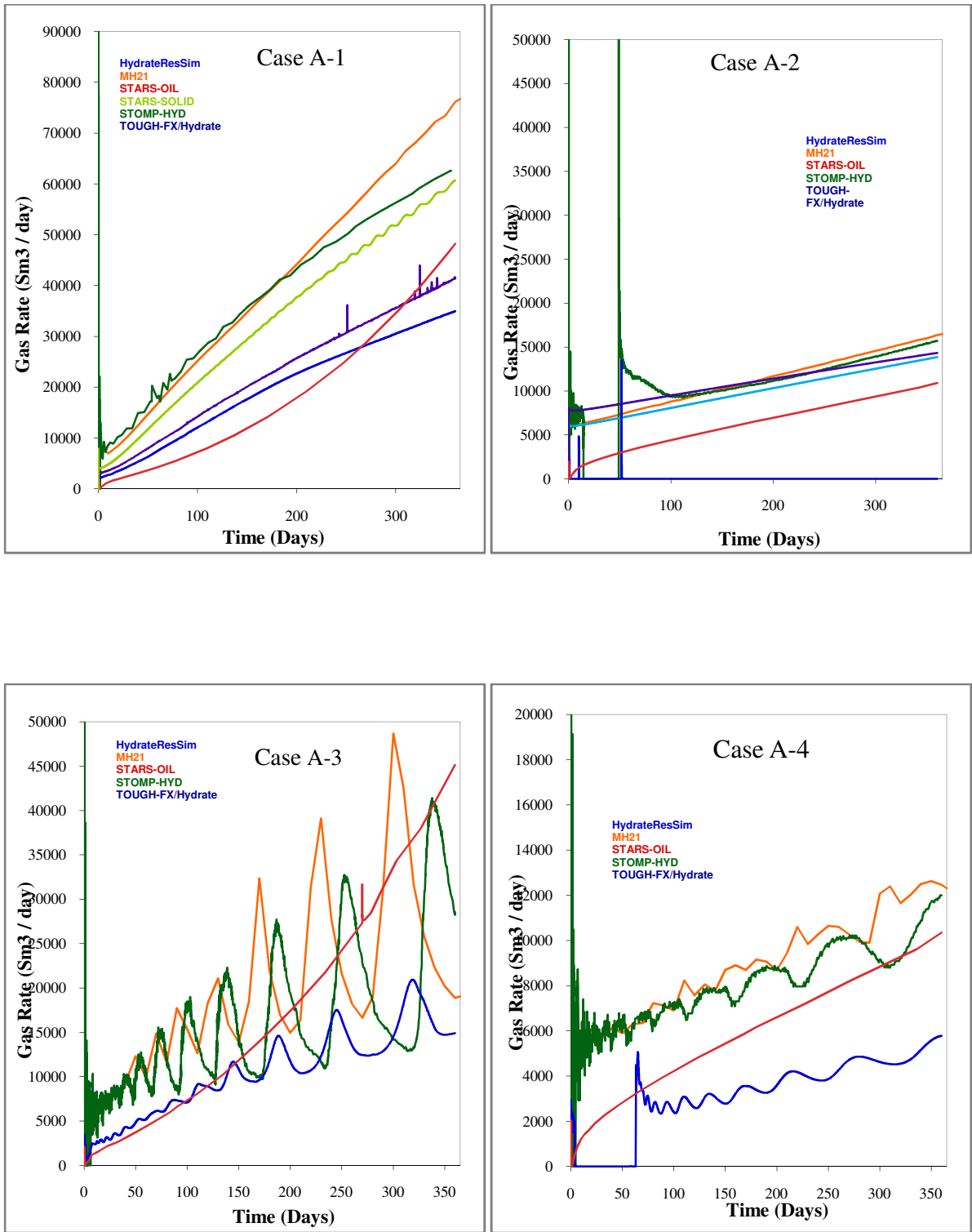


Figure 4-20 Gas Rates for problem 5 Cases A-1, A-2, A-3, A-4.

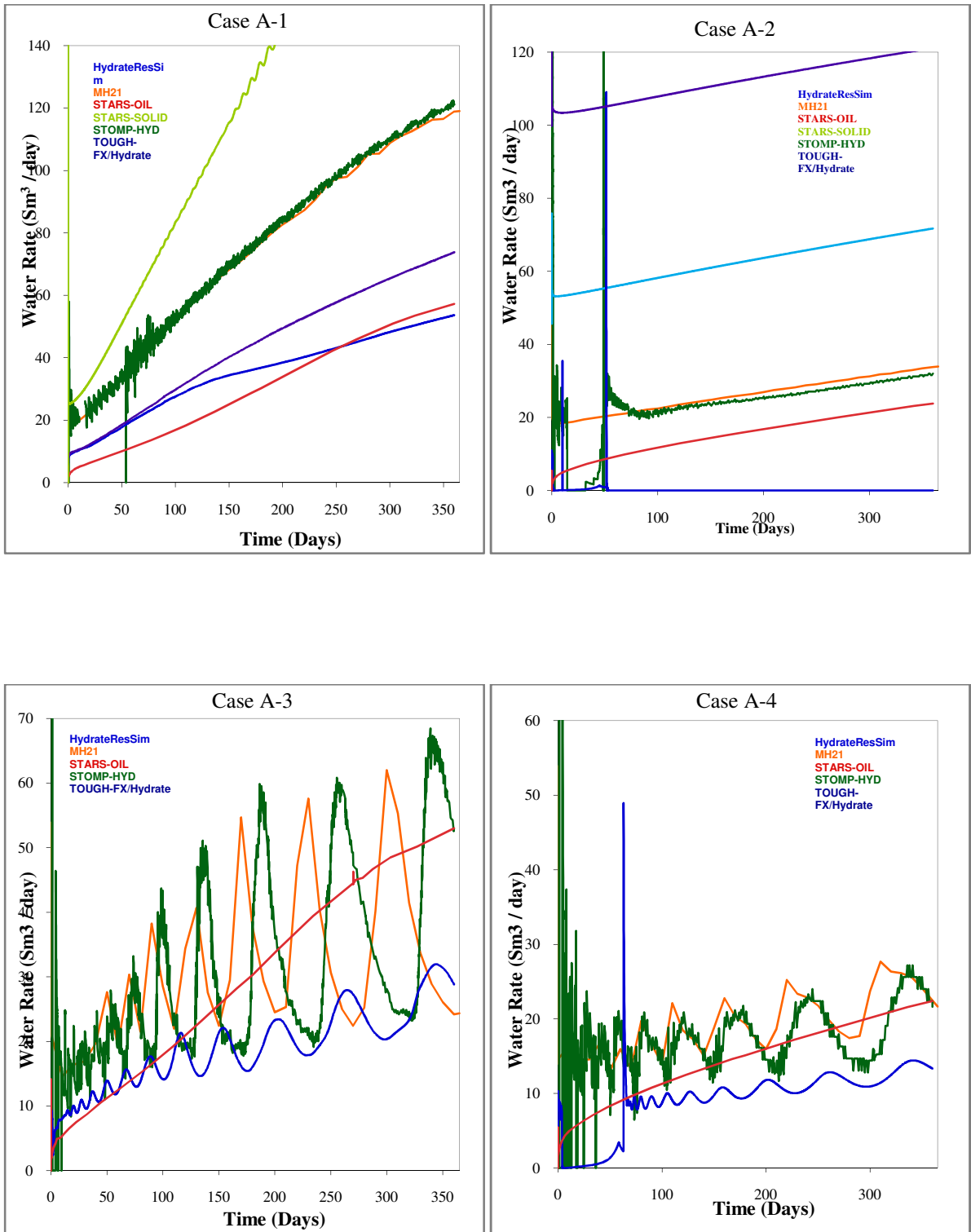


Figure 4-21 Gas Rates for problem 5 Cases A-1, A-2, A-3, A-4.

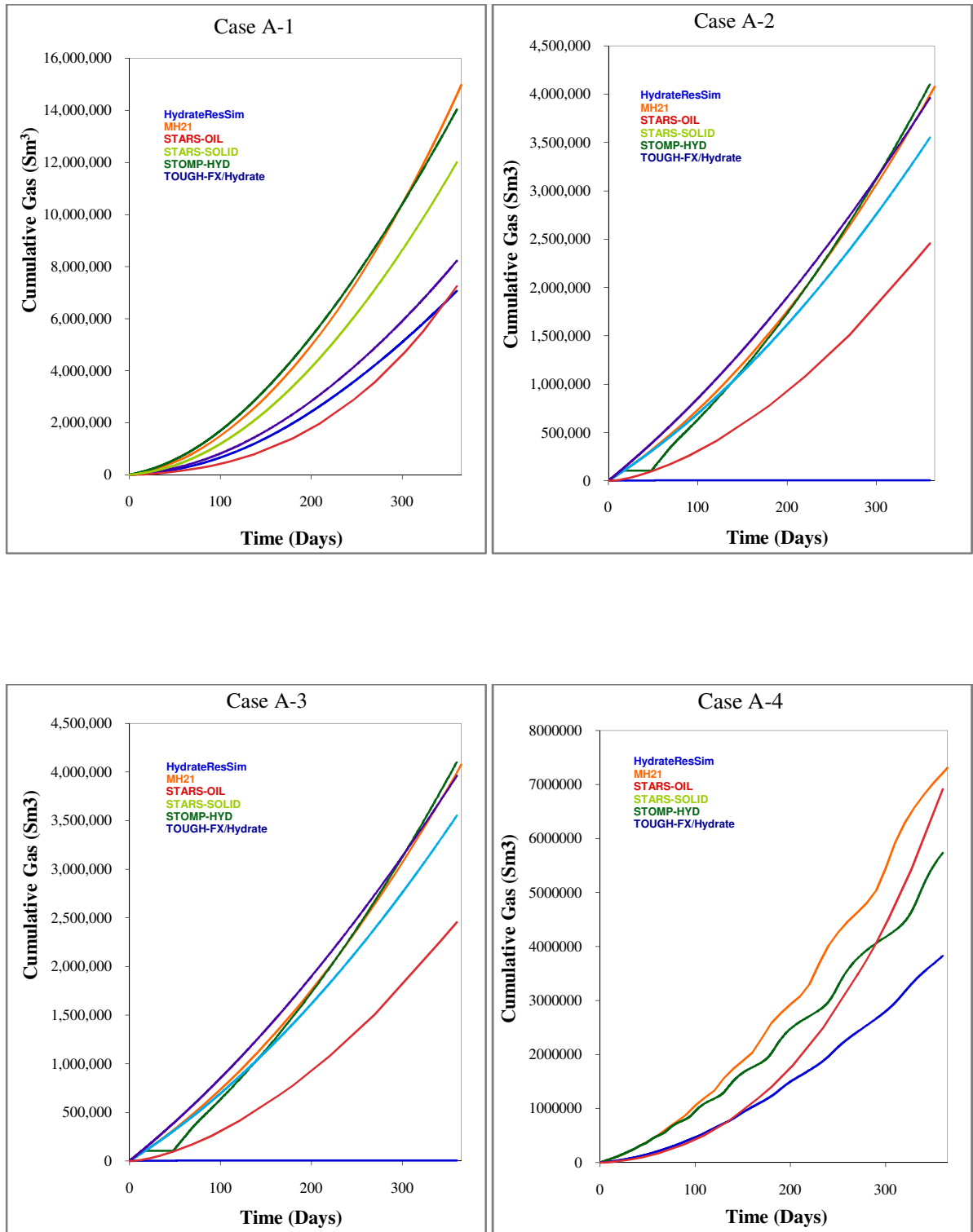


Figure 4-22 Cumulative gas production for problem 5 Cases A-1, A-2, A-3, A-4.

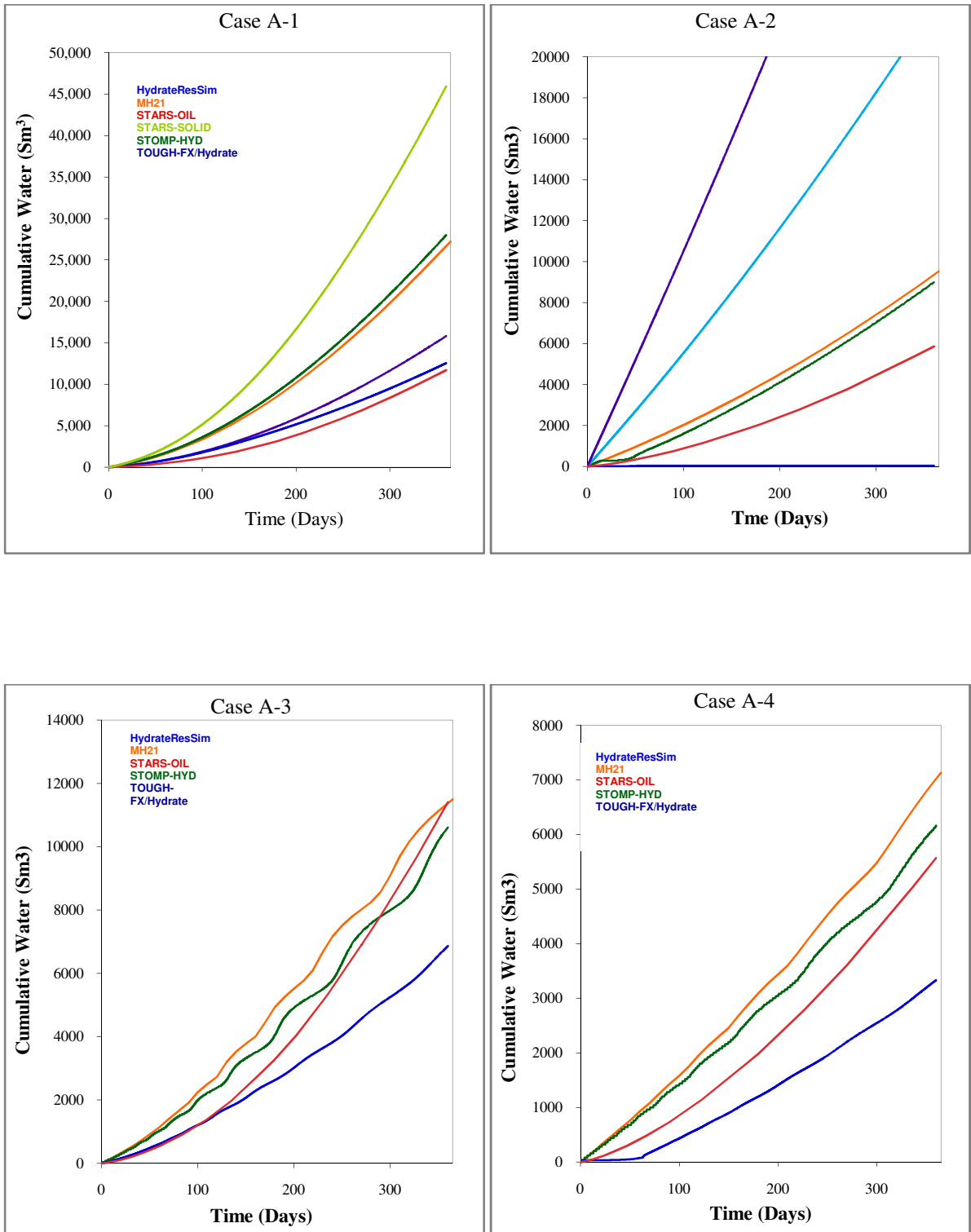


Figure 4-23 Cumulative water production for Problem 5 Cases A-1, A-2, A-3, A-4.

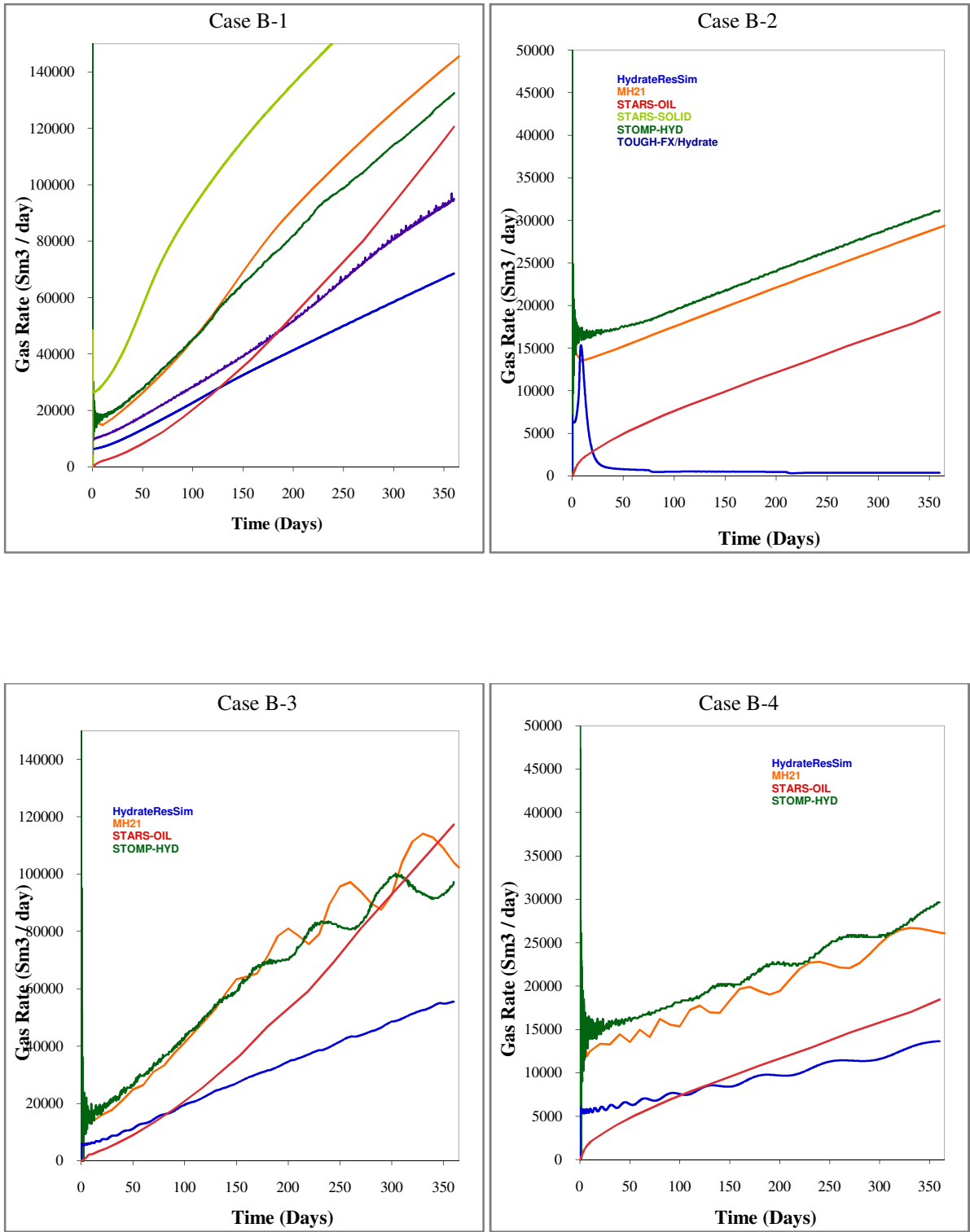


Figure 4-24 Gas rates for problem 5 Cases B-1, B-2, B-3, B-4.

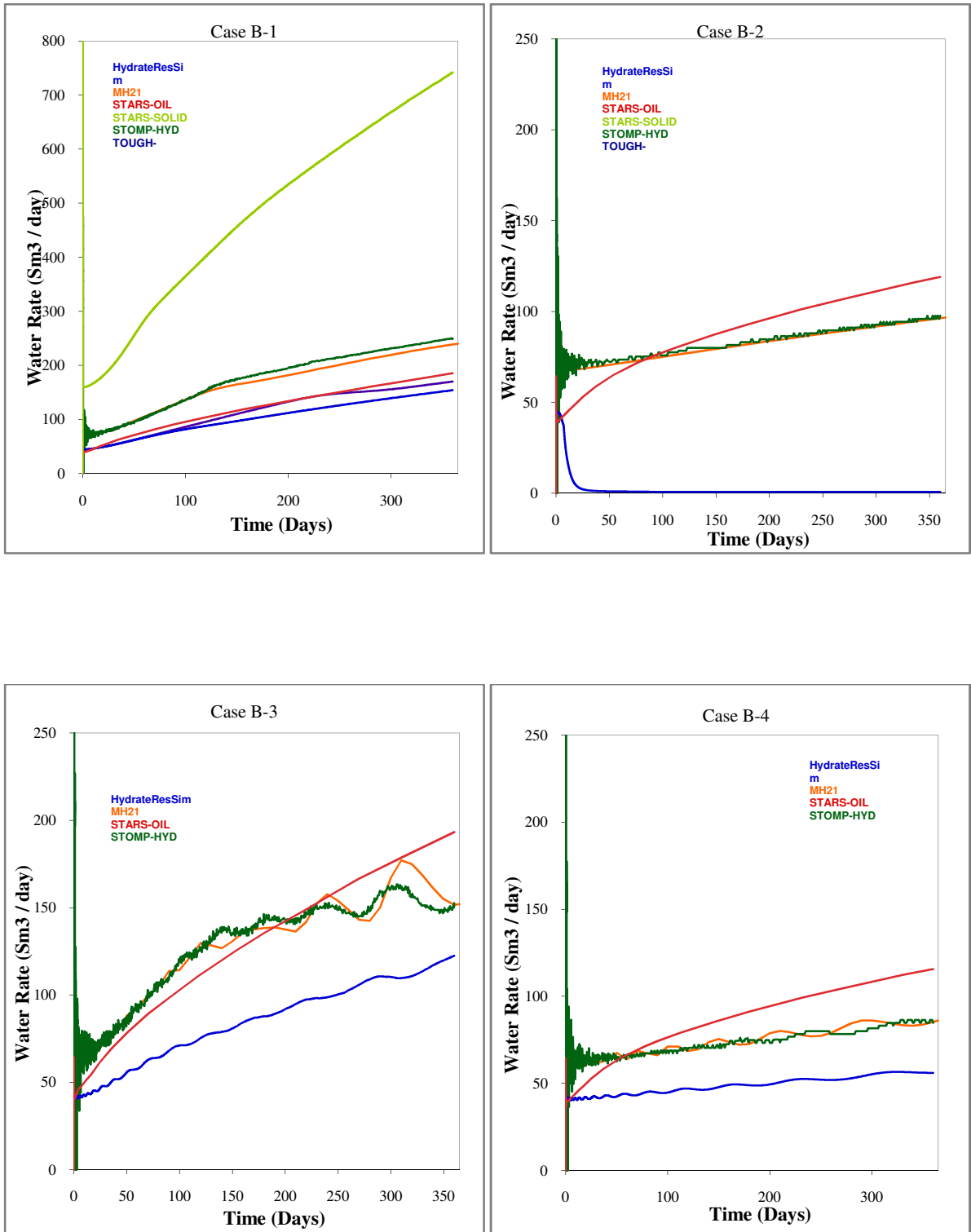


Figure 4-25 Water rates for problem 5 Cases B-1, B-2, B-3, B-4.

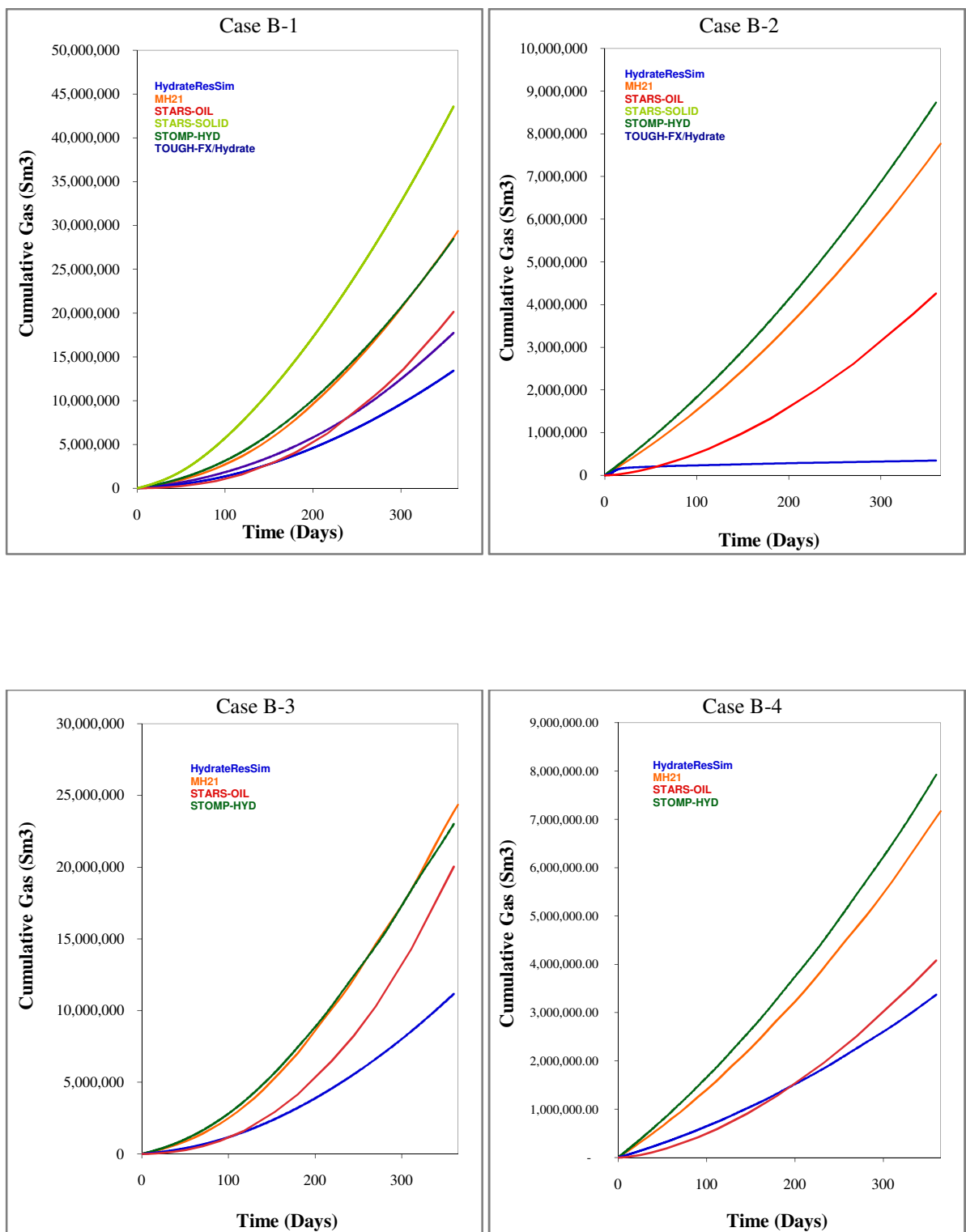


Figure 4-26 Cumulative gas production for problem 5 Cases B-1, B-2, B-3, B-4.

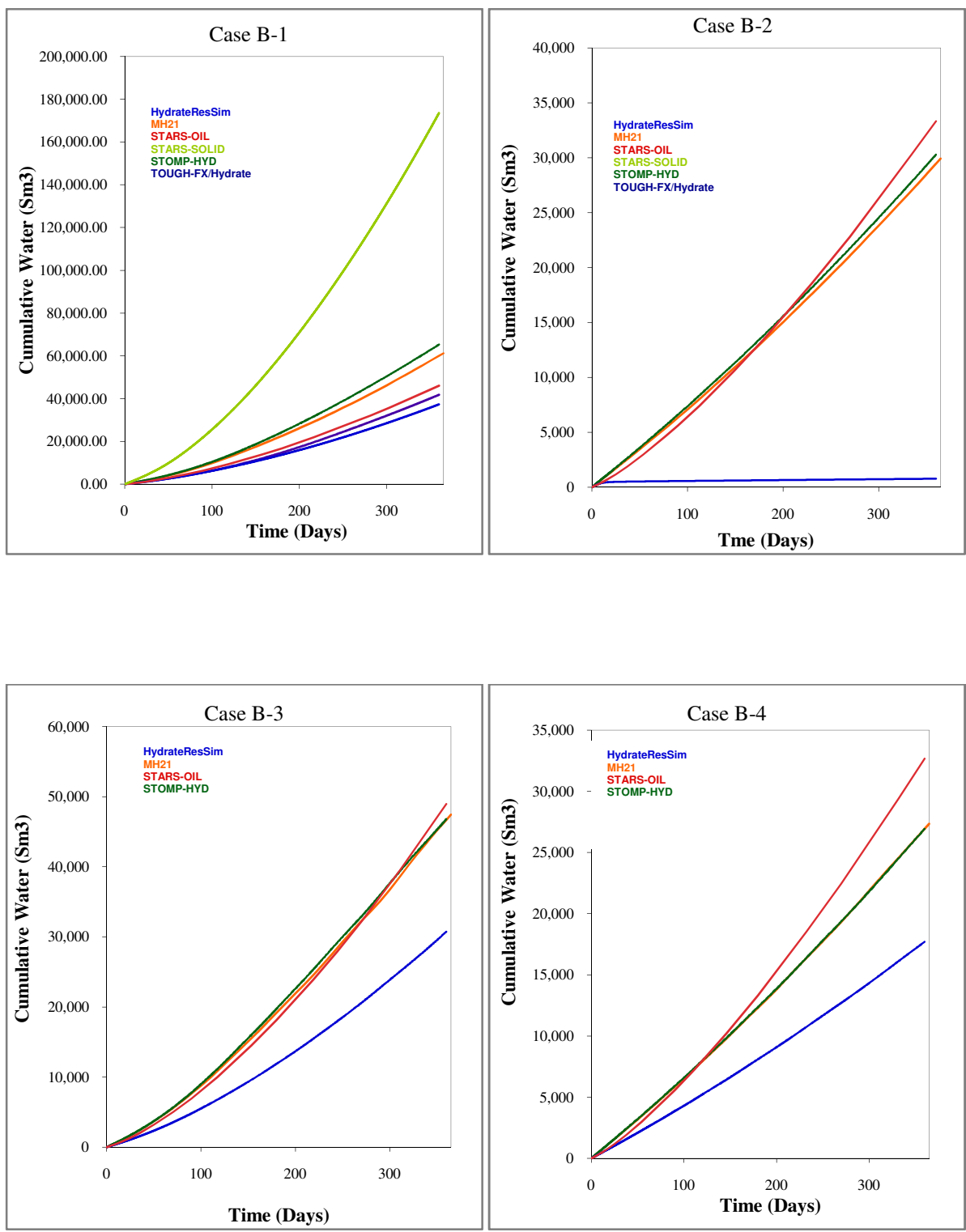


Figure 4-27 Cumulative water production for problem 5 Cases B-1, B-2, B-3, B-4.

5. Long term simulations on Prudhoe Bay and Mt. Elbert like sites

The Majority of the permafrost gas hydrates of the United States are found in the Alaskan region because of the geologic conditions that are compatible to permafrost hydrate formation.

Three different sites are chosen the Mt. Elbert site at Milne Point, the Prudhoe Bay L-Pad deposit and a theoretical accumulation of Prudhoe Bay L-Pad site. These have been preferred since Mt. Elbert was the site of the BP/US DOE Modular Dynamics Testing in, February 2007 and has extensive well log data. Prudhoe Bay sites are deeper reservoirs.

For simplicity in this study, the anisotropy of the reservoirs has been replaced with the average of each of the reservoir parameters obtained from NMR well log data.

Problem 7a is based on the Mt. Elbert site. It is a cold reservoir and hydrate can be extremely stable making it difficult to produce gas from Mt. Elbert. It is solved using a radial cylindrical domain. The hydrate bearing layer is bound by two shale zones.

Problem 7b originates from Prudhoe Bay L-Pad site. This reservoir consists of two hydrate bearing layers surrounded by shale zones. It is warmer than the reservoir specified in Problem 7a.

Problem 7c uses the same reservoir as that of Problem 7b; only difference being that is deeper, and thus warmer than the 7b reservoir.

5.1 Problem 7a

Geometry of the grid:

The whole structure of a grid is a cylinder with a vertical production well at the axis of the cylinder. There is distribution of cells in the grid in radial as well as vertical directions. The outer radius of the entire grid is 450 m and is 152.5 m deep. A schematic view of the grid is given in Figure 5-1.

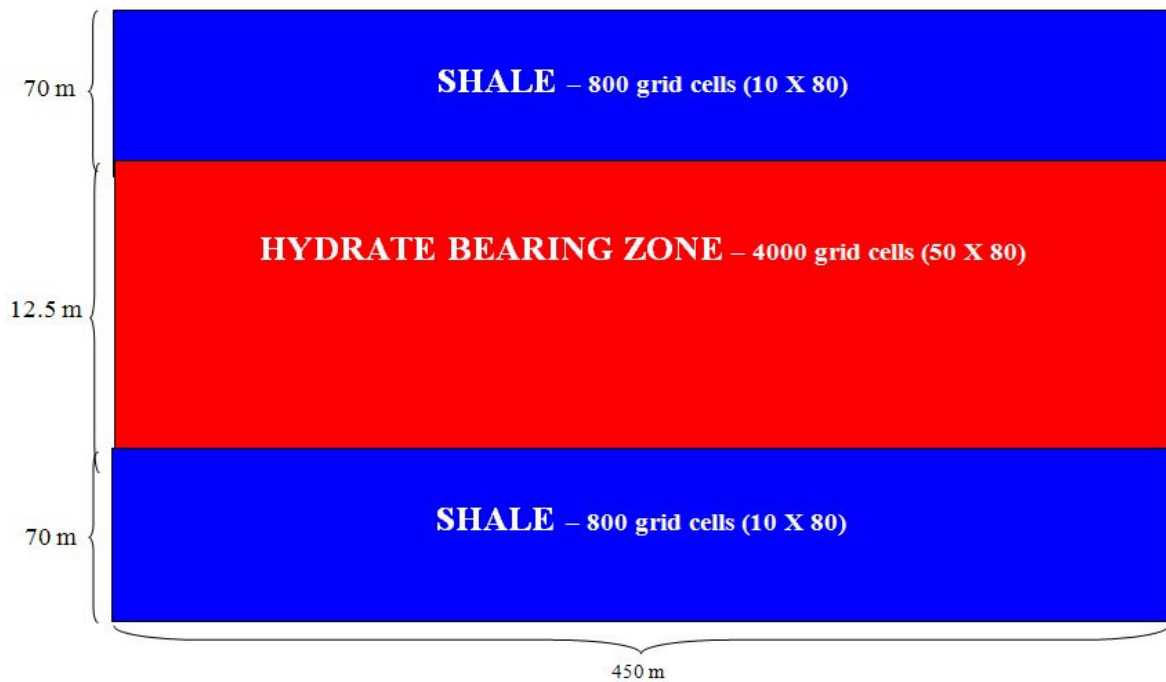


Figure 5-1 Schematic view of the grid for problem 7a.

Discretization of the grid:

r-direction: There are 80 cells distributed logarithmically from $r = r_w = 0.111\text{m}$. ($r_w =$ well bore radius) to $r = 450\text{m}$. The radius of the individual cells is given in Table 5-1.

Table 5-1 Radius of the individual cells

Cell	Radius, m	Cell	Radius, m	Cell	Radius, m	Cell	Radius, m
r1	0.131	r21	1.414	r41	10.287	r61	71.627
r2	0.153	r22	1.567	r42	11.340	r62	78.906
r3	0.177	r23	1.735	r43	12.500	r63	86.923
r4	0.204	r24	1.919	r44	13.777	r64	95.755
r5	0.233	r25	2.123	r45	15.184	r65	105.482
r6	0.266	r26	2.347	r46	16.734	r66	116.198
r7	0.302	r27	2.594	r47	18.442	r67	128.000
r8	0.341	r28	2.866	r48	20.322	r68	141.001
r9	0.384	r29	3.166	r49	22.394	r69	155.321
r10	0.432	r30	3.496	r50	24.675	r70	171.095
r11	0.485	r31	3.859	r51	27.188	r71	188.469
r12	0.543	r32	4.260	r52	29.957	r72	207.607
r13	0.606	r33	4.701	r53	33.006	r73	228.688
r14	0.677	r34	5.187	r54	36.365	r74	251.909
r15	0.754	r35	5.722	r55	40.065	r75	277.486
r16	0.839	r36	6.311	r56	44.140	r76	305.659
r17	0.933	r37	6.961	r57	48.629	r77	336.692
r18	1.037	r38	7.676	r58	53.573	r78	370.874
r19	1.151	r39	8.464	r59	59.020	r79	408.526
r20	1.276	r40	9.331	r60	65.019	r80	450.000

z-direction:

The cells in the hydrate bearing sediment are uniform in thickness and there are total of 50 cells in the hydrate layer. In each shale layer, there are 10 cells and the cell adjacent to the hydrate layer has a thickness of 0.25 m. From the center to the periphery, the cells increase in size logarithmically according to the equation $dz_i=dz_{i-1} * 1.694831$. Values of thickness of the cells in the z direction are given in Table 5-2

Table 5-2 Cell discretization in the z -direction for Problem 7a

Cell Number	dz	z(outer boundary)	z(center)
1	0.250	0.250	0.125
2	0.424	0.674	0.462
3	0.718	1.392	1.033
4	1.217	2.609	2.000
5	2.063	4.672	3.640
6	3.496	8.168	6.420
7	5.925	14.093	11.130
8	10.042	24.135	19.114
9	17.020	41.155	32.645
10	28.846	70.000	55.577

Initial conditions:

Hydrate Saturation and Water Saturation:

The hydrate saturation is 65% in the hydrate layer and water saturation is 35%. This 65 % is the average of the hydrate saturation data obtained from the NMR well log data obtained from Mt. Elbert site. In the shale layer, there is no hydrate and water saturation is 100%. In the z -direction, there is a geothermal gradient of 35.5 K/km and a hydrostatic pressure gradient of 9792 Pa/m. Following these gradients the pressures and temperatures at different depths are calculated and tabulated in Table 5-3.

Table 5- 3 Pressure and Temperature values for the reservoir modeled in Problem 7a

Cell	Region	Z	Z	T	T	P/MPa	P/MPa
		(boundary)	(center)	(boundary)	(center)	(boundary)	(center)
		0.000		273.295		6.035	
1	Shale	28.845	14.423	274.319	273.807	6.317	6.176
2	Shale	45.865	37.355	274.923	274.621	6.484	6.400
3	Shale	55.907	50.886	275.280	275.101	6.582	6.533
4	Shale	61.832	58.870	275.490	275.385	6.640	6.611
5	Shale	65.328	63.580	275.614	275.552	6.674	6.657
6	Shale	67.391	66.360	275.687	275.651	6.694	6.684
7	Shale	68.608	68.000	275.731	275.709	6.706	6.700
8	Shale	69.326	68.967	275.756	275.743	6.713	6.710
9	Shale	69.750	69.538	275.771	275.764	6.718	6.715
10	Shale	70.000	69.875	275.780	275.776	6.720	6.719
11	Hydrate	70.250	70.125	275.789	275.784	6.722	6.721
12	Hydrate	70.500	70.375	275.798	275.793	6.725	6.724
13	Hydrate	70.750	70.625	275.807	275.802	6.727	6.726
14	Hydrate	71.000	70.875	275.816	275.811	6.730	6.729
15	Hydrate	71.250	71.125	275.824	275.820	6.732	6.731
16	Hydrate	71.500	71.375	275.833	275.829	6.735	6.733
17	Hydrate	71.750	71.625	275.842	275.838	6.737	6.736
18	Hydrate	72.000	71.875	275.851	275.847	6.740	6.738
19	Hydrate	72.250	72.125	275.860	275.855	6.742	6.741
20	Hydrate	72.500	72.375	275.869	275.864	6.744	6.743
21	Hydrate	72.750	72.625	275.878	275.873	6.747	6.746
22	Hydrate	73.000	72.875	275.887	275.882	6.749	6.748
23	Hydrate	73.250	73.125	275.895	275.891	6.752	6.751
24	Hydrate	73.500	73.375	275.904	275.900	6.754	6.753
25	Hydrate	73.750	73.625	275.913	275.909	6.757	6.755
26	Hydrate	74.000	73.875	275.922	275.918	6.759	6.758
27	Hydrate	74.250	74.125	275.931	275.926	6.762	6.760
28	Hydrate	74.500	74.375	275.940	275.935	6.764	6.763
29	Hydrate	74.750	74.625	275.949	275.944	6.767	6.765
30	Hydrate	75.000	74.875	275.958	275.953	6.769	6.768
31	Hydrate	75.250	75.125	275.966	275.962	6.771	6.770
32	Hydrate	75.500	75.375	275.975	275.971	6.774	6.773
33	Hydrate	75.750	75.625	275.984	275.980	6.776	6.775
34	Hydrate	76.000	75.875	275.993	275.989	6.779	6.778
35	Hydrate	76.250	76.125	276.002	275.997	6.781	6.780

Table 5- 3 (contd....)

Cell	Region	Z	Z	T	T	P/MPa	P/MPa
		(boundary)	(center)	(boundary)	(center)	(boundary)	(center)
36	Hydrate	76.500	76.375	276.011	276.006	6.784	6.782
37	Hydrate	76.750	76.625	276.020	276.015	6.786	6.785
38	Hydrate	77.000	76.875	276.029	276.024	6.789	6.787
39	Hydrate	77.250	77.125	276.037	276.033	6.791	6.790
40	Hydrate	77.500	77.375	276.046	276.042	6.793	6.792
41	Hydrate	77.750	77.625	276.055	276.051	6.796	6.795
42	Hydrate	78.000	77.875	276.064	276.060	6.798	6.797
43	Hydrate	78.250	78.125	276.073	276.068	6.801	6.800
44	Hydrate	78.500	78.375	276.082	276.077	6.803	6.802
45	Hydrate	78.750	78.625	276.091	276.086	6.806	6.804
46	Hydrate	79.000	78.875	276.100	276.095	6.808	6.807
47	Hydrate	79.250	79.125	276.108	276.104	6.811	6.809
48	Hydrate	79.500	79.375	276.117	276.113	6.813	6.812
49	Hydrate	79.750	79.625	276.126	276.122	6.815	6.814
50	Hydrate	80.000	79.875	276.135	276.131	6.818	6.817
51	Hydrate	80.250	80.125	276.144	276.139	6.820	6.819
52	Hydrate	80.500	80.375	276.153	276.148	6.823	6.822
53	Hydrate	80.750	80.625	276.162	276.157	6.825	6.824
54	Hydrate	81.000	80.875	276.171	276.166	6.828	6.826
55	Hydrate	81.250	81.125	276.179	276.175	6.830	6.829
56	Hydrate	81.500	81.375	276.188	276.184	6.833	6.831
57	Hydrate	81.750	81.625	276.197	276.193	6.835	6.834
58	Hydrate	82.000	81.875	276.206	276.202	6.838	6.836
59	Hydrate	82.250	82.125	276.215	276.210	6.840	6.839
60	Hydrate	82.500	82.375	276.224	276.219	6.842	6.841
61	Shale	82.750	82.625	276.233	276.228	6.845	6.844
62	Shale	83.174	82.962	276.248	276.240	6.849	6.847
63	Shale	83.892	83.533	276.273	276.260	6.856	6.853
64	Shale	85.109	84.500	276.316	276.295	6.868	6.862
65	Shale	87.172	86.140	276.390	276.353	6.888	6.878
66	Shale	90.668	88.920	276.514	276.452	6.922	6.905
67	Shale	96.593	93.630	276.724	276.619	6.980	6.951
68	Shale	106.635	101.614	277.081	276.902	7.079	7.030
69	Shale	123.655	115.145	277.685	277.383	7.245	7.162
70	Shale	152.500	138.077	278.709	278.197	7.528	7.387

Boundary Conditions:

There is no net mass transport between the reservoir and the surroundings. The upper boundary temperature is held constant at 274.715 K and the lower boundary temperature is held at constant at 277.271 K.

Medium properties:

Medium properties like permeability porosity are specified in Table 5-4.

Table 5-4 Medium Properties for the Problem 5

Property	Value
Permeability, mD	Shale - 0.0
	Hydrate layer - 1000 (r direction)
	Hydrate layer - 100 (z direction)
Porosity, %	Shale - 10
	Hydrate zone - 35
pore Compressibility (1/Pa)	1.00E-08
Rock Density (kg/m ³)	2650
Rock Specific Heat (J/kg/K)	1000

Relative Permeability Models:

A relative permeability model developed by Stone + Aziz is used in this problem. The parameters were fixed so that every simulator has the same values.

Water Relative Permeability

$$k_{rw} = \left\{ \frac{(S_w - S_{wir})}{(1 - S_{wir})} \right\}^{4.52} ; S_{wir} = 0.248$$

Gas Relative Permeability

$$k_{rg} = \left\{ \frac{(S_G - S_{Gir})}{(1 - S_{Wir})} \right\}^{3.16} \quad S_{Wir} = 0. \quad S_{Gir} = 0.$$

S_{Wir} and S_{Gir} represents irreducible water and gas saturation. Gas and water relative permeability curves are shown in Figure 5-2.

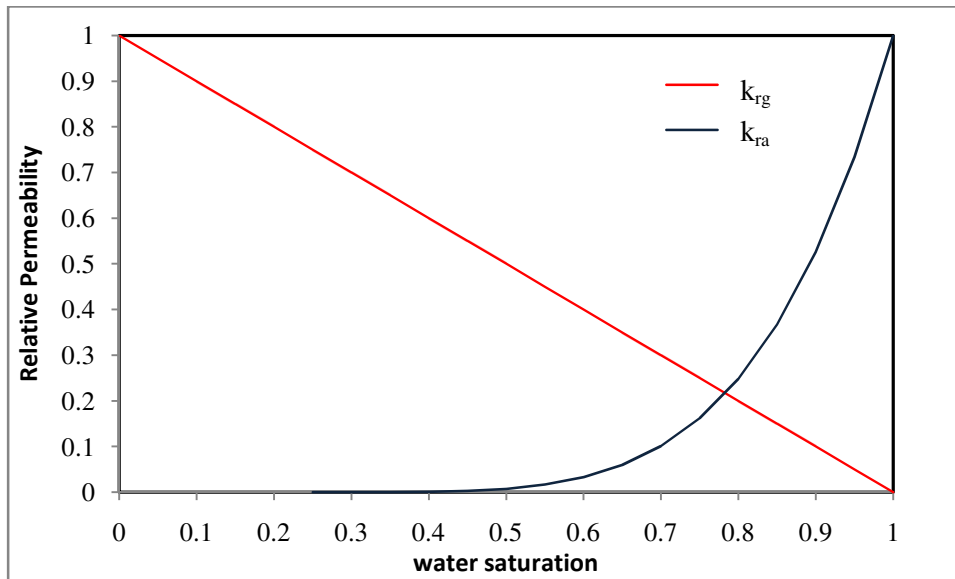


Figure 5- 2 Aqueous and Gas relative Permeability curves for Problem 7a.

Capillary Pressure Model:

Van Genuchten Capillary pressure Model is used just like in other problems.

$$\bar{s}_l = \frac{(s_l - s_{lr})}{(1 - s_{lr})} = \left(1 - \left(\alpha \beta_{gl} \left\{ \frac{(P_g - P_l)}{\rho_l g} \right\}^n \right)^m \right)^{-m} :$$

$$\alpha = 10.204 \text{ 1/m}, \beta_{gl} = 1.0, n = 4.432, m = 0.7744, s_{lr} = 0.28$$

where \bar{s}_l is the effective aqueous saturation, s_l is the aqueous saturation, β_{gl} is the interfacial tension scaling factor, and h_{gl} is the gas-aqueous capillary pressure head. Figure 5-3 shows the variation of capillary pressure with water saturation.

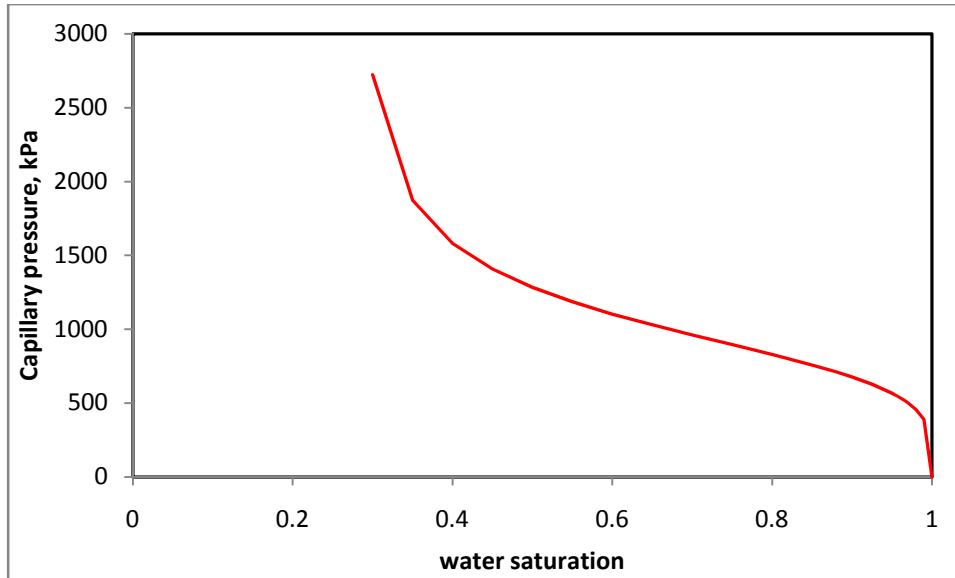


Figure 5-3 Capillary Pressure as a function of water saturation

Well Information:

Wellbore Radius is selected to be 0.111 m. The Bottom hole pressure is chosen to be 2.7MPa to avoid ice formation in the system.

Data and Sampling Frequency:

The simulations are carried out until all the hydrate dissociates and equilibrium is reached or over a time period of 50 years. Data for gas production rate, water production rate, cumulative gas production and cumulative water production is recorded with a time step of 90 days for 50 years.

5.1.1 Solution to Problem 7a

The input data file for the problem starts with the definition of the cylindrical grid.

Permeability porosity are specified as per the problem description.

```

**$ *****
**$ Definition of fundamental cylindrical grid
**$ *****
GRID RADIAL 80 1 70 *RW          0.111
KDIR DOWN
DI IVAR
0.020  0.022  0.024  0.027  0.029  0.033  0.036  0.039  0.043  0.048  0.053  0.058
      0.063  0.071  0.077  0.085  0.094  0.104  0.114  0.125  0.138  0.153  0.168
      0.184  0.204  0.224  0.247  0.272  0.300  0.330  0.363  0.401  0.441  0.486
      0.535  0.589  0.650  0.715  0.788  0.867  0.956  1.053  1.160  1.277  1.407
      1.550  1.708  1.880  2.072  2.281  2.513  2.769  3.049  3.359  3.700  4.075
      4.489  4.944  5.447  5.999  6.608  7.279  8.017  8.832  9.727 10.716 11.802
      13.001 14.320 15.774 17.374 19.138 21.081 23.221 25.577 28.173 31.033 34.182
      37.652 47.474
DJ JVAR          360
DK kvar
28.8455
17.0197
10.0421
5.92514
3.496
2.06275
1.21708
0.71811
0.42371
0.25
0.25  0.25  0.25  0.25  0.25  0.25  0.25  0.25  0.25  0.25
0.25  0.25  0.25  0.25  0.25  0.25  0.25  0.25  0.25  0.25
0.25  0.25  0.25  0.25  0.25  0.25  0.25  0.25  0.25  0.25
0.25  0.25  0.25  0.25  0.25  0.25  0.25  0.25  0.25  0.25
0.25  0.25  0.25  0.25  0.25  0.25  0.25  0.25  0.25  0.25
0.25
0.42371
0.71811
1.21708
2.06275
3.496
5.92514
10.0421
17.0197
28.8455
DTOP
80*500
CORNER-TOL 0.05
**$ Property: NULL Blocks Max: 1 Min: 1
**$ 0 = null block, 1 = active block
NULL CON          1
**$ Property: Porosity Max: 0.35 Min: 0.1
POR KVAR
  10*0.1 50*0.35 10*0.1
**$ Property: Permeability I (md) Max: 1000 Min: 0
PERMI KVAR
  10*0 50*1000 10*0
**$ Property: Permeability J (md) Max: 1000 Min: 0
PERMJ KVAR
  10*0 50*1000 10*0
**$ Property: Permeability K (md) Max: 100 Min: 0
PERMK KVAR
  10*0 50*100 10*0
END-GRID

```

Thermal properties, components description are as per the problem description.

```

ROCKTYPE 1
PRPOR 101.0
CPOR 5.0E-7
ROCKCP 2.0e+6 0
THCONR 1.728E+5
THCONS 1.728E+5
THCONW 5.183E+4
THCONO 3.395E+4
THCONG 7.4E+3
THCONMIX TEMPER
PERMCK 5

**$ Property: Thermal/rock Set Num Max: 1 Min: 1
THTYPE CON 1

**$ Model and number of components
MODEL 3 3 3 1

COMPNAME 'H2O' 'CH4' 'hydrate'

CMM 0 16.043e-3 127.333e-3
PCRIT 0 4.600E+3 1e4
TCRIT 0 -8.255E+1 1e3
KV1 1.186e7 3.65e9 0
KV4 -3816.44 -1942 0
KV5 -227.02 -265.99 0
CPG1 0.0E+0 1.9251E+1 0
CPG2 0.0E+0 5.213E-2 0
CPG3 0.0E+0 1.197E-5 0
CPG4 0.0E+0 -1.132E-8 0
CPL1 0.0E+0 0.0E+0 0
CPL2 0.0E+0 0.0E+0 0
CPL3 0.0E+0 0.0E+0 0
CPL4 0.0E+0 0.0E+0 0
MOLDEN 0 31800 7458
CP 0 5e-14 5e-14
CT1 0.0E+0 0 0
CT2 0.0E+0 0 0
AVG 0.0E+0 0.012198 0
BVG 0.0E+0 0.0E+0 0
AVISC 0.46642 0.137849 1e9
BVISC 0 114.14 0

** Reaction 1: 1 HYDRATE ---> 6.176 WATER + 1 CH4

**$ Reaction specification
STOREAC 1 0 1
STOPROD 7.176 1 0
RORDER 1 0 1
FREQFAC 1.e24
RENTN -51857.9364
EACT 146711.70
RXEQFOR 'H2O' 9.02843e15 0 0 -7893.6136 -273.15

** Reaction 2: 6.176 WATER + 1 CH4 --> 1 HYDRATE

**$ Reaction specification
STOREAC 6.176 1 0
STOPROD 0 0 1
RORDER 1 1 0
FREQFAC 1.e20
RENTN 51857.9364
EACT 146711.70
RXEQBAK 'H2O' 9.02843e15 0 0 -7893.6136 -273.15

```

Rock fluid properties, initial conditions such as pressure, temperature, and saturations are calculated based on models specified in the problem description.

```

ROCKFLUID
RPT 1 LININTERP WATWET
**SW      KRW      KROW      PCOW      **      kw
SWT
**$
      Sw      krw      krow      Pcow
0.248      0      0.00000008      960.48
0.3      5.69942E-06      0.00000007      599.3754829
0.35      0.000119776      0.00000006      481.4413657
0.4      0.000726823      0.00000005      419.5019542
0.45      0.002628352      0.00000004      375.2776708
0.5      0.007142098      0.00000003      340.2284612
0.55      0.016185523      0.00000002      310.8987242
0.6      0.032349547      0.00000001      285.5166471
0.65      0.058965383      0.000000009      263.0426992
0.7      0.100166174      0.000000008      242.8106796
0.75      0.160944508      0.000000007      224.3660077
0.8      0.24720656      0.000000006      207.3835797
0.85      0.365823416      0.000000005      191.6222293
0.9      0.52467998      0.000000004      176.8977346
0.95      0.732721791      0.000000003      163.0659502
1      1      0      150.0118032

```

```

** SL      KRG      KROG      PCOG
SLT
**$
      Sl      krg      krog      Pcog
0.29375      0.333202872      0      0
0.340625      0.26819991      0      0
0.3875      0.212449275      0      0
0.434375      0.165192515      0      0
0.48125      0.125680421      0      0
0.528125      0.093173674      0      0
0.575      0.066943593      0      0
0.621875      0.046273019      0      0
0.66875      0.030457384      0      0
0.715625      0.018806019      0      0
0.7625      0.010643808      0.00000005      0
0.809375      0.005313349      0.00000006      0
0.85625      0.002177914      0.00000007      0
0.903125      0.000625791      0.00000008      0
0.95      7.74008E-05      0.00000008      0
1      0      0.00000008      0

```

**\$ Property: Rel Perm Set Number Max: 1 Min: 1

```

KRTYPE IVAR 80*1
INITIAL
VERTICAL OFF
INITREGION 1

```

**\$ Property: Pressure (kPa) Max: 7387 Min: 6176

```

PRES KVAR
6176      6710      6731      6748      6765      6782      6800      6817      6834      6862
6400      6715      6733      6751      6768      6785      6802      6819      6836      6878
6533      6719      6736      6753      6770      6787      6804      6822      6839      6905
6611      6721      6738      6755      6773      6790      6807      6824      6841      6951
6657      6724      6741      6758      6775      6792      6809      6826      6844      7030
6684      6726      6743      6760      6778      6795      6812      6829      6847      7162
6700      6729      6746      6763      6780      6797      6814      6831      6853      7387

```

**\$ Property: Temperature (C) Max: 5.047 Min: 0.85

TEMP	KVAR									
0.85	2.593	2.67	2.732	2.794	2.856	2.918	2.981	3.043	3.145	
1.471	2.614	2.679	2.741	2.803	2.865	2.927	2.989	3.052	3.203	
1.951	2.626	2.688	2.75	2.812	2.874	2.936	2.998	3.06	3.302	
2.235	2.634	2.697	2.759	2.821	2.883	2.945	3.007	3.069	3.469	
2.402	2.643	2.705	2.768	2.83	2.892	2.954	3.016	3.078	3.752	
2.501	2.652	2.714	2.776	2.839	2.901	2.963	3.025	3.09	4.233	
2.559	2.661	2.723	2.785	2.847	2.91	2.972	3.034	3.11		
5.047										

```

**$ Property: Water Saturation Max: 1 Min: 0.35
SW KVAR
 10*1 50*0.35 10*1
**$ Property: Oil Saturation Max: 0.65 Min: 0
SO KVAR
 10*0
 50*0.65
 10*0
**$ Property: Gas Saturation Max: 0 Min: 0
SG CON 0
**$ Property: Water Mole Fraction(H2O) Max: 1 Min: 1
MFRAC_WAT 'H2O' CON 1
**$ Property: Oil Mole Fraction(hydrate) Max: 1 Min: 1
MFRAC_OIL 'hydrate' CON 1
**$ Property: Gas Mole Fraction(CH4) Max: 1 Min: 1
MFRAC_GAS 'CH4' CON 1
NUMERICAL
NORTH 150
ITERMAX 200
UPSTREAM KLEVEL
NCUTS 99
Newtoncyc 15
converge totres normal
maxsteps 999999
RUN

```

Simulation is started at time=0, and is run for 50 years. Reservoir is depressurized at a bottom hole pressure of 2700 kPa. This low bottom hole pressure is slowly put in practice by depressurizing first at time=0, BHP=4160kPa and then to BHP=2700 kPa at time=2 days

```

TIME 0
DTWELL 0.001
**$
WELL 'Well-1'
PRODUCER 'Well-1'
OPERATE MIN BHP 4160. CONT
**OPERATE MAX BHG 60000. CONT
**$ rad geofac wfrac skin
GEOMETRY K 0.111 0.249 1. 0.
PERF GEO 'Well-1'
1 1 1:10 1.0 CLOSED FLOW-TO 'SURFACE' REFLAYER
 1 1 11 1.0 OPEN FLOW-TO 1
 1 1 12:60 1.0 OPEN FLOW-TO 1
 1 1 61:70 1.0 CLOSED FLOW-TO 1

TIME 0.000694444
PRODUCER 'Well-1' OPERATE MIN BHP 4160
TIME 1.0
** STOP
PRODUCER 'Well-1' OPERATE MIN BHP 3500.0
TIME 1.01
TIME 1.02

```


TIME 1.09
 TIME 1.1
 TIME 1.11
 TIME 1.12
 TIME 1.19
 TIME 1.2
 PRODUCER 'Well-1' OPERATE MIN BHP 3000.0
 DTMAX .1
 TIME 1.21
 TIME 1.51
 TIME 1.75
 TIME 1.76
 TIME 1.77

TIME 2
 PRODUCER 'Well-1' OPERATE MIN BHP 2700.0

TIME 3	TIME 1247.22	TIME 5295	TIME 10226
TIME 4	TIME 1277.64	TIME 5386	TIME 10317
TIME 5	TIME 1308.06	TIME 5478	TIME 10409
TIME 6	TIME 1338.48	TIME 5569	TIME 10500
TIME 8	TIME 1368.9	TIME 5660	TIME 10591
DTMAX 30.42	TIME 1399.32	TIME 5752	TIME 10683
TIME 12	TIME 1429.74	TIME 5843	TIME 10774
TIME 20	TIME 1460.16	TIME 5934	TIME 10865
TIME 30.42	TIME 1490.58	TIME 6026	TIME 10957
TIME 40.	TIME 1521	TIME 6117	TIME 11048
TIME 50.42	TIME 1551.42	TIME 6208	TIME 11139
TIME 55.42	TIME 1581.84	TIME 6300	TIME 11230
TIME 60.84	TIME 1612.26	TIME 6391	TIME 11322
TIME 60.9	TIME 1642.68	TIME 6482	TIME 11413
TIME 91.26	TIME 1643	TIME 6574	TIME 11504
TIME 121.68	TIME 1734	TIME 6665	TIME 11596
TIME 152.1	TIME 1825	TIME 6756	TIME 11687
TIME 182.52	TIME 1917	TIME 6847	TIME 11778
TIME 212.8	TIME 2008	TIME 6939	TIME 11870
TIME 231.	TIME 2099	TIME 7030	TIME 11961
TIME 243.36	TIME 2191	TIME 7121	TIME 12052
TIME 273.78	TIME 2282	TIME 7213	TIME 12144
TIME 304.2	TIME 2373	TIME 7304	TIME 12235
TIME 334.62	TIME 2464	TIME 7395	TIME 12326
TIME 365.04	TIME 2556	TIME 7487	TIME 12418
DTMAX 90.	TIME 2647	TIME 7578	TIME 12509
TIME 395.46	TIME 2738	TIME 7669	TIME 12600
TIME 425.88	TIME 2830	TIME 7761	TIME 12691
TIME 456.3	TIME 2921	TIME 7852	TIME 12783
TIME 486.72	TIME 3012	TIME 7943	TIME 12874
TIME 517.14	TIME 3104	TIME 8035	TIME 12965
TIME 547.56	TIME 3195	TIME 8126	TIME 13057
TIME 577.98	TIME 3286	TIME 8217	TIME 13148
TIME 608.4	TIME 3378	TIME 8308	TIME 13239
TIME 638.82	TIME 3469	TIME 8400	TIME 13331
TIME 669.24	TIME 3560	TIME 8491	TIME 13422
TIME 699.66	TIME 3652	TIME 8582	TIME 13513
TIME 730.08	TIME 3743	TIME 8674	TIME 13605
TIME 760.5	TIME 3834	TIME 8765	TIME 13696
TIME 790.92	TIME 3925	TIME 8856	TIME 13787
TIME 821.34	TIME 4017	TIME 8948	TIME 13879
TIME 851.76	TIME 4108	TIME 9039	TIME 13970
TIME 882.18	TIME 4199	TIME 9130	TIME 14061
TIME 912.6	TIME 4291	TIME 9222	TIME 14152
TIME 943.02	TIME 4382	TIME 9313	TIME 14244
TIME 973.44	TIME 4473	TIME 9404	TIME 14335
TIME 1003.86	TIME 4565	TIME 9496	TIME 14426
TIME 1034.28	TIME 4656	TIME 9587	TIME 14518
TIME 1064.7	TIME 4747	TIME 9678	TIME 14609
TIME 1095.12	TIME 4839	TIME 9769	TIME 14700
TIME 1125.54	TIME 4930	TIME 9861	TIME 14792
TIME 1155.96	TIME 5021	TIME 9952	TIME 14883
TIME 1186.38	TIME 5113	TIME 10043	TIME 14974
TIME 1216.8	TIME 5204	TIME 10135	TIME 15066

TIME	15157	TIME	15979	TIME	16801	TIME	17622
TIME	15248	TIME	16070	TIME	16892	TIME	17714
TIME	15340	TIME	16161	TIME	16983	TIME	17805
TIME	15431	TIME	16253	TIME	17074	TIME	17896
TIME	15522	TIME	16344	TIME	17166	TIME	17988
TIME	15613	TIME	16435	TIME	17257	TIME	18079
TIME	15705	TIME	16527	TIME	17348	TIME	18170
TIME	15796	TIME	16618	TIME	17440	TIME	18262
TIME	15887	TIME	16709	TIME	17531	TIME	STOP

Simulation is stopped after 50 years.

Results of gas rate, water rate, cumulative gas rate, cumulative water rate are compared with other codes. To simplify the project CMG STARS results are compared with only MH21.

The characteristic part of Problem 7a is there is no gas for 1st 10 years. HydrateResim, TOUGH and CMG STARS agreed on this result. MH21 and STOMP took a little longer time to produce gas. However there is a small change in the magnitude of gas rates during the course of the simulation, the cumulative gas at the end of 50 years is almost same for all reservoir simulators. Every simulator is different in the way it calculates all the properties at each time step. So this small difference in magnitude can be expected from each simulator as the problem becomes more complex. Gas rate and Cumulative gas rate for STARS and MH21 are shown in Figure 5-4 and Figure 5-5.

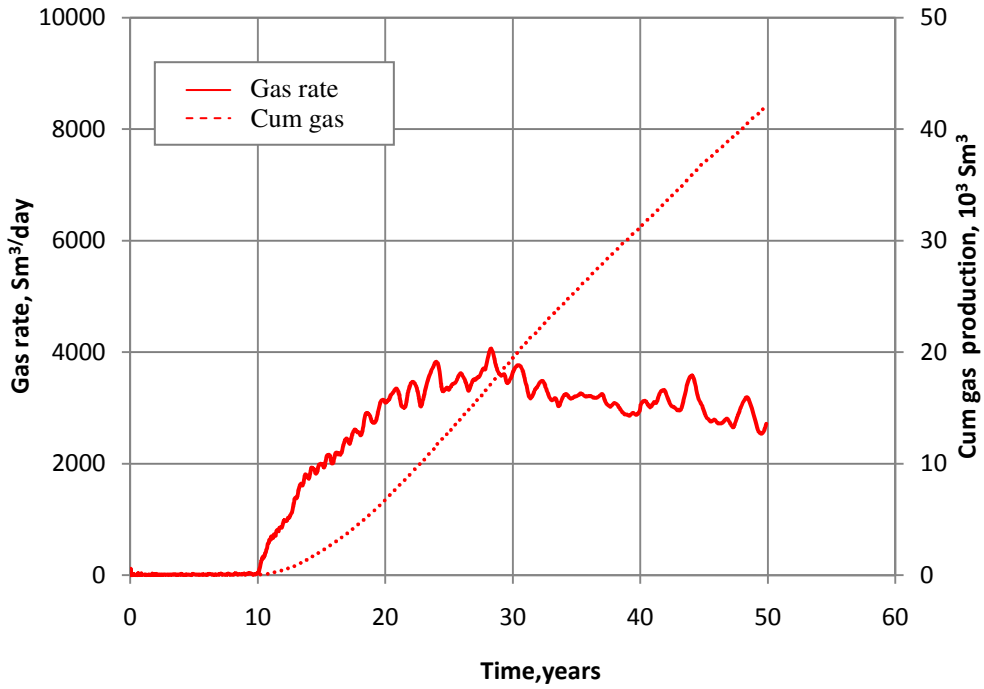


Figure 5-4 Gas rate and cumulative gas rate for 50 years using CMG STARS

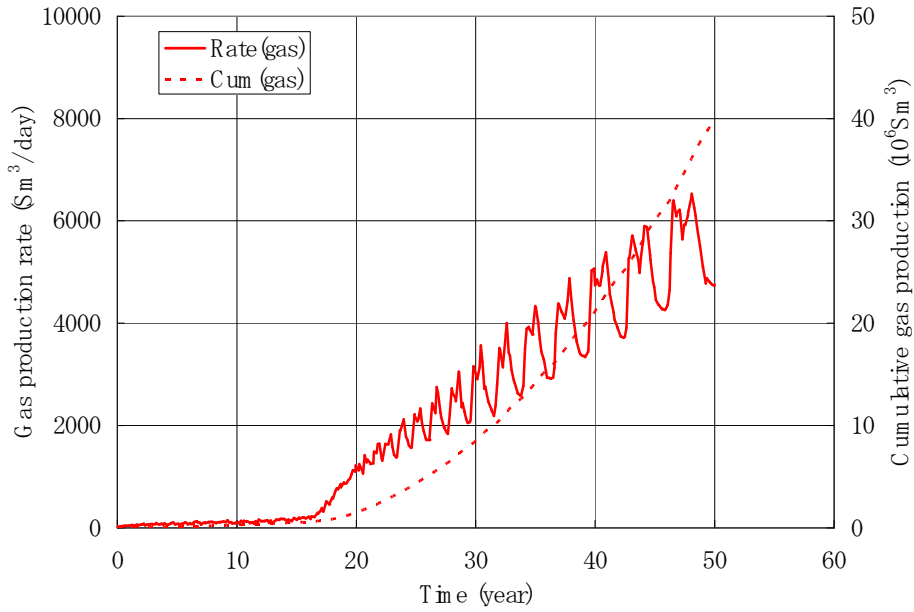


Figure 5-5 Gas rate and cumulative gas rate for 50 years using MH21

Water rates and cumulative water rates for CMG STARS and MH21 are in good agreement. Figures 5-6 and 5-7 show results for CMG STARS and MH21.

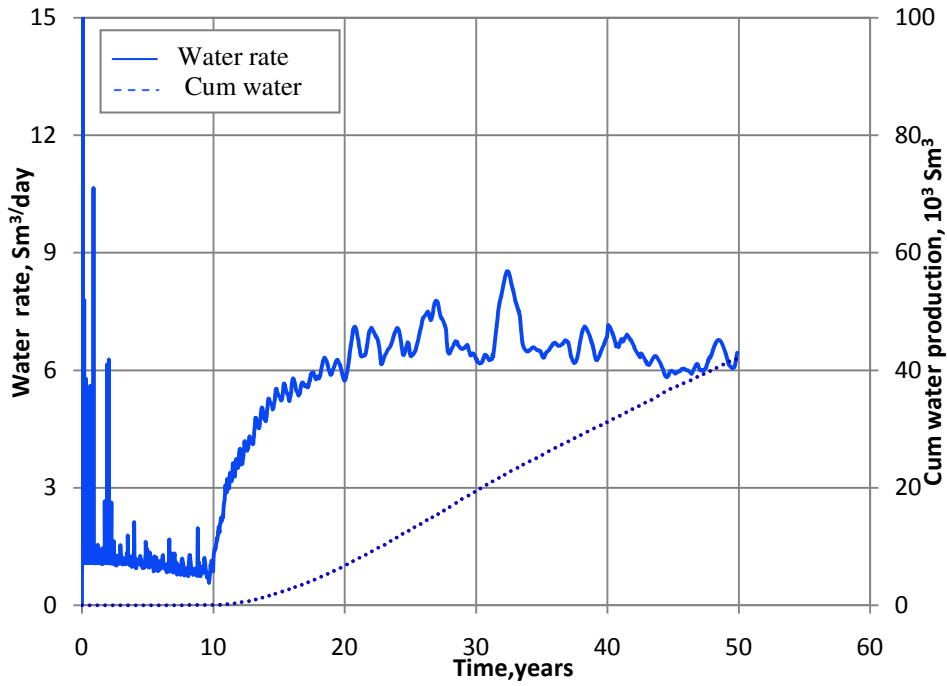


Figure 5-6 Water rate and cumulative water rate for 50 years using CMG STARS

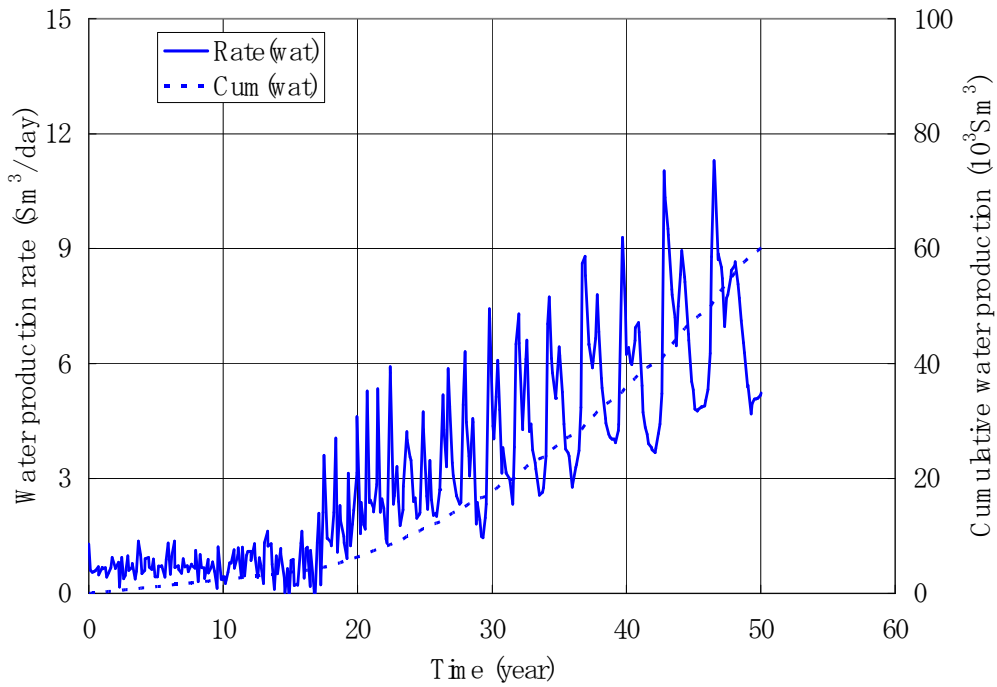


Figure 5-7 Water rate and cumulative water rate for 50 years using MH21

5.2 Problem 7b: PBU L-Pad

Geometry of the Grid

A radial grid of outer radius 450 m and 240 m deep is considered in this problem. Unlike Problem 7a there are two hydrate bearing layers bounded by three shale zones. A schematic view of the grid is shown in Figure 5-8.

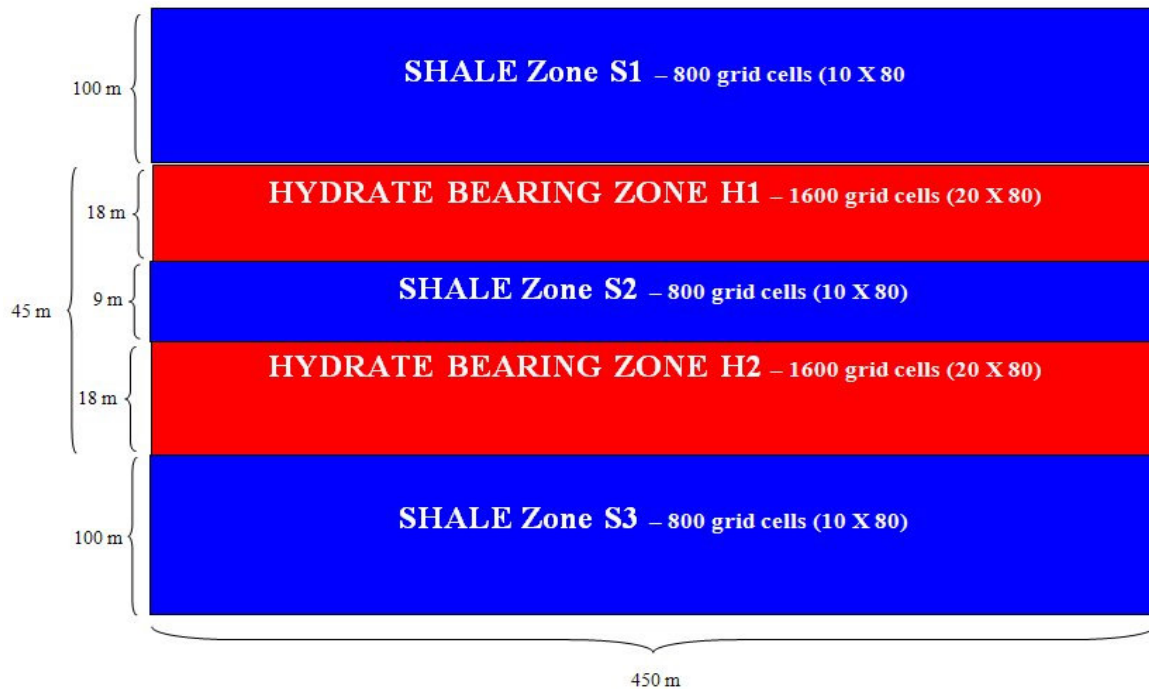


Figure 5- 8 Schematic view of the grid for Problem 7b.

Discretization of the Grid:

***r*-direction:** The radial discretization is same as in Problem 7a.

***z*-direction:** The hydrate bearing zones (H1 & H2) and the shale layer between them (S2) are uniformly discretized and the upper and lower shale zones (S1 & S3) are logarithmically discretized.

In both of these shale zones, the first grid block (next to the hydrate zone) is the same size as those in the hydrate bearing zone (0.9 m). For each subsequent cell, the dz obeys $dz_i=dz_{i-1}^*1.49587$ (as one moves away from the hydrate zone). This leads to the following z values given in Table 5-5

Table 5-5 Discretization of the grid in z direction

Cell number	dz	z (boundary)	z (center)
1	0.900	0.900	0.450
2	1.346	2.246	1.573
3	2.014	4.260	3.253
4	3.012	7.273	5.766
5	4.506	11.779	9.526
6	6.741	18.520	15.149
7	10.083	28.603	23.561
8	15.083	43.686	36.145
9	22.563	66.249	54.968
10	33.751	100.000	83.125

Initial Conditions

Hydrate Saturation and Water Saturation:

The hydrate saturation in hydrate bearing zones (H1 & H2) is 75 % and water saturation is 25%.

In the shale zones (S1, S2 & S3), there is no hydrate and water saturation is 100%.

Pressure & Temperature:

The top of hydrate bearing zone (H1) is 62 m below the top of the hydrate bearing zone. Pressure temperature of the Hydrate bearing zone are 7.327 MPa and 278.15 K. Pressure and temperature values for each cell are calculated using a hydrostatic pressure gradient of 9792 Pa/m and geothermal gradient of 0.03 K/m as given in Table 5-6.

Table 5-6 Pressure and Temperature values for Problem 7b

Cell	Region	Z (boundary)	Z (center)	T (boundary)	T (center)	P/Mpa (boundary)	P/MPa (center)
		0.000		275.150		6.348	
1	Shale	33.751	16.875	276.163	275.656	6.678	6.513
2	Shale	56.314	45.032	276.839	276.501	6.899	6.789
3	Shale	71.397	63.855	277.292	277.066	7.047	6.973
4	Shale	81.480	76.439	277.594	277.443	7.146	7.096
5	Shale	88.221	84.851	277.797	277.696	7.212	7.179
6	Shale	92.727	90.474	277.932	277.864	7.256	7.234
7	Shale	95.740	94.234	278.022	277.977	7.285	7.271
8	Shale	97.754	96.747	278.083	278.052	7.305	7.295
9	Shale	99.100	98.427	278.123	278.103	7.318	7.312
10	Shale	100.000	99.550	278.150	278.137	7.327	7.323
11	Hydrate	100.900	100.450	278.177	278.164	7.336	7.331
12	Hydrate	101.800	101.350	278.204	278.191	7.345	7.340
13	Hydrate	102.700	102.250	278.231	278.218	7.353	7.349
14	Hydrate	103.600	103.150	278.258	278.245	7.362	7.358
15	Hydrate	104.500	104.050	278.285	278.272	7.371	7.367
16	Hydrate	105.400	104.950	278.312	278.299	7.380	7.375
17	Hydrate	106.300	105.850	278.339	278.326	7.389	7.384
18	Hydrate	107.200	106.750	278.366	278.353	7.398	7.393
19	Hydrate	108.100	107.650	278.393	278.380	7.406	7.402
20	Hydrate	109.000	108.550	278.420	278.407	7.415	7.411
21	Hydrate	109.900	109.450	278.447	278.434	7.424	7.420
22	Hydrate	110.800	110.350	278.474	278.461	7.433	7.428
23	Hydrate	111.700	111.250	278.501	278.488	7.442	7.437
24	Hydrate	112.600	112.150	278.528	278.515	7.450	7.446
25	Hydrate	113.500	113.050	278.555	278.542	7.459	7.455

Table 5-6 (contd....)

Cell	Region	Z (boundary)	Z (center)	T (boundary)	T (center)	P/Mpa (boundary)	P/MPa (center)
26	Hydrate	114.400	113.950	278.582	278.569	7.468	7.464
27	Hydrate	115.300	114.850	278.609	278.596	7.477	7.472
28	Hydrate	116.200	115.750	278.636	278.623	7.486	7.481
29	Hydrate	117.100	116.650	278.663	278.650	7.494	7.490
30	Hydrate	118.000	117.550	278.690	278.677	7.503	7.499
31	Shale	118.900	118.450	278.717	278.704	7.512	7.508
32	Shale	119.800	119.350	278.744	278.731	7.521	7.516
33	Shale	120.700	120.250	278.771	278.758	7.530	7.525
34	Shale	121.600	121.150	278.798	278.785	7.539	7.534
35	Shale	122.500	122.050	278.825	278.812	7.547	7.543
36	Shale	123.400	122.950	278.852	278.839	7.556	7.552
37	Shale	124.300	123.850	278.879	278.866	7.565	7.561
38	Shale	125.200	124.750	278.906	278.893	7.574	7.569
45	Hydrate	131.500	131.050	279.095	279.082	7.635	7.631
46	Hydrate	132.400	131.950	279.122	279.109	7.644	7.640
47	Hydrate	133.300	132.850	279.149	279.136	7.653	7.649
48	Hydrate	134.200	133.750	279.176	279.163	7.662	7.657
49	Hydrate	135.100	134.650	279.203	279.190	7.671	7.666
50	Hydrate	136.000	135.550	279.230	279.217	7.680	7.675
51	Hydrate	136.900	136.450	279.257	279.244	7.688	7.684
52	Hydrate	137.800	137.350	279.284	279.271	7.697	7.693
53	Hydrate	138.700	138.250	279.311	279.298	7.706	7.702
54	Hydrate	139.600	139.150	279.338	279.325	7.715	7.710
55	Hydrate	140.500	140.050	279.365	279.352	7.724	7.719
56	Hydrate	141.400	140.950	279.392	279.379	7.732	7.728
57	Hydrate	142.300	141.850	279.419	279.406	7.741	7.737
58	Hydrate	143.200	142.750	279.446	279.433	7.750	7.746
59	Hydrate	144.100	143.650	279.473	279.460	7.759	7.754
60	Hydrate	145.000	144.550	279.500	279.487	7.768	7.763

Table 5-6 (contd....)

Cell	Region	Z (boundary)	Z (center)	T (boundary)	T (center)	P/Mpa (boundary)	P/MPa (center)
61	Shale	145.900	145.450	279.527	279.514	7.776	7.772
62	Shale	147.246	146.573	279.567	279.547	7.790	7.783
63	Shale	149.260	148.253	279.628	279.598	7.809	7.799
64	Shale	152.273	150.766	279.718	279.673	7.839	7.824
65	Shale	156.779	154.526	279.853	279.786	7.883	7.861
66	Shale	163.520	160.149	280.056	279.954	7.949	7.916
67	Shale	173.603	168.561	280.358	280.207	8.048	7.998
68	Shale	188.686	181.145	280.811	280.584	8.195	8.122
69	Shale	211.249	199.968	281.487	281.149	8.416	8.306
70	Shale	245.000	228.125	282.500	281.994	8.747	8.582

Boundary Conditions:

There is no net mass transport between the reservoir and the surroundings. The upper boundary temperature is held constant at 275.150 K and the lower boundary temperature is held at constant at 282.500 K.

Relative Permeability Models:

A relative permeability model developed by Stone³⁶ + Aziz³⁷ is used in this problem. The parameters were fixed so that every simulator has the same values.

Water Relative Permeability

$$k_{rw} = \left\{ \frac{(S_w - S_{wir})}{(1 - S_{wir})} \right\}^{5.04} ; S_{wir} = 0.10$$

Gas Relative Permeability

$$k_{rg} = \left\{ \frac{(S_G - S_{Gir})}{(1 - S_{Wir})} \right\}^{3.16} \quad S_{Wir} = 0. \quad S_{Gir} = 0.$$
 S_{Wir} and S_{Gir} represents irreducible water and gas saturation. Gas and water relative permeability curves are shown in Figure 5-9.

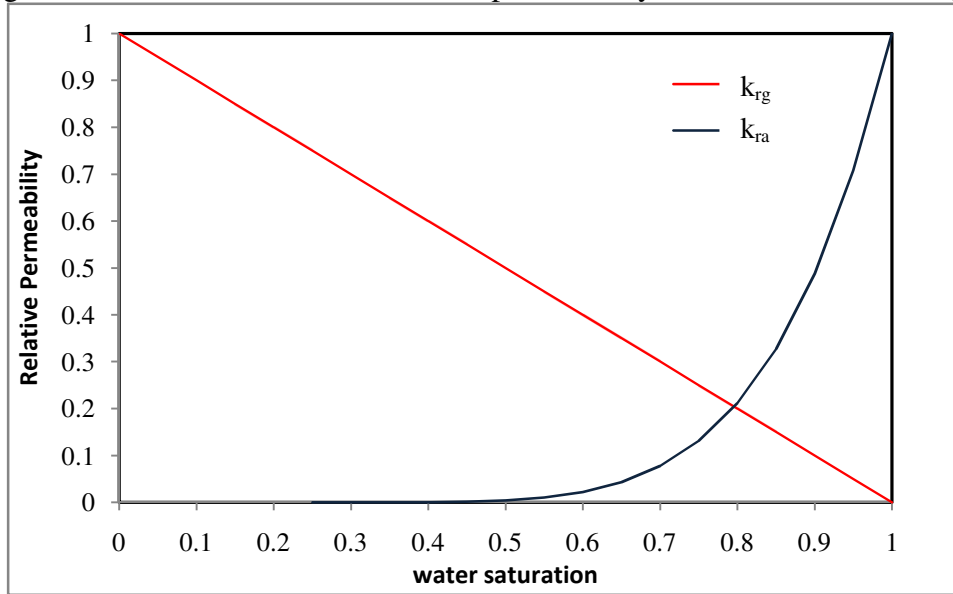


Figure 5- 9 Aqueous and Gas relative Permeability curves for problem 7b.

Medium properties:

Medium properties like permeability porosity are specified in Table 5-7

Table 5-7 Medium Properties for Problem 7b

Property	Value
Permeability, mD	Shale - 0.0
	Hydrate layer - 1000 (r direction)
	Hydrate layer - 100 (z direction)
Porosity, %	Shale - 10
	Hydrate zone - 35
Pore Compressibility (1/Pa)	1.00E-08
Rock Density (kg/m ³)	2650
Rock Specific Heat (J/kg/K)	1000

Capillary Pressure Model:

The capillary Pressure Model used in this problem is the same as in Problem 7a.

Well Information:

The wellbore Radius is selected to be 0.111 m. The bottom-hole pressure is chosen to be 2.7MPa to avoid ice formation in the system.

Data and Sampling Frequency:

The simulations are carried out until all the hydrate dissociates and equilibrium is reached or over a time period of 50 years. Data for gas production rate, water production rate, cumulative gas production and cumulative water production is recorded with a frequency of 90 days for 50 years.

5.2.1 Solution to Problem 7b

The grid description in this problem is different from Problem 7a.

The grid has two hydrate layers bounded by shale zones. The discretization in the r direction is same as in 7a but is different in the z direction. Porosity, permeability and rock fluid properties are specified as per the problem description. The properties that are same as in Problem 7a are not included in the data file given below.

```
*****
**$ Definition of fundamental cylindrical grid
*****
GRID RADIAL 80 1 70 *RW          0.111
KDIR DOWN

DI IVAR
** Discretization same as 7a

DJ JVAR          360

DK kvar

33.751  2.014  0.9  0.9  0.9  0.9  0.9  0.9  0.9  3.013
22.563  1.346  0.9  0.9  0.9  0.9  0.9  0.9  0.9  4.506
15.083  0.9  0.9  0.9  0.9  0.9  0.9  0.9  0.9  6.741
10.083  0.9  0.9  0.9  0.9  0.9  0.9  0.9  0.9  10.083
6.741  0.9  0.9  0.9  0.9  0.9  0.9  0.9  0.9  15.083
4.506  0.9  0.9  0.9  0.9  0.9  0.9  0.9  1.346  22.563
3.013  0.9  0.9  0.9  0.9  0.9  0.9  0.9  2.014  33.751

DTOP
80*500
**$ Property: NULL Blocks Max: 1 Min: 1
**$ 0 = null block, 1 = active block
NULL CON          1
**$ Property: Porosity Max: 0.4 Min: 0.1
POR KVAR
 10*0.0 20*.4 10*0.0 20*.4 10*0.0
**$ Property: Permeability I (md) Max: 1000 Min: 0
PERMI KVAR
10*0.0 20*1000 10*0.0 20*1000.0 10*0.0
**$ Property: Permeability J (md) Max: 1000 Min: 0
PERMJ KVAR
10*0.0 20*1000 10*0.0 20*1000.0 10*0.0
**$ Property: Permeability K (md) Max: 1000 Min: 0
PERMK KVAR
 10*0.0 20*100 10*0.0 20*100.0 10*0.0
END-GRID

ROCKTYPE 1
** same as problem 7a
**$ Model and number of components
** same as problem 7a
ROCKFLUID
RPT 1 LININTERP WATWET
```

```

**SW      KRW      KROW      PCOW      **      kw
SWT
**$      Sw      krw      krow      Pcow
0.1      0      0      0.00000008      599.3754829
0.15     4.7144E-07      0.00000007      599.3754829
0.2      1.55102E-05      0.00000007      599.3754829
0.248    0.000111876      0.00000007      599.3754829
0.3      0.00051028      0.00000007      599.3754829
0.35     0.001571214      0.00000006      481.4413657
0.4      0.003938301      0.00000005      419.5019542
0.45     0.008564868      0.00000004      375.2776708
0.5      0.016788044      0.00000003      340.2284612
0.55     0.030395467      0.00000002      310.8987242
0.6      0.051692385      0.00000001      285.5166471
0.65     0.083569097      0.000000009      263.0426992
0.7      0.129568686      0.000000008      242.8106796
0.75     0.19395504      0.000000007      224.3660077
0.8      0.281781109      0.000000006      207.3835797
0.85     0.398957395      0.000000005      191.6222293
0.9      0.552320658      0.000000004      176.8977346
0.95     0.749702809      0.000000003      163.0659502
1      1      1      0      150.0118032

```

```

** SL      KRG      KROG      PCOG
SLT
**$      Sl      krg      krog      Pcoc
0.29375  0.333202872      0      0
0.340625  0.26819991      0      0
0.3875   0.212449275      0      0
0.434375  0.165192515      0      0
0.48125   0.125680421      0      0
0.528125  0.093173674      0      0
0.575     0.066943593      0      0
0.621875  0.046273019      0      0
0.66875   0.030457384      0      0
0.715625  0.018806019      0      0
0.7625    0.010643808      0.000000005      0
0.809375  0.005313349      0.000000006      0
0.85625   0.002177914      0.000000007      0
0.903125  0.000625791      0.000000008      0
0.95     7.74008E-05      0.000000008      0
1      1      0      0.000000008      0

```

**\$ Property: Rel Perm Set Number Max: 1 Min: 1
KRTYPE IVAR 80*1

INITIAL
VERTICAL OFF

The pressure, temperature and saturations are specified as per the problem description. Well conditions are same as per the previous problem.

```

INITREGION 1
**$ Property: Pressure (kPa) Max: 7387 Min: 6176
PRES KVAR
6513      7295      7367      7428      7490      7552      7613      7675      7737      7824
6789      7312      7375      7437      7499      7561      7622      7684      7746      7861
6973      7323      7384      7446      7508      7569      7631      7693      7754      7916
7096      7331      7393      7455      7516      7578      7640      7702      7763      7998
7179      7340      7402      7464      7525      7587      7649      7710      7772      8122
7234      7349      7411      7472      7534      7596      7657      7719      7783      8306
7271      7358      7420      7481      7543      7605      7666      7728      7799      8582

```

```

**$ Property: Temperature (C)    Max: 5.047  Min: 0.85

TEMP KVAR
2.506    4.902    5.122    5.311    5.5    5.689    5.878    6.067    6.256    6.523
3.351    4.953    5.149    5.338    5.527    5.716    5.905    6.094    6.283    6.636
3.916    4.987    5.176    5.365    5.554    5.743    5.932    6.121    6.31    6.804
4.293    5.014    5.203    5.392    5.581    5.77    5.959    6.148    6.337    7.057
4.546    5.041    5.23    5.419    5.608    5.797    5.986    6.175    6.364    7.434
4.714    5.068    5.257    5.446    5.635    5.824    6.013    6.202    6.397    7.999
4.827    5.095    5.284    5.473    5.662    5.851    6.04    6.229    6.448    8.844

SW KVAR
10*1.0 20*.25 10*1.0 20*.25 10*1.0
**$ Property: Oil Saturation Max: 0.75  Min: 0
SO KVAR
10*0.0 20*0.75 10*0.0 20*0.75 10*0.0
**$ Property: Gas Saturation Max: 0  Min: 0
SG CON    0
**$ Property: Water Mole Fraction(H2O) Max: 1  Min: 1
MFRAC_WAT 'H2O' CON    1
**$ Property: Oil Mole Fraction(hydrate) Max: 1  Min: 1
MFRAC_OIL 'hydrate' CON    1
**$ Property: Gas Mole Fraction(CH4) Max: 1  Min: 1
MFRAC_GAS 'CH4' CON    1
NUMERICAL
** rest of the data file is same as 7a

```

The gas rate and cumulative gas rates for CMG STARS are in good agreement with other codes. This reservoir is warmer than the previous case leading to higher production rates.

Figure 5-10 and Figure 5-11 shows cumulative gas and gas rates for CMG STARS and MH21. Cumulative water and water rate are given in Figure 5-12 and 5-13.

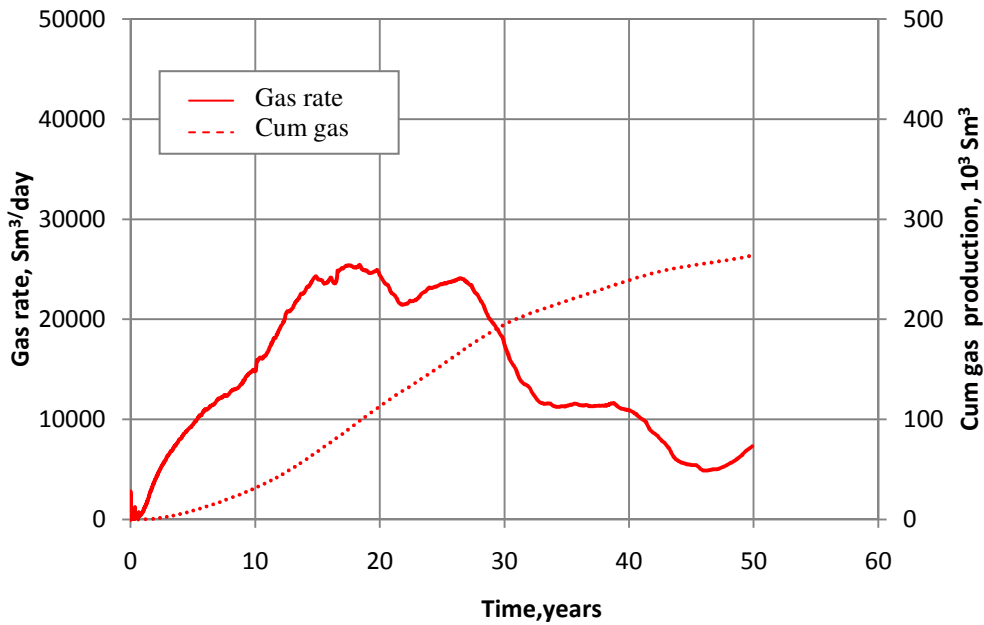


Figure 5-10 Gas rate and cumulative gas rate for 50 years using CMG STARS

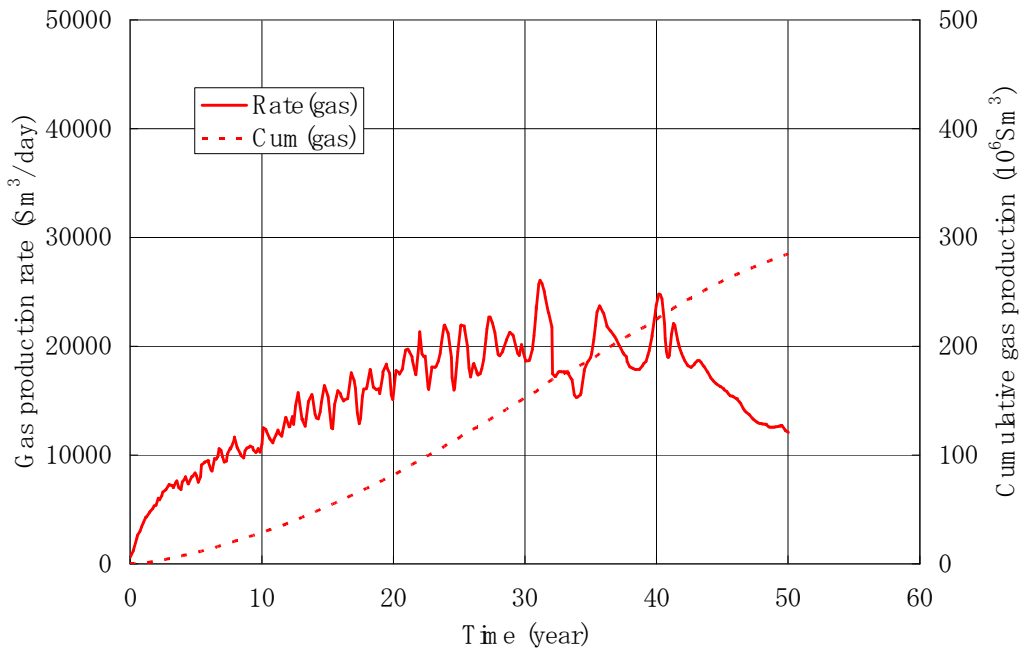


Figure 5-11 Gas rate and cumulative gas rate for 50 years using MH21

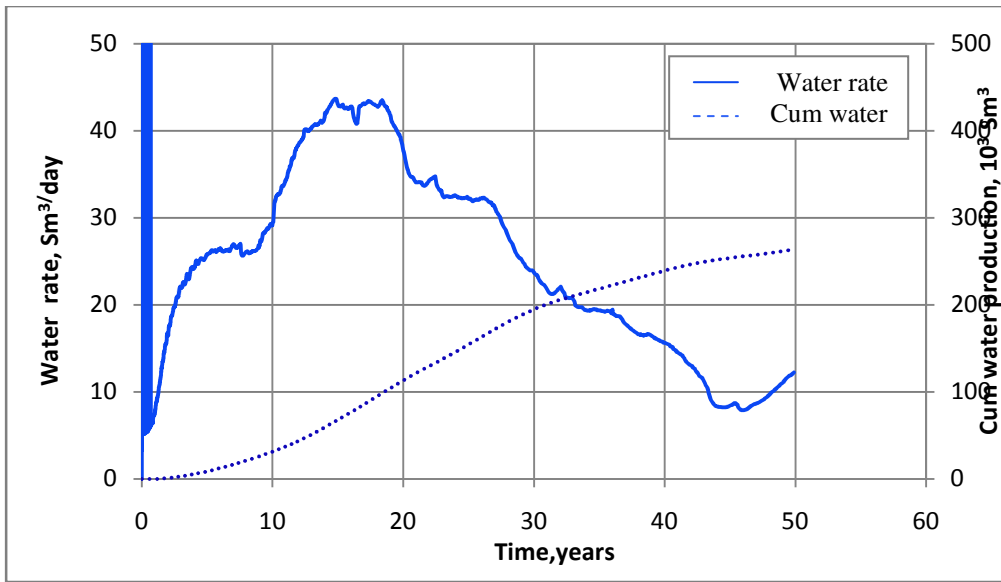


Figure 5-12 Water rate and cumulative water rate for 50 years using CMG STARS

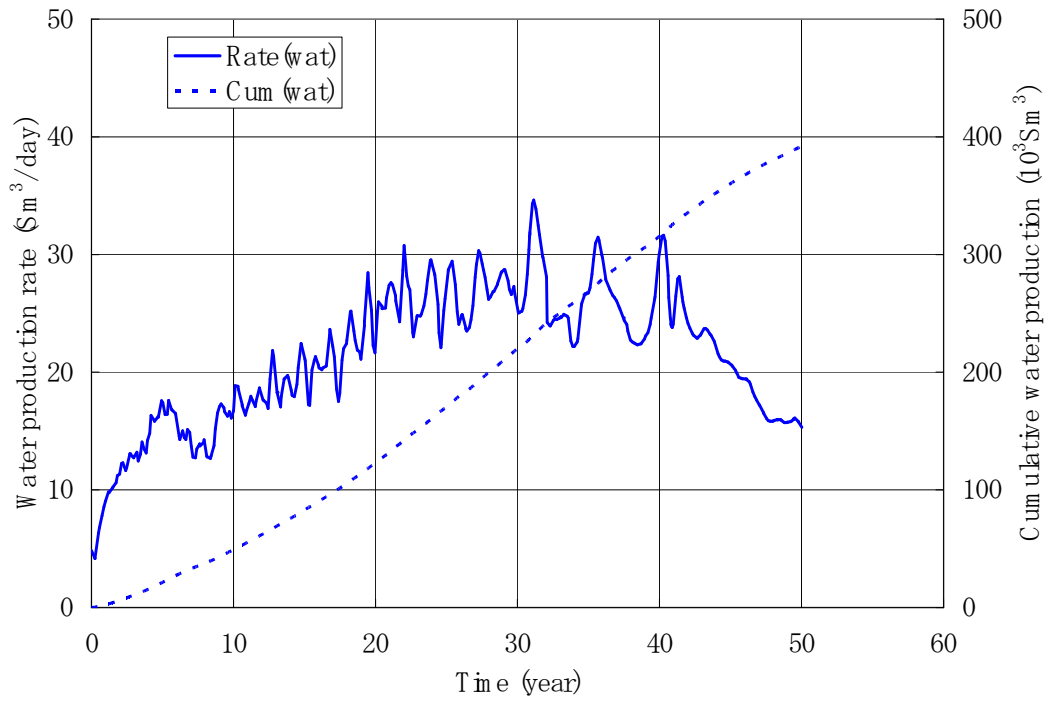


Figure 5-13 Water rate and cumulative water rate for 50 years using MH21

5.3 Problem 7c

Reservoir grid in this problem is same as in Problem 7b. All Parameters and conditions are the same as problem 7b except those that are modified are discussed in this part of the study.

Boundary Conditions: There is no net mass transport between the reservoir and the surroundings. The upper boundary temperature is held constant at 280.800 K and the lower boundary temperature is held at constant at 288.150 K.

Initial Conditions: A reservoir warmer than in previous cases is considered in this problem. The pressure and temperature of the bottom of the hydrate bearing zone are chosen as 12°C and 9.1 MPa. These high values are chosen considering the base of the hydrate stability zone. Pressure and temperature values of the entire reservoir are calculated based on the gradients specified in Problem 7b.

Table 5-8 Pressure and Temperature values for Problem 7c

Cell	Region	Z (boundary)	Z (center)	T (boundary)	T (center)	P/MPa (boundary)	P/MPa (center)
		0.000		280.800		7.680	
1	Shale	33.751	16.875	281.813	281.306	8.011	7.845
2	Shale	56.314	45.032	282.489	282.151	8.232	8.121
3	Shale	71.397	63.855	282.942	282.716	8.379	8.305
4	Shale	81.480	76.439	283.244	283.093	8.478	8.429
5	Shale	88.221	84.851	283.447	283.346	8.544	8.511
6	Shale	92.727	90.474	283.582	283.514	8.588	8.566
7	Shale	95.740	94.234	283.672	283.627	8.618	8.603
8	Shale	97.754	96.747	283.733	283.702	8.637	8.628
9	Shale	99.100	98.427	283.773	283.753	8.651	8.644

Table 5-8 (contd....)

Cell	Region	Z (boundary)	Z (center)	T (boundary)	T (center)	P/MPa (boundary)	P/MPa (center)
11	Hydrate	100.900	100.450	283.827	283.814	8.668	8.664
12	Hydrate	101.800	101.350	283.854	283.841	8.677	8.673
13	Hydrate	102.700	102.250	283.881	283.868	8.686	8.681
14	Hydrate	103.600	103.150	283.908	283.895	8.695	8.690
15	Hydrate	104.500	104.050	283.935	283.922	8.703	8.699
16	Hydrate	105.400	104.950	283.962	283.949	8.712	8.708
17	Hydrate	106.300	105.850	283.989	283.976	8.721	8.717
18	Hydrate	107.200	106.750	284.016	284.003	8.730	8.725
19	Hydrate	108.100	107.650	284.043	284.030	8.739	8.734
20	Hydrate	109.000	108.550	284.070	284.057	8.747	8.743
21	Hydrate	109.900	109.450	284.097	284.084	8.756	8.752
22	Hydrate	110.800	110.350	284.124	284.111	8.765	8.761
23	Hydrate	111.700	111.250	284.151	284.138	8.774	8.770
24	Hydrate	112.600	112.150	284.178	284.165	8.783	8.778
25	Hydrate	113.500	113.050	284.205	284.192	8.792	8.787
26	Hydrate	114.400	113.950	284.232	284.219	8.800	8.796
27	Hydrate	115.300	114.850	284.259	284.246	8.809	8.805
28	Hydrate	116.200	115.750	284.286	284.273	8.818	8.814
29	Hydrate	117.100	116.650	284.313	284.300	8.827	8.822
30	Hydrate	118.000	117.550	284.340	284.327	8.836	8.831
31	Shale	118.900	118.450	284.367	284.354	8.844	8.840
32	Shale	119.800	119.350	284.394	284.381	8.853	8.849
33	Shale	120.700	120.250	284.421	284.408	8.862	8.858
34	Shale	121.600	121.150	284.448	284.435	8.871	8.866
35	Shale	122.500	122.050	284.475	284.462	8.880	8.875
36	Shale	123.400	122.950	284.502	284.489	8.888	8.884
37	Shale	124.300	123.850	284.529	284.516	8.897	8.893
38	Shale	125.200	124.750	284.556	284.543	8.906	8.902
39	Shale	126.100	125.650	284.583	284.570	8.915	8.911

Table 5-8 (contd....)

Cell	Region	Z (boundary)	Z (center)	T (boundary)	T (center)	P/MPa (boundary)	P/MPa (center)
40	Shale	127.000	126.550	284.610	284.597	8.924	8.919
41	Hydrate	127.900	127.450	284.637	284.624	8.933	8.928
42	Hydrate	128.800	128.350	284.664	284.651	8.941	8.937
43	Hydrate	129.700	129.250	284.691	284.678	8.950	8.946
44	Hydrate	130.600	130.150	284.718	284.705	8.959	8.955
45	Hydrate	131.500	131.050	284.745	284.732	8.968	8.963
46	Hydrate	132.400	131.950	284.772	284.759	8.977	8.972
47	Hydrate	133.300	132.850	284.799	284.786	8.985	8.981
48	Hydrate	134.200	133.750	284.826	284.813	8.994	8.990
49	Hydrate	135.100	134.650	284.853	284.840	9.003	8.999
50	Hydrate	136.000	135.550	284.880	284.867	9.012	9.007
51	Hydrate	136.900	136.450	284.907	284.894	9.021	9.016
52	Hydrate	137.800	137.350	284.934	284.921	9.029	9.025
53	Hydrate	138.700	138.250	284.961	284.948	9.038	9.034
54	Hydrate	139.600	139.150	284.988	284.975	9.047	9.043
55	Hydrate	140.500	140.050	285.015	285.002	9.056	9.052
56	Hydrate	141.400	140.950	285.042	285.029	9.065	9.060
57	Hydrate	142.300	141.850	285.069	285.056	9.074	9.069
58	Hydrate	143.200	142.750	285.096	285.083	9.082	9.078
59	Hydrate	144.100	143.650	285.123	285.110	9.091	9.087
60	Hydrate	145.000	144.550	285.150	285.137	9.100	9.096
61	Shale	145.900	145.450	285.177	285.164	9.109	9.104
62	Shale	147.246	146.573	285.217	285.197	9.122	9.115
63	Shale	149.260	148.253	285.278	285.248	9.142	9.132
64	Shale	152.273	150.766	285.368	285.323	9.171	9.156
65	Shale	156.779	154.526	285.503	285.436	9.215	9.193
66	Shale	163.520	160.149	285.706	285.604	9.281	9.248
67	Shale	173.603	168.561	286.008	285.857	9.380	9.331
68	Shale	188.686	181.145	286.461	286.234	9.528	9.454
69	Shale	211.249	199.968	287.137	286.799	9.749	9.638
70	Shale	245.000	228.125	288.150	287.644	10.079	9.914

Permeability models, Capillary pressure model, medium properties, well specifications, data and sampling frequency are same as in Problem 7b.

5.3.1 Solution to Problem 7c

A warmer reservoir is considered in this problem. Pressure, temperature, saturations are different from the previous case. Every other property including grid and well properties are same as Problem 7b. Only the parameters that need to be changed and that are different from the previous problem are specified below.

**\$ Property: Pressure (kPa) Max: 7387 Min: 6176

PRES KVAR

7845	8628	8699	8761	8822	8884	8946	9007	9069	9156
8121	8644	8708	8770	8831	8893	8955	9016	9078	9193
8305	8655	8717	8778	8840	8902	8963	9025	9087	9248
8429	8664	8725	8787	8849	8911	8972	9034	9096	9331
8511	8673	8734	8796	8858	8919	8981	9043	9104	9454
8566	8681	8743	8805	8866	8928	8990	9052	9115	9638
8603	8690	8752	8814	8875	8937	8999	9060	9132	
9914									

**\$ Property: Temperature (C) Max: 5.047 Min: 0.85

TEMP KVAR

8.156	10.552	10.772	10.961	11.15	11.339	11.528	11.717	11.906	12.173
9.001	10.603	10.799	10.988	11.177	11.366	11.555	11.744	11.933	12.286
9.566	10.637	10.826	11.015	11.204	11.393	11.582	11.771	11.96	12.454
9.943	10.664	10.853	11.042	11.231	11.42	11.609	11.798	11.987	12.707
10.196	10.691	10.88	11.069	11.258	11.447	11.636	11.825	12.014	13.084
10.364	10.718	10.907	11.096	11.285	11.474	11.663	11.852	12.047	13.649
10.477	10.745	10.934	11.123	11.312	11.501	11.69	11.879	12.098	14.494

**\$ Property: Water Saturation Max: 1 Min: 0.25

SW KVAR

10*1.0 20*.25 10*1.0 20*.25 10*1.0

**\$ Property: Oil Saturation Max: 0.75 Min: 0

SO KVAR

10*0.0 20*0.75 10*0.0 20*0.75 10*0.0

**\$ Property: Gas Saturation Max: 0 Min: 0

SG CON 0

Gas rate and cumulative gas rates shows good agreement with other codes

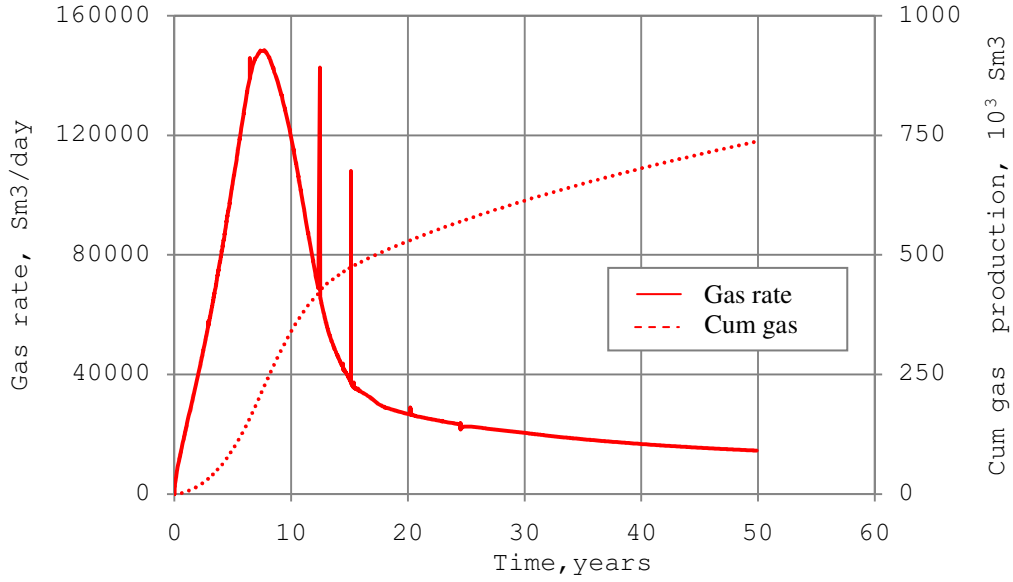


Figure 5-14 Gas rate and cumulative gas production for 50 years using CMG STARS

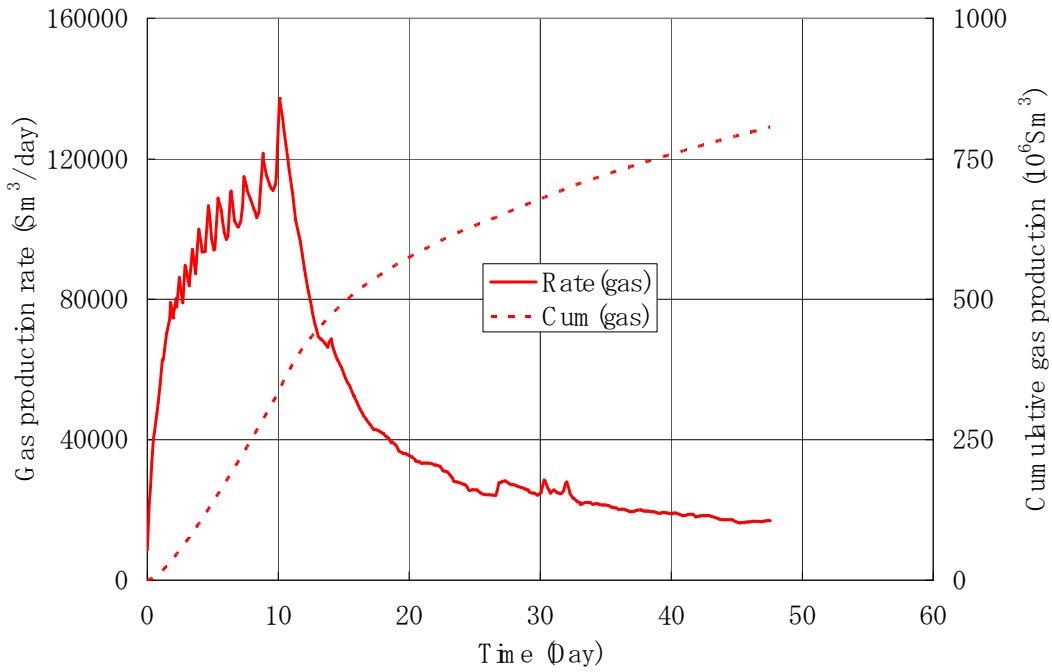


Figure 5-15 Gas production rate and cumulative gas production for 50 years using MH21

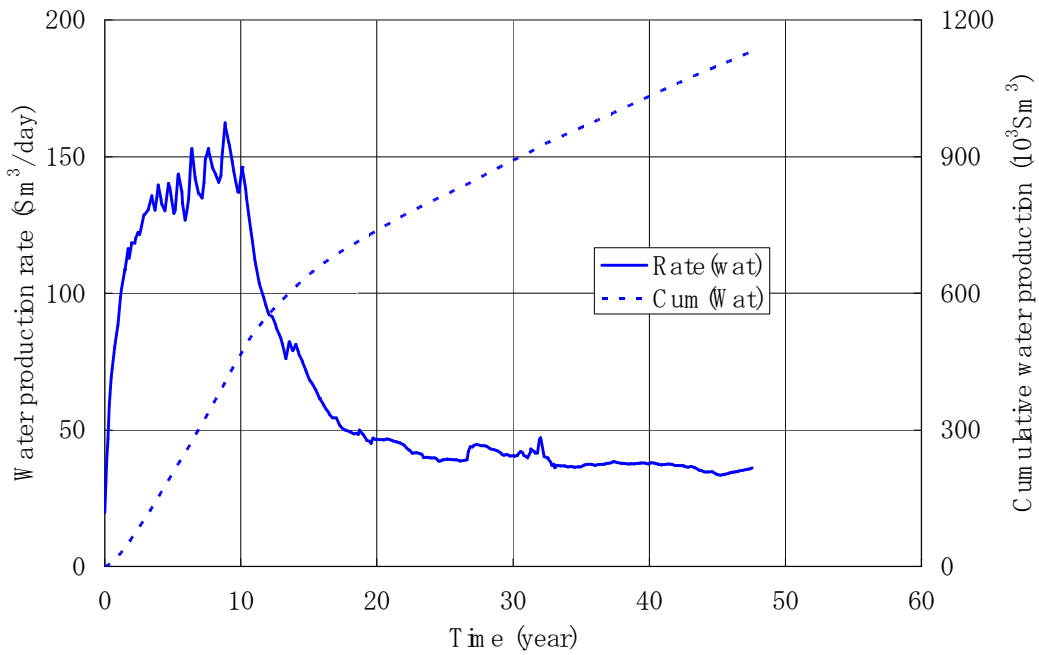


Figure 5-16 Water rate and Cumulative water production for 50 years using MH21

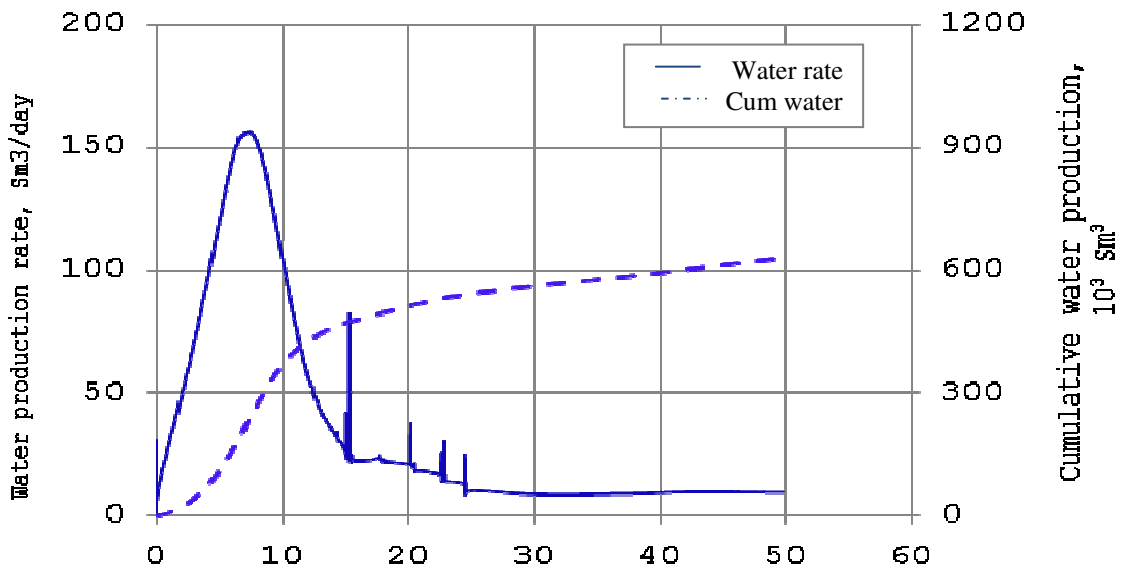


Figure 5-17 Water rate and Cumulative water production for 50 years using CMG STARS

6. Sensitivity Analysis of Reservoir Parameters

Typically in a reservoir simulation, all the parameters are recalculated for every time step. Various parameters influence the production of gas from methane hydrates. If the production rates are correlated parametrically, the correlation can be generalized and can be applied to another situation with much more confidence. This could potentially save time and money. Sensitivity analysis helps in reaching a consensus on such a correlation. That is why sensitivity analysis for this case is considered important.

Sensitivity analysis is done to systematically prove the relative importance of the model's parameters, here in this case the simulation's parameters. It highlights the impact of independent variables on a dependent variable. There are many universally accepted procedures for doing sensitivity analysis; a common approach is to explore the effects of changing parameters one at a time on the production rates. For the sensitivity analysis, seven factors have been chosen. They are pressure, temperature, Hydrate saturation, permeability, Bottom-hole pressure, Porosity and Free Water saturation.

There are various ways to conduct a sensitivity analysis and two methods chosen here are

1. **One at a Time Effect³⁸ (OAAT)**: In OAAT one parameter is varied keeping the rest of the factors constant.
2. **Plackett-Burman Design³⁸**: This method allows simultaneous examination of the entire suite of parameters. Effects of individual parameters and 2-way interaction of the pairs of parameters is also studied in this method. All the parameters are changed in a certain design that will be discussed in the section 6.2.

6.1 One at a Time Effect:

The One At A Time effect (OAAT) is studied by changing one parameter at a time and other simulation properties are same as the base case problem.

Base Case Description:

Base case problem is Problem 7b except that the hydrate saturation, water saturation in the hydrate bearing zone and the bottom-hole pressure applied in the reservoir are changed. Hydrate saturation and water saturation in the hydrate bearing zone are 0.7 and 0.3. Bottom-hole pressure is considered to be 2900 kPa. All the parameters are changed from base case to lower or higher end, also preset by judgment, one at a time. Table 5.1 illustrates the factors and their values used in this study. Pressure and temperature values given below are for the uppermost part of the shale zone.

Table 6-1 Factors and their values used for OAAT effect calculations

Factor	Lower end	Base Case	Upper end
Porosity, %	30	40	50
Permeability(r/Z), mD	750/75	1000/100	1250/125
Hydrate saturation, %	60	70	80
Free Water Saturation, %	13	15	18
Temperature, °C	0.85	2.5	4.5
Pressure, kPa	5800	6513	7200
Bottom-hole Pressure, kPa	2700	2900	3000

Simulations are carried for 20 years with a data sampling frequency of 1 year and cumulative gas production are compared to evaluate the effect of each parameter.

Effect of Porosity:

As porosity increases, it is expected that the ability to flow should increase. Porosity is varied from a reference value of 0.4 to 0.3 & 0.5. All other parameters like permeability, water saturation, hydrate saturation, free water saturation, bottom hole pressure, temperature and pressure of the reservoir are held constant and are same as that of the base case. No particular trend is observed in the reservoir behavior with respect to porosity changes as shown in Fig. 6-1.

Effect of porosity on gas production rates depends upon the variation chosen. If porosity is varied from 0.3 to 0.2 and 0.4 a different result can be expected. Conventional thought would suggest that higher porosity gives high production rates due to more available pore volume in the reservoir. Depending on the value picked for porosity in the simulation, there is a change in the output from the reservoir. There is ample uncertainty associated with porosity changes.

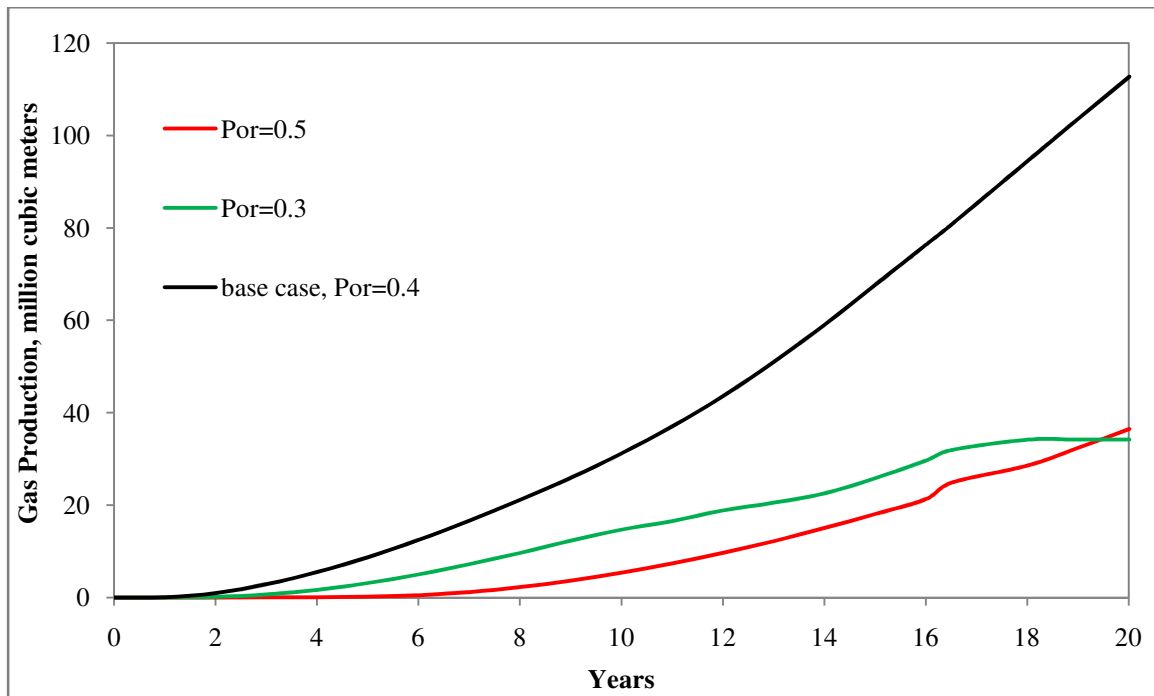


Figure 6-1 Effect of Porosity on gas production

Effect of Permeability:

Permeability for the base case is 1000mD in the radial direction and 100mD in the vertical direction. Two cases are considered in which absolute permeability is changed from 1000/100 mD (r/z direction) to 1250/125 mD and 750/75 mD. Increasing permeability has increased production rates as shown in Figure 6-2.

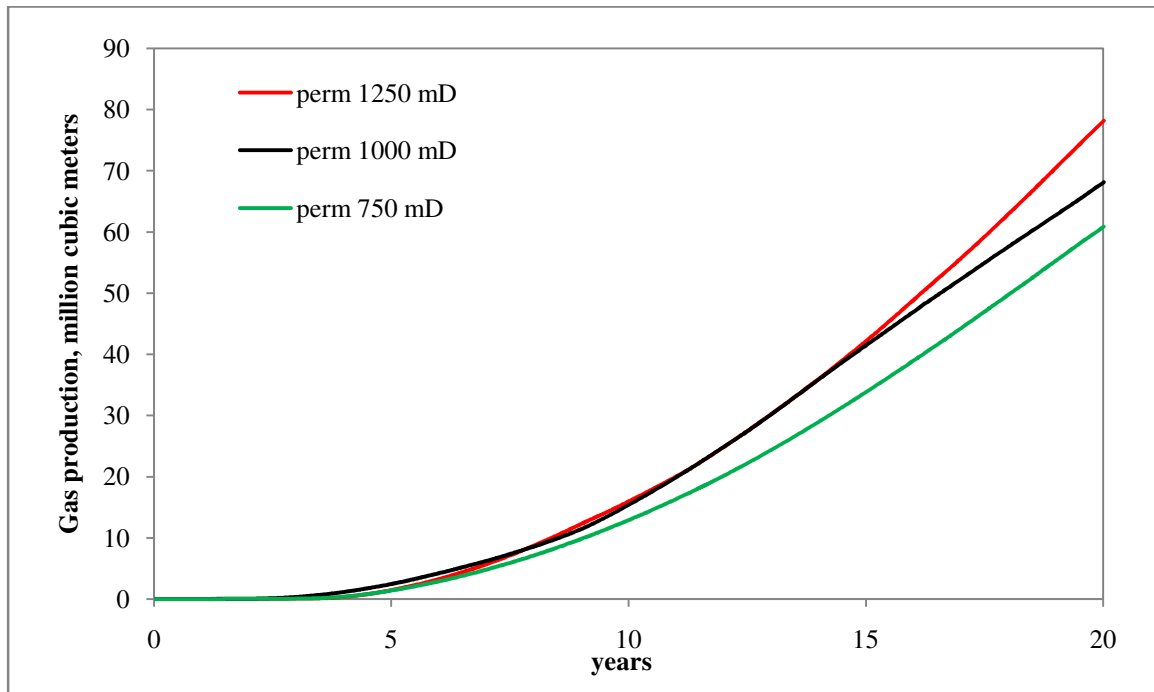


Figure 6-2 Effect of permeability on gas production

Effect of Hydrate saturation:

Higher the hydrate saturation, more the methane in the reservoir. This might be an interesting factor to consider seeing if higher hydrate saturations yielded higher gas. Hydrate saturation is assumed to be uniform in the hydrate bearing zone. It is varied from 0.7 (base case) to 0.6 and 0.8.

This is an interesting and informative result obtained. Higher hydrate saturation gave lesser production rates. Hydrate dissociation is endothermic and it cools the reservoir. Hence, higher hydrate saturation rapidly cools the reservoir preventing further hydrate dissociation and contributes to fall in gas production rates. These production rates however depend on the values of the hydrate saturation chosen. Therefore, a detailed experiment has to be designed in order to study the reservoir behavior in total. In Figure 6-3, decrease in hydrate saturation shows an increase in production rates.

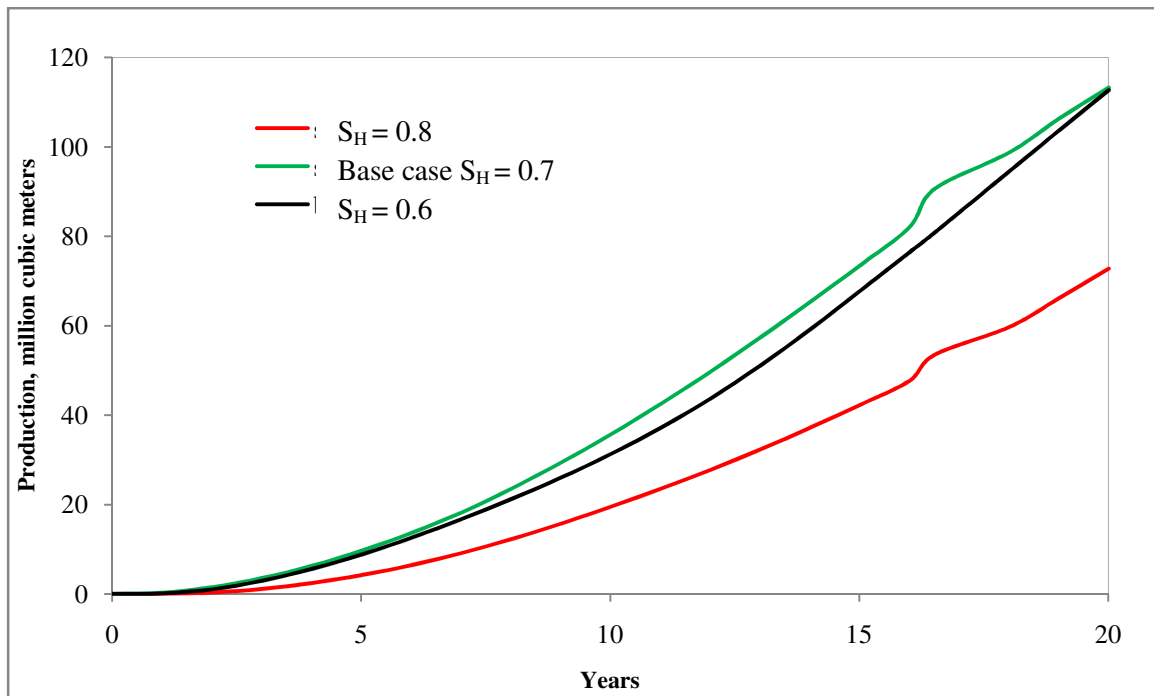


Figure 6-3 Effect of hydrate saturation on gas production

Effect of temperature:

At high temperature, the hydrate is perturbed from its equilibrium and easier becomes dissociation. So, warmer reservoirs could lead to higher gas rates. In the base case, the temperature at the uppermost part of the shale zone is 2.5 °C. The geothermal gradient is

+0.03°C/m and the temperature of the remaining cells is calculated using the geothermal gradient. This temperature is changed to 0.85°C and 4.5°C for the OAAT effect calculation.

The geothermal gradient remains the same.

As expected, higher reservoir temperature lead to higher gas production and this can be attributed to more available heat in the system as shown in Figure 6-4.

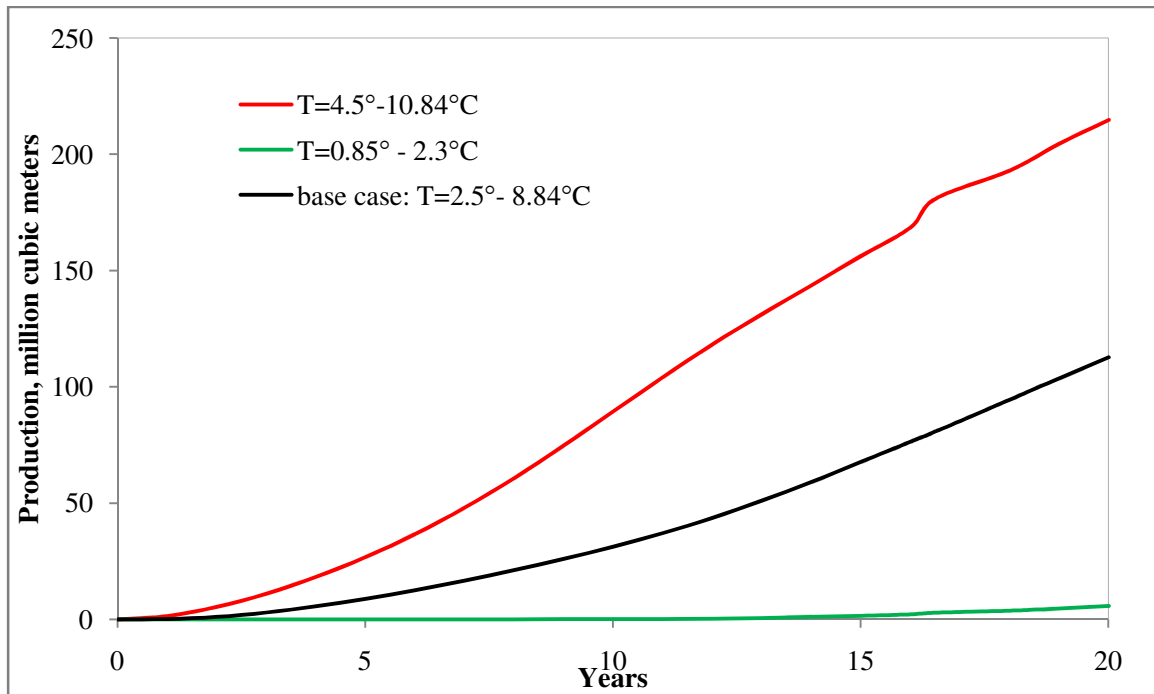


Figure 6-4 Effect of temperature on gas production

Effect of Pressure:

In the base case, the pressure at the uppermost part of the Shale zone is 6513 kPa. The hydrostatic pressure gradient is 9792 Pa/m and the pressure of the remaining cells is calculated using the hydrostatic pressure gradient. This pressure is changed to 5800 kPa and 7200 kPa for the OAAT effect calculation. The hydrostatic pressure gradient remains the same. These values of temperature and pressure are chosen to ensure the stability of the

hydrate. Hydrate can also form in the reservoir depending upon the pressure and temperature values, which also can reduce gas production rates. In this case higher gas production rates are found with increase in the difference between the pressure of the reservoir and the bottom hole pressure applied in the reservoir. Figure 6-5 shows the cumulative gas production at different pressures.

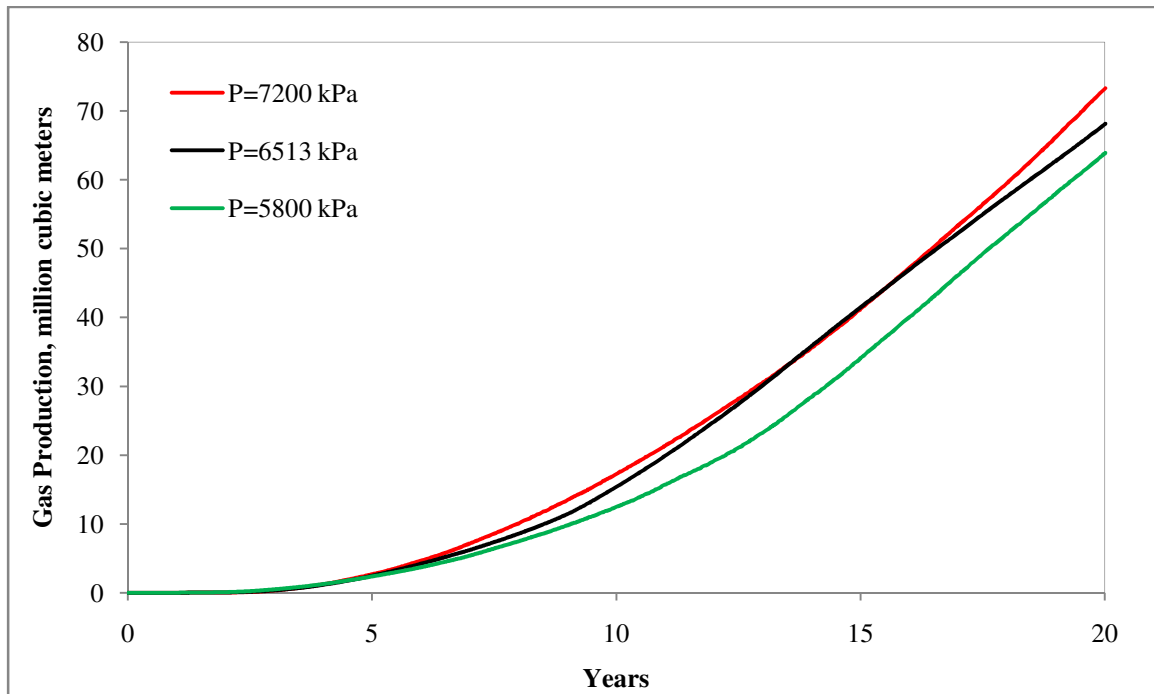


Figure 6-5 Effect of pressure on gas production

Effect of Bottom-hole Pressure:

A lower bottom-hole pressure (BHP) is ideal to produce gas because it depressurizes more. But there is also a limitation to this. At BHP lower than 2700kPa, Ice formation is seen and hence the least value of BHP that could be possible is 2700kPa. Bottom-hole pressure is changed from 2900kPa in the base case to 2700kPa and 3000kPa.

Production rates for BHP of 2900 kPa and 2700 kPa are nearly the same as shown in the Figure 6-6 Increase in the BHP means there is lesser depressurization in the reservoir owing to lesser production rates.

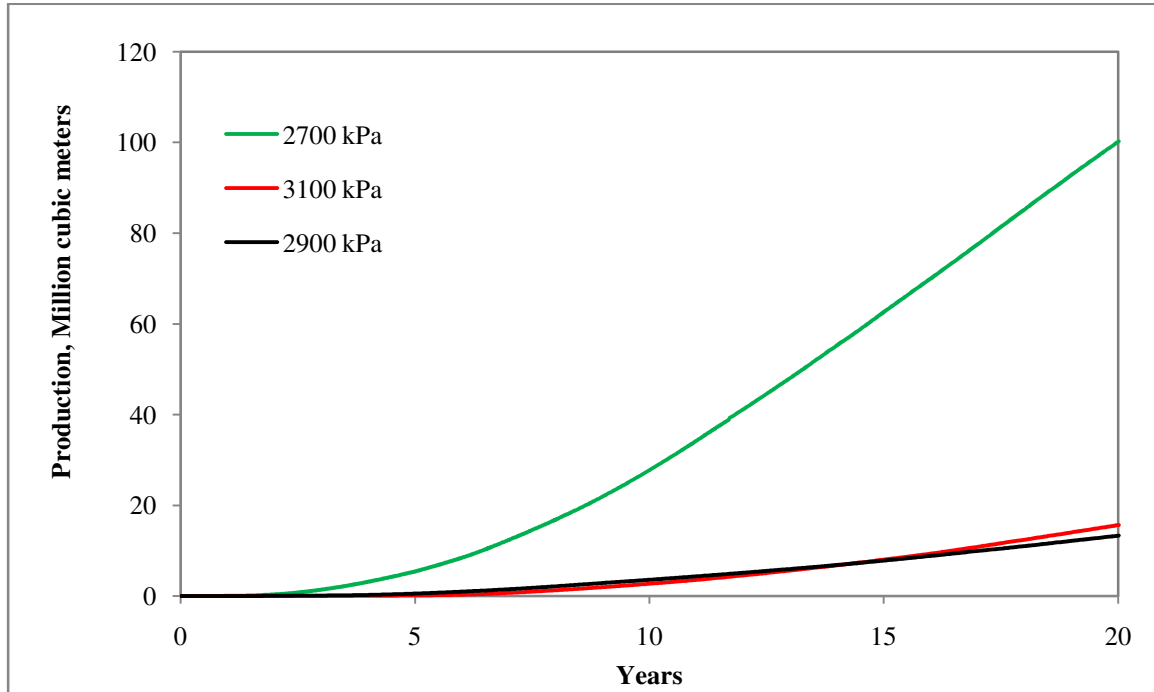


Figure 6-6 Effect of bottom- hole pressure on gas production

Effect of free water saturation:

Free water saturation for the base case is 15%. It is changed to 13% and 18% for the OAAT effect calculation. Free water saturation is related to the irreducible water saturation as seen in the following equation, $S_{irw} = S_w - S_{free}$. Changing irreducible water saturation changes all the permeability properties of the reservoir. So, free water saturation is a very important factor to be taken care of. Table 6-1 lists all the factors and changes in the factors from the base case.

Keeping the water saturation constant, if free water saturation is changed, irreducible water saturation also changes which affects the permeability curves. So, increase in gas production is observed with increase in free water saturation as shown in Figure 6-7.

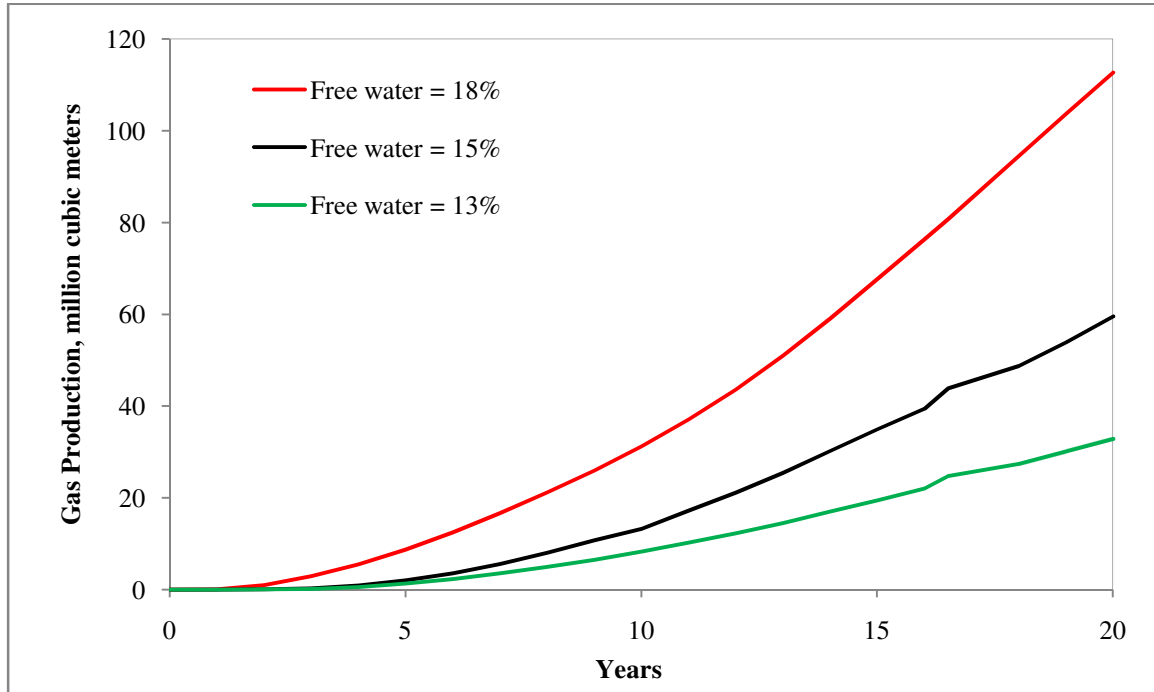


Figure 6-7 Effect of free water saturation on gas production

6.2 Plackett Burman Design.

One common way to obtain interactions between the parameters is to perform a complete factorial design. A complete factorial design consists of all possible permutations of the parameters starting from a high and low value for each parameter. The number of scenarios required for completing the factorial design is 2^n where n is the number of parameters and “2” is a consequence of using 2 values (high, low) for each parameter. To perform one complete factorial design, a cumbersome 128 (2^7) runs are to be conducted.

The Plackett Burman design is an alternative method which is convenient and informative. The design specifies a subset of scenarios used for a complete factorial design. The number of scenarios for the design is 2 times that multiple of 4, which is greater than the number of parameters. In this case 16 runs are conducted for seven reservoir parameters. The algorithm to implement the sensitivity analysis involves the following steps.

- Select a base case
- Determine the possible upper and lower ends of the parameters.
- Create Plackett-Burman sensitivity analysis matrix.
- Run the scenarios.
- Calculate effect of each parameter on production rates.
- Interpret the results.

The base case for this sensitivity analysis is problem 7b. Problem 7b has been validated with all other simulators that participated in the study. The same input data file is used in the following sensitivity analysis changing certain parameters in the problem according to the design. The details of the design are given later in this chapter.

Upper and lower values for each parameter are selected. These values are obtained by increasing or decreasing the value of the parameter by certain fixed percentage in order to gain maximum benefit from this design. Eight different reservoir scenarios (designs) are considered in this study because seven factors are being studied for sensitivity and 8 is the least multiple of 4 greater than 7. The seven reservoir parameters with their higher and lower values for Design 1 are shown in Figure 5.1. All the parameter values for different designs are given in Table 5.2. Pressure and temperature values specified in Table 5.2 are for the uppermost part of the shale zone. The corresponding values of pressure and temperature are calculated using the gradients specified in the base case.

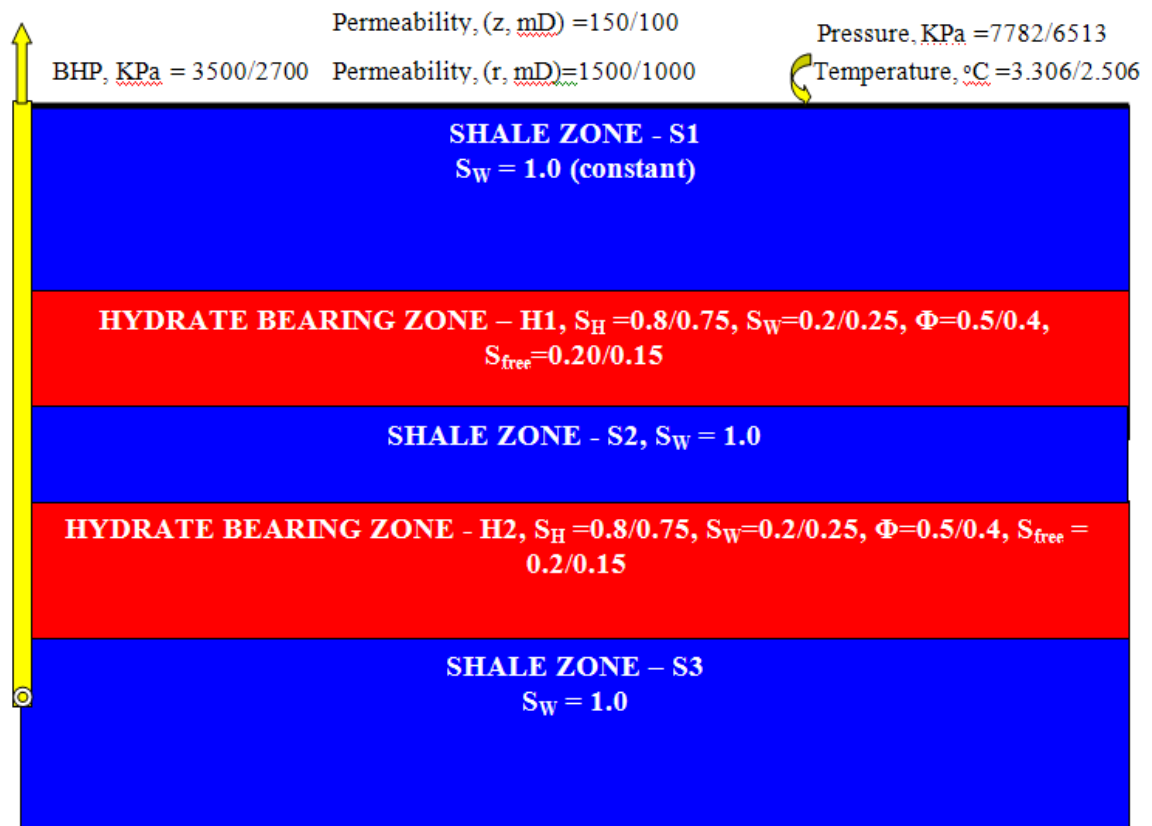


Figure 6-8 Parameter specifications for Design 1

Table 6- 2 Parameter specifications for different scenarios

Parameters	Design 1		Design 2		Design 3	
Pressure(kPa)	7782	6513	5243	6513	5878	6513
Temperature(°C)	3.306	2.506	1.706	2.506	2.306	2.506
Hydrate Sat.	0.8	0.75	0.5	0.75	0.65	0.75
Permeability(mD)	1500/150	1000/100	500/50	1000/100	750/75	1000/100
BHP(kPa)	3500	2700	2700	3000	2700	2900
Porosity	0.5	0.4	0.3	0.4	0.3	0.4
Free Water	0.2	0.15	0.1	0.15	0.12	0.15

Table 6-2 (contd...)

Parameters	Design 4		Design 5		Design 6	
Pressure(kPa)	5878	6513	7148	6513	5878	6513
Temperature(°C)	7.391	8.157	5.56	5.11	4.65	5.11
Hydrate Sat.	0.65	0.75	0.8	0.7	0.6	0.7
Permeability(mD)	750/75	1000/100	1250/125	1000/100	750/75	1000/100
BHP(kPa)	2700	2900	3000	2900	2700	2900
Porosity	0.3	0.4	0.5	0.4	0.3	0.4
Free Water	0.12	0.15	0.18	0.15	0.12	0.15

Table 6-2 (contd...)

Parameters	Design 7		Design 8	
Pressure(kPa)	5878	6513	7148	6513
Temperature(°C)	4.65	5.11	8.92	8.157
Hydrate Sat.	0.6	0.7	0.5	0.4
Permeability(mD)	750/75	1000/100	1250/125	1000/100
BHP(kPa)	2700	2900	2900	2700
Porosity	0.3	0.4	0.4	0.3
Free Water	0.12	0.15	0.18	0.15

Considering seven factors, a design of size eight is needed and the design matrix is given in Table 6-3. The ‘plus’ and the ‘minus’ in the matrix is replaced with higher and lower values for each parameter elaborated in Table 6-2.

Table 6-3 Plackett-Burman sensitivity analysis matrix

Run Number	Pressure	Temperature	Hydrate Saturation	Permeability	Bottom hole Pressure	Porosity	Free water
1	+	+	+	-	+	-	-
2	-	+	+	+	-	+	-
3	-	-	+	+	+	-	+
4	+	-	-	+	+	+	-
5	-	+	-	-	+	+	+
6	+	-	+	-	-	+	+
7	+	+	-	+	-	-	+
8	-	-	-	-	-	-	-
9	-	-	-	+	-	+	+
10	+	-	-	-	+	-	+
11	+	+	-	-	-	+	-
12	-	+	+	-	-	-	+
13	+	-	+	+	-	-	-
14	-	+	-	+	+	-	-
15	-	-	+	-	+	+	-
16	+	+	+	+	+	+	+

A total of 16 runs are conducted for each design by changing the parameters for every run as shown in Tables 6-2 & 6-3. Hydrate saturation, water saturation, free water saturation and irreducible water saturation are linked together by the following equations.

$$S_w + S_H = 1, S_G = 0 \text{ (initially)}, S_{irw} = S_w - S_{free}$$

For example in Run 1 (Table 6-3) hydrate saturation has a ‘plus’ sign and free water saturation has a ‘minus’ sign which indicates that the higher value among the two, for hydrate saturation and lower value of the two, for free water saturation is used. Water saturation and irreducible water saturation are recalculated from the above equations which in turn change the relative permeability curves. All these direct or indirect effects are taken

into consideration for each run. All other properties not mentioned in this chapter are same as that of the base case.

Simulations are run using CMG STARS for 20 years with a data sampling frequency of 1 year.

Results

A range of production rates were obtained in each design. The Figure 6-9 gives a visual description of the range of production rates observed in each design. Each of the area plots show how sensitive the production rates are with respect to the parameter changes. Designs 1, 2 and 3 especially showed lower production rates. This is because they are cold reservoirs. Warmer reservoirs, Designs 4 – 8 showed better production rates than Designs 1 – 3.

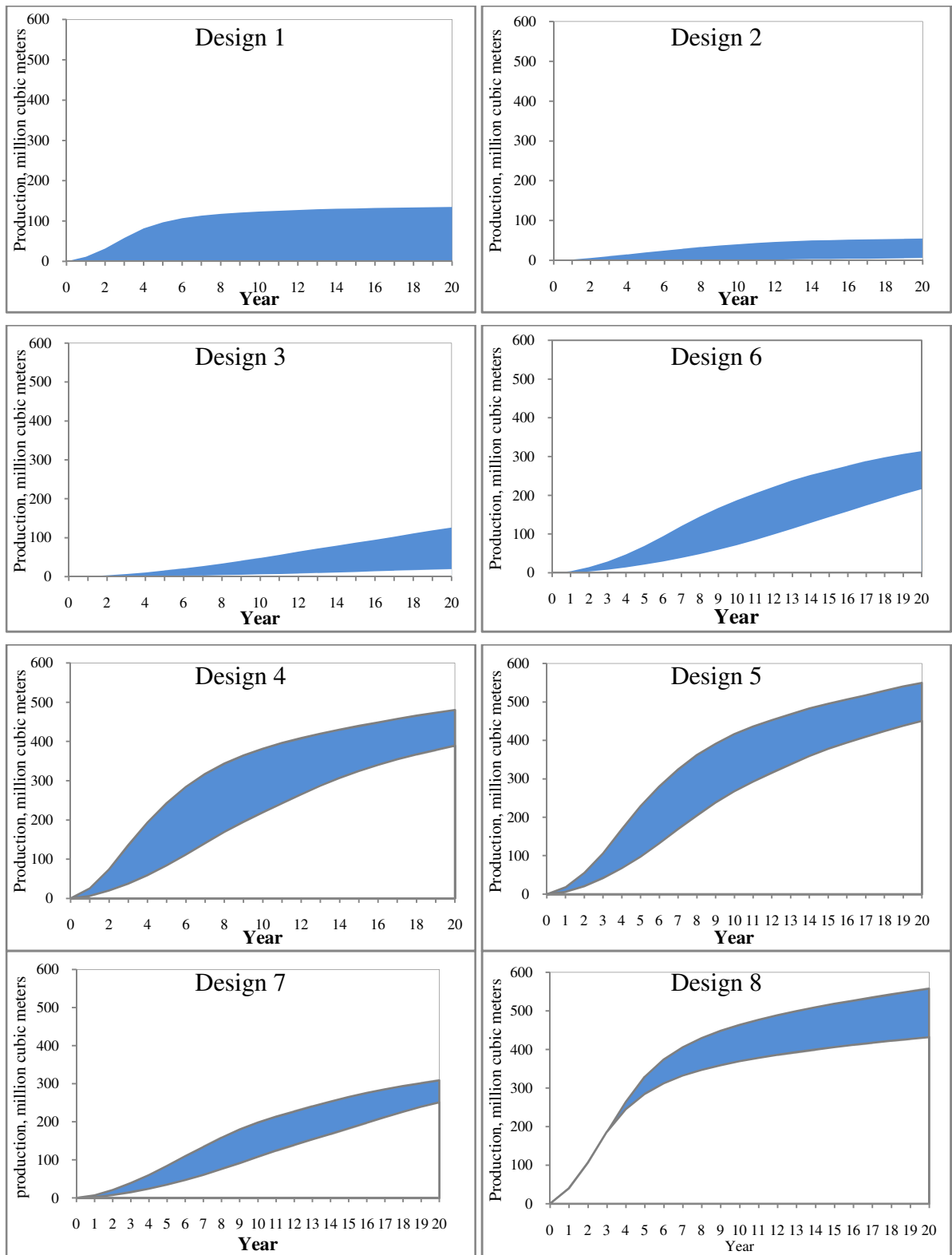


Figure 6- 9 Cumulative gas production for designs 1-8

The effects of the PB design are found out as follows. For the run n, (n = 1, 2, 3...16)

$$S_n = \sum_{i=0}^{20} \frac{P_i}{(1 + 0.15)^i}$$

where P_i = Annual Production and the factor 0.15 is used to discount the future production rate to a number that can be added to today's value to give a present value of the total production in the predicted future. Thus, S_n s ($S_1, S_2...S_{16}$) are calculated. In order to calculate the effect of a parameter, the following equation is used.

$$E_j = \sum \frac{\pm S_n}{8 * \% \text{ change in } E_j}$$

where $j = 1, 2...7$, '+' is taken before the S_n when there is a corresponding '+' in the matrix column for that specific parameter and '-' is taken before the S_n when there is a corresponding '-' in the matrix column for that specific parameter.

For example, in Design 1, the effect of pressure is given as $E_1 = (+S_1-S_2-S_3+S_4-S_5+S_6+S_7-S_8-S_9+S_{10}+S_{11}-S_{12}+S_{13}-S_{14}-S_{15}+S_{16}) \div (8*\% \text{ Change in Pressure})$

Results

The effects are calculated using equation for E_j . The effects of various factors/parameters are plotted against those factors. A positive higher effect indicates that an increase in that factor increases the production rate and a negative effect value means that an increase in that factor decreases the production rate. The effects of all the design parameters are shown in Figure 6-10. For pressure, some effects were higher and some effects were lower than zero. This means that it depends on the other factors in the scenario.

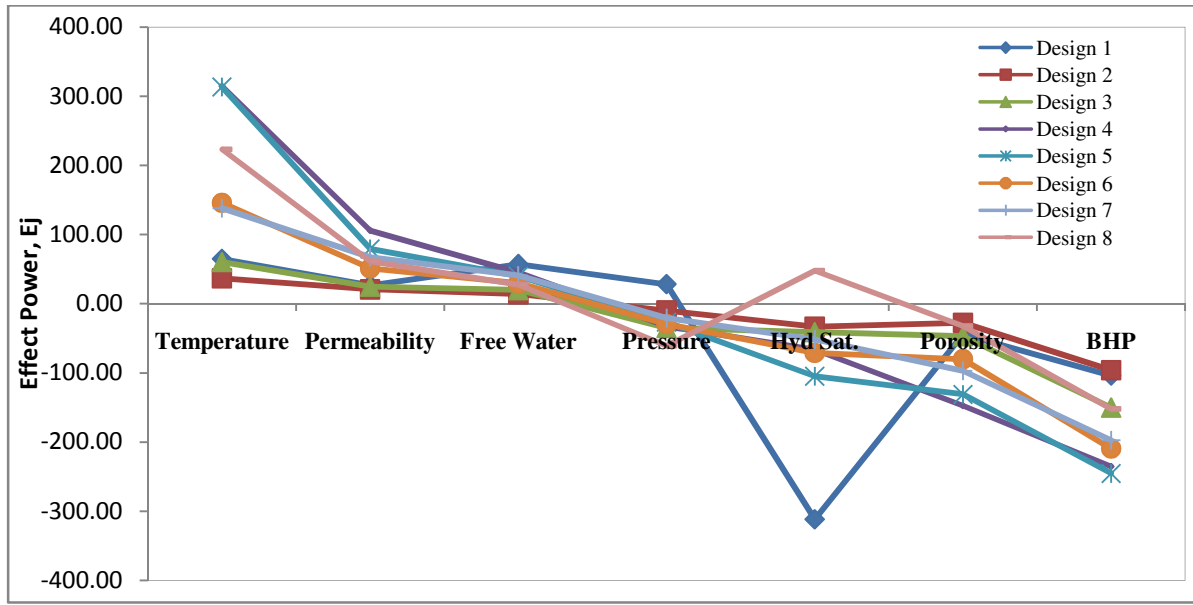


Figure 6- 10 Effects of the parameters on gas production.

Table 6-4 Effects of variable input parameters on cumulative gas production

Design	Temp.	Perm.	Free Water	Pressure	Hyd Sat.	Porosity	BHP
1	64.66	26.71	57.03	28.26	-311.77	-44.11	-103.86
2	36.61	20.78	13.79	-9.87	-33.17	-27.68	-96.00
3	60.44	24.76	19.99	-35.11	-40.90	-46.93	-150.28
4	314.49	105.64	45.19	-32.31	-66.14	-147.40	-235.17
5	313.07	79.09	39.82	-26.64	-104.86	-131.06	-245.29
6	145.70	50.83	29.43	-29.56	-71.31	-80.28	-209.52
7	138.16	67.59	40.99	-20.70	-51.75	-96.93	-197.27
8	223.30	61.41	27.65	-60.86	47.83	-32.27	-152.03

Each of the parameters has been ranked based on the magnitude of the effect calculated. BHP was ranked the strongest in all the designs except design 8, which is warm reservoir and has less hydrate saturation. Temperature is observed to be the next most important factor in determining the productivity of the reservoir.

Table 6-5 Rankings for different parameters involved in each design

Design	1	2	3	4	5	6	7	8
Pressure	6	7	5	7	7	6	7	4
Temperature	3	2	2	1	1	2	2	7
Hyd. Sat.	1	3	4	4	4	4	5	3
Permeability	7	5	6	5	5	5	4	6
BHP	2	1	1	2	2	1	1	5
Porosity	5	4	3	3	3	3	3	1
Free water	4	6	7	6	6	7	6	2

7. Importance and Incorporation of Heterogeneity in Reservoirs

Heterogeneities in the characteristic of geologic systems are commonly seen. It is true that everywhere in nature, there is diversity. We have incorporated heterogeneity into the reservoir models to make it resemble a natural reservoir. So far, homogeneous properties have been assumed throughout the reservoir. These homogeneous property values are actually the average values of the distribution of the parameters. Measured data for these properties are obtained from the distribution of properties from the Mt Elbert Stratigraphic test well. This data is generally specified with respect to the depth of the reservoir. The variability in permeability, porosity, hydrate saturation, water saturation and irreducible water saturation is taken into account in this part of the study. Figure 7-1 and 7-2 show a distribution of hydrate saturation, permeability, porosity and irreducible water saturation from a depth of 2130 ft to 2170 ft which is obtained from Mt. Elbert site³⁹.

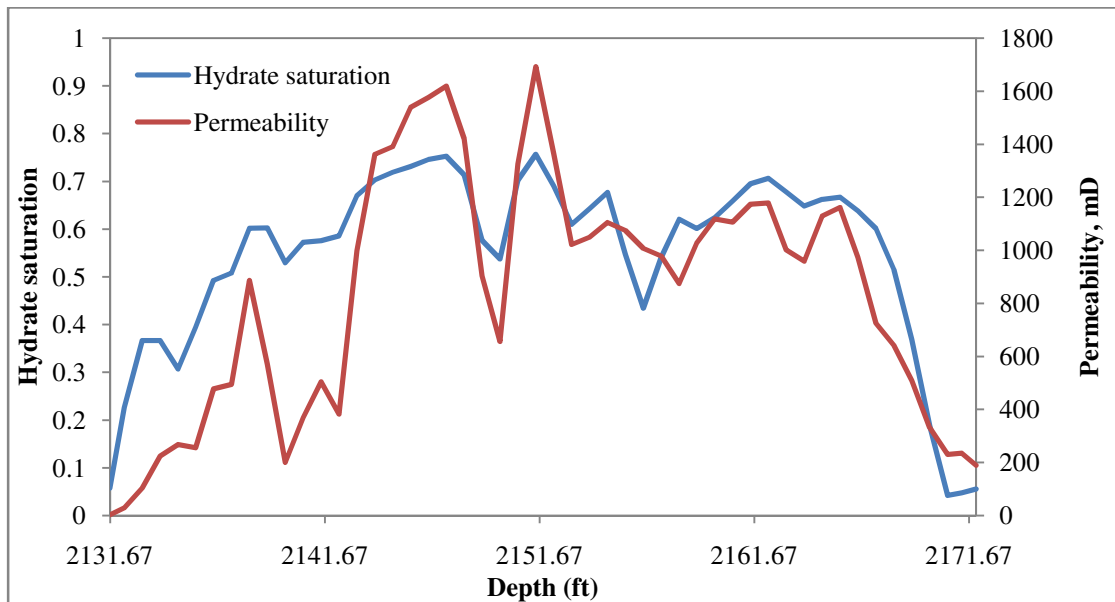


Figure 7-1 Hydrate saturation and Permeability distribution data from Mt Elbert Stratigraphic test well

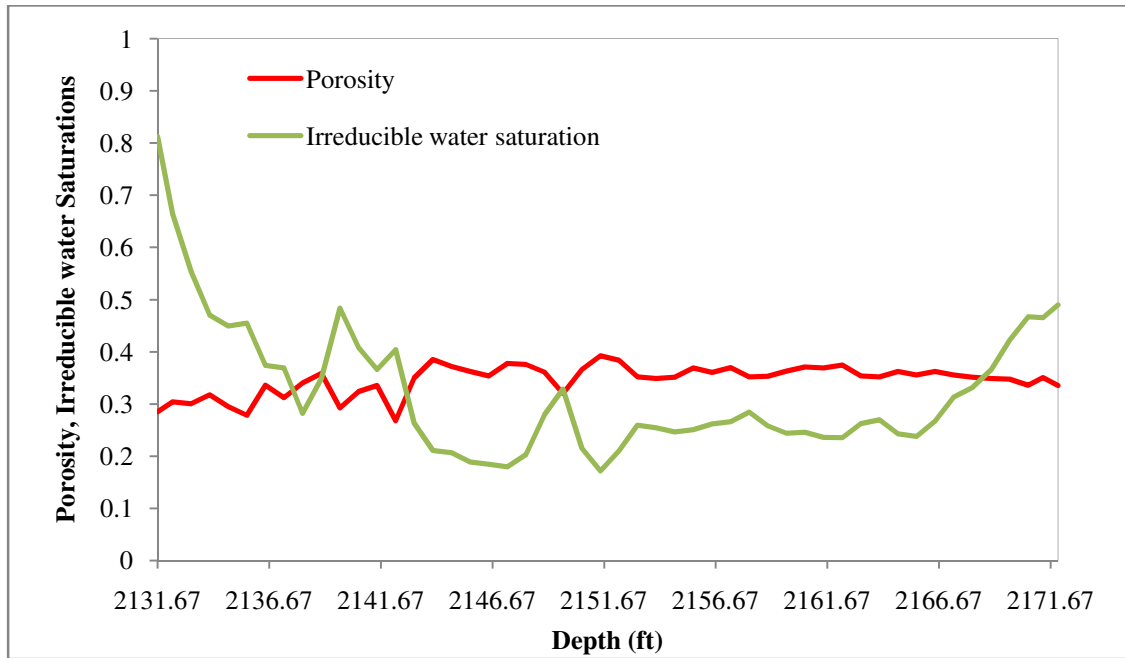


Figure 7-2 Porosity and Irreducible water saturation data from Mt Elbert Stratigraphic test well

It can be seen from Figure 7-1 that hydrate saturation and permeability are low at 2130 ft and 2170 ft and higher at other points. This can be due to higher clay concentrations at those points which is shown in Figure 7-2 in the form of higher irreducible water saturation. Instead of specifying a constant uniform property in the entire reservoir these variations in properties are specified in the input data file and variations in gas production are studied.

Base case

As seen in the results of Problem 7a (Figure 7-3) no gas was produced for the first 10 years. It is very important to check whether the production rates are same even after introducing heterogeneity in the system. This made us to choose Problem 7a (Mt Elbert like deposit) as the base case and heterogeneities in different properties are incorporated using the Mt Elbert

Stratigraphic test well data. Three different cases with difference in the heterogeneity of properties are being studied.

Case 1

In Problem 7a, Porosity (0.1-Shale Zone, 0.35-Hydrate Zone), Hydrate saturation (0.0-Shale Zone, 0.65-Hydrate Zone), Permeability (1000 mD/100 mD), Irreducible water saturation (0.248) are constant for the entire reservoir. In this case variability in properties like hydrate saturation, permeability, porosity and irreducible water saturation as shown in Figures 7-1 and 7-2 are included in Problem 7a data file. Irreducible water saturation for each layer is different and so 50 relative permeability tables have been included for 50 layers in the hydrate bearing zone of Problem 7a. Variations in Porosity, Permeability, hydrate saturation and irreducible water saturations are specified in the data file as below.

```

Por
10*0.1
  0.28426  0.29398  0.32222  0.36982  0.37972  0.37501  0.35830  0.36267  0.35184  0.34788
  0.29388  0.31994  0.31212  0.36786  0.35679  0.35935  0.35701  0.36552  0.35309  0.34509
  0.30152  0.32115  0.31170  0.35733  0.33170  0.34630  0.35164  0.36297  0.35909  0.33069
  0.30570  0.33477  0.31075  0.36006  0.35691  0.34949  0.35079  0.35547  0.35651  0.33032
  0.28711  0.34545  0.34477  0.36705  0.37842  0.35816  0.35780  0.35024  0.35000  0.33939
10*0.1

PERMI KVAR & PERMJ JVAR
10*0
  2.053  255.838  199.683  1361.843  1421.303  1364.303  1006.938  1105.914  1129.347  508.473
  28.558  477.572  369.510  1391.727  904.047  1022.109  977.957  1174.095  1162.216  331.048
  103.396  494.724  504.766  1539.624  656.058  1049.961  874.970  1179.020  973.308  230.385
  224.637  886.225  382.626  1577.072  1326.622  1105.361  1027.493  1002.020  725.017  234.475
  267.802  571.090  999.316  1619.529  1693.079  1075.644  1119.034  959.168  642.321  189.283
10*0

PERMK KVAR
10*0
  0.205  25.584  19.968  136.184  142.130  136.430  100.694  110.591  112.935  50.847
  2.856  47.757  36.951  139.173  90.405  102.211  97.796  117.409  116.222  33.105
  10.340  49.472  50.477  153.962  65.606  104.996  87.497  117.902  97.331  23.039
  22.464  88.623  38.263  157.707  132.662  110.536  102.749  100.202  72.502  23.447
  26.780  57.109  99.932  161.953  169.308  107.564  111.903  95.917  64.232  18.928
10*0

```

So KVAR									
10*0									
0.057	0.394	0.529	0.703	0.714	0.690	0.434	0.659	0.662	0.368
0.227	0.493	0.572	0.719	0.576	0.610	0.541	0.695	0.666	0.188
0.366	0.508	0.576	0.731	0.538	0.643	0.621	0.706	0.638	0.042
0.367	0.602	0.585	0.746	0.703	0.677	0.601	0.677	0.601	0.047
0.307	0.602	0.670	0.753	0.757	0.547	0.624	0.648	0.515	0.055
10*0									
SWIRG KVAR									
10*0.248									
0.812	0.455	0.484	0.211	0.203	0.210	0.262	0.246	0.243	0.365
0.664	0.374	0.408	0.207	0.279	0.259	0.266	0.236	0.238	0.423
0.554	0.369	0.366	0.189	0.328	0.255	0.284	0.235	0.267	0.467
0.470	0.282	0.404	0.185	0.215	0.246	0.258	0.262	0.313	0.465
0.449	0.349	0.263	0.180	0.172	0.251	0.244	0.270	0.332	0.490
10*0.248									

Case 2

In this case the effect of heterogeneity in hydrate saturation on production rates is studied. Other Properties like porosity permeability irreducible water saturation are set constant as the base case.

Case 3

This case is similar to case 1 except that, a uniform permeability of 1000 mD and 100 mD in the radial and horizontal direction are considered. This case is studied to understand the effect of variable permeability on production rates.

Results

All the cases were run for 10 years. It was noticed from the simulations that in all cases gas was produced in the first 10 years as shown in Figure 7.3.

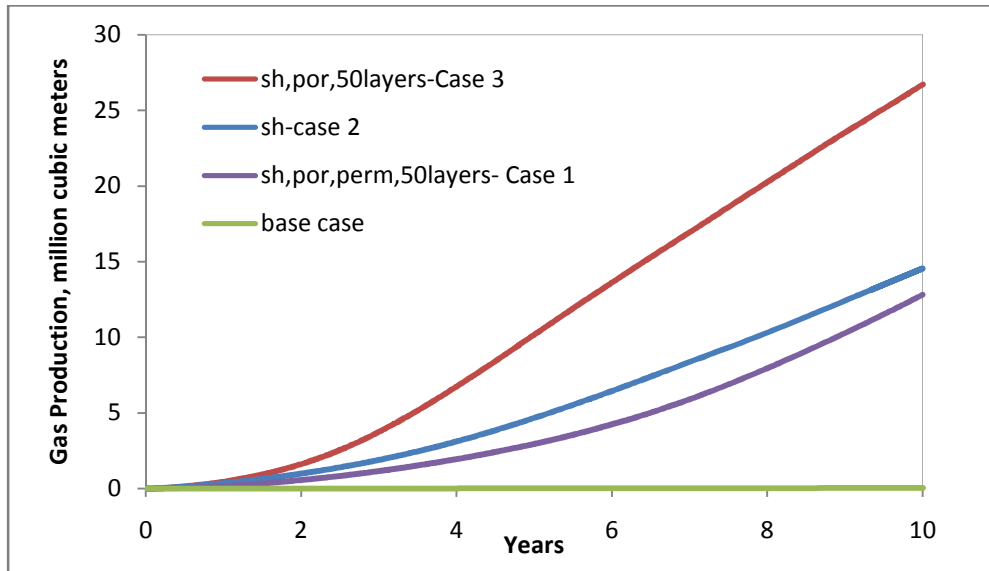


Figure 7-3 Gas production for Case 1, 2 and 3. Case 1 refers to the reservoir which includes anisotropy in permeability, porosity, hydrate saturation and irreducible water saturation. Only heterogeneity in hydrate saturation is considered in Case 2. Anisotropy in hydrate saturation, porosity and irreducible water saturation (50 layers) is considered in Case 3

8. Conclusions Recommendations and Future work

8.1 Conclusions

- Depressurization is better method for gas hydrate production yielding higher production rates than in the case of thermal stimulation.
- Capillary pressure of water-gas is introduced in the water-oil table as PCOW when the oil phase is absent. Gas-water capillary pressure is introduced as PCOG in the gas-oil table when hydrate is modeled as an oil phase. These differences in the specification of gas-water capillary pressure have created problems matching the results of capillary pressure for CMG STARS with other codes.
- Capillary pressure and gas phase relative permeability are a function of water saturation but they can be specified only as a function of liquid saturation (water + oil) in STARS input data file. This has created problems in matching the relative permeability curves with other simulators.
- Results for hydrate modeled as an oil phase with the exception of problems resulting in the formation of ice in the system for all the reservoir simulators are in good agreement.
- Using the inbuilt ICE model in STARS can lead to differences in the results. Specifying ICE as a component is preferred to encounter the ice formation in the system.
- Sharp hydrate dissociation is not observed for CMG STARS when hydrate is specified as an oil component.

- Incorporating heterogeneities in properties like porosity, permeability, hydrate saturation, irreducible water saturation has increased production rates.
- Sensitivity analysis was performed using Plackett-Burman Design and results showed that temperature, bottom-hole pressure are the most sensitive parameters. Hydrate saturations above 60% have a negative impact on production rates. Hydrate saturations of about 40-50% has showed a positive impact on gas production rates.

8.2 Recommendations and Future work

- The ICE model inbuilt in CMG STARS could be compared / validated by conducting several small runs with the reaction chemistry specified and to find out the difference between the model used in STARS and other codes.
- Definition of more cases with ice as a part of the system and solving them in comparison with other hydrate codes being used.
- Lab scale experiments on hydrate core samples could be conducted and the situation can be converted to a code comparison problem, thus provides a controlled comparison to experimental data.
- The introduction of horizontal wells into the reservoir scenario and comparison with vertical wells should be performed.
- So far, only one method of hydrate dissociation has been used in this study at a time. It would be of interest to use more than one method of hydrate dissociation for the same system at different times and this could lead to knowledge of the best combination of methods of hydrate dissociation for that particular system.

- Conducting Plackett Burman design for different scenarios including anisotropy in all the parameters and to compare with the case already studied in the project.
- Implementation of different techniques of design of experiments like Monte-Carlo, taguchi, full factorial, half factorial and studies of the effects of different factors in a reservoir simulation should be performed.
- An economic model can be developed to cross check the economic feasibility of the gas hydrate wells in order to gain confidence over the production rates obtained from reservoir simulations.
- Effect of different variables like reservoir thickness, well completion, well spacing on production rates should be studied.

References

1. Kvenvolden, K. A. (1993) Gas hydrates-Geological Perspective and global change. *Reviews of Geophysics* 31, 173-187
2. National Energy Technology Laboratory, http://www.netl.doe.gov/technologies/oil-gas/FutureSupply/MethaneHydrates/MH_CodeCompare/MH_CodeCompare.html. 2008.
3. Moridis, G.J., M.B. Kowalsky, and K. Pruess, *TOUGH-Fx/HYDRATE v1. 0 User's Manual: A code for the simulation of system behavior in hydrate-bearing geologic media*. Report LBNL-58950. Lawrence Berkeley National Laboratory, Berkeley, CA, 2005.
4. MH-21 Research Consortium, <http://www.mh21japan.gr.jp/english/>.
5. Moridis, G.J., M.B. Kowalsky, and K. Pruess, *HydrateResSim Users Manual: A Numerical Simulator for Modeling the Behavior of Hydrates in Geologic Media*. Department of Energy, Contract No. DE-AC03-76SF00098. Lawrence Berkeley National Laboratory, Berkeley, CA, 2005.
6. Computer Modeling Group Ltd, *CMG STARS*. 2007: Calgary, Alberta, Canada.
7. White, M.D. and M. Oostrom., *STOMP Subsurface Transport Over Multiple Phase: User's Guide PNNL-15782 (UC-2010)*. Pacific Northwest National Laboratory, Richland, Washington, 2006.
8. EIA (U.S. Energy Information Administration), Annual Energy Outlook 2008 http://www.eia.doe.gov/oil_gas/natural_gas/info_glance/natural_gas.html

9. Forests and energy, Key Issues, Food and Agriculture Organization of the United States, 2008. <ftp://ftp.fao.org/docrep/fao/010/i0139e/i0139e00.pdf>
10. EIA (U.S. Energy Information Administration), Annual Energy Outlook 2007, Report: DOE/EIA 0383-2007, February 2006.
11. U.S. Department of Energy, Office of Fossil Energy Overview of Methane Hydrate: Future Energy Within Our Grasp
http://fossil.energy.gov/programs/oilgas/publications/methane_hydrates/MHydrate_overview_06-2007.pdf
12. Michael D. Max et al. (eds.), Economic Geology of Natural Gas Hydrate, 191-206. © 2006 Springer. Printed in the Netherlands.
13. Collett T.S. et al., Occurrence of Marine gas hydrates in the Indian continental margin. Results of the Indian national gas hydrate program (NGHP). American Geophysical Union, Fall Meeting 2007.
14. Alaska Gas hydrate Studies With The BPXA-USDOE-USGS Resource Studies
http://www.netl.doe.gov/technologies/oil-gas/FutureSupply/MethaneHydrates/rd-program/ANSWell/ANSWell_main.html.
15. New Energy and Fuel, Apr 23, 2008
<http://newenergyandfuel.com/http://newenergyandfuel.com/2008/04/23/a-breakthrough-in-fuel-supplying-from-methane-hydrates/>
16. Michael D. Max. *Natural Gas Hydrate: In Oceanic and Permafrost Environments*, 2000 P-1

17. Yuri F. Makogon, *Hydrates of Hydrocarbons*, **1997**
18. Hammerschidt, E. G. *Ind. Eng. Chem.* 1934, 26, 851.
19. Tofimuk, A.A., Cherskiy, N.V., Tsarev, V.P., *Future Supply of Nature-Made Petroleum and Gas* (Meyer, R.F., ed.), Pergamon Press, New York, 919 (1977).
20. Klauda, J.B., Sandler, S.I., *Energy and Fuels*, 19, 469 (2005).
21. Mineral Management Service: Methane gas hydrates (USGS)
http://geology.usgs.gov/connections/mms/joint_projects/methane.htm
22. Clathrate Hydrates of Natural Gases p-540 Dendy Sloan estimates
23. Kvenvolden, K.A., "Gas Hydrates as a Potential Energy Resource", U.S. Geological Survey Professional Paper 1570, pg. 555-561, 1993.
24. Mc Mullan, R.K., Jeffrey, G.A., *J. Chem. Phys.*, 42, 2725 (1965).
25. Ripmeester, J.A., Tse, J.S., Ratcliffe, C.T., Powell, B.M., *Nature*, 325, 135 (1987).
26. Sloan, E.D.; Koh, C. A. *Clathrate hydrates of natural gases*, 3rd ed, 2007 p-70
27. Sloan, E.D.; Koh, C. A. *Clathrate hydrates of natural gases*, 3rd ed, 2007 p-540
28. Williams, E. T., Millheim, K., and Liddell, B., "Methane Hydrate Production from Alaskan Permafrost," DOE final report, Maurer Technology Inc. and Andarko Petroleum Corp., TX, March 2005.
29. Michael D. Max. *Natural Gas Hydrate: In Oceanic and Permafrost Environments*, **2000** P-5
30. United States Environmental Protection Agency: www.epa.gov/methane/
31. Khalil, M.A.K., C.L. Butenhoff, and R.A. Rasmussen, 2007, 41, 2131-2137. *Atmospheric Methane: Trends and Cycles of Sources and Sinks. Environmental Science and Technology.*

32. D. Archer "Methane hydrate stability and anthropogenic climatic change", *Biogeosciences*, 4, 521-544, 2007
33. Kelley, Joseph T., et al; "Giant Sea-Bed Pockmarks: Evidence for Gas Escape from Belfast Bay, Maine," *Geology*, 22:59, 1994.
34. Van Genuchten, M.T., *A closed-form equation for predicting the hydraulic conductivity of unsaturated soils*. *Soil Sci. Soc. Am. J*, 1980. **44**(5): p. 892-898
35. Mualem, Y., *A New Model for Predicting the Hydraulic Conductivity of Unsaturated Porous Media*. 1976
36. Stone, H.L., *Probability model for estimating three-phase relative permeability*. *J. Pet. Tech*, 1970. **22**(2): p. 214-218.
37. Aziz, K. and A. Settari, *Petroleum Reservoir Simulation*. 1979: Applied Science Publishers.
38. Diane L. Beres and Douglas M. Hawkins., "Plackett-Burman technique for sensitivity analysis of many-parameter models" *Ecological Modeling* 141 (2001) 171-183.
39. Anderson, B., et al. Analysis of Modular Dynamic Formation Test Results from the "Mount Elbert" Stratigraphic Test Well, Milne Point, Alaska. in Proceedings of the 6th International Conference on Gas Hydrates. 2008. Vancouver, British Columbia, Canada.